THE INFLUENCE OF BOTTOM CURRENTS ON THE SEDIMENTARY EVOLUTION OF THE ALBORAN SEA DURING THE PLIOCENE AND QUATERNARY

Carmen Juan Valenzuela

La influencia de las corrientes de fondo
en la evolución sedimentaria del Mar de Alborán
durante el Plioceno y Cuaternario

Tesis Doctoral 2016

UNIVERSITAT DE BARCELONA

CSIC
CONSEJO SUPERIOR DE INVESTIGACIONES CIENTÍFICAS

iCM Institut de Ciències del Mar

Departament d'Estratigrafia, Paleontologia i Geociències Marines.

Universitat de Barcelona.

Programa de Doctorado en Ciencias del Mar.

Bienio 2009-2010

The influence of bottom currents on the sedimentary evolution of the Alboran Sea during the Pliocene and Quaternary

La influencia de las corrientes de fondo en la evolución sedimentaria del Mar de Alborán durante el Plioceno y Cuaternario

Memoria de Tesis Doctoral presentada por:

Carmen Juan Valenzuela

2016

Memoria de Tesis Doctoral presentada por:

Carmen Juan Valenzuela

para optar al título de Doctora por la Universitat de Barcelona

Tesis realizada en el Departamento de Geociencias
Marinas del Institut de Ciències del Mar (ICM),
perteneciente al Consejo Superior de Investigaciones
Científicas (CSIC) en Barcelona

La doctoranda:
Carmen Juan Valenzuela

Los directores de la Tesis:

Dra. Gemma Ercilla Zarraga
Departamento de Geociencias Marinas
Institut de Ciències del Mar
ICM-CSIC

Dr. F. Javier Hernández Molina
Department of Earth Sciences
Royal Holloway, University of London

El tutor de la Tesis:

Dra. Teresa Medialdea Cela
Recursos y Geología Marina
Instituto Geológico y Minero de España
IGME (Sede Ríos Rosas)

Dr. Miquel Canals Artigas
Departament d'Estratigrafia, Paleontologia
i Geociències Marines
Universitat de Barcelona

Agradecimientos

En el centro de la Tierra la fuerza de gravedad se neutraliza. Allí todo cambia su naturaleza y su comportamiento, y el resultado de ese fenómeno es un misterio para el hombre.
Si hay agua, estará flotando en lagos esféricos. Si hay fuego, formará tormentas de viento circular, o tal vez será un pequeño sol interior.
Quizás haya agua y fuego al mismo tiempo en constante lucha, creando un eterno e increíble espectáculo.
Sea como fuere, me encanta recordar que eso está ocurriendo ahora mismo debajo de nuestros pies.

Ciruelo Cabral

Cuaderno de Viajes

INDEX

Presentation and objectives of this PhD thesis

Bottom current processes have an important impact on the shape of the seafloor through erosion, transport and deposition, generating extensive contourite features (e.g., Stow *et al.*, 2002a; Rebesco and Camerlenghi, 2008; Rebesco *et al.*, 2014). Interest in the sediments and features related to bottom currents has increased over the past 15 years, as they provide records of palaeoceanographic and palaeoclimatic changes (Knutz, 2008), offer potential for hydrocarbon exploration (Viana *et al.*, 2007), and can also be related to geohazards (Holbrook *et al.*, 2002).

Globally, new detailed maps of continental margins and abyssal plains have encouraged research into the sedimentary processes behind contourite formation (e.g., Rebesco and Camerlenghi, 2008, and references therein; Shanmugam, 2012). Water-masses circulating in modern oceans and seas can transport sediment over long distances, and their bottom component can re-suspend and advect seafloor sediments or pirate sediments from other sedimentary processes (e.g., gravity flows). Moreover, deep-water circulation is a relatively long-term process, with periods of activity ranging from decades to millions of years that are closely linked to basin physiography and climatic and eustatic changes (Stow *et al.*, 2008; Mulder *et al.*, 2011). In spite of this significant role played by deep-sea currents in sedimentation, contourites have been largely overlooked in comparison to downslope gravitational processes and other continental shelf processes such as waves and storms. This is mainly due to the traditional focus on turbidites and their economic importance in hydrocarbon exploration, as well as to the difficulty in recognizing contourites.

Most of the sedimentary and stratigraphic studies performed on the Pliocene and Quaternary deposits in the deep-sea areas of the Alboran Sea have failed to approach the sedimentary record and the active circulation that characterises this sea, as an integrated system (e.g., Stanley *et al.*, 1975; Alonso and Maldonado, 1992; Maldonado *et al.*, 1992; Ercilla *et al.*, 1994; Chiocci *et al.*, 1997). In fact, although the Alboran Sea is a key oceanographic location in the Mediterranean Sea because of its proximity to the Strait of Gibraltar, the role of bottom currents in sedimentation has been reported only at a local scale (Ercilla *et al.*, 2002; Palomino *et al.*, 2011).

This PhD thesis is aimed at understanding the influence of bottom currents on basin-scale sedimentation in the deep-water environments of the Alboran Sea and how this influence has evolved during the Pliocene and Quaternary, since the opening of the Strait of Gibraltar. In order to achieve this, the work has the following specific objectives:

a) To determine the importance of bottom currents in shaping the deep-water environments of the Alboran Sea.

b) To analyse in detail the Pliocene and Quaternary seismic stratigraphy to demonstrate the widespread dominance of bottom-current processes in the Alboran Sea since the opening of the Strait of Gibraltar.

c) To establish the architectural model of the Alboran Sea in terms of sedimentary systems in order to carry out the geological approach to define the palaeoceanographic processes.

d) To analyse the interaction between bottom current alongslope and gravity flow downslope sedimentary processes in the turbidite systems.

This thesis is organised into 9 chapters. These chapters deal with the database and methods, the description, interpretation, and discussion of the results, and the main conclusions of this study.

Chapter I *"Introduction"*, focuses on some basic aspects of distal continental margins, the main sedimentary systems, and the study area.

Chapter II **"Database and methods"**, presents the data used in this study, obtained during various scientific and commercial cruises and through collaboration with French and Moroccan institutions. It also describes the different geophysical and sedimentologic techniques used for data acquisition as well as the type of analysis performed on both the sedimentary record and the water column.

Chapter III **"Significance of bottom currents in the deep-sea morphodynamics of the Alboran Sea"**, combines a classical geological approach based on a seismic study of the major morphosedimentary features with an oceanographic study of the water masses.

Chapter IV *"Seismic evidence of current-controlled sedimentation in the Alboran Sea during the Pliocene and Quaternary: Palaeoceanographic scenarios"*, presents a new seismic stratigraphy for the Alboran Sea and a detailed analysis of the seismic facies that provide evidence of the contourite features, their controlling factors and the palaeoceanographic scenarios since the opening of the Strait of Gibraltar.

Chapter V ***"Pliocene and Quaternary sedimentary systems and an architecture model for the Alboran Sea. A geological perspective to palaeoceanographic processes".*** This chapter looks in depth at the architectural model in terms of sedimentary systems with special emphasis on determining the geological approach to defining palaeoceanographic processes.

Chapter VI ***"Bottom current signatures in the uneven turbidite systems of the Alboran Sea"***. This chapter analyses the interaction between alongslope and downslope sedimentary processes through their morphological and sedimentary imprints in the turbidite systems of the Alboran Sea during the Pliocene and Quaternary.

Chapter VII ***"Conclusions"*** sets out the conclusions of this PhD thesis.

Chapter VIII ***"References"*** is a compilation of all the literature used in this study.

Chapter IX ***"Annex: scientific contributions"***, provides the scientific contributions (abstracts and papers) that were published throughout this study.

Abstract

An interdisciplinary study of the geomorphology, sedimentology, stratigraphy and physical oceanography of the deep-sea environments of the Alboran Sea (south-western Mediterranean Sea) has been carried out with the purpose of evidencing and understanding the role of bottom currents in the sedimentary evolution of the Spanish and Moroccan continental margins and adjacent basins during the Pliocene and Quaternary. This study was conducted using swath bathymetry data, more than 1900 profiles consisting of parametric, single- and multi-channel seismic records, scientific and commercial wells, sediment cores, and hydrographic data comprising: Conductivity, Temperature and Depth (CTD) profiles, Acoustic Doppler Current (ADCP) profiles, and EK60 echograms.

Here, for the first time, a morphosedimentary scenario with a wide spectrum of depositional (plastered, sheeted, channel-related, mounded confined, elongated and separated drifts) and erosional (terraces, escarpments, moats, channels and furrows) contourite features are described in the Alboran Sea, from the shelf break to the basin floor. Hydrographic data offers new insights into the distribution of the Mediterranean water masses, and reveals that the bottom circulation of the Western Intermediate Water (WIW) and the Levantine Intermediate Water (LIW) interact with the Spanish slope, and the Western Mediterranean Deep Water (WMDW) with the Moroccan slope, Spanish base-of-slope and deep basins. The integration of distinct datasets and approaches allow a new sedimentary model to be proposed for the Alboran Sea that underlines the significance of bottom current processes in shaping deep-sea morphology. This model suggests that the bottom circulation of water masses governs physiography, that the interface positions of water-masses with contrasting densities sculpt terraces at a regional scale, and that morphological obstacles play an essential role in the local control of processes and water-mass distribution.

An analysis of the seismic stratigraphy from the Pliocene and Quaternary sequences has enabled to update and rename the stratigraphic boundaries and establish a new seismic stratigraphy for the Alboran Sea, after relocating the base of the Quaternary from 1.8 to 2.6Ma. Additionally, the seismic analysis involves the presentation and discussion of the evidence for contourite features reaching the scale of the Alboran Basin. Contourite drifts (plastered, sheeted, elongated separated and confined mounded drifts) and erosive features (terraces, escarpments, moats, channels, furrows) were developed under the continuous influence of Mediterranean water masses after the opening of the Strait of Gibraltar (~5.33Ma). At least two primary factors have controlled the contourite features

in this sea: i) tectonics, which has governed the relocation of the main Mediterranean flow pathways and their circulation patterns; and ii) climate, which has influenced both water-mass conditions (depth and density contrast of the interfaces) and hinterland sediment sources, conditioning the morphoseismic expression and growth pattern of drifts and terrace formation (dimensions). The distribution of contourite features through time and space allows to propose three main scenarios for ocean circulation since the opening of the Strait of Gibraltar: i) Atlantic Zanclean flooding; ii) the Pliocene sea, with two different stages for the dense circulation and characterised by poorly-defined and unstable interfaces for the Atlantic Waters (AW), light and dense Mediterranean waters and the presence of a strong countercurrent in the Western Basin; and iii) the Quaternary sea, characterised by tabular Mediterranean water masses with multiple current dynamics, increasingly important density contrasts, and climate shifts causing major vertical and horizontal displacement of the interfaces. These stages reflect variability in the bottom current regimes and related alongslope efficiency in terms of transport, deposition and erosion.

The detailed seismic analysis of the units making up the Pliocene and Quaternary sequences allows for the first time, to make an in-depth analysis of the contourite features, turbidite systems and mass-movement deposits, and map them through time. These maps are enormously helpful when it comes to understanding the sedimentary architecture of the Spanish and Moroccan continental margins and basins, as well as for decoding the palaeoceanographic processes from a geological perspective. Two main contourite depositional systems are defined: the Intermediate Contourite Depositional System (ICDS), formed under the action of the Light Mediterranean Waters (LMW) on the Spanish margin, and the Deep Contourite Depositional System (DCMW), formed under the action of the Dense Mediterranean Waters (DMW) mainly on the Moroccan margin and basins. The characterisation of the terraces as contourite features that form under the combination of two water masses, has also led to the definition of the Atlantic Contourite Depositional System (ACDS). The occurrence of several contourite depositional systems has led to the suggestion of a new term, not heretofore considered in the literature: Multiple Contourite Depositional System (MCDS), which refers to the set of different CDSs that occurs in the same area and evolving under the action of multiple water masses. In addition, twenty turbidite systems have been characterised, revealing that they are responsible for the different sedimentary architecture of the Spanish margin, where they coexist with contourites, as on the Moroccan margin the turbidite systems are less well developed. The mass-movement deposits are mainly related to the reworking of the contourites draping the highs. Mainly contourites but also turbidites, allowed to define from a geological

12

perspective the basic oceanographic processes and to determine their occurrence, relative magnitude and energy, and time of action.

This PhD thesis also explains the uneven development of the turbidite systems in the Alboran Sea, which is interpreted to be conditioned by the interaction of alongslope with downslope processes. Several morphological and sedimentary signatures produced by the interaction between both processes have been identified in the Pliocene and Quaternary records, as well as on the present-day seafloor of the Alboran Sea. The interaction scenarios move between two-end-members: from bottom currents dominating gravity flows to gravity flows dominating contour currents. In between these extreme cases, the alternation and mutual influence of both processes can occur. Two different conceptual models of interaction are proposed for the Spanish and Moroccan margins. i) On the Spanish margin, the alongslope and downslope interaction is especially complex and varied, with both regional and local effects on the turbidite systems. This is because here the turbidite systems are influenced at different water depths by Atlantic and Mediterranean water masses and their interfaces, with current flows that change across- and downslope. ii) On the Moroccan margin, the vigorous action of the WMDW primarily inhibits the formation of canyons and associated deposits.

The findings of this PhD thesis suggest that the relevance of bottom-water processes in deep sea must be reevaluated. It is concluded that understanding the influence of bottom currents is not only essential for reconstructing present and past water mass circulation, but also for recognising sea floor morphologies and decoding the sedimentary stacking pattern and evolution of deposits, as well as global climate and periods of eustatic variation.

Resumen

En el presente trabajo se ha llevado a cabo un estudio multidisciplinar de la geomorfología, sedimentología, estratigrafía y oceanografía física de los ambientes profundos del Mar de Alborán (extremo sur-oeste del Mar Mediterráneo), con el propósito de comprender el papel que los procesos asociados a las corrientes de fondo juegan en la evolución sedimentaria de los márgenes continentales de España y Marruecos, así como de las cuencas adyacentes, durante el Plioceno y el Cuaternario. Este estudio se ha llevado a cabo empleando datos de batimetría multihaz, más de 1900 registros sísmicos de sonda paramétrica, mono- y multi-canal, sondeos científicos e industriales, testigos de sedimento, y varios tipos de datos hidrográficos que comprenden: perfiles de conductividad, temperatura y profundidad (CTD), perfiles obtenidos con un correntómetro acústico Doppler (ADCP), y ecogramas registrados con una ecosonda EK60.

Por primera vez en el Mar de Alborán, se ha sido descrito un contexto morfosedimentario compuesto por un amplio espectro de rasgos contorníticos deposicionales (crestas adosadas, laminares, asociadas a canales, monticulares confinadas y elongadas separadas) y erosivos (terrazas, escarpes, fosas, canales y surcos erosivos), desde el borde de la plataforma continental hasta las cuencas. Los datos hidrográficos han ofrecido nueva información sobre la distribución de las masas de agua mediterráneas, y han revelado que la circulación de fondo del Agua Intermedia Occidental (Winter Intermediate Water, WIW) y el Agua Intermedia Levantina (Levantine Intermediate Water, LIW) interaccionan con el talud continental del margen español, mientras que el Agua Mediterránea Occidental Profunda (Western Mediterranean Deep Water, WMDW) interactúa con el talud continental del margen marroquí, la base de talud del margen español y las cuencas profundas. La integración de diversas bases de datos y de distintas disciplinas ha permitido proponer un nuevo modelo sedimentario para el Mar de Alborán el cual enfatiza la importancia de los procesos sedimentarios asociados a corrientes de fondo en el moldeado de los fondos marinos. Este modelo sugiere que la circulación de fondo de las masas de agua condiciona la fisiografía, que la posición de las interfaces de las masas agua con un importante contraste en sus densidades, es capaz de esculpir terrazas a escala regional, y que los altos morfológicos desempeñan un papel esencial en el control local de procesos y en la distribución de las masas de agua.

El análisis de la estratigrafía sísmica de las secuencias Pliocena y Cuaternaria ha permitido actualizar y renombrar los límites estratigráficos del Mar de Alborán, tras la reubicación además de la base del Cuaternario de 1,8 a 2.6 Ma, así como establecer una

aproximación cronológica a los mismos. Asimismo, este análisis sísmico ha permitido presentar y discutir evidencias de depósitos contorníticos a escala del Mar de Alborán. Los rasgos contorníticos de tipo deposicional (crestas adosadas, laminares, elongadas separadas y confinadas) y erosivo (terrazas, escarpes, fosas, canales y surcos) se desarrollaron bajo la influencia continua de las masas de agua mediterráneas tras la apertura del Estrecho de Gibraltar (~5.33 Ma). Al menos dos factores principales han controlado los rasgos contorníticos en esta cuenca: i) la tectónica, que rige la reubicación de los principales flujos mediterráneos y por tanto sus patrones de circulación; y ii) el clima, que ha influido en las condiciones de las masas de agua (profundidad y contraste de densidad en las interfaces) y en las áreas fuentes de sedimento en tierra, condicionando la expresión morfo-sísmica y los patrones de crecimiento de los depósitos contorníticos así como la formación de terrazas (dimensiones). La distribución de los elementos contorníticos en el espacio y el tiempo, permite proponer tres escenarios principales para explicar la circulación de las masas de agua desde la apertura del Estrecho de Gibraltar: i) la inundación atlántica en el Zancliense; ii) el mar Plioceno, con dos etapas diferentes para la circulación profunda y que en general se caracteriza por la presencia de interfaces poco definidas e inestables entre las aguas atlánticas (AW), y las aguas mediterráneas ligeras y densas, así como por la presencia de una fuerte contracorriente en la cuenca occidental de Alborán; por último, iii) el mar Cuaternario, que se caracteriza por masas de agua mediterráneas con flujo mayormente tabular pero con múltiples dinámicas de flujo a nivel local, una creciente influencia de los contrastes de densidad, y grandes cambios climáticos que provocan desplazamientos verticales y horizontales de las interfaces. Estas tres grandes etapas reflejan la variabilidad en los regímenes de corrientes de fondo, y la eficiencia en el transporte de sedimento, sedimentación y erosión a lo largo del margen.

El estudio sísmico detallado de las unidades que componen las secuencias Pliocena y Cuaternaria ha permitido por primera vez el análisis y la cartografía a lo largo del tiempo de los rasgos contorníticos, los sistemas turbidíticos y los depósitos de inestabilidad sedimentaria. Estos mapas han permitido comprender la arquitectura sedimentaria de los márgenes continentales español y marroquí y de las cuencas, así como definir los procesos paleoceanográficos desde un enfoque geológico. Se han definido dos grandes sistemas deposicionales contorníticos: el Sistema Deposicional Contornítico Intermedio (SDCI), formado bajo la acción de las aguas mediterráneas de menor densidad en el margen español, y el Sistema Deposicional Contornítico Profundo (SDCP), formado bajo la acción de las aguas mediterráneas densas principalmente en el margen marroquí y en las cuencas. La caracterización de las terrazas como rasgos contorníticos formados bajo la acción combinada de dos masas de agua ha llevado también a definir el Sistema

16

Deposicional Contornítico Atlántico (SDCA). El desarrollo de varios sistemas deposicionales contorníticos ha dado lugar a la definición de un nuevo término no planteado previamente en la literatura: el Sistema Deposicional Contornítico Múltiple (SDCM), referido a un conjunto de diferentes SDC que se forman en una misma zona bajo la acción de múltiples masas de agua. Asimismo, se han caracterizado veinte sistemas turbidíticos que son la causa principal de las diferencias en la arquitectura sedimentaria que presentan el margen español, en el que coexisten con las contornitas, y el margen marroquí, donde están menos desarrollados. Con respecto a los depósitos de inestabilidad sedimentaria, su formación está relacionada principalmente con el retrabajamiento de las contornitas que recubren los altos. Las contornitas principalmente, pero también las turbiditas, han permitido definir desde una perspectiva geológica los principales procesos oceanográficos así como determinar su ocurrencia, magnitud y energía relativas, y su tiempo de acción.

En esta Tesis se explica también el desarrollo desigual que presentan los sistemas turbidíticos en el mar de Alborán, y que ha sido interpretado como resultado de la interacción entre los procesos sedimentarios paralelos (asociados a las corrientes de fondo) y perpendiculares (asociados a los procesos de flujos gravitativos) al margen. En los registros Plioceno y Cuaternario, así como en el fondo marino actual del mar de Alborán, se han identificado rasgos de tipo morfológico, sedimentario y sedimentológico producidas por la interacción entre ambos procesos. Los escenarios de interacción varían entre dos situaciones extremas: las corrientes de fondo dominan sobre los flujos gravitativos, y los flujos gravitativos dominan sobre la acción de las corrientes de fondo. Entre ambos extremos puede producirse la alternancia y la influencia mutua de ambos procesos. Se han propuesto dos modelos de interacción conceptuales para los márgenes español y marroquí. i) En el margen español la interacción es especialmente compleja y variada, con efectos regionales y locales sobre los sistemas turbidíticos. Esto ocurre debido a que los sistemas turbidíticos están influenciados a diferentes profundidades por las masas de agua atlánticas y mediterráneas y sus interfaces, con una dinámica además que varía longitudinal y perpendicularmente al margen. ii) En el margen marroquí, la acción intensa de la WMDW inhibe en gran parte la formación de cañones y depósitos asociados.

Los resultados de esta Tesis sugieren que la importancia de los procesos relacionados con corrientes de fondo en ambientes marinos profundos debería ser reevaluada. Se concluye que una mayor comprensión de su influencia es esencial no sólo para reconstruir los patrones de circulación recientes y pasados, sino también para identificar

determinados rasgos morfosedimentarios, descifrar sus patrones de sedimentación y evolución, así como establecer tendencias en el clima y variaciones eustáticas a nivel global.

Acronyms

ACDS - Atlantic Contourite Depositional System
AW - Atlantic Water
CDC - Contourite depositional complex
CDS - Contourite depositional system
CSIC - Spanish National Research Council (Consejo Superior de Investigaciones Científicas)
DCDS - Deep Contourite Depositional System
EAB - Eastern Alboran Basin
EAG - Eastern Alboran Gyre
EMDW - Eastern Deep Mediterranean Water
DMW Dense Mediterranean waters (nowadays comprising WMDW)
ICDS - Intermediate Contourite Depositional System
ICM - Marine Sciences Institute (Institut de Ciències del Mar)
IEO - Spanish Oceanographic Institute (Instituto Español de Oceanografía)
IGME - Geological and Mining Institute of Spain (Instituto Geológico y Minero de España)
LMW - Light Mediterranean waters (nowadays comprising WIW+LIW)
LIW - Levantine Intermediate Water
MAW - Modified Atlantic Water
MOW - Mediterranean Outflow Water
MB - Motril Basin
MW - Mediterranean Water
Psu - Practical salinity units
RV - Research Vessel
SAB - Southern Alboran Basin
ShW - Shelf water
TDW - Tyrrhenian Dense Water
TS - Turbidite system
WAB - Western Alboran Basin
WAG - Western Alboran Gyre
WIW - Western Intermediate Water
WMDW - Western Mediterranean Deep Water

Chapter I - Introduction

Chapter I - Introduction

1. The geology of the passive continental margins

The continental margins represent the transition between continents and oceans, and are the areas with major sediment accumulation on Earth (Kennett, 1981; Divins, 2003). They are the subject of interest of many disciplines, of oceanography in general and of marine geology in particular, as their sedimentary registers contain relevant information about the tectonic evolution of the margins, the palaeoclimatology and the hydrology of the adjacent areas, the glacioeustatic changes or the subaerial erosion.

1.1. Main physiographic provinces

Three main physiographic provinces can be defined in the continental margins based on gradients, width and water depths: the continental shelf, the continental slope and the continental rise (Fig. 1.1). The break points between the shelf and slope (named shelf break), and between the slope and rise are relatively sharp and can be distinguished due to their different seafloor gradients (Fig. 1.1).
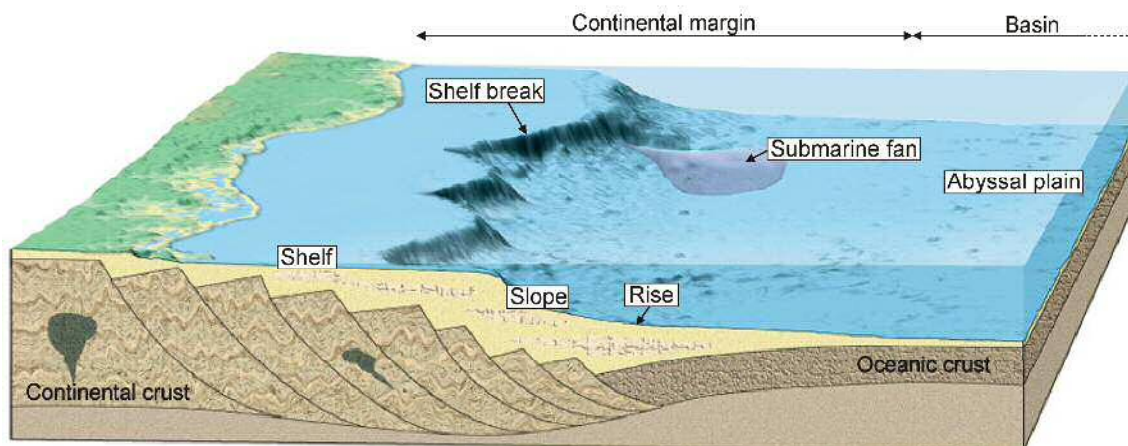
Fig. 1. 1 - Diagram of a passive continental margin. Modified from Tarbuck *et al.* (2005)

The *continental shelf* province is a relatively flat surface characterized by gentle gradients (0.1º to 1º), that extends from the present-day coastline to the shelf break. The width of the continental shelf averages 80 km (Johnson and Baldwin, 1996), although it can be almost absent in tectonically active margins and reach up to 1200 km (Siberia, Russia) in some passive margins. This shelf surface is submerged during transgressions and highstands of the sea level (with the shelf break typically located at 120-130 m water

depth -w.d.-), and can be completely exposed to subaerial conditions during regressive and lowstands.

The *continental slope* province is typically rather narrow (~20 km), beginning at the shelf break and dropping from ~120 m w.d. to hundreds/thousands meters deep (Kennett, 1981). The average slope values are of ~3 to 5º (Kennett, 1981), but locally can reach up to 25º (Pratson and Haxby, 1996; Stow et al., 1996). It can be a quite complex province, including seamounts, canyons, intra-slope basins, terraces, marginal plateaus, etc. The continental slope frequently coincides with the transition between continental and oceanic crust (Tarbuck et al., 2005).

The *continental rise* is a wide area (100-1000 km; Kennett, 1981) with lower gradients (~0.33º, Tarbuck et al., 2005) where most of the sediments transported from the continents to the deep-sea environments accumulate. This physiographic province begins with a drastic variation in the seafloor gradient that gradually diminishes towards the adjacent abyssal plain. This physiographic province only develops in passive margins, as a result of sedimentation of different types of sedimentary bodies, as turbiditic fan, mass movement deposits, etc.

1.2. Sedimentary processes shaping and outbuilding the distal continental margins

Literature establishes that there are three main types of sedimentary processes shaping the distal margins. They can be defined based on the interplay between the source of sediment and the transport mechanism, and are: gravitational processes, bottom currents and (hemi)pelagic settling, that represent extremes in a continuum (Rebesco et al., 2014).

1.2.1. Gravitational processes

Gravitational processes result from the loss or lack of stability of sediments previously deposited in all the physiographic environments from the shelf to deeper domains (Ercilla and Casas, 2012) and frequently shape the slopes of the continental margins transporting sediments hundreds of kilometres downslope (Einsele, 1992; Casas et al., 2011; Masson et al., 2011; Ercilla and Casas, 2012; Casas et al., 2015; García et al., 2015).

These processes can occur due to high rate of sediment deposition (Einsele, 1992; Einsele et al., 1996) or deformation of the slope (Vázquez et al., 2010) until reaching a point where sediment becomes unstable (Nardin et al., 1979; Prior and Coleman, 1984; Booth et al., 1985; Masson et al., 1996; Iglesias, 2009; Casas et al., 2011), or due to the

action of a trigger. The potential triggering mechanisms are: earthquakes, erosion due to the impinging of water masses or associated oceanographic processes (as internal waves, etc.), gas release (Casas *et al.*, 2011), dense shelf water cascading (Einsele *et al.*, 1996) and sea level falls (Prior, 1984; Einsele *et al.*, 1996; Locat and Lee, 2000; Casas *et al.*, 2011).

Once the instability is initiated, the process can be described and classified according to its mechanical behaviour (rheology), transport mechanism, concentration of the particles, sedimentary structures and resulting seismic features downslope (Mutti and Ricci Lucchi, 1975; Mulder and Cochonat, 1996; Locat and Lee, 2000; Shanmugam, 2000; Mulder and Alexander, 2001; Gani, 2004; Masson *et al.*, 2006; Casas *et al.*, 2015). The most important types of mass transport processes observed in the marine environment are the slumps and slides, mass-flows, debris-rock avalanches and turbiditic flows (Table 1.1, Casas *et al.*, 2015).

Process	Rheology/ transport mechanism	Sedimentary structures	Seismic features
Slide	Elastoplastic/Coulomb Shear failure along discrete shear planes	Undeformed continuous bedding	The deposits show little internal deformation and pre-existing bedding is preserved. Plastic deformation can occur at the base of the failed deposit.
Slump	Elastoplastic/Coulomb Shear failure with rotation along discrete shear surface	Plastic deformation at the toe, folds, tension faults, rotational blocks.	Compressional ridges, irregular upper bedding contacts, contorted layers.
Debris flow	Viscoplastic Cohesive flow: Strength is principally from cohesion due to clay content.	Generally a poor grading and fabric. Massive beds with some blocks at the top of the flow. Typical hummocky surface on the seafloor.	Convex-up shape with low amplitude to transparent facies. The presence of blocks generates hyperbolic reflectors.
Rock/ debris avalanches	Non cohesive flow: Strength is principally from grain-to grain interaction	Poorly sorted ungraded to normally graded breccia or conglomerate with little matrix. Finer grained tail over the coarse grained head	Widespread, hummocky depositional lobes.
Turbiditic flow	Newtonian Supported by fluid turbulence	Normal size grading, sharp basal contacts, gradational upper contacts. Bouma sequence	Lobate or laterally continuous reflectors.

Table 1. 1 - Most frequent types of mass movement processes in the marine environment. Compiled from Moscardelli and Wood (2008) and Mulder *et al.* (2011) by Casas *et al.* (2015).

The *slumps and slides* are the movement of sediment or rock along a shear plane with relatively low shear resistance (Fig. 1.2). Slumps imply rotational movement and slides translational movement. The *mass flows* are cohesive flows characterized by a high cohesion between clay and fine silt particles and a pseudoplastic rheology (Fig. 1.2). Depending on the grain size, cohesive flows can be classified into mudflows and debris flows. Mudflows comprise clay-rich flows (> 40% clay) and silt flows (<25% clay). *Debris flows* consist of poorly sorted flows with plastic behaviour in which clasts float in a fine-grained matrix (Casas *et al.*, 2015). The *debris-rock avalanches* are a non-cohesive flow that involves large volumes of fragmented bedrock or consolidated sediment, often allowing large blocks of material (metric to kilometric size) to accumulate in different

parts of the flow (Prior and Doyle, 1985; Blikra and Nemec, 1998; Casas *et al.*, 2015). *Turbidity flows* are diluted gravity flows characterized by their high energy, where the particles are maintained in suspension due to fluid turbulence, and represent the main mechanism of sediment transfer from hinterland areas to the deep-sea basins (Kuenen, 1938, 1951; Kuenen and Migliorini, 1950). Velocity and density decrease upwards, and the flow is structured into a mainly erosional head (where the coarsest material concentrates) that mixes the eroded sediment with the running flow (Gervais *et al.*, 2006), and a mainly depositional neck, body and tail (diluted, thinner back part of the flow) (Mulder, 2011). The sediment transported by turbidity flows deposits after a change in the slope gradient (at the base of the slope or at intra-slope basins).
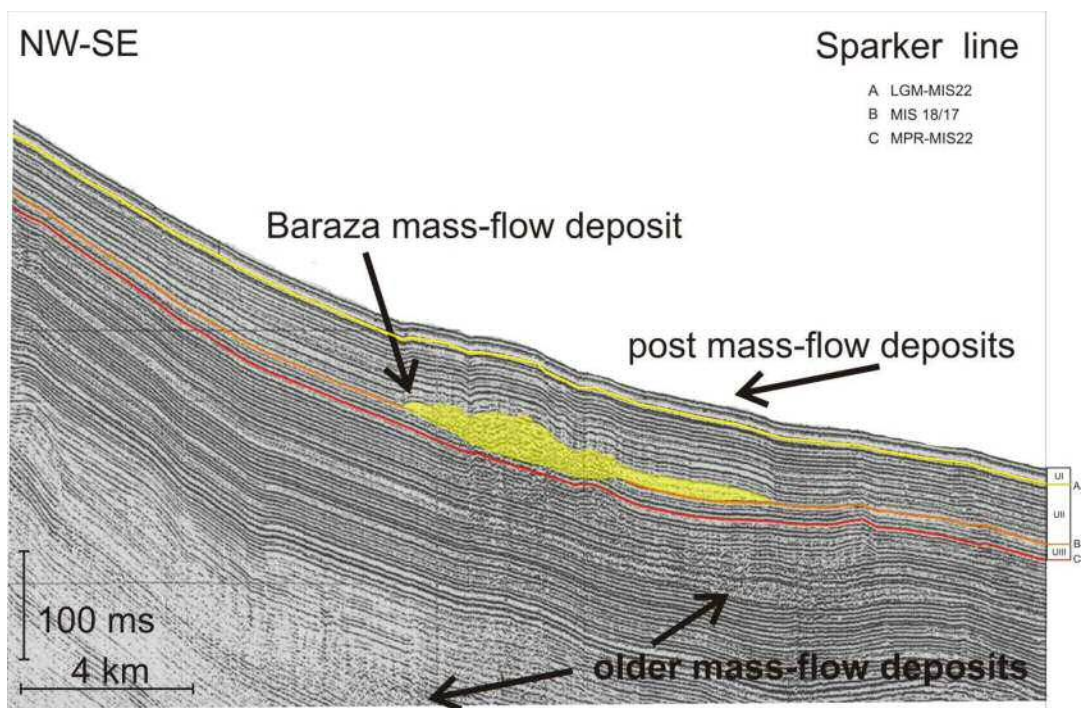
Fig. 1. 2 - Seismic profile illustrating the occurrence of mass-flow features on the slope of the Alboran Sea. From Casas *et al.* (2011).

1.2.2. Bottom currents

Bottom currents are generically defined as any persistent water current flowing near the sea-floor (Rebesco *et al.* 2008, 2014) (Fig. 1.3), and their continuous action on the seafloor can re-suspend and advect the seafloor sediments, pirate sediments from other sedimentary processes (e.g., gravity flows), transport the sediment over long distances and cause contourite sedimentation, generating altogether a large variety of erosive (e.g., channels, abraded surfaces) and depositional features (e.g., sediment waves, and large sedimentary drifts). Different oceanographic processes that generate bottom currents have been described in literature:
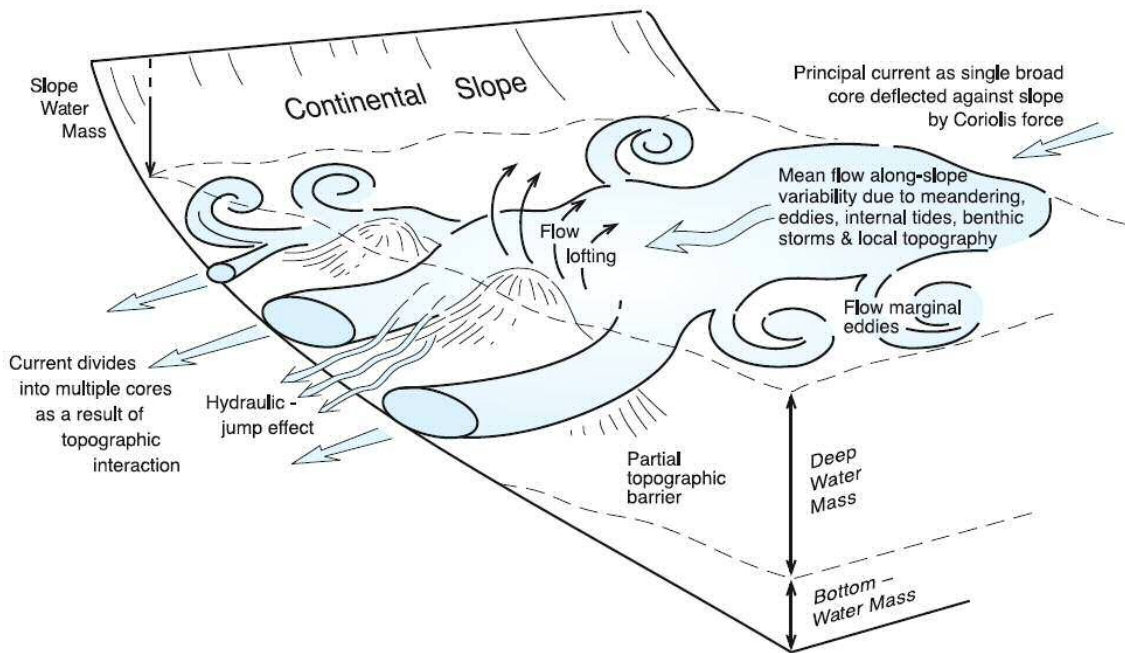
Fig. 1. 3 - Schematic diagram illustrating the effect of the bottom-currents on a slope. From Stow *et al.* (2008).

a) *Density-driven currents and thermohaline circulation.* These currents tend to flow in geostrophic balance parallel to depth contours (i.e., Wåhlin and Walin, 2001; Legg *et al.,* 2009; Rebesco *et al.,* 2014). Their density forcing can be maintained by cooling, evaporation or both (Rebesco *et al.,* 2014), and their speed is proportional to the slope of the bottom and to their density difference with the overlying water mass (Rebesco *et al.,* 2014); local heterogeneities such as topographic obstacles contribute in accelerating the deep currents. The intensification of the slow thermohaline circulation on the western oceanic margins leads to faster deep boundary currents capable of eroding, transporting and depositing fine-grained sediment (Stow and Lovell, 1979). A sufficiently active bottom current acting on geological time scales can cause a relevant effect on the seafloor by winnowing fine-grained sediments, generating erosive and depositional features (Stow *et al.,* 2002b; Rebesco and Camerlenghi, 2008; Rebesco *et al.,* 2014; Hernández-Molina *et al.,* 2015).

b) *Overflows.* These hydrographic structures are defined as the flow of a dense gravity current, carrying a particular water over a topographic barrier (either from a regional basin into the open ocean or from open-ocean flow into an isolated regional basin) until it reaches density equilibrium (Hernández-Molina *et al.,* 2015) (Fig. 1.4).
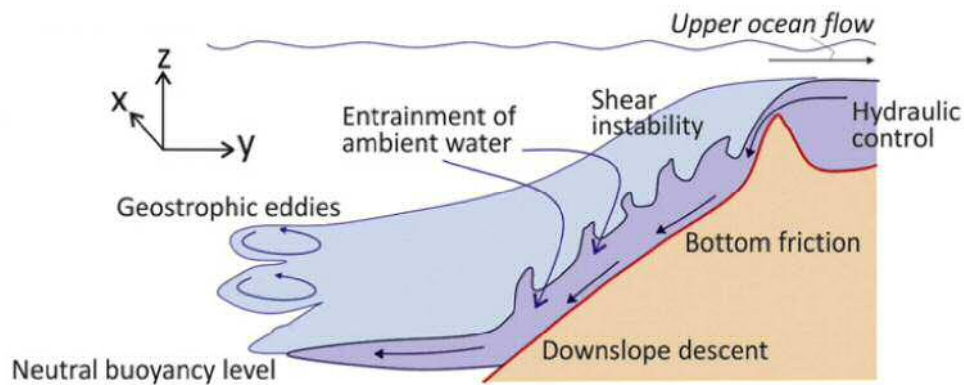
Fig. 1. 4 - Schematic diagram representing the physical processes acting during an overflow event. Adapted from Legg *et al.*, 2009 by Rebesco *et al.*, 2014.

c) *Processes at the interface between water masses.* The interface between water masses (pycnocline) can be sharp and well defined, or diffuse with a gradual transition from one water mass to the other (Hernández-Molina *et al.*, 2009, 2015; Preu *et al.*, 2013; Rebesco *et al.*, 2014). Turbulent mixing of water masses caused by tides, eddies (e.g., Piola and Matano, 2001; Arhan *et al.*, 2002, 2003) and internal waves (Puig *et al.*, 2004) can disrupt it (Rebesco *et al.*, 2014; Hernández-Molina *et al.*, 2015). Energetic current patterns associated with these disruptions strongly affect the seafloor through erosion and re-suspension (Dickson and McCave, 1986; Cacchione *et al.*, 2002; Puig *et al.*, 2004; Shanmugam, 2013a, 2014; Rebesco *et al.*, 2014; Hernández-Molina *et al.*, 2015).

d) *Deep-water tidal currents.* The energy of surface tides (barotropic tides driven by the gravitational pull of the Sun and the Moon) may generate deep baroclinic tides in stratified fluids. Both types of tides can influence deep-water environments (Dykstra, 2012), typically having a stronger effect on continental slopes with submarine canyons (e.g., Shepard, 1976; Shepard *et al.*, 1979; Viana *et al.*, 1998; Kunze *et al.*, 2002; Garrett, 2003; Shanmugam, 2012a, 2013b; Gómez-Ballesteros *et al.*, 2014; Gong *et al.*, 2013; Rebesco *et al.*, 2014; Hernández-Molina *et al.*, 2015).

e) *Deep-sea storms.* Benthic storms, also known as deep-sea storms or abyssal storms, are an intermittent deep-water process that occurs at a frequency of about 8 to 10 events per year (Holger, 1987), closely related to eddy formation (Rebesco *et al.*, 2014). Benthic storms are strong, intensified bottom currents affecting the seafloor in which bottom-current velocity can increase by a factor of 2-5 times (average 15-20 cm/s with peaks of over 43 cm/s) over a period of a few days (2 to 25 days) to several weeks (Hernández-Molina *et al.*, 2015). Benthic storm-related flows can have much longer-lasting effects on the suspension of bottom sediment (Rebesco *et al.*, 2014). Once ripped up by the erosional

effects of increased bottom shear, sediments can be transported by bottom currents and deposited in quiet regions downstream (Hollister and McCave, 1984; Flood and Shor, 1988; Von Lom-Keil *et al.*, 2002; Rebesco *et al.*, 2014) (Fig. 1.5).

f) *Eddies.* Eddies occur when a water mass interleaves into a stratified environment, or when current flows meet a seafloor irregularity such as a canyon, seamount or cape (Roden, 1987; Rogers, 1994; Arhan *et al.*, 2002; Serra *et al.*, 2010). Instabilities in bottom currents can also generate vortices (Serra *et al.*, 2010; Rebesco *et al.*, 2014; Hernández-Molina *et al.*, 2015) and contribute to the formation of nepheloid layers and long-distance sediment transport (Fig. 1.5).
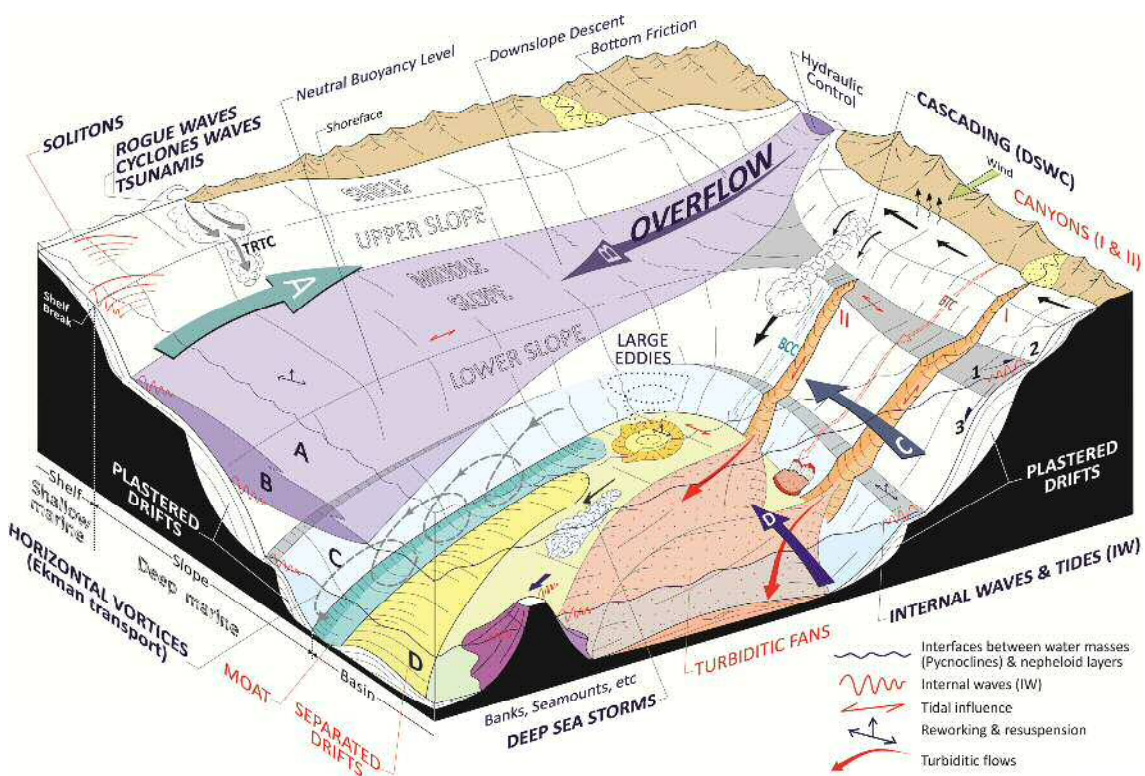
Fig. 1. 5 - 3D sketch depicting the possible oceanographic processes in deep-water environments. In addition to density currents and overflows, the velocity at the seafloor can also be affected by barotropic currents or intermittent processes such as cascading, giant eddies, deep sea storms, vortices, internal waves, internal tides, tsunamis, cyclone waves and rogue waves. From Rebesco *et al.* (2014).

g) *Secondary circulation.* The main cores of deep-water currents typically run parallel to isobaths (Rebesco *et al.*, 2014; Hernández-Molina *et al.*, 2015). The combined effect of bottom friction and the Coriolis effect in the Ekman layer usually results in a clockwise secondary circulation or helicoidal flow around the core of the current (Wåhlin and Walin, 2001; Wåhlin, 2004; Muench *et al.*, 2009b; Cossu *et al.*, 2010; Cossu and Wells, 2013;

Rebesco *et al.,* 2014; Hernández-Molina *et al.,* 2015) (Fig. 1.5). These flows can generate furrows with oblique trend relative to the main contourite bodies of the prevailing bottom currents (Rebesco *et al.,* 2014; Hernández-Molina *et al.,* 2015).

h) *Dense shelf water cascades.* Dense water masses can generate in shelf areas as a result from cooling, evaporation, freezing and/or salinization in the surface layer, forming a density-driven flow over the shelf edge, down along and across the slope area and reaching the continental slope (Simpson, 1982; Killworth, 1983; Ivanov *et al.,* 2004) (Fig. 1.5). Dense water cascading is mostly driven by density, gravity effects and the Coriolis Effect, but is slowed by friction and mixing (Rebesco *et al.,* 2014; Hernández-Molina *et al.,* 2015). Dense shelf water cascading can cause significant sediment transport (Palanques *et al.,* 2009) and has been suggested to cause massive sand beds within submarine canyons (Gaudin *et al.,* 2006).

i) *Internal waves and solitons.* These processes typically occur in stratified fluids after a water parcel displaced from its equilibrium position returns to its stable depth, causing an oscillation along the interface between two water masses of different densities (Farmer and Armi, 1999; Apel, 2000, 2004; Rebesco *et al.,* 2014) (Fig. 1.6). Internal waves are characterized by low frequencies (periods ranging from tens of minutes to days) and high amplitudes (hundreds of metres) (Rebesco *et al.,* 2014; Hernández-Molina *et al.,* 2015). The displacement and transference of energy also affects the water parcels at shallower and deeper levels (Shanmugam, 2012b, 2013a, 2014; Rebesco *et al.,* 2014; Hernández-Molina *et al.,* 2015). High amplitude internal wave generation in the Strait of Gibraltar around the Camarinal Sill and other minor sills located nearby strongly affects the Iberian (Puig *et al.,* 2004, Fig. 1.7A) and African margins (Fig. 1.7B).
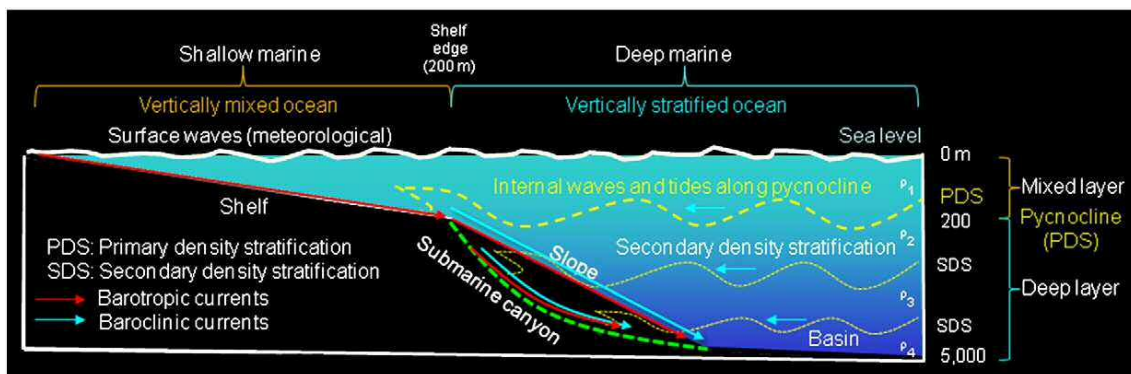
Fig. 1. 6 - Schematic diagram showing the position of the pycnocline (i.e., primary density stratification), where density gradient is the sharpest, and between ocean layers of different densities. Internal waves and tides propagate along boundaries of both primary and secondary density stratifications. Not to scale. From Shanmugam *et al.* (2012a).
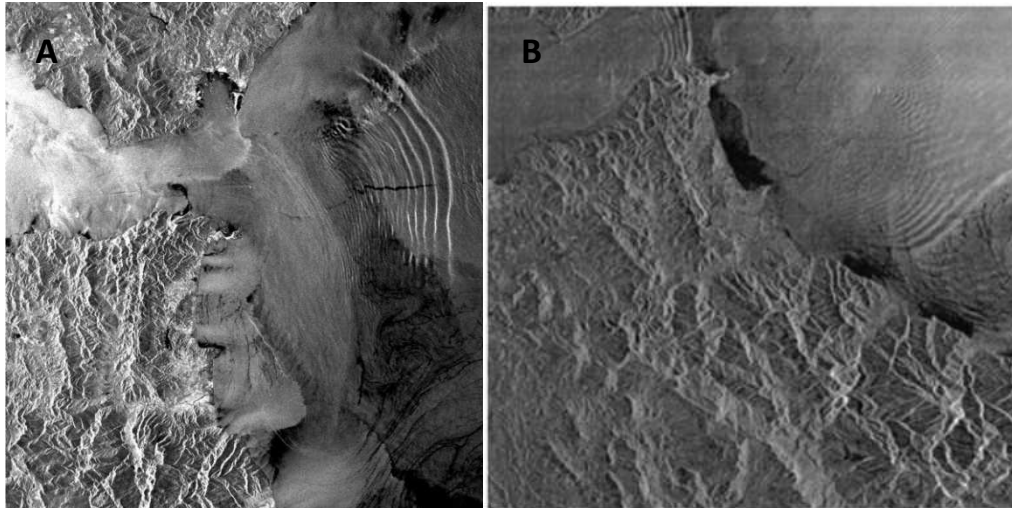
Fig. 1. 7 - Sea surface manifestations in Synthetic Aperture Radar (SAR) of internal wave packets generated in the Strait of Gibraltar a) with ENE trend (The dark line intersecting the internal wave packet originates from a ship which has discharged oil en route), acquired with ERS-1 satellite, and b) with a SE trend, acquired with ERS-2 satellite (from Vázquez et al., 2008).

j) *Tsunami-related traction currents, cyclone waves and rogue waves* are intermittent processes with similar effects (Rebesco *et al.,* 2014). All of them can trigger bottom currents and generate large hydrodynamic pressures on the sea floor that produce submarine mudflows and slope instabilities (Wright and Rathje, 2003) (Fig. 1.5), accelerating deep-water sedimentation and/or reworking previous deposits (Rebesco *et al.,* 2014; Hernández-Molina *et al.,* 2015). Tsunamis consist of a wave or series of waves involving the whole water column, caused by an abrupt vertical displacement of the ocean bottom due to earthquakes, landslides submarine volcanic eruptions or meteorite impacts (Shanmugam, 2006, 2011; 2012a; Rebesco *et al.,* 2014; Hernández-Molina *et al.,* 2015). Tsunami waves do not displace the water horizontally, nor do they transport sediment in open ocean. However, during the transformation stage of the wave when approaching a land mass, tsunami waves erode and incorporate sediment. Tsunami-related traction currents can thus transport large concentrations of sediment in suspension (Abrantes *et al.,* 2008; Shanmugam, 2006, 2012a) in the upper margins and the shelf. Oceanic rogue waves (also known as freak waves, killer waves, monster waves, abnormal waves, etc.) are surface gravity waves whose wave heights are at least twice as large as the significant wave height expected for the sea state (Shanmugam, 2012a; Hernández-Molina *et al.,* 2015). Last, tropical cyclones are large, rotating (due to the Coriolis force) systems of clouds, winds and thunder storms. However, it is not possible to differentiate between deposits generated by tsunamis and those generated by cyclonic or rogue waves (Shanmugam, 2011; Rebesco *et al.,* 2014).

1.2.3. (Hemi)pelagic settling

The (hemi)pelagic settling consists on the export of organic matter and other suspended particles from the surface waters, and their slow settling until reaching the seafloor. These processes can occur in the distal portion of the margins under high productivity conditions (Hüneke and Henrich, 2011) or favoured by conditions of low terrigenous sediment input (Garrison, 1981). Pelagic sediments are mostly composed by biogenic (autochthonous) particles mostly consisting of organic matter and calcareous and siliceous skeletal elements (Masqué *et al.,* 2003), whereas hemipelagic sediments are mixtures of biogenic and terrigenous (allochthonous) sediments that are deposited by a combination of vertical (pelagic) settling and slow lateral advection (Stow and Tabrez, 1998). There is a complete gradation between pelagites and hemipelagites (Stow *et al.,* 1996; Stow and Tabrez, 1998).

1.3. Deep-sea sediments

The aforementioned sedimentary processes represent extremes in a continuum of deep-sea sedimentary facies (Rebesco *et al.,* 2014). Interbedded hemipelagites, mass-wasting deposits, turbidites and contourites are common, especially in continental slope and rise environments, and adjacent deep sea areas (Stow and Lovell, 1979).

1.3.1. Mass movement deposits

Mass movement deposits (also named submarine sedimentary instability deposits, submarine slides, mass wasting deposits, mass transport deposits and gravity deposits) are features that have similar characteristics to the onshore mass movement deposits, with exceptions such as turbidites, which are exclusive to aquatic environments (Casas *et al.,* 2015; García *et al.,* 2015). For that reason, the terminology applied to submarine instability deposits is inherited from that of subaerial environments (e.g., Locat and Lee, 2000; Lee *et al.,* 2009; Hungr *et al.,* 2014; Casas *et al.,* 2015). Mass movement deposits frequently contribute in shaping the slopes of the continental margins (Casas *et al.,* 2011, 2015), and may develop in various environments and geological contexts (shelf, slope, rise and basins) (Ercilla and Casas 2012; Casas *et al.,* 2015 and references therein), although they commonly occur in areas with thick sedimentary deposits, sloping seafloors and high environmental stresses (Hampton *et al.,* 1996; Casas *et al.,* 2015). Mass movement deposits range greatly in size, (centimetric to decametric thickness; metric to hundreds of km in length) (Ercilla and Casas 2012), affecting huge areas of the seafloor (i.e., Storegga Slide, 95000 km^2, Fig. 1.8; Canals *et al.,* 2004; Haflidason *et al.,* 2004; Masson *et al.,* 2006).
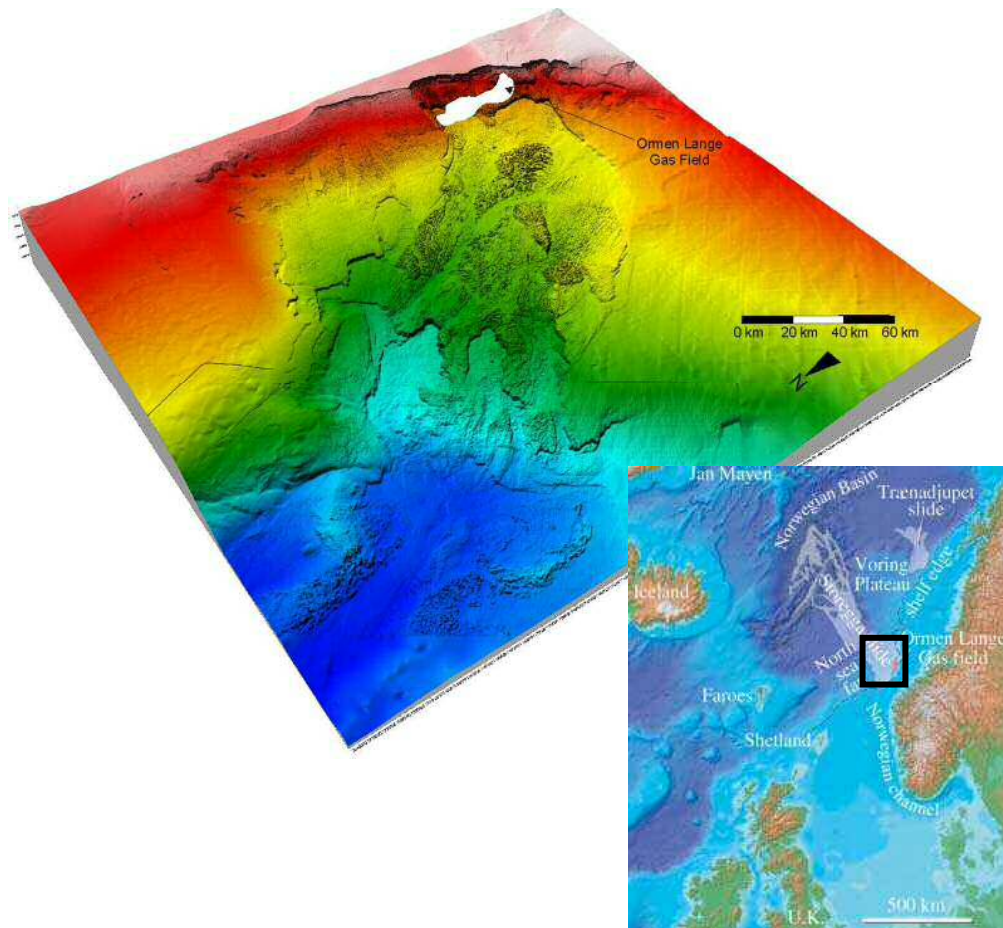
Fig. 1. 8 - Three-dimensional image of the upper Storegga slide based on swath bathymetry. This slide occurred 8200 years ago, and is considered the largest known landslide. Modified from Wille *et al.* (2005) and Masson *et al.* (2006).

The deposits that result from a sediment failure can be divided into slumps (rotational movement) and slides (translational movement) that can exhibit multiple phases of sediment displacement that propagate upslope (retrogressive failures) (e.g., Prior and Suhayada, 1979; Mulder and Cochonat, 1996; Casas *et al.*, 2015). The deposits that result from mass flows and avalanches are typically named as mass flow deposits and/or debrites, and debris avalanche deposits, respectively (Shanmugam, 2000 and references therein). Slumps/slides and mass-flow deposits appear associated forming complex depositional bodies that usually involve elements of both sedimentary processes, sliding and mass-flows (Masson *et al.*, 2006).

Several major factors control the deposition of mass movement deposits, such as the quantity and the type of sediment available (Alonso *et al.*, 1991; Mutti and Normark, 1991; Normark *et al.*, 1993; Bellaiche and Mart, 1995; Alonso and Ercilla, 2003). In turn, these factors depend on the size and the relief of the drainage basins (Kenyon, 2001; Alonso and

Ercilla, 2002, 2003), the rainfall (Bellaiche *et al.*, 2002; Panin and Jipa, 2002), tectonics (Gaullier *et al.*, 2002; Loncke *et al.*, 2002) and sea level fluctuations (Alonso and Ercilla, 2003). Thus, the sedimentary record of mass-movement deposits may inform about active tectonism, seabed fluid flow, glacioeustatic variations, etc. (Ercilla and Casas, 2012).

1.3.2. Turbidite systems

Turbidite systems (TSs) or submarine fans are defined as deep-sea clastic systems where the dominant process is a turbidity current (e.g., Pickering *et al.*, 1989; Normark *et al.*, 1993; Reading and Richards, 1994; Richards and Bowman, 1998; Richards *et al.*, 1998; Hüneke and Mulder, 2011). Their vertical stacking and plan-view morphology depends on the sediment input and on the morphology of the margin (Fig. 1.9). TSs have been the focus of research since the 1950s because they form relevant clastic accumulations in the deep seas that allow to decode the Earth's past climate and the regional oceanographic history and as potential hydrocarbon reservoirs (e.g., Shepard and Dill, 1966; Kenyon *et al.*, 1978; Pickering *et al.*, 1989; Richards and Bowman, 1998; Stow and Mayall, 2000; Alonso and Ercilla, 2000, 2003; García *et al.*, 2006, 2015).

Other mass movement deposits, as well as (hemi)pelagites and sediment piracing by deep water currents may simultaneously occur in these systems (Shanmugam, 2008; García *et al.*, 2015).

According to Mutti and Normark (1991), the main architectural elements defining a turbidite system are large-scale erosive features (i.e., canyons and channels), and depositional elements (i.e., channel-fill deposits, overbank deposits and lobes) (Fig. 1.10).

Submarine canyons are narrow (few km) and deep (hundreds of m) easily recognizable features with V-shaped and U-shaped cross-sections and steep walls, that originate on the continental shelf and upper slope and cross the slope with a mostly perpendicular trend, acting as the main conduits for sediment transfer to the deep basins (Fig. 1.9). These features can also exhibit complex trajectories caused by the presence of tectonic lineations or obstacles such as seamounts (Boillot *et al.*, 1974; Belderson and Kenyon, 1976; Cremer, 1981; Kenyon, 1987; Ercilla *et al.*, 2008b; Iglesias, 2009). Submarine canyons can initiate as a result of subaerial erosion during lowstands of sea level, submarine erosion by retrogressive mass movements, erosion of tectonic depressions, forward erosion by continuous steady flows and bypassing on prograding margins (Shepard, 1981; Mulder *et al.*, 2004; García *et al.*, 2015), and coalescence of smaller tributary canyons and gullies that frequently feed the main canyon (Ercilla *et al.*, 1992; Blum and Okamura, 1992; Field *et al.*,

1999; Orange, 1999; García *et al.,* 2006). The canyons transport a great variety of sediment types (gravels to clay) that will affect the morphology of the downslope turbidite deposits (Fig. 1.9).
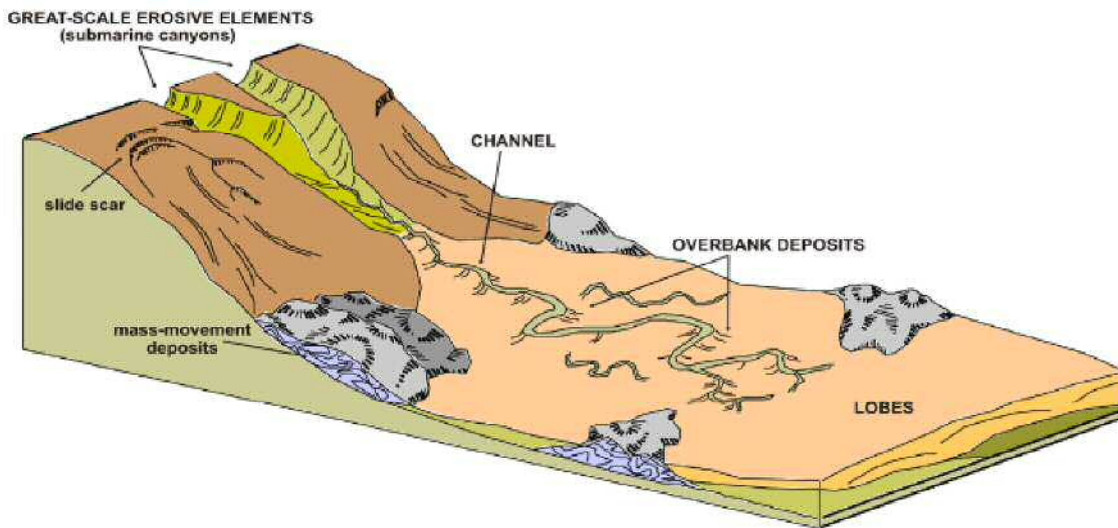
Fig. 1. 9 - Schematic diagram representing the main architectural elements of a turbidite system. Modified from Normark *et al.* (1993) by Alonso and Ercilla (2000).

The *channels* are rectilinear to highly meandriform features that develop basinward from the canyon mouth (Figs. 1.9 and 1.10), and considered to be mixed features maintained by a combination of erosion incising the channel and infill deposits (Normark *et al.,* 1993). The geometry of the turbidite channels is related to the type of sediment that feeds the turbidite fan: long and sinuous channels are mostly fed by muddy sediment, and straight and short channels are mostly fed by sandy sediment (García *et al.,* 2015). The dimensions of the turbidite channels progressively decrease, branching into minor distributary channels that ultimately disappear basinward. The coarsest sediment fraction is deposited in the channel axis, generating high-amplitude reflections (Flood *et al.,* 1991; Deptuck *et al.,* 2003; García *et al.,* 2015), and the finest sediment fraction feeds the overbank deposits. The lateral migration and avulsion of the turbidite channels occurs as a result of high-energy events (Wynn *et al.,* 2007).

The *overbank deposits* are fine-grained and thin-bedded sediments that develop adjacent to the main turbidity channels (Figs. 1.9 and 1.10). Their outbuilt mostly results from the spillover of the upper turbidity currents, but also due to the centrifugal force when the channel abruptly changes its direction (Piper and Normark, 1983; Normark *et*

al., 1993; Hiscott *et al.*, 1997; Mulder, 2011; García *et al.*, 2015). The overbank area can be divided into: a) the proximal levee (Fig. 1.10), characterized by a constructive positive relief that occasionally shows sediment wave fields and furrows caused by the spillover processes; and b) its lateral prolongation, where the deposit evolves laterally to a practically flat domain (García *et al.*, 2015). Due to the Coriolis force, the right-hand levee downflow is better developed in the northern hemisphere and the opposite levee in the southern hemisphere.
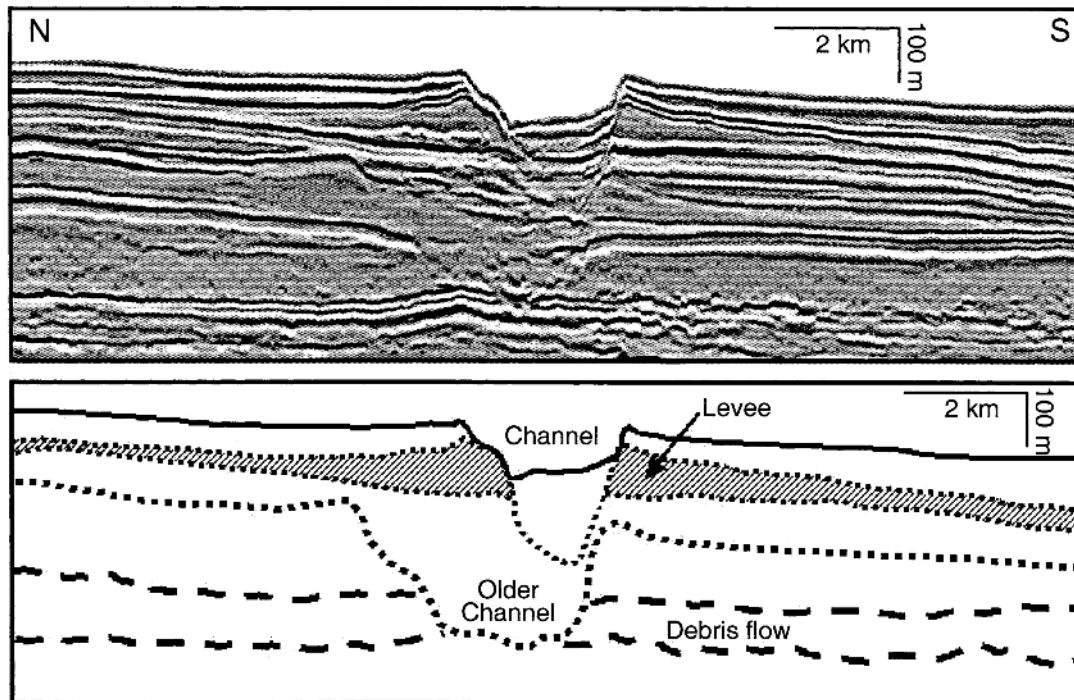
Fig. 1. 10 - Seismic-reflection profile oriented transverse to a high-sinuosity leveed channel in deep-water offshore Nigeria. The levees thin from 110-120 m to less than 5 m over a distance of 10-12 km away from the margins of the channel. From Normark *et al.* (2002).

The *lobe* domain is fed by channelised and unchannelised turbidity flows, and occurs in the distal part of a turbidite system (Fig. 1.9). The lobe domain displays three morphosedimentary domains: proximal, dominated by distributary channels; middle, characterized by the vertical stacking of lens-shaped bodies; and distal, dominated by thin levels of fine sediment (silty clay and clay) (García *et al.*, 2015). Literature contains the term fanlobe that cannot be confused with the lobe domain here described. Fanlobe, defined by Shanmugam and Moiola (1988), represents the sedimentary body integrated by the main leveed channel, channelized lobe, and distal lobe fringe.

In recent years, several attempts have been made to classify TSs in order to provide predictive paradigms for outcrop and subsurface analysis (Reading and Richards, 1994;

Richards *et al.,* 1998). The high variability in geometry, size and internal character of TSs leads to differences in sedimentary architecture. A few turbidite system classifications are found in the literature, being the most widely-used classification that one proposed by Richards *et al.,* 1998 (Fig. 1.11), in which twelve classes were presented based on a combination of the following parameters: mud-rich, mixed mud-sand-rich, sand-rich, gravel-rich, and slope apron, submarine fan and ramp*.*
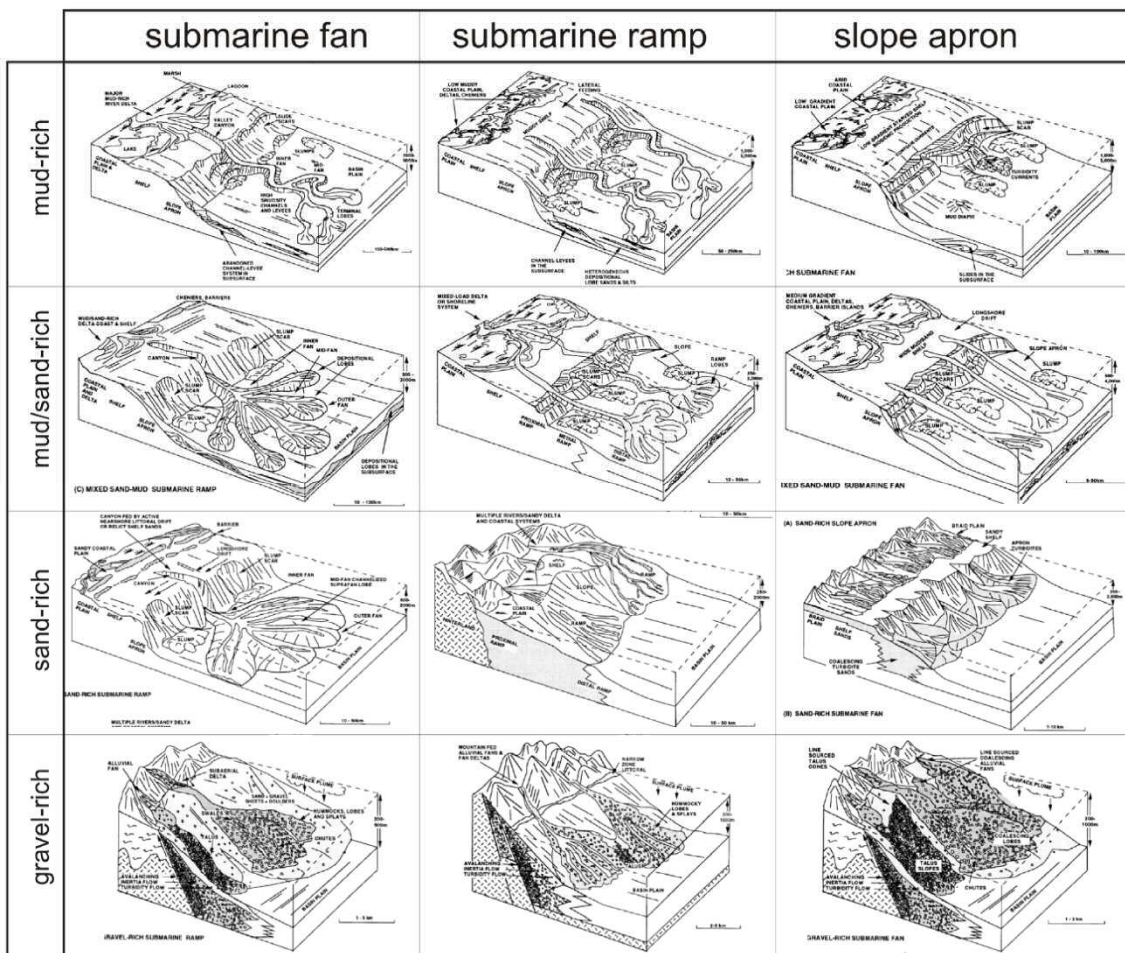
Fig. 1. 11 - Classification of deep-sea clastic systems proposed by Richards *et al.* (1998).

1.3.3. Contourite systems

Contourites are defined as sediments deposited or substantially reworked by the persistent action of bottom currents (Stow *et al.,* 2002a; Rebesco, 2005; Rebesco *et al.,* 2008). There are two different terms defining the association of contourite features: *Contourite Depositional System (CDS)* comprises depositional and erosive features sculpted by the same water mass in the same area (Hernández-Molina *et al.,* 2003, 2006a; Rebesco and Camerlenghi, 2008); *Contourite Depositional Complex (CDC)* is defined by different

CDSs formed by the same water mass in the same or adjacent subbasins (Hernández-Molina *et al.*, 2008b; Rebesco *et al.*, 2014).

Despite the significant role played by deep-sea currents in sedimentation, contourites have been largely overlooked compared to deposits formed by downslope gravitational processes and other continental shelf processes (i.e., waves and storms). This scarcity on contourite studies relates to the wide variety of bottom-current processes that might affect deposition, similarities and interactions with other processes (mostly turbidites), the lack of diagnostic criteria for contourite facies in sediment cores, and the difficulties in identifying contourites in the onshore geologic record (Rebesco *et al.*, 2008, 2014).

Most contourite features are located in the western margin of the largest oceanic basins and extend from the upper slope to the abyssal plains (Rebesco *et al.*, 2014), being associated to shallow (Sivkov *et al.*, 2002; Viana *et al.*, 2002; Verdiccio and Trincardi, 2008; Vandorpe *et al.*, 2011), intermediate (Gonthier *et al.*, 1984; Mulder *et al.*, 2003; Hernández-Molina *et al.*, 2006a; Llave *et al.*, 2007; Hübscher *et al.*, 2010; Toucanne *et al.*, 2012; Roque *et al.*, 2012; Preu *et al.*, 2013) and deep water masses (Heezen *et al.*, 1966; Hunter *et al.*, 2007; Moraes *et al.*, 2007; Shanmugam, 2008; Borisov *et al.*, 2013; Martos *et al.*, 2013). Contourite deposits have also been described in lakes (Ceramicola *et al.*, 2001; Wagner *et al.*, 2012).

Large-scale elongated erosive features and thick, extensive accumulations referred to as contourite drifts can be sculpted by bottom currents; these deposits could also be wiped out by highly intermittent or episodic oceanographic processes (Rebesco *et al.*, 2014). The depositional contourite drifts can be >100 km wide, hundreds of kilometres long, up to 2 km thick and up to 1.5 km in relief. Their dimensions range from ca. 100 km^2 (small patch drifts) to >100,000 km^2 (giant elongated drifts), and locally to ~ 1,000.000 km^2 (sheeted drifts in abyssal plains) (Hernández-Molina *et al.*, 2008b).

The most frequent classification system is based on drift morphology and associated accelerated deep-water filaments (McCave and Tucholke, 1986; Faugères *et al.*, 1993, 1999; Rebesco and Stow, 2001; Rebesco, 2005; Faugères and Stow, 2008; Ercilla *et al.*, 2016). According to this classification, the drifts can be roughly divided into elongated (with two subtypes, detached and separated drifts), sheeted (with two subtypes, abyssal sheets and plastered drifts), channel-related (with two subtypes, axial and lateral patch drifts, and contourite fans), confined, patch, infill, fault-controlled and mixed drifts (Fig. 1.12). However, the different drift types often show intermediate characteristics and must be considered within a continuous spectrum of deposits (Rebesco *et al.*, 2014).
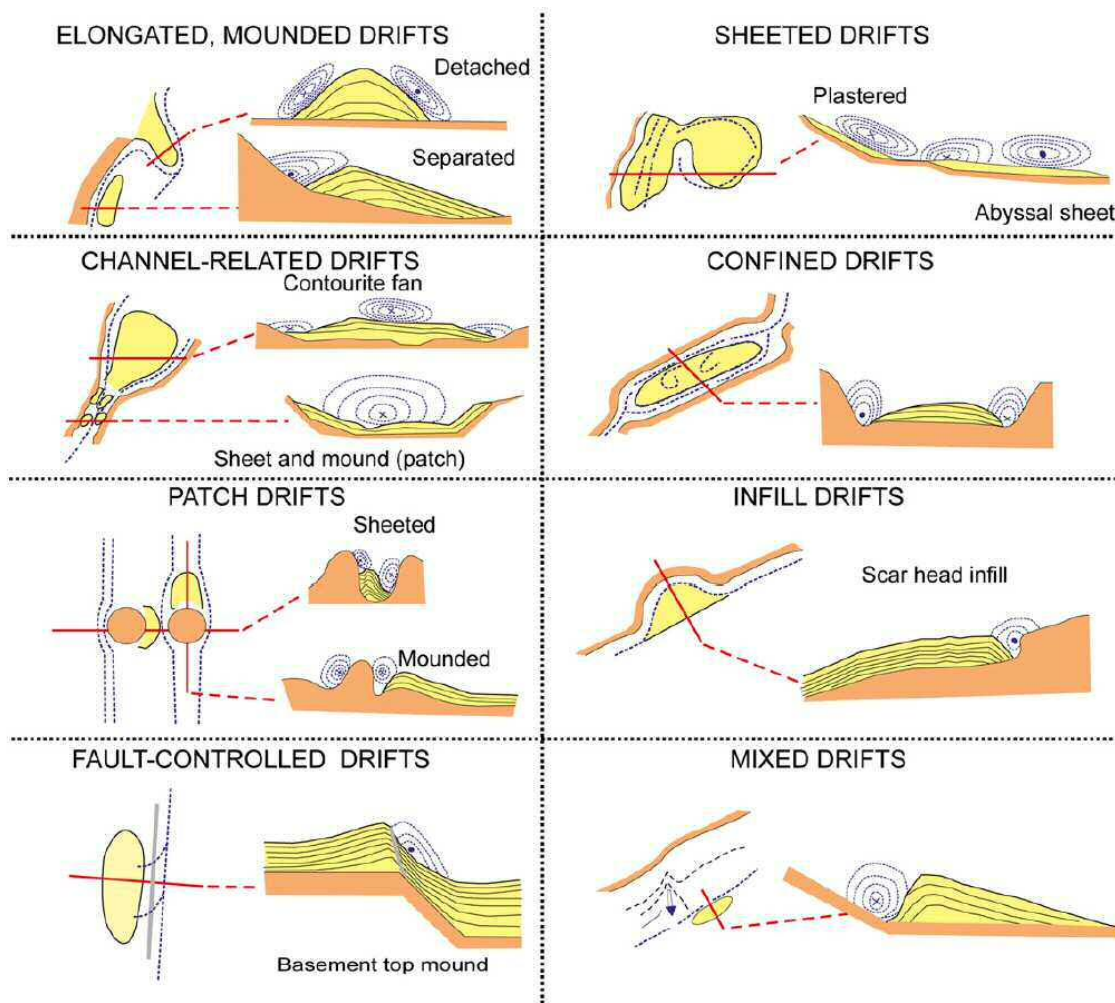
Fig. 1. 12 - Sediment drift types and inferred bottom-current paths. Modified from work by Rebesco (2005) and by Hernández-Molina *et al.* (2008b).

-*Elongated separated drifts* are frequently associated to steep slopes, from which they are separated by a distinct erosional/non-depositional moat (e.g. Faro-Albufeira drift, Stow *et al.,* 2002b) and with alongslope migration downstream of the current flow (Faugères *et al.,* 1999).

-*Elongated detached drifts* typically result from a change in the margin's trend, and are a seaward elongation from the adjacent slope (e.g. Eirik Drift, Hunter *et al.,* 2007) with predominant downslope migration (Faugères *et al.,* 1999) and without a moat separating it from the slope.

-*Sheeted drifts* are characterized by a broad, relatively uniform thickness with very slight thinning towards the margins and a predominantly aggradational stacking pattern (e.g. Gloria Drift; Egloff and Johnson, 1975). The *plastered drifts* are generally located along a gentle slope swept by relatively low velocity currents (e.g. Preu *et al.,*

2013; Rebesco *et al.,* 2013), and also have an alongslope migration downstream of the current flow (Faugères *et al.,* 1999).

-The *channel-related axial and lateral patch drifts* are deposited along a gateway in which currents are constrained and forced to speed up, and *fan drifts* are deposited at the exit the gateway, characterized by random lateral migration (e.g. Vema Channel, Brazil, Mézerais *et al.,* 1993 and Jane Basin, Antarctica, Maldonado *et al.,* 2005). All channel-related drifts have predominant downcurrent migration (Faugères *et al.,* 1999).

-*Confined drifts* are mounded features with limited lateral migration and with distinct moats along both flanks, and develop in between high tectonic (e.g. Lake Baikal, Ceramicola *et al.,* 2001) or volcanic reliefs (Faugères *et al.,* 1999).

-*Patch drifts* are small, irregular drifts characterized by a random distribution controlled by the interaction of the bottom currents with the irregular seafloor morphology (Hernández-Molina *et al.,* 2006b).

-*Infill drifts* typically form at the head of a scar and are characterized by a mounded geometry, moderate relief and limited extension until infilling the topographic depression (Laberg *et al.,* 2001).

-*Fault-controlled drifts* develop either at the base or at the top of a fault-generated relief, which causes perturbations in the bottom-current flow pattern (Rebesco, 2005).

-Last, *mixed drifts* are those that involve the significant interaction of alongslope contour currents with other depositional processes (e.g., Camerlenghi *et al.,* 1997; Hernández-Molina *et al.,* 2009; Llave *et al.,* 2007; Brackenridge *et al.,* 2013).

The many interrelated factors that control drift morphology include basin physiography, tectonic setting, current regime, sediment input, interacting processes and changes in climate and in sea level (e.g., Stow *et al.,* 2008; Mulder *et al.,* 2011; Rebesco *et al.,* 2014), as well as the length of time that these processes have operated (Faugères *et al.,* 1993; Rebesco, 2005; Faugères and Stow, 2008; Ercilla *et al.,* 2008a, 2011; Rebesco *et al.,* 2014).

The erosive contourites comprise three main types of submarine valleys: contourite moats, contourite channels and marginal valleys (Hernández-Molina *et al.,* 2008b; García *et al.,* 2009; Rebesco *et al.,* 2014) (Fig. 1.13), as well as planar erosional features: abraded surfaces and terraces.
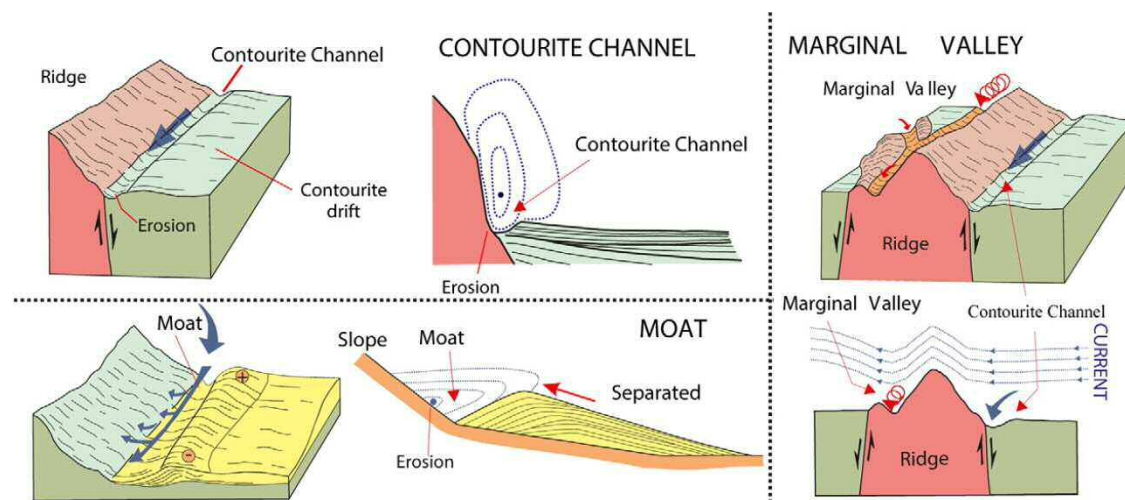
Fig. 1. 13 - Main characteristics of large-scale contourite erosional features. Modified from Hernández-Molina *et al.* (2008b) and García *et al.* (2009), by Rebesco *et al.* (2014).

-*Contourite moats* are channels parallel to a slope or an obstacle (i.e., seamounts) and originate by localized erosion or non-deposition beneath the core of the bottom current, accentuated by the Coriolis force. Moats are characterized by coarser sediment, and appear typically associated to separated and confined drifts (Fig. 1.13, García *et al.*, 2009; Rebesco *et al.*, 2014).

-*Contourite channels* are large (tens to hundreds of km), elongated erosional depressions characterized by the presence of truncated reflections, formed mainly by the action of bottom currents. Contourite channels can exhibit alongslope, sinuous and oblique trends (García *et al.*, 2009; Rebesco *et al.*, 2014).

-*Marginal valleys* (also named scours) are elongated erosional channels generated by a bottom current impinging against and around topographic obstacles (e.g. seamounts, diapiric ridges, and mud volcanoes) (García *et al.*, 2009; Rebesco *et al.*, 2014).

-*Abraded surfaces* are localised areas eroded by strong tabular currents (i.e., contourite escarpments). They are often found in association with scours, sediment waves, dunes and sand banks Hernández-Molina *et al.*, 2011a; Ercilla *et al.*, 2011; Sweeney *et al.*, 2012; Rebesco *et al.*, 2014).

-Last, *contourite terraces* are broad, low-gradient and slightly seaward-dipping, alongslope surfaces produced by the erosion of an interface in the proximal slope and drift deposition in the outer slope (Hernández-Molina *et al.*, 2009; Preu *et al.*, 2013; Rebesco *et al.*, 2014). For that reason, some authors also consider contourite terraces as mixed erosive/depositional features (Preu *et al.*, 2013) (Figs. 1.14 and 1.15).
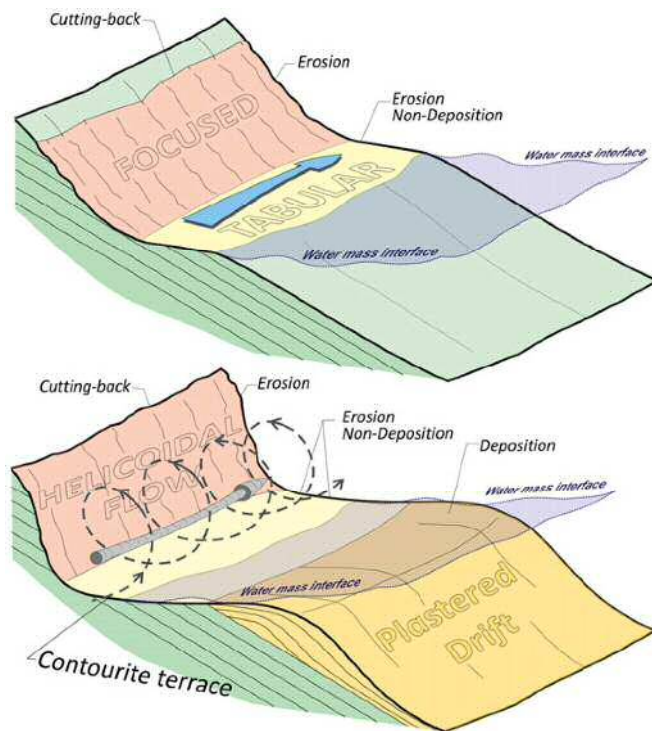
Fig. 1. 14 - Diagram showing how contourite terraces are moulded by the action of alongslope processes. Modified from Preu *et al.* (2013).
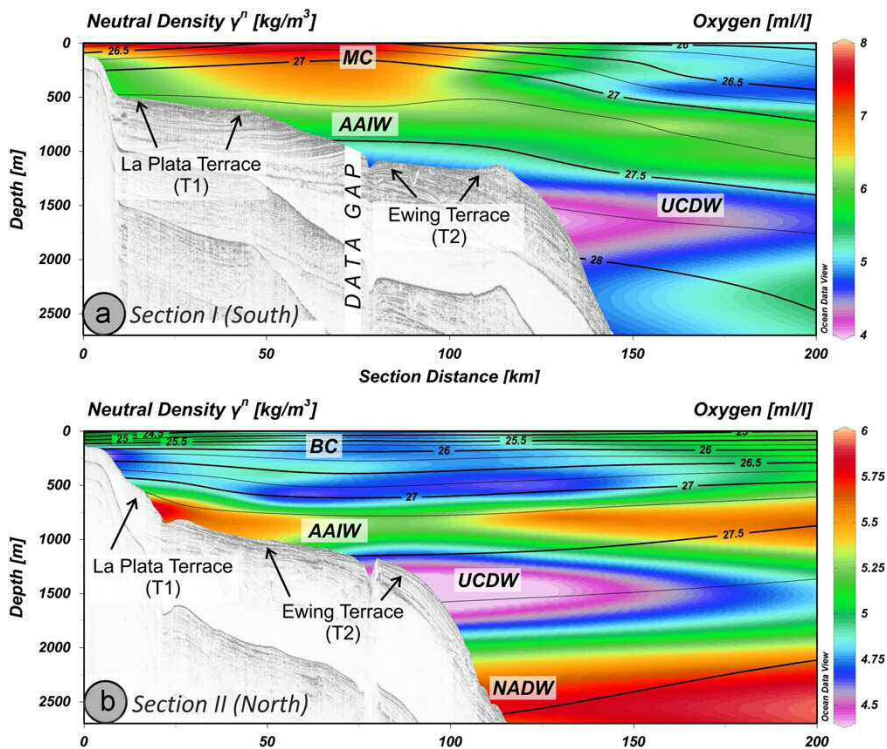
Fig. 1. 15 - Contourite terraces located south (a) and north (b) of the Mar del Plata Canyon, displayed in seismic–hydrographic sections. Legend: AAIW—Antarctic Intermediate Water; BC—Brazil Current; MC—Malvinas Current; NADW - North Atlantic Deep Water; UCDW - Upper Circumpolar Deep Water. From Preu *et al.* (2013).

Contourite features have a worldwide distribution and have been described in all the oceanic basins (Atlantic, Indian, Pacific, Arctic and Antarctic Basins) and the Mediterranean Sea (Rebesco *et al.,* 2014) (Fig. 1.16). The presence of contourites in the Mediterranean Basin has been examined for this work (Table 1.2), including details about their location, depth, morphology and their possible causes. The most striking contourites appear at intermediate water depths, suggesting that the Levantine Intermediate Water is the main bottom current affecting Mediterranean margins (Roveri *et al.,* 2002). Its analysis reveals a higher abundance of contourite features in the Western Basin when compared with the Eastern Basin, but the higher tectonism of the eastern Mediterranean basin could be masking their presence.
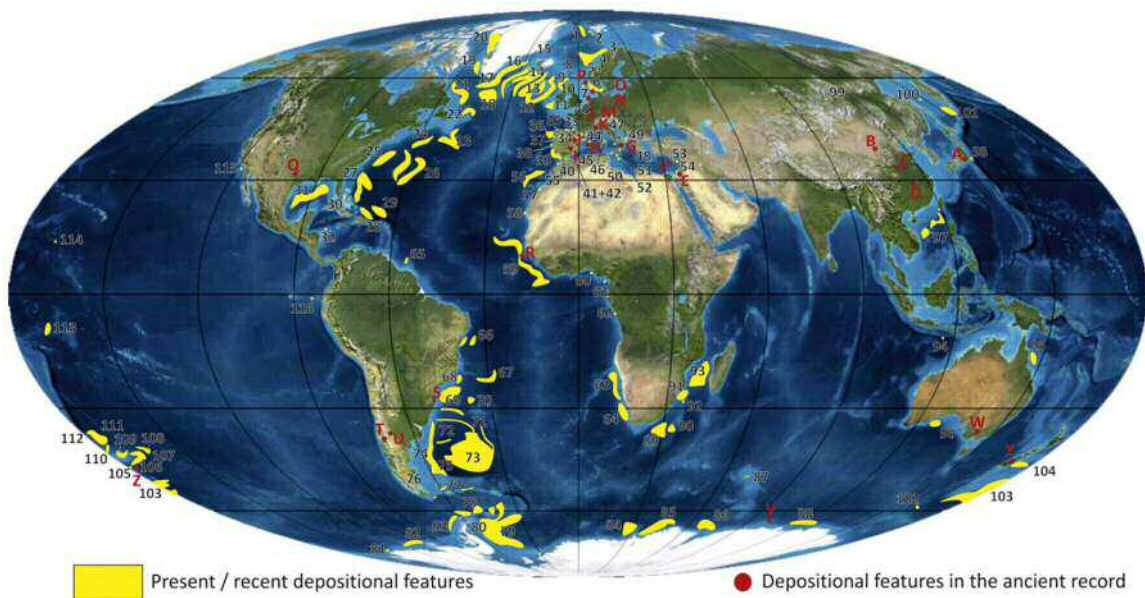
Fig. 1. 16 - Occurrence of large contourite deposits in the present ocean basins or from the recent past (116 yellow areas) and in the ancient sedimentary record (red points). From Rebesco *et al.* (2014)

Contourite deposit(s)	Location	Description	Depth range (m)	Interpretation/Cause	Reference(s)
Ceuta Drift (part of Alboran CDS)	SW Alboran Sea	Elongated mound, 100 km long, 28 km wide, 400 m high, 700 ms thick. Concave erosive feature in the basin floor bounding the drift.	200-700	Results from the action of the Mediterranean deep current redistributing and depositing sediment. At the NW end of the drift this current reaches velocities between 100 and 300 cm/s, causing larger discontinuity surfaces.	Ercilla *et al.*, 2002
Djibouti drifts (part of Alboran CDS)	Seamounts on the Motril Marginal Plateau (northern Alboran Sea)	Drift (mounded, plastered, confined and sheeted) deposits and related bottom-current features (moats, scour marks and terraces) .Up to 300 m thick.	700-950	Interaction of intermediate and deep Mediterranean water masses with the seafloor topography, and especially with the distribution of seamounts	Palomino *et al.*, 2011
Valencia sediment waves	Valencia Slope (Spain)	Several fields of sediment waves. Wave heights from 2 m and up to 50m. Wavelengths between 500-1000m.	250-850	Sculpted by strong near-inertial internal wave activity. The erosive surfaces are apparently linked to eustatic sea level oscillations.	Ribó *et al.*, 2013
Menorca drift	North Minorca (Balearic Islands, Spain)	Elongated separated drift 150 km long, 25 km wide, with sediment waves on the drift (2.5-5 km wavelength, 5-17 m high)	>2000	The Balearic Promontory acts as a topographic barrier and forces the WMDW to flow eastward and southeastward, parallel to the Minorca base of slope.	Velasco *et al.*, 1996 and Frigola *et al.*, 2007
Mallorca CDS	Shelf and shelf edge, SW Mallorca (Balearic Islands, Spain)	Elongate-mounded drift.	150-275	Feature affected by a major fault displacement (150 m). Suggested to result from an offshoot of the Balearic Current, which flows through the Mallorca Channel.	Vandorpe *et al.*, 2011
	Shelf and upper slope, SW Mallorca (Balearic Islands, Spain)	Alongslope drift and upslope drift with pronounced mounded geometry, and sediment wave field (10–15 m high and 400–800 m in wavelength.	Drifts: 250 to 600. Sediment wave field: 170–310.	Probably controlled by LIW (alongslope drift) and Algerian mesoscale gyres (upslope drift). The scar of giant landslides caused the creation of new drift units.	Lüdmann *et al.*, 2012
Rosas shelf channel	Catalan continental shelf (Spain)	Sediment waves and alongslope shelf channel	50-150	Eddy circulation of the southwestward Northern Current over the Catalan continental shelf and dense shelf water cascading	Duran *et al.*, 2014
Pianosa CDS	Corsica Channel (North Tyrrhenian Sea)	Plastered and elongated separated drifts	300	Related to particular sea-bottom morphologies that may accelerate the local deep currents	Marani *et al.*, 1993
		Elongated separated drifts, to plastered sheeted drift (30 km long, < 10 km wide)	300-600	Acceleration due to topographic constriction and slope topography of the northward flowing LIW.	Roveri *et al.*, 2002
		Elongated multi-crested mound morphologies (~10km long) and deep moats	600–750	Contourite drifts could record LIW intensification and enhanced ventilation throughout the last glacial interval	Cattaneo *et al.*, 2014
		Small longitudinal mounded drifts and multi-crested drifts. Small contourite drifts	200-1000	Acceleration of bottom currents with millennial scale variability, possibly linked to sea level changes.	Miramontes *et al.*, 2014
Paola Basin drift	Eastern Tyrrhenian Sea, Calabria Slope	Elongated separated drift (80 m thick) draped by 10 m of sediment.	600-750	Related to particular sea-bottom morphologies that may accelerate the local deep currents	Marani *et al.*, 1993
Cape Vaticano drift	Tyrrhenian Sea	Elongated separated drift, 10 km long, 250-300 m thick	~700	Acceleration due to coastal promontory	Martorelli *et al.*, 2010

Contourite deposit(s)	Location	Description	Depth range (m)	Interpretation/Cause	Reference(s)
Cefalu slope sediment waves	Tyrrhenian Sea, northern Sicily	Buried sediment waves of 30 m of amplitude and 1-1.2 km of wavelength.	~1500	Morphology of causing the intensification of the local circulation pattern.	Marani *et al.*, 1993
Sicily Channel scours	10 Km away from the Sicily Channel sill	Twin scours against the steep walls of a tectonic basin. Up to 70 m of vertical incision and 3 km width.	>900	Bottom currents accelerated in the Sicily Channel sill and focused along the basin walls.	Marani *et al.*, 1993
Sicily Channel drifts	Panterellia Island (Sicily Channel)	Widespread occurrence of rather small elongated separated drifts (up to 10 km long and 3.3 km wide) and erosional elements	~250–750	Northwestward outflow of Levantine Intermediate Water and transitional Eastern Mediterranean Deep Water via the Sicily Channel, strongly influenced by morphological features.	Martorelli *et al.*, 2011,
Messina Rise sediment waves	Ionian Sea	Asymmetric sediment waves, 25-35 m of amplitude and 1.3 km in wavelength.	~2300	Morphology of causing the intensification of the local circulation pattern.	Marani *et al.*, 1993
Shelf-edge contourites in the Gela margin	Gela margin (southern Sicily)	Erosional moats parallel to the shelf edge, buried sediment waves, and low-mounded (occasionally multi-crested) muddy drifts	170-250	Long-term impact of the Mediterranean thermohaline circulation, particularly the upper LIW, as well as off-shelf cascading in the Adriatic margin	Verdicchio and Trincardi, 2008
Gargano drifts	South Adriatic margin	Elongated separated shelf-edge contourite drifts	Upstream: 500-600. Down-stream: 270-500	Dynamical interaction of the LIW and off-shelf cascading of dense shelf waters and acceleration due to coastal promontory	Verdicchio and Trincardi, 2008; Martorelli *et al.*, 2010
Pelagosa sill to Otranto strait drifts	South West Adriatic Margin	Large variety of erosional and depositional features including giant sediment drifts and sediment waves	From the shelf edge, down to 1200	The dense shelf waters follow a slope-parallel direction almost perpendicular to the pre-existing slope canyons.	Foglini *et al.*, 2015
Otranto channel drift	Northern Ionian Sea, Apulian Ridge	Low-relief elongated separated drift (~2-3 Km wide, ~50 m high)	1250-1300	Related to particular sea-bottom morphologies that may accelerate the local deep currents	Marani *et al.*, 1993
Malta-Sicily Escarpment drift	Upper Malta-Sicily Escarpment (MSE)	Plastered drift in the steeper northern wall of a channel	Not described	Sediment fed by down-canyon transport	Micallef *et al.*, 2013a
NE Malta drift	N of Gozo and NE of Malta	Elongated separated mounded drift ~10 km long, 1.3 km wide and 10 m high	130-150	Formed by prevailing south-eastern bottom currents, which are confined to the base of the steep fault-related escarpments	Micallef *et al.*, 2013b
Latakia drift	Latakia Ridge (off Syria)	Erosive channel, fault-related elongated plastered drifts, sediment waves (300-500 m wavelength and 5 m high)	~375-1300	Northward directed contour current along the Latakia Ridge and westward deflection of this current	Tahchi *et al.*, 2010
Ashdod scour moats	Continental shelf off Ashdod and Haifa, Israel	Current-scoured moats associated with small outcropping mounds	90-110	SW to NE shore-parallel sediment transport	Golik, 1993
Other	NE Cyclades Plateau shelf, Aegean Sea	Not described (presence confirmed by seismic-reflection profiles)	Not described	Dense shelf water cascading after strong cold winter winds	Salusti *et al.*, 2015
	Khayr al Din area (Algeria margin)	Sediment waves or contourite drifts	Not described	The area is suggested to have a tectonic origin mixed with hydrodynamic processes	Domzig *et al.*, 2006

Table 1. 2 - Main Mediterranean contourite features described in the literature

Pelagites comprise biogenic oozes and red clays, and lack prominent sedimentary structures, being characterized by occasional faint clay laminations and few flocculates (Garrison, 1981). The pelagic oozes are characterized by a high percentage of biogenic material (>70%) and a clay sized terrigenous component; abyssal red clays are characterized by a low biogenic content (<30%) and a high clay content (>70%)(Stow and Tabrez, 1998). None of them show a significant silt or sand fraction (Stow and Tabrez, 1998). Their accumulation rates are <1cm/ka (Garrison, 1981; Stow and Tabrez, 1998). The pelagic sediments are produced in open ocean surface water, where the production of mineralized skeletal elements is controlled by insolation, nutrient abundance and temperature (Hüneke and Henrich, 2011).

Hemipelagites comprise muddy oozes, calcareous and siliceous muds or marls, as well as organic-rich, volcaniclastic-rich and glacigenic-rich muds (Stow and Tabrez, 1998) that cover ~20% of the present-day sea floor. When deposited in open water oxygenated conditions, hemipelagites are completely devoid of primary sedimentary structures, but mottled and highly bioturbated (Stow and Tabrez, 1998). Hemipelagites can appear in most deep-sea environments, especially those close to continental margins (Garrison, 1981; Stow and Tabrez, 1998) where the higher productivity and the presence of terrigenous sediments in suspension favour a more rapid sedimentation (>1 cm/ka and typically between 5 and 15 cm/ka.; Garrison, 1981; Stow and Tabrez, 1998). On the other hand, when deposited in poorly oxygenated or completely anoxic waters, weak to well-developed parallel lamination is preserved and bioturbation is rare or absent (Kemp 1990; Brodie and Kemp 1994; Stow and Tabrez, 1998). Hemipelagites associated with upwelling systems are characterized by abundant biogenic material and well-preserved organic matter (Stow and Tabrez, 1998), and their potential as source rocks has long been recognized (Garrison, 1981).

2. Regional background: the Alboran Sea

The Alboran Sea is a partly land-locked, east-west oriented Neogene extensional basin (Biju-Duval *et al.*, 1978; Dewey *et al.*, 1989; Platt and Vissers, 1989; Cloething *et al.*, 1992; García-Dueñas *et al.*, 1992; Jabaloy *et al.*, 1993; Estrada *et al.*, 1997, 2011; Comas *et al.*, 1999; Martínez-García *et al.*, 2010, 2013; Do Couto *et al.*, 2016, among many others) of approximately 150 km wide and 350 km long, located in the south-western Mediterranean

Sea (Fig. 1.17). This basin is limited by the Iberian Peninsula (Spanish margin) and north Africa (Moroccan margin), and is bounded by the Algero-Balear Basin in the east and the Strait of Gibraltar in the west (Figs. 1.17C, 1.18).
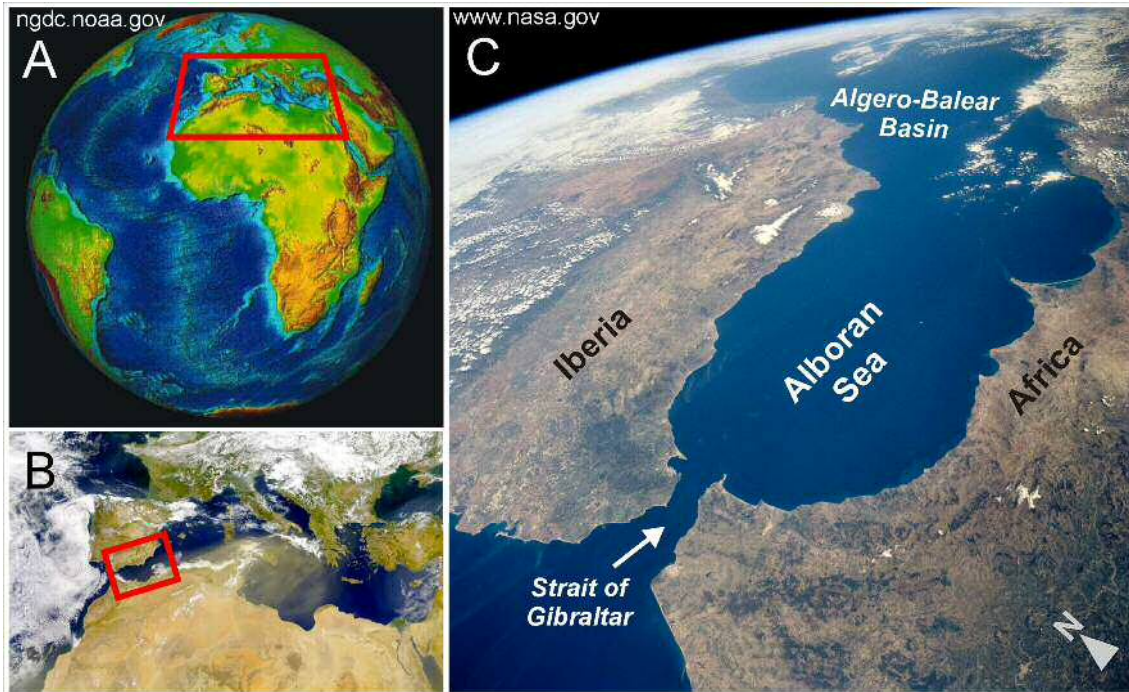
Fig. 1. 17 - Location of the study area in the westernmost Mediterranean Sea. A) Elevation and ocean depth in shaded relief on a spherical globe (ngdc.noaa.gov). B) The Alboran Sea in the context of the Mediterranean Sea (NASA - SeaWiFS). C) Satellite image of the Alboran Sea (www.nasa.gov).

2.1. Geological setting

2.1.1. Geodynamic

The Alboran Sea is located within the Gibraltar Arc System, an arcuate Alpine feature that is part of the Betic-Rif-Tell orogen (Fig. 1.18), which developed since the Early Miocene (Platt and Vissers, 1989; Comas *et al.*, 1992). The Gibraltar Arc is constituted by three main pre-Neogene crustal domains: the Internal Zones (allochtonous continental units displaced westward ca. 300 km, Duggen *et al.*, 2008), the Flysch units (a stack of turbiditic sediments accumulated within the pre-existing oceanic basin) marking the suture zone, and the External Zones, originated on two distinct palaeomargins (Iberia and Africa) (Fig. 1.18). The first two domains show structural continuity north and south of the Alboran Sea, while the later does not display any stratigraphic or structural continuity in the Iberian and African sections of the Gibraltar Arc (Chalouan *et al.*, 2008).
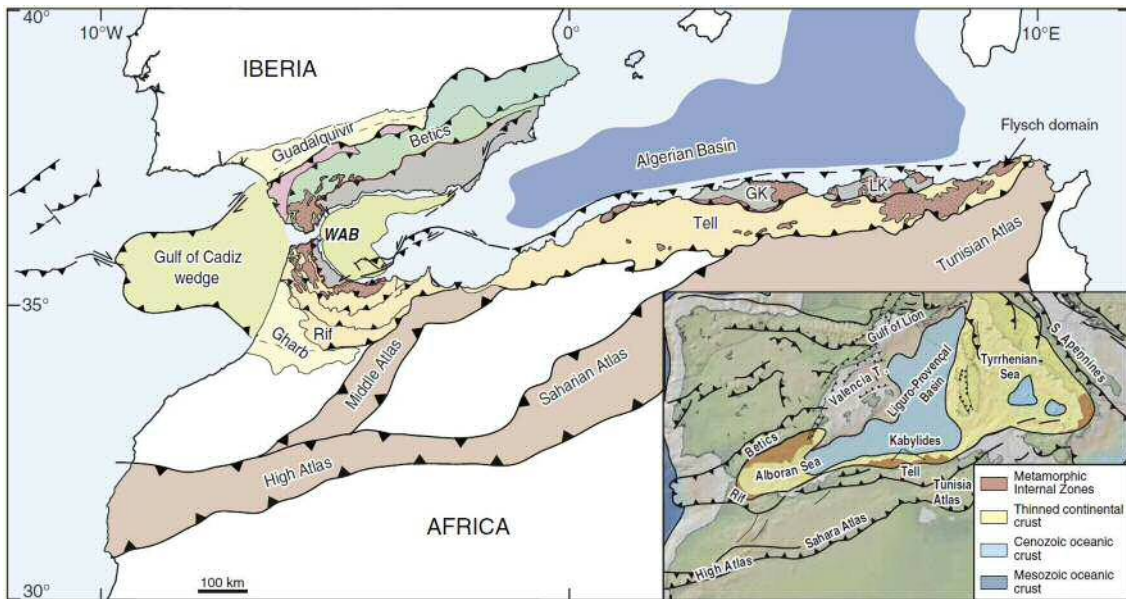
Fig. 1. 18 - Structural map of the southwestern Mediterranean Sea, representing the main tectonic units. The location of the Apennines, Tellian, Rif and Betic fold and thrust belts in the context of the western Mediterranean is represented in the inset map. (GK: Greater Kabylide; LK: Lesser Kabylide). From Do Couto et al. (2016). Legend: WAB, Western Alboran Basin.

The geodynamic evolution of the Alboran Basin, still under debate, is determined by the relative motion between Eurasia and Africa (Dewey et al., 1989) (Fig. 1.18). Extension in the Alboran Sea is contemporaneous with convergence between the African and European plates (Biju-Duval et al., 1978; Dillon et al., 1980; Dewey et al., 1989; Estrada et al., 1997; Duggen et al., 2008). Many authors have tried to explain the specific characteristics of the Alboran Basin such as the eastward crustal thinning transition to the Algerian-Balearic Basin oceanic crust (Comas et al., 1995; Booth-Rea et al., 2007; Ammar et al., 2007; Chalouan et al., 2008) or the N-S symmetry vs. E-W asymmetry (Duggen et al., 2008). The most recent models consider the Alboran Domain as a result from Miocene subduction, collision and slab migration processes (Gutscher et al., 2002; Faccena et al., 2004; Spakman and Wortel, 2004; Jolivet et al., 2008; Do Couto et al., 2016).

The early tectonic evolution of the Alboran Basin was controlled by a regional N-S extensional phase during the Early Miocene, followed in the Middle Miocene by a relatively quiescent period with high sedimentation as a result of the continuous erosion of the uplifted hinterlands, and high subsidence rates due to an underlying dipping crustal slab (Fig. 1.19, Do Couto et al., 2016). A rotation in the direction of extension occurred in the Burdigalian, shifting from N-S to E-W extension. During the E-W extension period, the subsiding Western Alboran Basin (WAB) migrated westwards hundreds of kilometres (Duggen et al., 2008; Do Couto et al., 2016) without enduring significant deformation, moving on the edge of a westward-migrating slab from the Tethys lithosphere (Fig. 1.19,

Do Couto *et al.*, 2016). In the Middle Miocene the collision caused by the westward moving lithosphere slab resulted in the development of the Gulf of Cadiz sedimentary wedge in front of the migrating Arc of Gibraltar, and in the formation of the Guadalquivir Basin (Spanish margin) and Gharb Basin (Morocco margin) (Fig. 1.19, Do Couto *et al.*, 2016). Simultaneously, the subsidence within the arc continued.
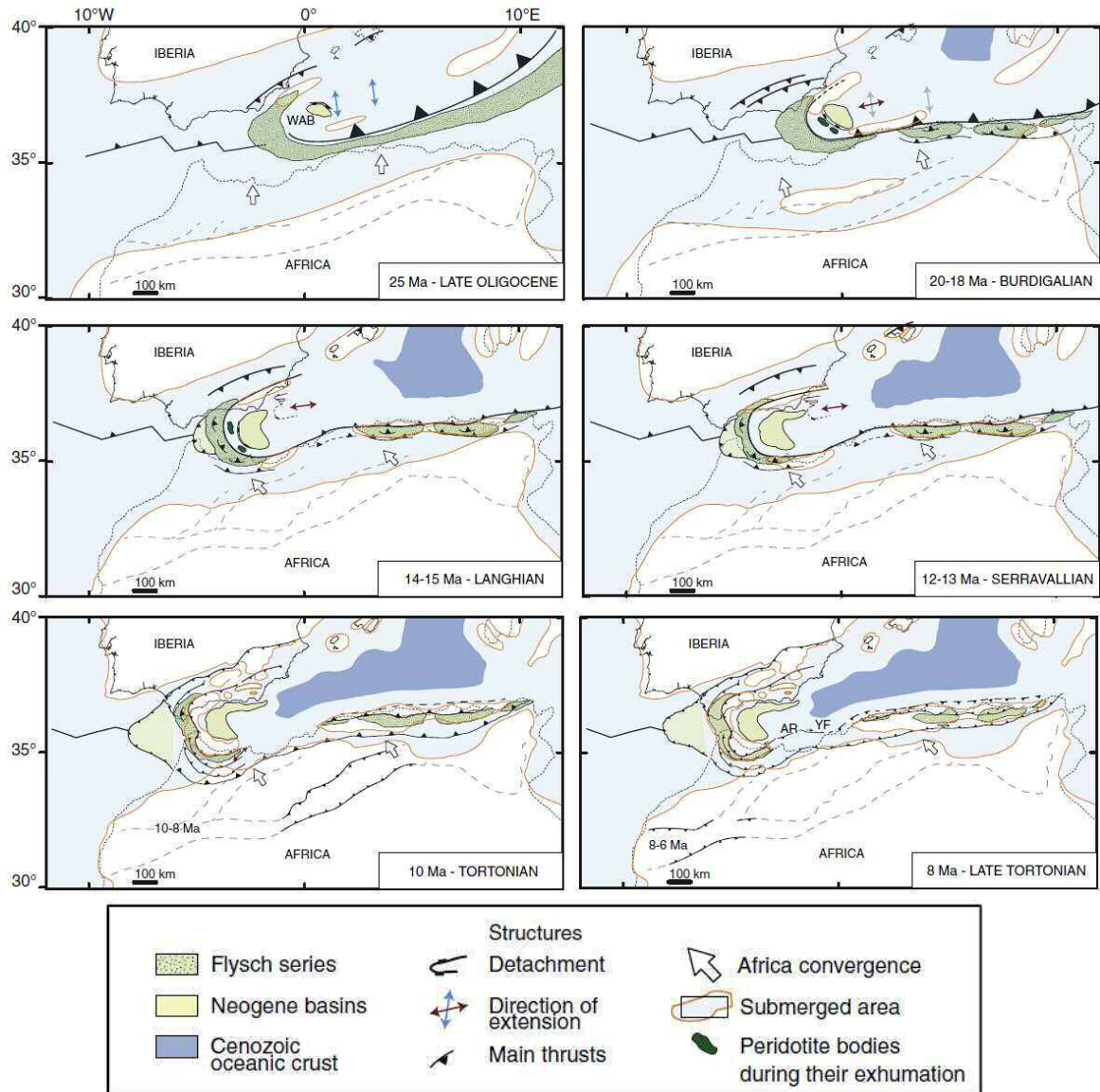
Fig. 1. 19 - Palaeogeographic reconstruction of the formation of the Alboran Domain, from the Early Oligocene to the late Messinian. AR= Alboran ridge; YF= Yusuf fault. From Do Couto *et al.*, 2016.

At the end of the Tortonian, the westward movement of the Alboran Domain nearly stopped with the renewal of N-S compression at ~7 Ma, which was accommodated by strike-slip faults and the progressive uplift of the intramontane basins (Iribarren *et al.*, 2009; Do Couto *et al.*, 2016). As a result of the formation of the Alboran Domain, the

tectonic subsidence of the Alboran Basin varies laterally along the margin from east to west (Docherty and Banda, 1992; Comas *et al.*, 1999), with greater amount of tectonic subsidence in the WAB (Docherty and Banda, 1995). At the end of the Miocene the most important volcanic activity occurred in the Alboran Sea, and formed most of the volcanic seamounts on the present-day seafloor (Hoernle *et al.*, 1999; Duggen *et al.*, 2004, 2008; Ammar *et al.*, 2007; Chalouan *et al.*, 2008).

Post-Tortonian tectonism modified the architecture of the Miocene basins and margins, and formed the present morpho-structure of the Alboran Sea (Comas *et al.*, 1992). Since then, the neotectonic processes have primarily modified the local dimensions of the basin and subbasins, favouring the uplift of the Alboran Ridge and some highs, as well as deforming and faulting the sedimentary record (e.g., Estrada *et al.*, 1997; Ammar *et al.*, 2007; Ballesteros *et al.*, 2008; Martínez-García *et al.*, 2011, 2013).

The Plio-Quaternary deformation of the Alboran Sea has been marked by a change from an extensional to a compressional regime after the earliest Pliocene (Campos *et al.*, 1992; Maldonado *et al.*, 1992; Woodside and Maldonado, 1992; Rodríguez-Fernández and Martin-Penela, 1993; Estrada *et al.*, 1997) and by a change in the orientation of the Eurasian/African plate convergence vector from NW-SE to WNW-ESE (Mazzoli and Helman, 1994; Rosenbaum *et al.*, 2002; Martínez-García *et al.*, 2013) that contributed to the reactivation and uplift of the SW-NE oriented ridges (Estrada *et al.*, 1997; Comas and Soto, 1999; Martínez-García *et al.*, 2013). Subsidence events have also been detected during the Pliocene, when local uplifted and subsided areas coexisted in the Alboran Basin (Comas *et al.*, 1999) and during the Pleistocene, from 2.5 Ma to present day (Comas *et al.*, 1992, 1999; Rodríguez-Fernández *et al.*, 1999).

A more detailed study carried out by Martínez-García *et al.* (2013) revealed that the Plio-Quaternary tectonic history of the Alboran Sea comprises three major shortening phases: a) earliest Pliocene (*ca.* 5.33-4.57 Ma) mainly deforming the Alboran Ridge, although the Yusuf and Al-Idrissi fault zones were also active; b) Late Pliocene (*ca.* 3.28–2.59 Ma), leading to the closure of the gateway that had connected the Southern Alboran Basin (SAB) and WAB until the Upper Pliocene; c) Pleistocene (*ca.* 1.81-1.19) (e.g., Estrada *et al.*, 1997; Martínez-García *et al.*, 2013), characterized by syn-sedimentary deformation and uplift of the Alboran Ridge, extensional to transtensional deformation in the Yusuf Lineament (Mauffret *et al.*, 1992, 2007; Alvarez-Marrón, 1999; Fernández-Ibáñez *et al.*, 2007; Martínez-García *et al.*, 2013), and the northwards propagation of the Al-Idrissi Fault zone (d'Acremont et al., 2014).

2.1.2. Sedimentation

The sedimentation in the Alboran Sea is mostly siliciclastic, originating primarily from rivers, coastal erosion, and dust from the Sahara Desert (e.g., Jiménez-Espejo *et al.,* 2008; Moreno *et al.,* 2002; Lobo *et al.,* 2015). The Spanish and Moroccan bordering margins are quite similar from the point of view of sediment sources. The Alboran Basin is characterized by numerous seasonally steep rivers and streams that erode the Betic Mountains (> 3000 m high) in the Spanish margin and the Rif Mountains (elevations above 2000 m) in the Moroccan margin. Their drainage basins vary between a few to several hundreds of km². The spacing and number of these hydrographic sources are comparable in both borders (Stanley *et al.,* 1975). The Alboran Sea receives sediments from these sources in variable quantities and with different grain sizes. Flood events from the larger rivers result in influential plumes of fine suspended sediments in both margins (Lobo *et al.,* 2006). Contrasting, the shorter rivers and streams remain dry most time of the year and have sporadic torrential regimes, discharging from gravels to silty sediments (El Moumni and Gensous, 1992; Liquete *et al.,* 2005; Lobo *et al.,* 2006; Fernández-Salas *et al.,* 2003, 2007). The regime of rivers and streams are conditioned by climate, which is also comparable in both margins with rainy activity mainly during autumn and winter (Stanley *et al.,* 1975; Liquete *et al.,* 2005; Lobo *et al.,* 2006). Rainfall increases toward the east and in lower elevations in both margins (Stanley *et al.,* 1975).

Two important events affect the sedimentary history of the Alboran Sea: the Messinian Salinity Crisis (MSC, starting at 5.96 Ma, Ryan *et al.,* 1973) and the subsequent opening of the Strait of Gibraltar at approximately 5.33 Ma. During the MSC (which affected the whole Mediterranean Sea), the Alboran Basin was widely affected by subaerial erosion. The later re-flooding after the opening of the Strait of Gibraltar (~5.33 Ma) also eroded the seafloor excavating prominent features such as the Zanclean Channel that crosses the entire Alboran Sea, terraces and escarpments in the WAB (Fig. 1.20, Estrada *et al.,* 2011). The overlying Pliocene and Quaternary stratigraphy has been primarily characterized along the Spanish margin and adjacent subbasins (Campillo *et al.,* 1992; Jurado and Comas, 1992; Ercilla *et al.,* 1992; Pérez-Belzuz *et al.,* 1997; Hernández-Molina *et al.,* 2002), whereas there are few studies of the Moroccan margin (Tesson *et al.,* 1987; Ercilla *et al.,* 2002; Somoza *et al.,* 2012). In those studies, the most common stratigraphic boundaries were defined in Ryan *et al.* (1973) and Campillo *et al.* (1992), primarily along the Spanish margin.
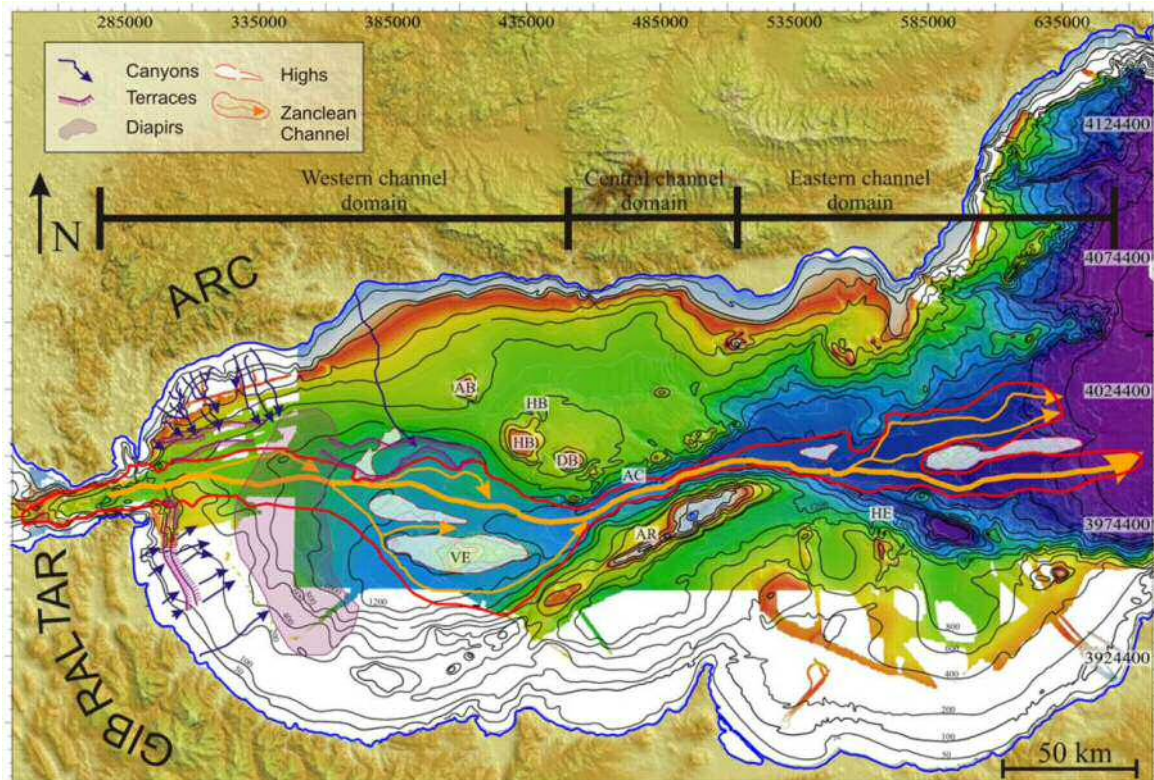
Fig. 1. 20- **Present-day bathymetric map showing the subaerial channels excavated during the Messinian Salinity Crisis and the Zanclean Channel and terraces excavated during the Atlantic Flooding. The location of major highs and other morphological features are also indicated. Legend: *AB* - Algarrobo Bank, *AC* - Alboran Channel, *AR* - Alboran Ridge, *DB* - Djibouti Bank, *HB* - Herradura Bank, *HE* - Habibas Escarpment, *VE* - Vizconde de Eza High (also known as Ibn Batouta Seamount). From Estrada *et al.* (2011).**

Most of the studies about the Plio-Quaternary sedimentary evolution of the Alboran Sea carried out over the last 30 years were focused on the sedimentary evolution of TSs in the Spanish margin (e.g., Alonso and Maldonado, 1992; Estrada *et al.*, 1997; Alonso *et al.*, 1999; Pérez-Belzuz, 1999; Alonso and Ercilla, 2000, 2003) and mass movement deposits on the Spanish margin and seamounts (Casas *et al.*, 2011; Martínez-García *et al.*, 2011; Alonso *et al.*, 2014a, Vázquez *et al.*, 2010), whereas the African margin has remained relatively unexplored (Auzende, 1975; Tesson *et al.*, 1987; Tesson and Gensous, 1989; Ercilla *et al.*, 2002; Somoza *et al.*, 2012). These studies concluded that confined and unconfined downslope processes, combined with a hemipelagic settling, have played a dominant role in outbuilding the continental margins and infilling basins, whereas the bottom currents have only had a local influence contributing to the building of the Ceuta drift in the westernmost Moroccan margin (Stanley *et al.*, 1975; Comas *et al.*, 1992; Alonso and Maldonado, 1992; Ercilla *et al.*, 1992, 1994; Ercilla and Alonso, 1996; Estrada *et al.*, 1997; Alonso *et al.*, 1999; Alonso and Ercilla, 2002; Ercilla *et al.*, 2002).

2.1.3. Present-day physiography

As a result of its origin and tectonic history, the Alboran Sea is nowadays characterized by a complex physiography. Five physiographic domains have been defined in the Alboran Sea: continental shelf, continental slope, base of slope, basins and seamounts (Fig. 1.21).
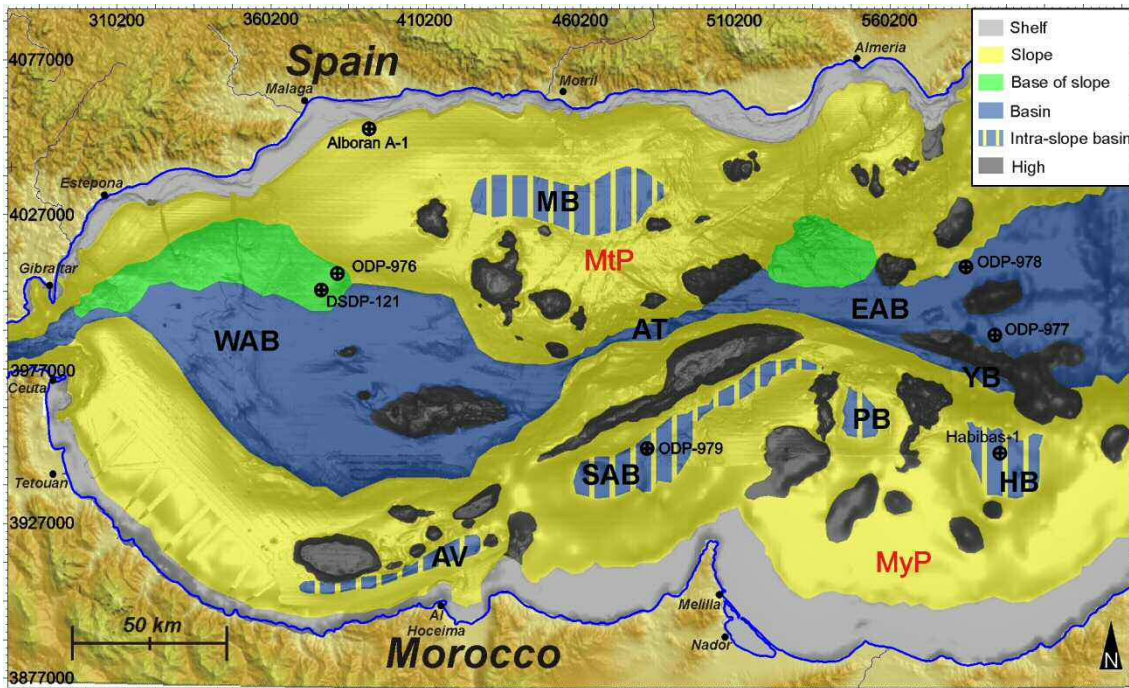
Fig. 1. 21 - Physiographic provinces of the Alboran Sea, showing the shelf, slopes, the two base of slope provinces in the Spanish margin, the basins (AT - Alboran Through; EAB - Eastern Alboran Basin; WAB - Western Alboran Basin; YB - Yusuf Basin), the intra-slope basins (AV - Al Hoceima Valley; HB - Habibas Basin; MB - Motril Basin; PB - Pytheas Basin; SAB - Southern Alboran Basin) and plateaus (MtP - Motril Plateau; MyP - Moulouya Plateau).

The continental shelf extends down to 90–115 m in the Spanish and 100–150 m in the Morocco margin, and is characterized by an abrupt outer limit (except in the easternmost Moroccan shelf, with a poorly defined ramp shape). The continental slopes of both margins are irregular: their dimensions range from 10 to 83 km wide for the Spanish, and 10 to 105 km wide for the Moroccan margin, extending to depths up to 945 m in the WAB and up to 2294 m in the Eastern Alboran Basin (EAB). The slopes also comprise intra-slope basins, among which the SAB, which is 1180 m deep, and the Motril Basin (MB), which is 920 m deep stand out. The other intra-slope basins are the Al Hoceima Valley (AV), the Habibas Basin (HB) and the Pytheas Basin (PB) (Fig. 1.21). The base of slope has been defined in the Alboran Sea due to an important decrease of the slope gradients (<2–0.8º) that mark a transition to a predominantly erosive-depositional environment (Alonso and Ercilla, 2003). This province is locally defined in the western Spanish margin at water

53

depths between 600 and 945 m, and in the eastern Spanish margin at water depths between 1400 and 1850m. The basin domain comprises: a) two main basins: the EAB, which is 1980 m deep, and the WAB, which is 1510 m deep; b) the northeast/southwest-oriented Alboran Trough (up to 1800 m deep); and c) the Yusuf Basin (up to 2340 m deep). Last, several morphologic highs (Fig. 1.22) dot the margins and basins, related to structural and volcanic highs, ridges and plateaus (400 to 1000 m high) (Palomino *et al.*, 2015). Among them, the largest one is the Alboran Ridge that crosses obliquely the Alboran Sea with a NE-SW trend (1750 m high).
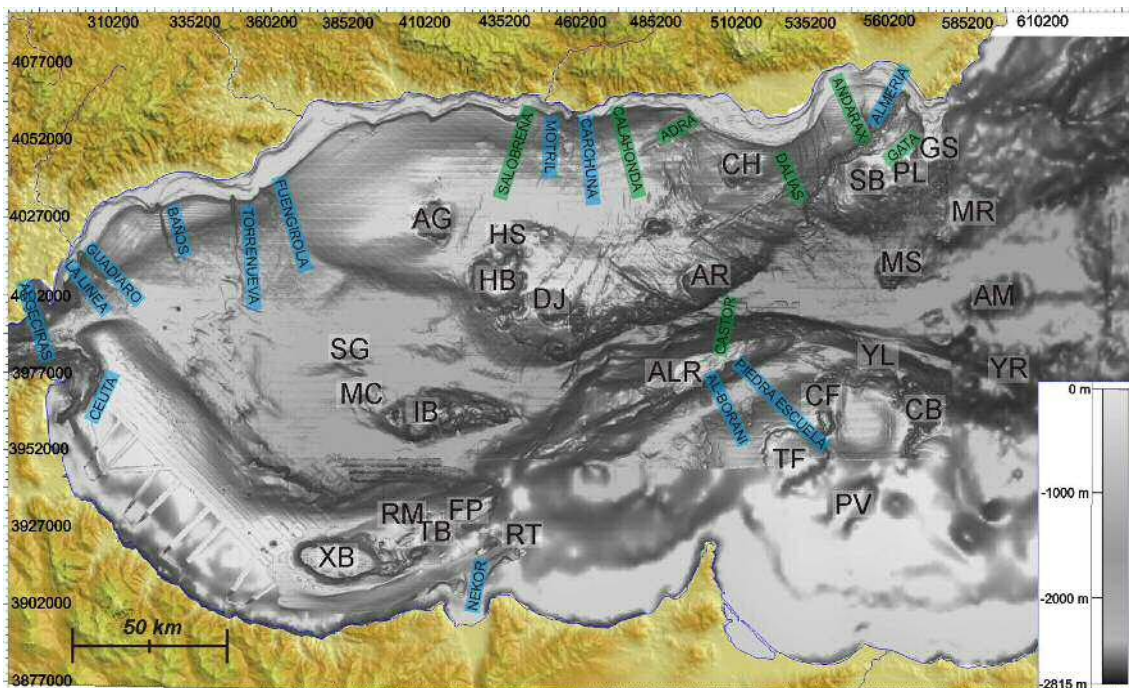
Fig. 1. 22 - Bathymetric map showing submarine canyons (in blue) and gullies (in green) system, as well as the structural highs dotting the margins and basins. Legend: AB - Alidade Bank; AG - Algarrobo Bank; ALR - Alboran Ridge; AM - Al-Mansour High; AR - Adra Ridge; CB - Câbliers Bank; CF - Catifas Bank; CH - Chella Bank; DJ - Djibouti Bank; GS - Cabo de Gata Spur; HB - Herradura Bank; HE - Habibas Escarpment; HS - Herradura Spur; IB - Ibn-Batouta Bank; MC - Maria del Carmen High; MS - Maimonides Seamount; MR - Maimonides Ridge; PL - Pollux Bank; PV - Provençaux Bank; RT - Ras Tarf Ridge; SB - El Sabinar Banks; SG - Segoviano High; TB - Tofiño Bank; TF - Tres Forcas Cape Ridge; XB - Xauen Bank; YL - Yusuf Lineament; YR - Yusuf Ridge.

The slope, base of slope, and walls of some seamounts are indented by submarine canyons and gullies (Fig. 1.22). In the Spanish margin, the main downslope features, from east to west, are: the Almeria System (composed by the Gata, Andarax and Dalias channels and gullies, and the Almeria Canyon), the Adra Channel, the Guadalfeo System (composed by the Calahonda and Salobreña gullies, and the Carchuna and Motril canyons), Fuengirola, Torre Nueva (also known as Calahonda Canyon), Baños (also known as Placer de las

Bóvedas Canyon), Guadiaro, La Linea and Algeciras canyons (Alonso and Maldonado, 1992; Ercilla *et al.,* 1992; Lobo *et al.,* 2008; Vázquez *et al.,* 2015). In the Moroccan margin only the Nekor and the Ceuta canyons are mapped. The northern and southern flanks of the Alboran Ridge are also indented by submarine canyons: the Al Borani and the Piedra Escuela canyons on the southeastern flank (Vázquez *et al.,* 2010, 2015), and the Castor Canyon and gullies on the northeastern side (Vázquez *et al.,* 2010, 2015; Martínez-García *et al.,* 2013). These submarine canyons are V-shaped in cross section and are generally short (< 10 km), with the exception of the 55 km long Almeria Canyon (Alonso and Ercilla, 2003).

2.2. Palaeoclimatic conditions in the Mediterranean Basin and its vicinities

The late Miocene North African climate was characterized by stable conditions (Köhler *et al.,* 2010), much more humid than present climate (Ruddiman *et al.,* 1989; Griffin, 2002; Lihoreau *et al.,* 2006; Gladstone *et al.,* 2007; Köhler *et al.,* 2008, 2010) and with rivers draining into the central Mediterranean (Köhler *et al.,* 2010). A denser vegetation than in present day contributed to withhold the soil and to a reduced dust production (Middleton, 1985; Larrasoaña *et al.,* 2003), favouring the fluvial input to dominate over eolian contributions (Köhler *et al.,* 2010). However, palynological evidences indicate a trend towards drier climate conditions in the same period when considering the whole Mediterranean Sea (Suc and Bessais, 1990), which may have triggered the change in the Mediterranean's water budget and circulation pattern. A major cooling episode associated to an increase in global ice volume has also been reported at 6.26 Ma (Hodell and Kennett, 1986; Hodell *et al.,* 2001).

The onset of evaporite deposition at 5.96 +0.02 Ma (Krijgsman *et al.,* 1999a) is not correlated to major changes in the benthic $\delta^{18}O$ signal, supporting the idea of local climatic conditions favouring the evaporation of the Mediterranean, instead of global climatic forcing (Weijermars, 1988; Martin and Braga, 1996; Krijgsman *et al.,* 1999b, 2001, Hodell *et al.,* 2001).

At a global scale, early Lower Pliocene was characterized by a progressive increase in solar radiation, in the concentration of CO_2 at the atmosphere and in the oceanic heat transport (Rind and Chandler, 1991) caused by changes in the ocean's termohaline circulation (Fauquette *et al.,* 1999). Local pollen studies in south France suggest an overall warm and wet period, with high rainfall that should diminish the salinity in the Gulf of Lion and thus difficult the deep water formation (Fauquette *et al.,* 1999). During the early

Pliocene the wet phase in Africa declined and its climate finally became drier at ~4.6 Ma (Griffin, 2002). The onset of the late Lower Pliocene is characterized by the establishment of high-frequency climatic oscillations modulated by precession at 4.5 Ma (Sprovieri, 1990; Thunell *et al.*, 1991; Aguirre, 2000), as well as the onset of a cold period (Suc and Zagwijin, 1983; Suc *et al.*, 1995; Fauquette *et al.*, 1999) at 3.2-3.1 Ma (Krantz, 1991). In the upper Pliocene (~3 Ma) the European and Mediterranean climate was again warmer, wetter and less seasonal than present-day climate (Haywood *et al.*, 2000). Large and abrupt climate changes (Mudelsee and Stattegger, 1997) ultimately lead to the appearance of the ice caps on the northern hemisphere at 2.6 Ma (e.g., Shackleton *et al.* 1984; Raymo 1994; Tiedemann *et al.* 1994). Due to the changes in the climate patterns, the Sahara region suffered a progressive desertification until the present-day, favouring a Mediterranean-wide increase in the eolian dust (Becker *et al.*, 2005) (Fig. 1.23).
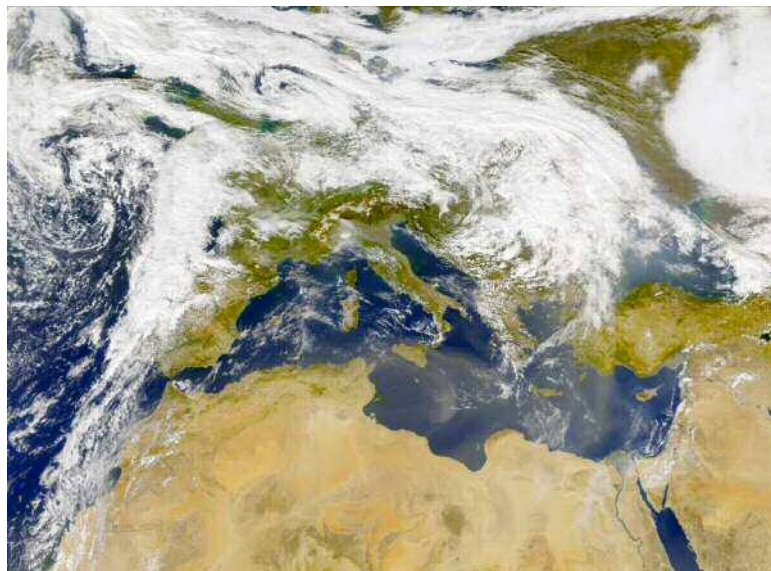
Fig. 1. 23 - Cloud of Saharan dust covering most Eastern Mediterranean Basin. SeaWiFS Project, NASA/Goddard Space Flight Center, ORBIMAGE

The Pleistocene was characterized by even larger climatic oscillations and abrupt changes (Mudelsee and Stattegger, 1997). The glacial cycles show an increasing asymmetry and a slight diminution in their amplitude, and after ~2.2 Ma also show shorter and colder interglacial events (Lisiecki and Raymo, 2005). At 1.4 Ma, a first abrupt decline in 41 ka cycles occurs (Lisiecki and Raymo, 2007). In the Middle Pleistocene occurs the transition from 41 ky to 100 ky glacial cycles (named Mid-Pleistocene Transition, MPT). The MPT is a multiple stage phenomenon that starts at 1.25-1.20 Ma with ~70 ky cycles and progressively increases in intensity until finally stabilizing at 0.7-0.65 Ma with cycles of 100 ky (Head *et al.*, 2008). The MPT also includes the Middle-Pleistocene

Revolution (MPR), which defines the marked prolongation and intensification of the climatic cycles between 900 and 650 ka (Maslin and Ridgwell, 2005). During the MPT, the asymmetry of the cycles and the contrast between warm and cold periods progressively increased (Mudelsee and Stattegger, 1997), with interglacial periods extremely warm and glacial periods extremely cold, favouring a remarkable ice volume variation (Maslin and Ridgwell, 2005). As a result of these intense changes, the Mediterranean area periodically endured a variety of palaeoclimates (cool-wet, cold-dry, warm-moist and warm-dry, Butzer, 1961). The analysis of pollen records, as well as fluvial and eolian inputs in sediment samples recovered in the Alboran Sea have revealed an increase of Saharan wind intensity during Heinrich events and Dansgaard-Oeschger stadial periods in the uppermost Pleistocene (Moreno *et al.*, 2002).

2.3. Oceanographic setting

The Alboran Sea adjoins with the Strait of Gibraltar, where the Atlantic and Mediterranean waters encounter and interact. The transition between these groups of water masses favours the occurrence of strong vertical and horizontal gradients (Millot, 1987; 1999; Cacho *et al.*, 2001; Sierro *et al.*, 2005; Jimenez-Espejo *et al.*, 2008; Rogerson *et al.*, 2010), which have also been documented for the latest Quaternary.

The exchange of water masses in the Strait of Gibraltar is conditioned by the high evaporation rates of the Mediterranean basin (exceeding precipitation and river runoff), being compensated by the inflow of Atlantic Waters. Estimations suggest that about 10% of the inflow is evaporated in the Mediterranean basin, whereas the other 90% is progressively modified until sinking and becoming intermediate and deep Mediterranean Waters (MWs), which ultimately flow towards the Strait of Gibraltar where they mix and become the Mediterranean Outflow Waters (MOW). The average residence time of the Mediterranean Basin is about 50-100 years (Millot and Taupier-Letage, 2005b).

Traditionally, three main water masses have been identified in the Alboran Sea (Parrilla *et al.*, 1986; Parrilla and Kinder, 1987; Millot, 1999): Atlantic Water (AW), Levantine Intermediate Water (LIW) and Western Mediterranean Deep Water (WMDW).

The incoming surface AW is relatively fresh (36-36.5 psu) and cool (16ºC in average), and enters into the Mediterranean Sea in pulses through the Strait of Gibraltar (moving to a maximum w.d. of 150–200 m at up to 1 m/s) and describes two anticyclonic gyres: the quasi-permanent Western (WAG) and the variable Eastern Alboran Gyres (EAG) (Fig. 1.24). In very cold winters the WAG can collapse, allowing the AW to form a coastal jet

flowing along the African shore (Bormans and Garrett, 1989; García-Lafuente, 2002; Periáñez, 2006, 2007; Vargas-Yáñez *et al.*, 2002). The AW progressively increases its temperature and salinity during its eastward movement because of evaporation and mixing (Parrilla *et al.*, 1986), becoming Modified Atlantic Water (MAW) (Gascard and Richez, 1985). The LIW (characterized by its high salinity and temperature) extends to a w.d. of 500–600 m, and preferentially circulates along the Spanish margin and central Alboran Sea with velocities up to 14 cm/s. The LIW presents interannual and decadal variations of its physical characteristics, mainly in temperature (T) or salinity (S) (Brankart and Pinardi, 2001). Last, the WMDW is characterized by its relatively high density (due to its lower temperature) and is mainly restricted to the Moroccan margin (Bryden and Stommel, 1982; Pistek *et al.*, 1985; Gascard and Richez, 1985, among others) and basins below 500–600 m w.d. Although its flow is mostly sluggish, locally can move in pulses with velocities up to 22 cm/s (Gascard and Richez, 1985; Fabrés *et al.*, 2002). On the western Moroccan slope, it mixes locally and seasonally with the AW, forming shelf waters (ShW, Gascard and Richez, 1985).
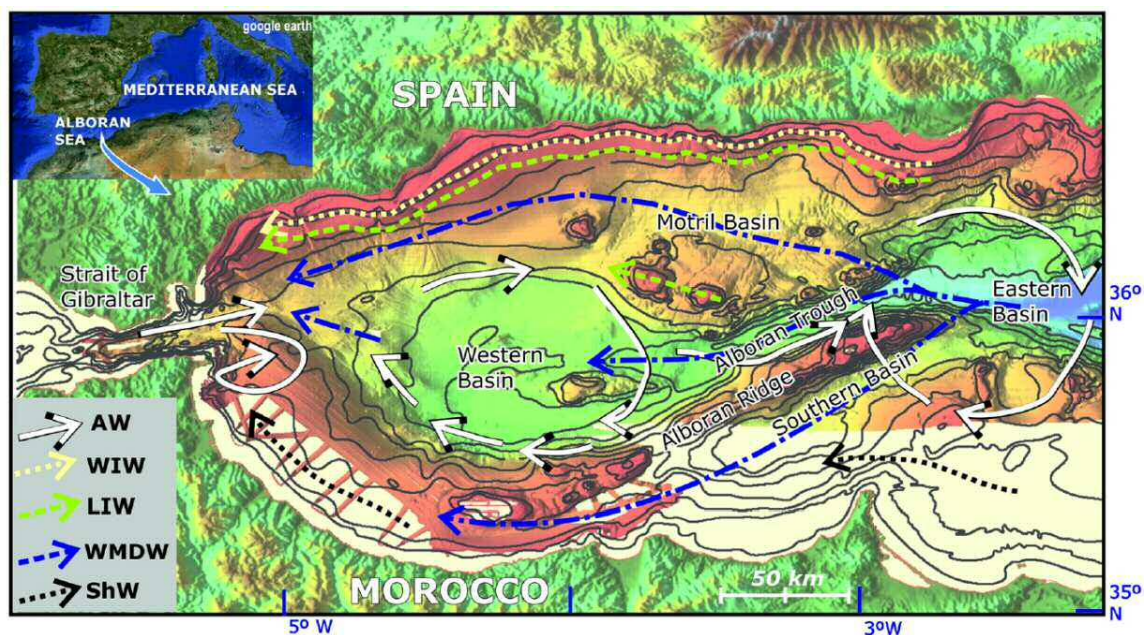
Fig. 1. 24 - Bathymetric map of the Alboran Sea with the present-day regional circulation model. Legend: AW: Atlantic Water; WIW: Western Intermediate Water; LIW: Levantine Intermediate Water; WMDW: Western Mediterranean Deep Water; ShW: Shelf waters (a mixture of AW and WMDW) (Ercilla *et al.*, 2016).

According to recent studies by Millot (2009, 2014) the MWs show a more complex structure and dynamic than the one considered traditionally, comprising four water masses instead of only two (Fig. 1.25). The water masses that were previously disregarded

are Western Intermediate Water WIW- between AW and LIW (characterized by a temperature minimum at 100-300 m), and Tyrrhenian Dense Water –TDW- flowing between LIW and WMDW. This was caused because a) WIW only appears intermittently, sometimes forming eddies detached from the coast and b) TDW shows a poorly-defined core and similar characteristics to that of the overlying and underlying waters (LIW and WMDW), with yearly variations.

The MWs converge at the Strait of Gibraltar, a constriction that leads to the acceleration of the outflowing waters, with exit measured velocities of 100 and 280 cm/s, and the formation of solitons that can reach 200 km into the Western Mediterranean (Heezen and Johnson, 1969; Bryden and Stommel, 1982; Dónde Va Group, 1984; Pomar *et al.*, 2012). The proportion of the various MWs display marked changes at a decadal scale (Fig. 1.25); mesoscale processes and internal tides largely contribute to the mixing of the water masses (Millot *et al.,* 2006) in the western sector of the Alboran Sea.
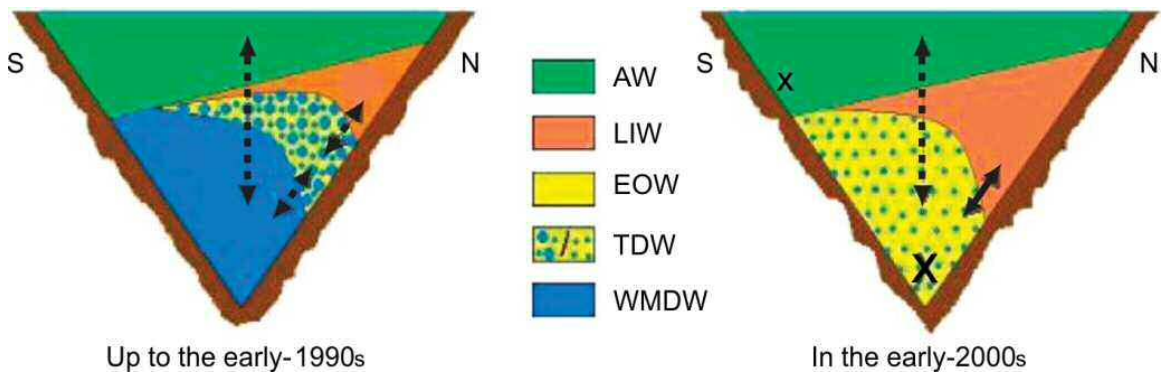
Fig. 1. 25 - Conceptual diagrams illustrating the decadal variations of the water masses in the Strait of Gibraltar. The full arrows represent mesoscale processes; the dashed arrows represent the effect of internal tides. From Millot *et al.,* 2006.

Chapter II - Database and methods

Chapter II - Database and methods

1. Database

This work is based on the analysis of a compilation of four main database types:

- i) Swath bathymetry data.

-ii) Seismic data comprise single- and multi-channel seismic profiles with different resolutions, from very high to low (a few metres to <1m).

-iii) Scientific and commercial wells.

-iv) Sediment cores.

-v) Hydrographic data comprising: Conductivity, Temperature and Depth (CTD) profiles, Acoustic Doppler Current (ADCP) profiles, and EK60 echograms.

These databases were recorded in many different campaigns conducted since the 70s in the Alboran Basin (http://www.icm.csic.es/geo/gma/SurveyMaps). However, six oceanographic cruises carried out in the last years deserve a special mention for providing new and relevant data that allowed to progressively infill the gaps of the former database:

-SAGAS cruise (2008), conducted onboard the research vessel (RV) Hespérides (Fig. 2.1A), and linked to the Spanish SAGAS project (CTM2005-08071-C03-02/MAR).

-SAGAS-Bis cruise (2010), conducted onboard the RV Sarmiento de Gamboa (Fig. 2.1B), and linked to the Spanish SAGAS-Bis project (CTM. 2009/07893-E/MAR).

-CONTOURIBER-I cruise (2010), onboard the RV Sarmiento de Gamboa (Fig. 2.1B) and linked to the Spanish CONTOURIBER project (CTM 2008-06399-C04).

-MARLBORO-I cruise (2011), conducted onboard the RV Côtes De La Manche (Fig. 2.1C) and linked to the French MARLBORO project (CNFC, INSU-2010-2011).

-MONTERA cruise (2012), onboard the RV Sarmiento de Gamboa (Fig. 2.1B) and linked to the Spanish MONTERA Project (CTM 2009-14157-C02-02).

-SARAS cruise (2012), conducted onboard the RV Ramon Margalef (Fig. 2.1D), and linked to the International Eurofleets SARAS project (FP7/2007-2013).
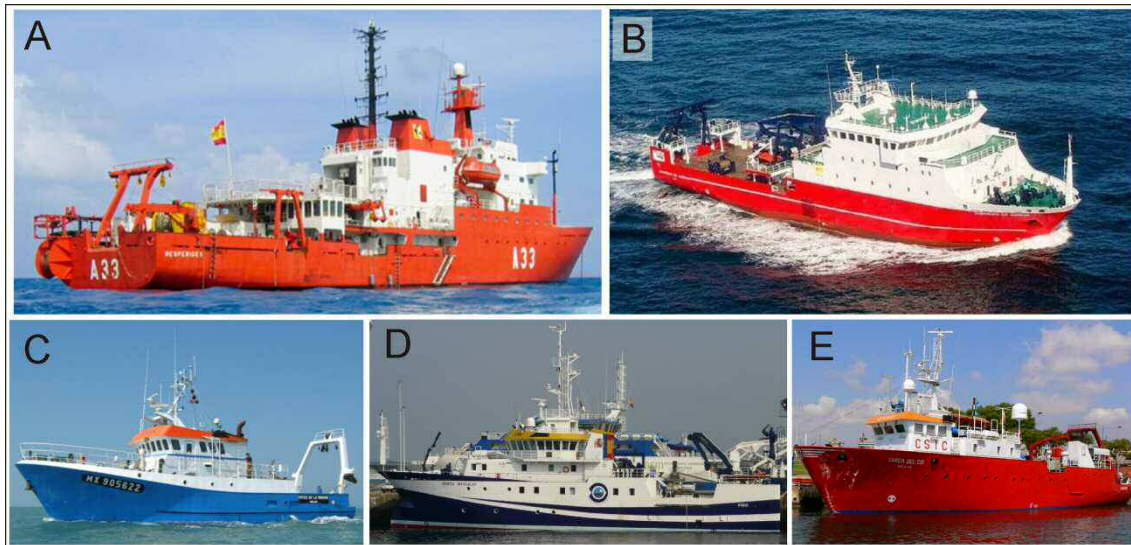
Fig. 2. 1 - Some oceanographic vessels that allowed recording the database used in this work: A) RV Hespérides; B) RV Sarmiento de Gamboa; C) RV Côtes De La Manche; D) RV Ramón Margalef; E) RV García del Cid.

1.1. Multibeam bathymetric database

The *multibeam bathymetric database* consists of compilation of high resolution swath bathymetry data acquired in different campaigns carried out since the 90s in the Alboran Basin, with Simrad EM12 and Atlas HYDROSWEEP DS multibeam echosounders and the Navipac Online Acquisition software (bathymetric data acquired by the Instituto Español de Oceanografía -IEO- for the Spanish Fisher Office, as well as ALBA, MARSIBAL, CONTOURIBER and SARAS cruises). The bathymetry has been gridded to a resolution of 25 m. The gaps in the bathymetric mosaic were completed with the regional bathymetry from the GEBCO Digital Atlas, resulting in a variable resolution mosaic (Fig. 2.2). The integration of these data has allowed the elaboration of a detailed bathymetric mosaic for the Alboran Sea that has been published in Ercilla *et al.* (2016). A KMZ file format with the bathymetric mosaic is available in the supplementary data of that article.

1.2. The seismic database

The main seismic database consists of a compilation of *high-to low-resolution seismic profiles* (single- and multi-channel seismic profiles, >1900 profiles) (Fig. 2.3).

The *very high-resolution seismic profiles* were acquired with TOPAS and Parasound systems simultaneously with other geophysical systems (seismic reflection systems, swath bathymetry) in the recent most campaigns (Fig. 2.3).
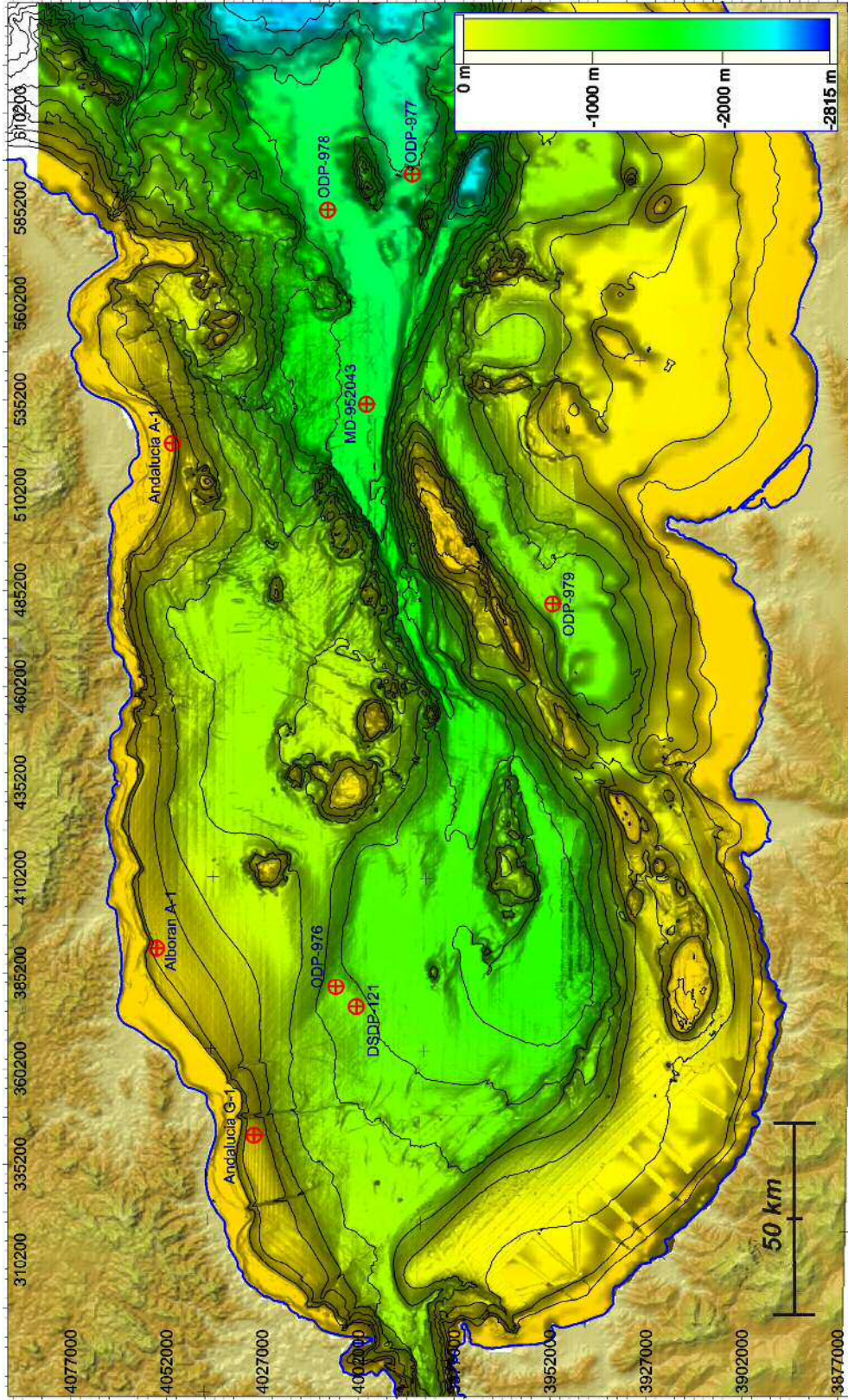
Fig. 2. 2 - Bathymetric map of the Alboran Basin (below 100 m water depth, contour lines are spaced 200m, built with Global Mapper v. 13) showing the scientific and commercial wells used for this work. Several multi-beam bathymetry datasets from the ALBA, MARSIBAL, CONTOURIBER and SARAS projects and the Fishing General Secretary-Spanish Government have been obtained, compiled and integrated for the present study. Data is gridded to a resolution of 25 m.

65
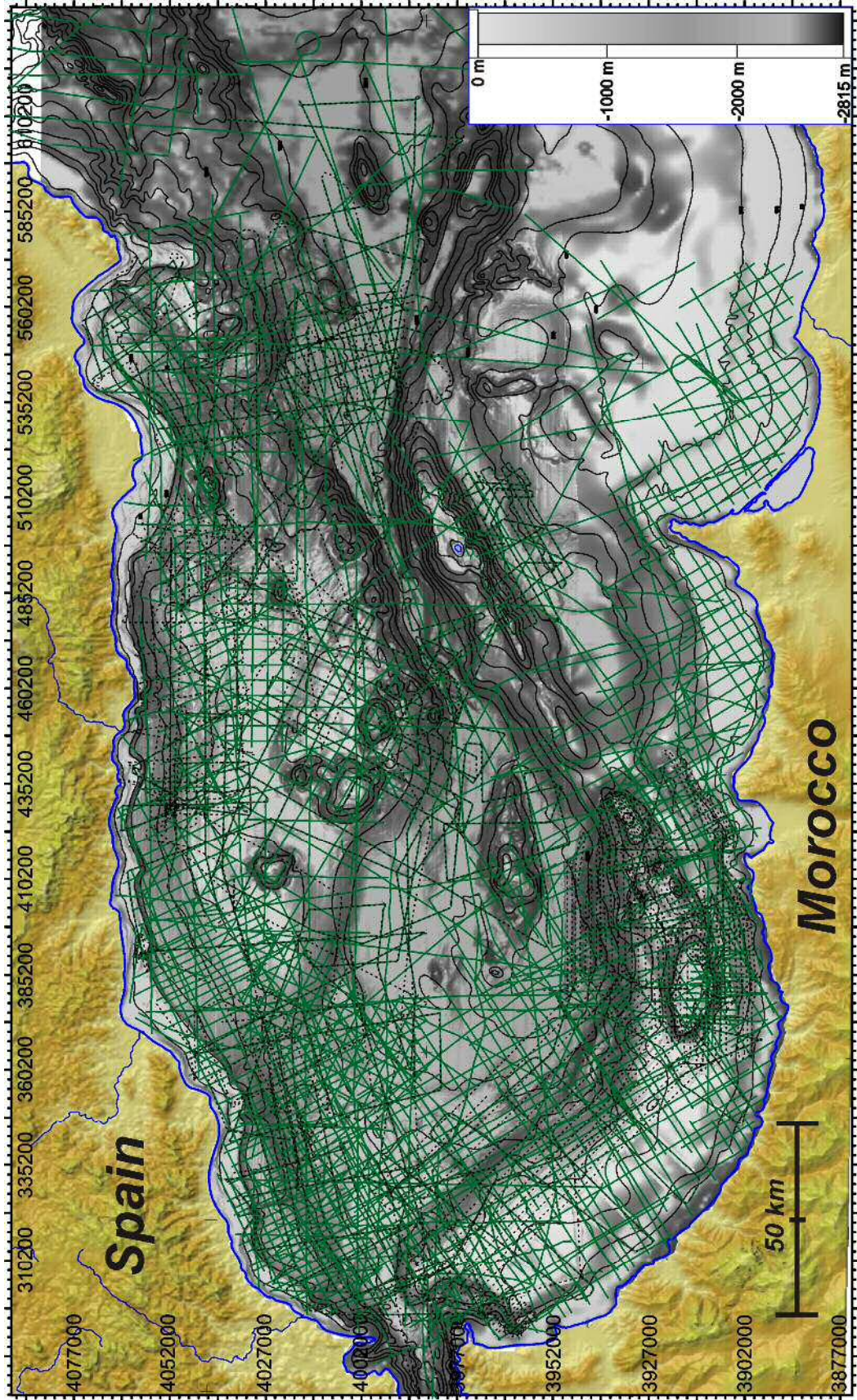
Fig. 2. 3 - Map showing the tracklines of the reflection seismic profiles (in green) and parametric seismic profiles (dashed, in black). The bathymetry map is also displayed in greyscale as background.

66

The *high- to low-resolution seismic data* (single- and multi-channel seismic profile) were obtained in 37 different cruises conducted between 1972 and 2012, comprising sparker, airgun, and multi-channel seismic profiles and extending to various depths and resolutions (Fig. 2.3):

(i) Single-channel seismic profiles (Fig. 2.4A) acquired with Sparker system during four oceanographic cruises (IGME GC-83-2, CEUTA UdP, AL HOCEIMA UdP, and SARAS).

(ii) Single-channel seismic profiles mostly acquired with airgun system (140-620 c.i.) during 12 oceanographic cruises (GC-89-1, GC-90-1, ODP GC-90-1, GC-90-2, TYRO-91, TTR-12, MARSIBAL-Project1, MARSIBAL 2006, MARGUA06, SAGAS Bis, CONTOURIBER-1 and MONTERA12-AL) (Fig. 2.4B).

(iii) Multi-channel seismic profiles also acquired mostly with Airgun system, recorded in 21 oceanographic cruises (RAY-72, IGME EAS-74, AS, AG, ALM, ALB, MC-75 Spain, MC-75 Morocco, MO-75, BRPM-79, 82AD, S-83, TALB, IZD, CONRAD, TSH, He-91-3, ESCI-ALB, CAB-00, CAB-01 and MARLBORO-1) (Fig. 2.4C).

These seismic profiles have been compiled in the framework of several Spanish and international research projects in collaboration with French and Moroccan institutions, as well as from commercial hydrocarbon exploration projects. The seismic profiles that comprise the database are available online at the Archivo Técnico de Hidrocarburos (*https://geoportal.minetur.gob.es/ATHv2/welcome.do*), the Institut de Ciències del Mar (ICM—CSIC) (*http://gma.icm.csic.es/sites/default/files/geowebs/surveymaps/index.htm*) and the Instituto Geológico y Minero de España (IGME) (*http://info.igme.es/catalogo/*) databases.

Although the acquisition and processing techniques were similar for all the different datasets, different software specifications, parameters and equipment (including different sources) were used in each oceanographic cruise.
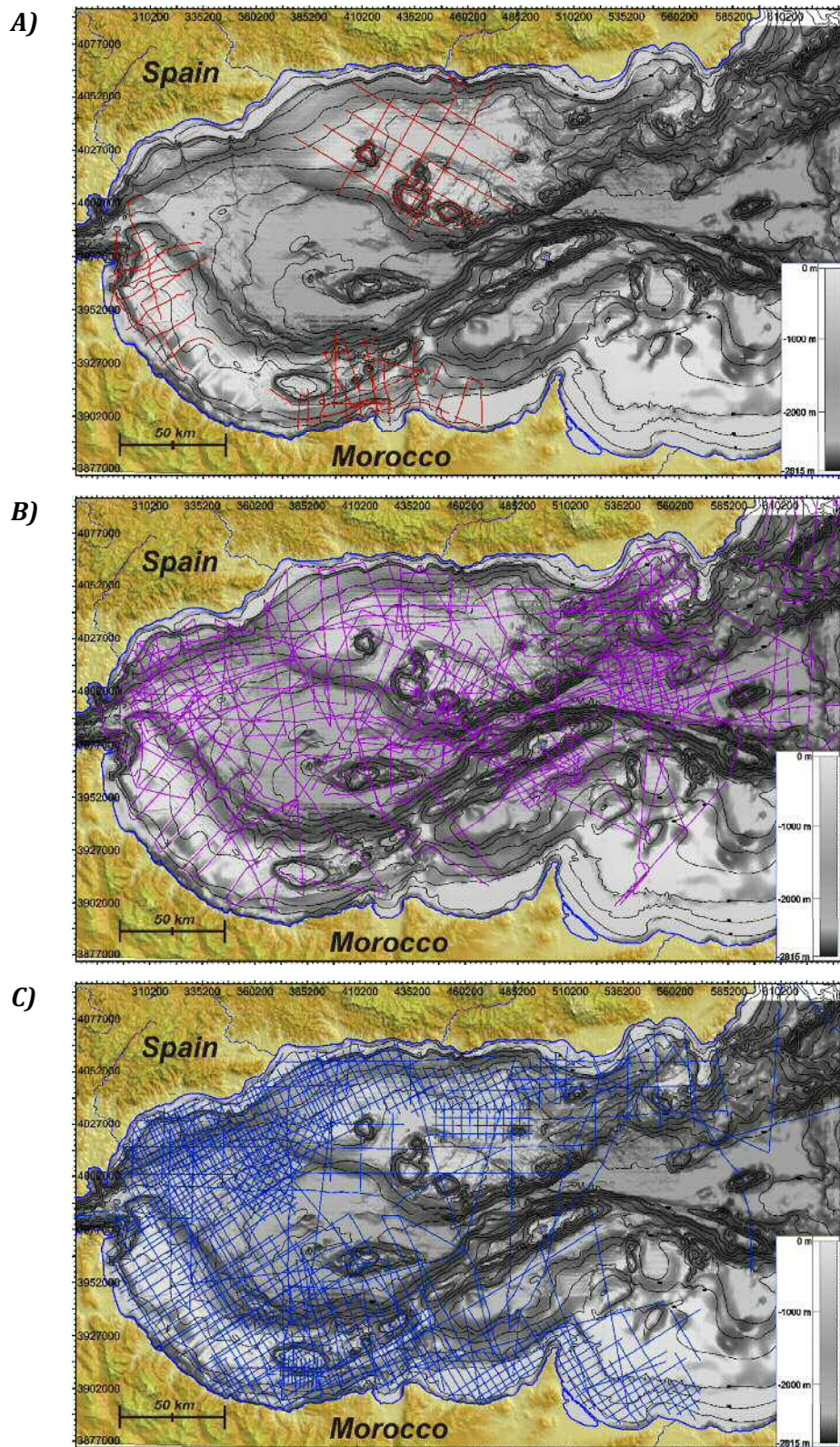
Fig. 2. 4 - Bathymetric map showing the tracklines of the seismic database: A) single-channel sparker seismic profiles, B) single-channel airgun seismic profiles, and C) multi-channel seismic profiles.

1.3. Scientific and commercial wells

The wells have been used for the establishment of Pliocene and Quaternary chronostratigraphic framework. The scientific wells for this work are the DSDP Site 121 drilled by the Deep Sea Drilling Project (DSDP) during Leg 13 (Ryan *et al.*, 1973), and the ODP Sites 976-979 drilled by the Ocean Drilling Program (ODP) during Leg 161 (Comas *et al.*, 1996, 1999). In addition, another scientific well (MD-952043) as well as commercial wells drilled during oil and gas exploration programs (Andalucía-G1; Andalucía-A1; Alboran-A1 and Habibas 1) have been used (Fig. 2.2). The chronostratigraphic framework for the Western Mediterranean adapted by Siesser and de Kaenel (1999) has been applied.

1.4. Sediment cores

The database of sediment cores (up to 5 m long) comprises seventeen cores recovered in some TSs located in the WAB and MB. The following sediment cores have been analysed: K-17, K-18, K-19 and K-20 piston cores and GDR5, GDR8 and GDR12 gravity cores in the Guadiaro TS; the K-23 piston core in the Ceuta Canyon mouth; the TG8, TG10, TG11, TG13, TG15a and TG15b gravity cores in the Motril Canyon, and the MTL16, MTL17 and MTL18 gravity cores in the Calahonda TS (Fig. 2.5). The sedimentological results of these cores are mostly available in Alonso *et al.* (1999), and a few of them in Pérez-Belzuz (1999) and Lebreiro and Alonso (1998).
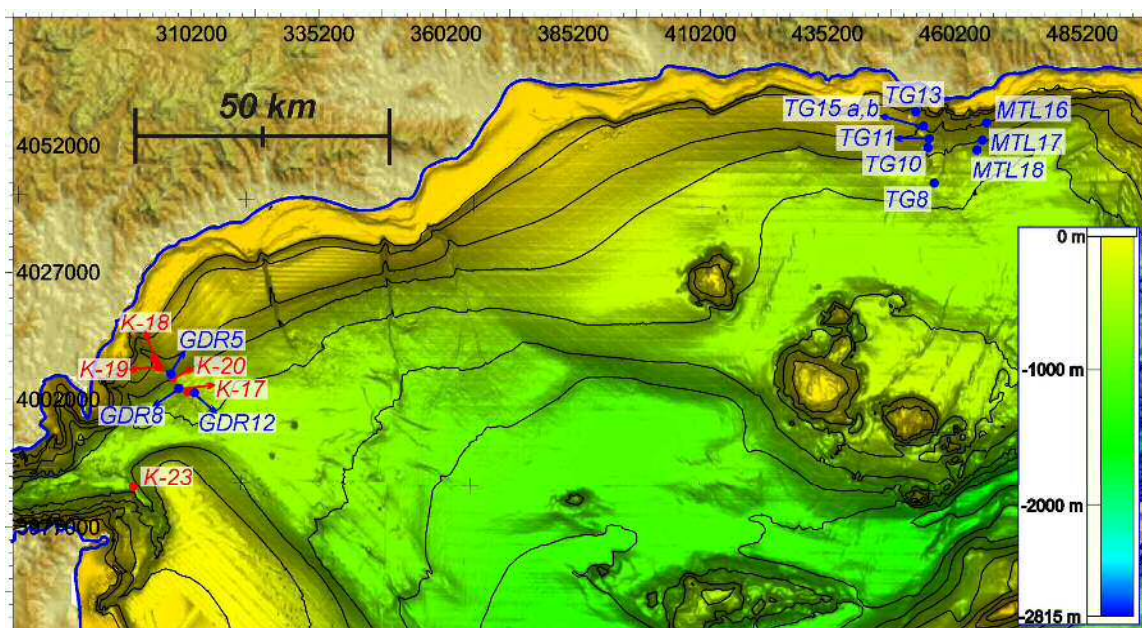
Fig. 2. 5 - Bathymetric map showing the location of the five piston cores (in red) and seven gravity cores (in blue) analysed in this work.

1.5. Hydrographic database

Three types of hydrographic database have been compiled for this study: Conductivity, Temperature and Depth profiler (CTD), Acoustic Doppler Current Profiler (ADCP) and EK60 echograms.

A large dataset of comprising more than 3000 *CTD profiles* registered from 1975 to the present day was downloaded from the open-access Sea Data Net service (*http://www.seadatanet.org/Data-Access*) and other platforms (e.g., the Medocean II database, *http://odv.awi.de/en/data/ocean/medatlasii/*) (Fig. 2.6).

Several profiles recorded by a hull-mounted *ADCP* during recentmost oceanographic campaigns in the Alboran Sea were also analysed (Fig. 2.6). The velocity profiles provide the module and direction of the different layers of the water column down to 700 m w.d.
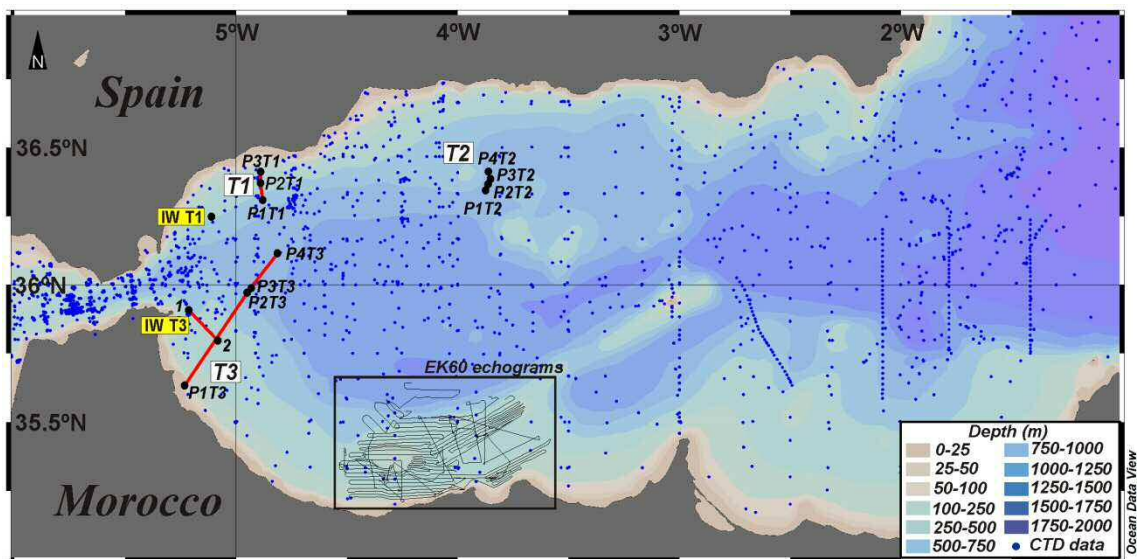
Fig. 2. 6 - GEBCO bathymetric map showing the location of the hydrographic database of this work: CTD profiles are represented by blue points; ADCP stations with vertical velocity profiles are represented by black points (stations P1T1, P2T1 and P3T1 on terrace T1, stations P1T2, P2T2, P3T2 and P4T2 on terrace T2 and P1T3, P2T3, P3T3 and P4T3 on terrace T3); ADCP transects are represented by red lines; ADCP transects or stations in which internal waves were detected in backscatter intensity plots are marked with yellow labels. The EK60 echograms recorded in the Morocco margin are represented by thin black lines.

Last, *EK60 echosounder data* were acquired during recentmost campaigns of the Alboran Sea. They provide hydrographic information of anomalies in the water column such as turbulence, turbidity, water mass interfaces or internal waves.

2. Data acquisition systems

2.1. Description of the multibeam bathymetric systems

The *multibeam bathymetric system* is based on the emission of a series of narrow acoustic pulses arranged in a fan and directed towards the seafloor (Fig. 2.7A). This echosounder is mounted in the hull of the vessel (Fig. 2.7B) and measures the two-way travel time (twtt) that requires the sound pulse to travel from the echosounder to the seafloor and reach the vessel again after being reflected in the seafloor. This information is automatically corrected and converted to depth using the sound velocity of the sea water that depends on water temperature and salinity; this data is registered using CTD and eXpendable Bathy-Termographs (XBT) profilers that are systematically deployed during the bathymetric survey. The modern systems operate with an acoustic frequency of 13 kHz and a power of 12 kW, and emits up to 141 equi-angular and equidistant acoustic beams reaching a maximum angle of 120º. The acoustic footprint (or swath coverage) depends on the depth of the seafloor and the beam angle, but typically is ~3.5 times the seafloor depth (20 km maximum).
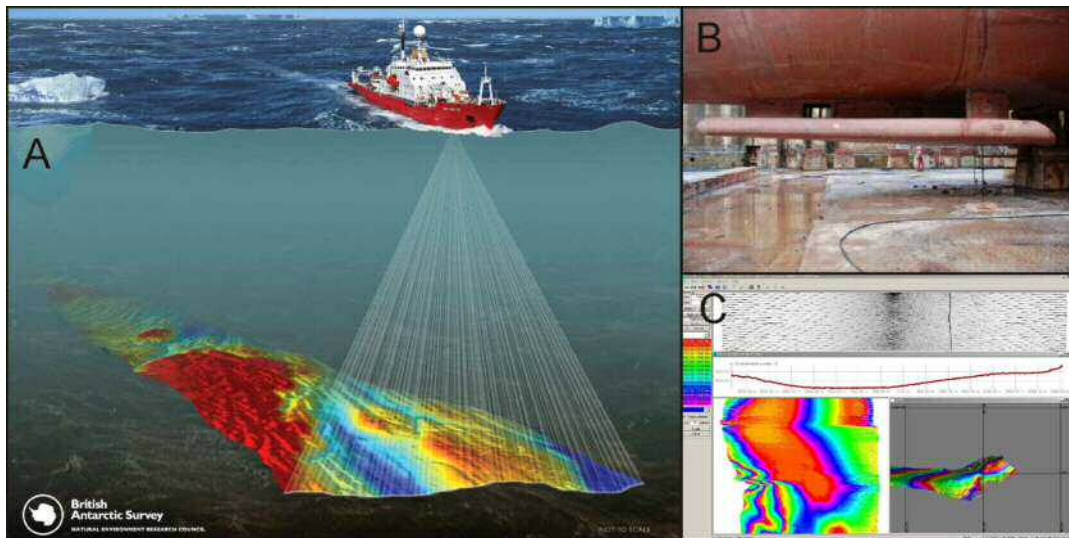
Fig. 2. 7 - A) Scheme of the multibeam bathymetric system showing the acoustic pulses and a bathymetric map of the seafloor (modified from the British Antarctic Survey). B) Side view of the 8 m gondola installed at the hull of the RV Sarmiento de Gamboa, including MB Atlas Hydrosweep DS-3 and MB Atlas Hydrosweep MD-3 echosounders, as well as the Atlas Parasound. C) Capture of the Navipac Online Acquisition software.

Multibeam data are displayed in real-time onboard with the Navipac Online Acquisition software (Fig. 2.7C), but require later processing with specific software (i.e., NEPTUNE, CARIS, CARAIBES) to apply other calibrations and corrections (i.e., tide, wave height,

motion of the vessel...). To position the soundings correctly, the multibeam echosounders are also connected to the onboard positioning system, recording data such as heading, velocity and motion. Unlike older techniques (leadline, single beam), multibeam swath bathymetry provides 100% seabed coverage, allowing the mapping of the seafloor with precise dimensions and geometry, as well as 360º view of the sedimentary systems and the structural elements. For that reason, swath bathymetry is considered nowadays a key tool for geological interpretation based on seismic records.

2.2. Description of the seismic systems

The seismic systems comprise three main components: the source of energy, the reception system, and the acquisition and recording system. The resolution and penetration of a dataset will depend on the energy of the source and the frequency of the resulting wave. In general, low penetration systems will result on high resolution, whilst high penetration systems will provide lower resolution.

2.2.1. High-resolution seismic system: subbottom parametric systems

The principle of the subbottom parametric system consists of the transmission of two primary sound signals at close frequencies (16 and 20 kHz for the TOPAS, 18 and 39 kHz for the Atlas Parasound). The simultaneous transmission of two sound signals at nearby frequencies generates a secondary low-frequency sound signal ranging 0.5 to 6 kHz (typically 3.5 kHz). The sound pulse of the parametric systems penetrates below the seafloor and refracts on the boundaries between sediment with different densities, providing excellent vertical resolution of shallow unconsolidated sediment due to the low frequency of the sound signal. The Simrad TOPAS (Topographic Parametric Sonar) and Atlas Parasound system are the two high resolution systems used in this work:

The Simrad TOPAS system consists of a directional multiple transducer (16 independent transducers) for transmission and reception of the sound pulse. The acoustic beam width ranges from 4 to 6˚, depending on the frequency, which allows obtaining higher penetration and resolution (https://www.km.kongsberg.com/). The penetration depends on the water depth and sediment characteristics, and typically reaches 50-80 m (https://www.km.kongsberg.com/, Webb, 1993). The TOPAS system is electronically stabilized to correct pitch, roll and heading of the vessel, and the returning wave signal is processed automatically (using TOPAS® software), allowing real-time visualization onboard of the vessel of the seafloor structures. However, it is also possible to re-process the raw data after the cruise.

The *Atlas Parasound system* consists of a single hull-mounted small transducer for the emission of the sound signal, which generates a narrow beam directed to the seafloor. Horizontal resolution can be improved by increasing the emission rate or by reducing the speed of the vessel. The transmitted signals were Chirp and CW type (1.5 kHz). This system is also connected to auxiliary sensors (position, sound velocity, motion of the vessel) electronically stabilized to correct all these parameters. Atlas Parasound system also allows real-time visualization of the data onboard and re-processing.

Although the maximum theoretical penetration of the Atlas Parasound system is 200 m under optimal conditions, a comparison with TOPAS profiles in the same area and with the same vertical distribution of sedimentary bodies reveals that the Atlas Parasound system provides lower penetration and resolution than the TOPAS system (Fig. 2.8) (Alonso *et al.*, 2010).
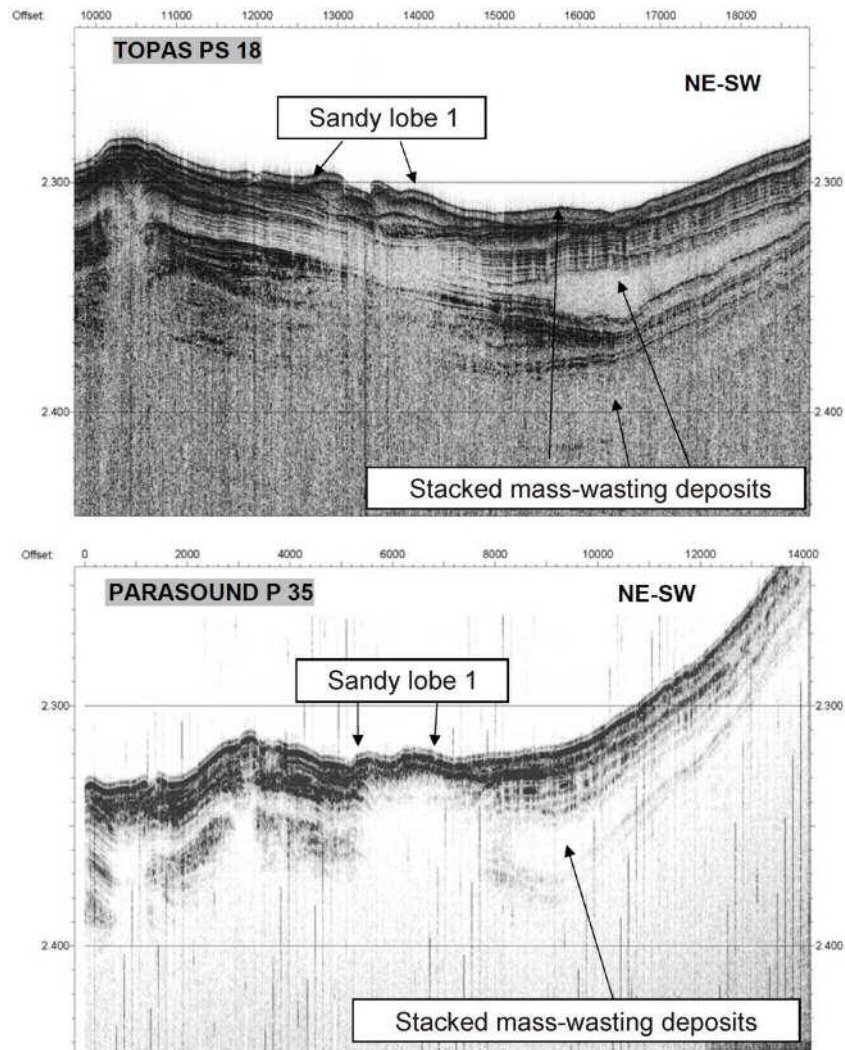
Fig. 2. 8 - Comparison of the resolution attained by the Simrad TOPAS PS-18 system (profile recorded during the MARSIBAL cruise) and the Atlas Parasound P-35 system (profile recorded during the SAGAS Bis) in the same area (Almeria continental margin) (Alonso *et al.*, 2010).

2.2.2. High- to low-resolution seismic systems: single- and multi-channel seismic systems

The Sparker is a high- to middle-resolution system with a high-voltage source that consists of a planar floating multi-tip spark-array (Fig. 2.9A,B) towed behind the ship. This systems was used in the SARAS cruise with the spark-array of 120 SIG sparker-electrodes that were triggered every 2 seconds. The system can reach an energy of 500J at discharge, and the frequency of the resulting signal is ∼6 kHz. A single-channel streamer towed behind the ship is also required for data reception.

This technique is suitable for surveys from 30 to ∼1000m water depth. Depending on the nature of the soil, the penetration of the sound signal can reach several hundred meters below the seafloor with a metric resolution. This data only requires a basic processing consisting of band-pass filtering (low cut at 200 Hz, high cut at 4000 Hz), in order to erase the noise, and swell filtering (Fig. 2.9C).
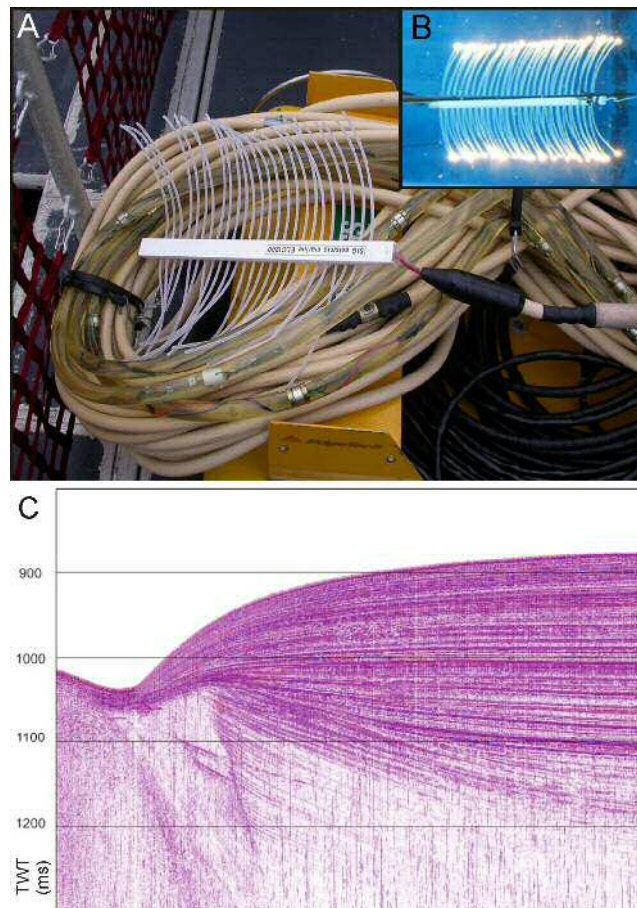
Fig. 2. 9 - A) Example of a Sparker system (USGS). B) Sparking electrode in salty water (SIG-Marine Seismic Equipments). C) Example of slightly processed sparker profile from SARAS cruise, showing an elongated separated drift in the northern part of the Tofiño Bank, from d'Acremont *et al.* (2012).

The *airgun system* (140-620 c.i.) is characterized by a source of one or more air-pressurized pneumatic chambers hanging from a float (Fig. 2.10), submerged and towed behind the vessel at ~5m deep. The airgun is air-pressurized when charged; when firing the airgun due to the retraction of a bolt, the air is suddenly released. The implosion of the air bubble generates a pulse of acoustic energy that travels to the seafloor, penetrates in the sediment (where is transmitted by compression and dilatation of the sediment) and is refracted in each interface between two sediment layers with different properties.

Fig. 2. 10 - Airgun working frame designed and mounted by the "Marine Technology Unit" of CSIC (Spain) for the RV Sarmiento de Gamboa. The airgun array consists of 6 Sercel GGUN-II canyons distributed in three clusters of various capacities, hanging from a float (Vázquez et al., 2012).

The reflected pulse is received by the hydrophones located in a neutrally buoyant SIG streamer towed behind the airgun source at 1.5 m water depth. The shooting frequency was controlled by the navigation system, which generates equidistant events every 12.5, 15 or 25 m. The average penetration of the acoustic signal was 1.5 s TWTT.

Real-time data was displayed in onboard monitors using the Delph® Seismic Plus acquisition software that allows to control most parametres of the airgun system (navigation, ping rate, activate or deactivate the firing of the airguns, logging...) and visualizing the raw data. The recorded raw data was later processed, and different filters and corrections were applied.

The multi-channel seismic system is also characterized by a source of low frequency (typically one or more air-pressurized pneumatic chambers). The main difference consists of using a streamer with multiple active sections of hydrophones (channels) that can be much longer (up to few km) than a single-channel streamer. The number of hydrophones per channel, the number of channels and the distance between channels can vary from a multi-channel configuration to another, resulting in variable penetration and resolution.

The most typical configuration for multi-channel seismic acquisition is called Common Mid-Point mode (CMP). CMP is defined as the point located halfway between the source and the receiver that is shared by several source-receiver pairs (Fig. 2.11). This is achieved by registering the reflected signal of the same shot into many receivers (which is called shot gather), and then moving the source position a multiple of the distance between the receivers (the CMPs are located at half the receiver spacing, Fig. 2.11).
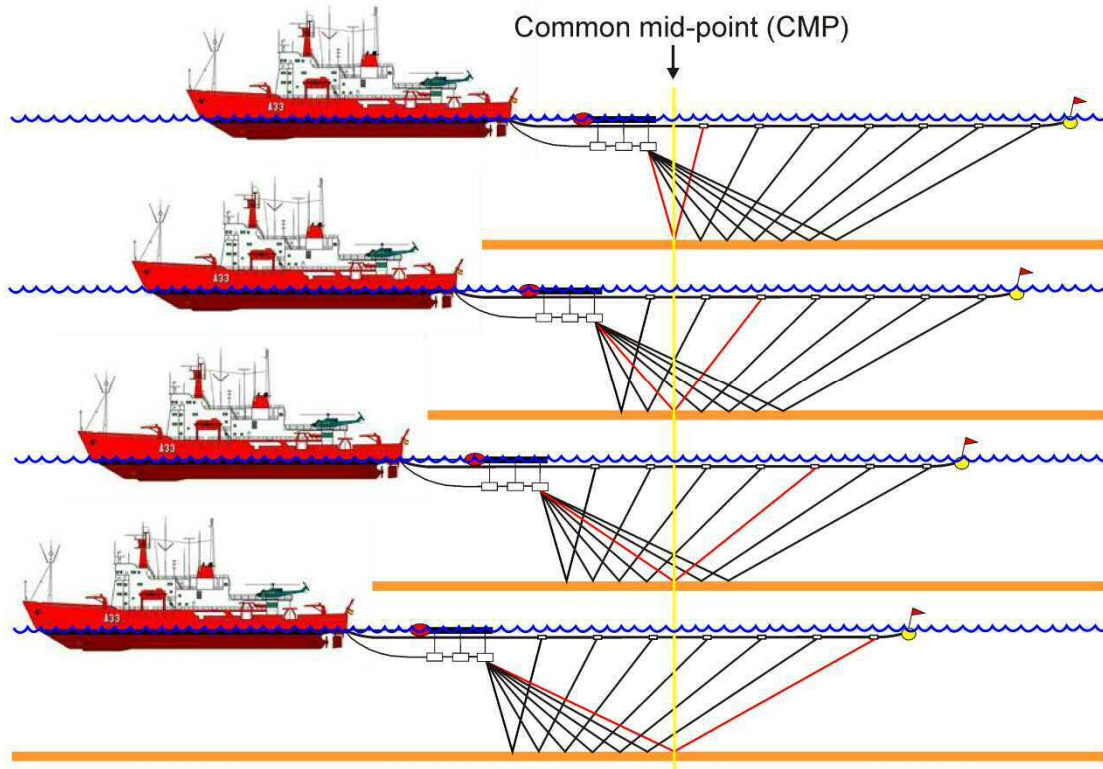
Fig. 2. 11 - Diagram explaining the common mid-point technique, considering four shots of the airgun array and seven active sections (channels) in the streamer, while the vessel is displacing to the left.

In the case of ideally flat layers of sediment, the pulse of acoustic energy will be reflected at a Common Depth Point (CDP) for each interface that will be located below the CMP. However, when sediment layers show a certain dipping angle, not all the traces reflect at the same mid-point location, and no CDP will be shared by multiple source-

receiver pairs. As a result, this seismic system requires important processing work after the cruise to reconstruct the geometry of the sediment layers: Dip Moveout Processing (DMO), migration, etc.

2.3. Description of the sediment sampling systems

Two different sampling systems were used to recover the sediment cores: seven of them were sampled at TSs in the MB using the gravity corer system, and five more cores were sampled at TSs near the Strait of Gibraltar using a piston corer system.

The gravity corer is a sampling system composed of a lead weight attached to a steel drilling shaft (with a PVC liner placed within to collect the drilled sedimentary column), and terminated by a core catcher system, that samples the sediment falling by gravity and inertia. The piston corer sampling system is very similar, but a piston is inserted inside the PVC liner and positioned at the bottom near the core catcher. A longer drilling shaft is used for the piston corer system, because the recovered samples are usually longer.
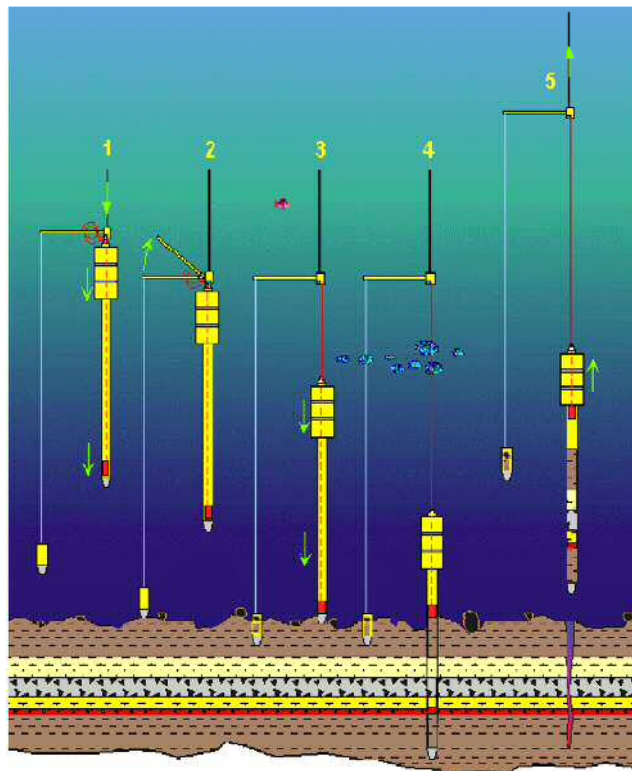
Fig. 2. 12 - Mechanical triggering system for the recovery of sediment cores. In this diagram, a piston is also represented within the drilling shaft (in red). Modified from Alonso *et al.* (2010).

A mechanical triggering system was used in both cases (Fig. 2.12). The free fall of the coring system is triggered by the landing of a small (1m) gravity corer that hangs from a

lever arm as a counterweight. The sudden displacement of the lever arm releases the cable of the lead weight and shaft, allowing the coring system to fall by gravity and drill the near surface sediment. In the case of a piston corer system, as the shaft penetrates the seafloor the piston inside stops at the sediment surface (Fig. 2.12), creating a pressure differential at the top of the sediment column that allows the soft material to enter the core liner without disruption, reduces internal friction and prevents plugging.

2.4. Description of the hydrographic systems

The *CTD system* measures conductivity (that is converted into salinity), temperature and hydrostatic pressure (that is converted to depth), and also allows calculating other variables such as density, sound velocity, etc. The main sensors commonly scan the water properties at a rate of 24 Hz. Other auxiliary sensors can be connected to the CTD profiler to measure dissolved oxygen, pH, turbidity, chlorophyll fluorescence, etc. The water properties can be observed in real time using a conducting cable that connects the CTD to an onboard computer, or the data can be downloaded once the equipment is onboard.

The *ADCP Ocean Surveyor 75 system* (76.8 kHz) works in the narrow band mode, using 4 beams at a ping rate of 0.7 Hz, 30º of aperture and a cell size of 8 m. The principle behind ADCP profilers consists of the emission of sound pulses (or pings) at a fixed frequency along the ship´s path. As the sound waves travel in the water column, those suspended materials floating in a water layer reflect the sound pulse back to the instrument. Due to the Doppler Effect, those sound pulses reflected due to the presence of suspended materials moving away from the profiler will have a slightly lowered frequency when they return; on the other hand, if the suspended materials are moving toward the instrument the reflected sound pulse will have higher frequency. The difference in frequency between the emitted and received pulses is called the Doppler shift. By measuring the time the pulses take to return and the Doppler shift, the profiler can calculate how fast the suspended materials (and the seawater around them) are moving. The ADCP can measure the current speed at many different depths with each series of pings, allowing to understand the current regime characteristics.

The *Simrad EK60 echosounder* is based on one transducer and one transceiver unit that operated at a frequency of 38 kHz to register the structures in the water column. Real-time data was displayed in onboard monitors and the recorded raw data was later processed, corrected and filtered.

3. Analysis of the sedimentary register and water column

Four main type of analysis have been carried out in this work: i) geomorphological and sedimentary, ii) seismic-stratigraphic and architecture, iii) sedimentological, and iv) hydrographic.

The *geomorphological and sedimentary analysis* (i) of the near-seafloor comprised the examination of the morphology (dimensions, geometry) and of the acoustic facies making up the sedimentary features. Morphosedimentary features were defined using bathymetric and seismic data, based on their overall morphology and geometry, alongslope and downslope elongations, acoustic facies and strata patterns. The production of bathymetric maps, topographic profiles and 3D elevation models were performed with the use of specific softwares, such as Surfer, Fledermaus and Global Mapper. All the subbottom seismic profiles were integrated into a Kingdom Suite project (IHS Kingdom) for their correlation and interpretation. The study of the acoustic facies followed the method described by Damuth (1980). The classifications for contourites from Faugères *et al.* (1999), García *et al.* (2009) and Rebesco (2005), for turbidites from Richards *et al.* (1998), and for mass movement deposits from Masson *et al.* (1996), Lee *et al.* (2009), and Casas *et al.*, (2015), were adapted for the definition of the morphosedimentary features.

The *seismic-stratigraphic and architecture analysis* (ii) of the deposits included the correlation of a time-stratigraphic sequence's and unit's framework, and the analysis of the sedimentary facies within the Pliocene and Quaternary sequences. All the sparker, airgun and multi-channel seismic profiles were also integrated into a Kingdom Suite project (IHS Kingdom) for their accurate correlation and interpretation.

For the correlation of a time-stratigraphic sequence's and unit's framework involved the identification and correlation across the Alboran Basin of Pliocene and Quaternary seismic boundaries previously identified in the literature (Alonso and Maldonado, 1992; Campillo *et al.*, 1992; Ercilla *et al.*, 1992, 2002; Jurado and Comas, 1992; Estrada *et al.*, 1997; Pérez-Belzuz *et al.*, 1997; Pérez-Belzuz, 1999; Hernández-Molina *et al.*, 2002; Somoza *et al.*, 2012; Juan *et al.*, 2012a,b) to have a stratigraphic time reference for the acoustic characterization of the morphosedimentary features.

The seismic boundaries were correlated and calibrated with the age-significant biostratigraphy events and log (sonic and density) data from the DSDP site 121 (Ryan *et al.*, 1973) and ODP sites 976, 977, 978 and 979 (Comas *et al.*, 1999; de Kaenel *et al.*, 1999; Siesser and de Kaenel, 1999; von Grafenstein *et al.*, 1999) the chronology of the seismic

stratigraphic boundaries based on the age calibration built with data from scientific and commercial wells (Fig. 2.13)(Ryan *et al.*, 1973; Armentrout, 1991; Comas *et al.*, 1996; Martínez-García *et al.*, 2013) were matched with the preliminary seismic interpretation, and also correlated with findings from other local-, regional- and global-scale studies (Alonso and Maldonado, 1992; Ercilla *et al.*, 1994; Comas *et al.*, 1996; de Kaenel *et al.*, 1999; Fauquette *et al.*, 1999; Zazo, 1999; González-Donoso *et al.*, 2000; Llave *et al.*, 2001, 2006, 2007; Hernández-Molina *et al.*, 2002, 2006a, 2014; Becker *et al.*, 2005; Lisiecki and Raymo, 2005, 2007; Hayward *et al.*, 2009; Van Rooij *et al.*, 2010; Miller *et al.*, 2011; Zazo *et al.*, 2013; Martínez-García *et al.*, 2013; Rohling *et al.*, 2014). The names of the Pliocene and Quaternary stratigraphic divisions have been updated, and also renamed several previous stratigraphic boundaries to obtain a straightforward nomenclature based on the recent age definition of the Quaternary base boundary (*http://www.stratigraphy.org/*; Morrison and Kukla, 1998). The sedimentary analysis of the morphosedimentary features is defined based on their overall morphology and geometry, alongslope and downslope elongations, acoustic facies and strata patterns, using bathymetric and seismic data and isochore maps obtained with IHS Kingdom Suite software.
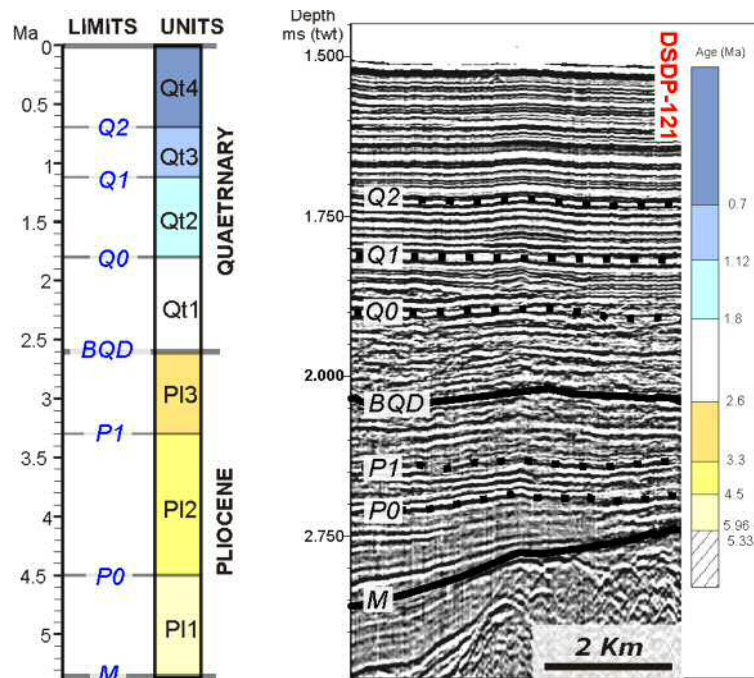
Fig. 2. 13- Seismic line crossing the location of the DSDP 121, showing the vertical stacking of the Pliocene and Quaternary units. The M (top of the Messinian surface) and BQD (base of Quaternary discontinuity) reflectors limiting the Pliocene (in yellow) and Quaternary (in blue) sequences are represented in black, whereas the internal boundaries of seismic units are represented with dashed lines. Legend: M, P0, P1, BQD, W0, Q1, Q2 refer to seismic boundaries of the seismic units.

A precise chronology of the seismic stratigraphic boundaries was developed primarily by correlating the seismic register with data from scientific wells (Fig. 2.13) for the chronostratigraphic attribution of the seismic boundaries identified in the seismic database. The combined data allowed a good degree of confidence in the correlations, despite the low sediment recovery in some scientific wells (i.e., 10% recovery in DSDP121; Ryan *et al.,* 1973). The chronostratigraphic framework adapted by Siesser and de Kaenel (1999) for the western Mediterranean has been applied to the Plio-Quaternary sequence.

The characterization of contourite drifts was based on the criteria of Faugères *et al.* (1999), Rebesco (2005), Stow and Faugères (2008), and Rebesco *et al.* (2008, 2014). We applied the terminology of Faugères *et al.* (1999), Rebesco (2005) and Rebesco *et al.* (2014) to the contourite drifts and that of Hernández-Molina *et al.* (2006a, 2014) and García *et al.* (2009) to the contourite erosional features. Likewise, we adopted the classifications from Normark *et al.* (1993), Richards *et al.* (1998), Richards and Bowman (1998) for turbidites, Mutti and Normark (1991) for defining the main architectural elements defining a turbidite system (TS), and that from Masson *et al.* (1996), Lee *et al.* (2009), and Casas *et al.,* (2015), for mass movement deposits.

The *sedimentological analysis* (iii) consisted on the sedimentary facies characterization, which was carried out based on grain-size distribution, carbonate content, presence of sedimentary structures, and sand fraction composition. Textural analysis were performed using settling-tube techniques for the coarse-grained fraction (<50 μm) and Sedigraph 5000D techniques for silt and clay fractions (< 50 μm). Textural statistical parameters (e.g. mean and standard deviation) were calculated using the moment measurements on sample populations containing quarter-phi interval classes in all fractions (Friedman and Sanders, 1978). The degree of sorting (standard deviation) was established using the Folk and Ward (1957). Total carbonate content was determined using a Bernard calcimeter (Alonso *et al.,* 1996). The sedimentary structures were examined based on digital images of the split cores. The sand fraction composition was examined using a binocular microscope. The terrigenous components were classified as quartz, mica, rock fragments, pyritized material and burrows, and glauconite. Biogenic components were classified as planktonic foraminifera (entire and fragments), benthic foraminifera, ostracods, bivalves, and gastropods.

The *hydrographic analysis* (iv) consisted in the treatment of CTD data, ADCP data and EK 60 echograms:

-The *CTD dataset* was analysed with the Ocean Data View (ODV) software (*http://odv.awi.de*) using T/S diagrams (Fig. 2.14), N-S (Fig. 2.15) and E-W transects of the key properties of the water masses (potential temperature, salinity, density and their derivatives with depth), as well as plots of the variation of these properties in the whole Alboran Basin at specific depths.

-The *ADCP data* were analysed in two different ways: first, the variation of the eastward and northward components of the water flow with depth was plotted and interpreted, backed by the multibeam bathymetric data; second, the variation in the backscatter intensity of these components along the vessel track was also analysed.

-The *EK60 echograms* were loaded on the IHS Kingdom suite software for their correlation and interpretation (Fig. 2.16), assuming that the reflectors in the water column result from the acoustic energy scattered by sediment and aggregations of phyto and zooplankton suspended on the interfaces between water masses and due to turbulence.

The T/S diagrams consist on the scatter representation of the potential temperature (Θ, the temperature that would have a volume of water if raised to the surface without any interaction with the surrounding waters, Stewart, 2008; Völker, 2007) and salinity values, measured at different depths, in a Cartesian diagram (Figs. 2.14, 2.15). If the potential density (σ_Θ, the density of a parcel of water if raised adiabatically to the surface without change in salinity) is represented for a number of paired values of potential temperature and salinity, the values with equal density draw curves called isopycnals (Figs. 2.14, 2.15), along which the water masses will move (neutral path) (Eden and Willebrand, 1999; Stewart, 2008) (i.e., the LIW was recently tracked along the whole Mediterranean basin by Millot, 2013 using this technique).

Since the number of possible combinations of Θ and S is limited, T/S diagrams allow to recognize a reasonable number of water masses in the oceans. The different water masses were identified (Fig. 2.15) considering the published ranges for temperature, salinity and vertical and horizontal gradient data of the water masses present in the area compiled from literature (Gascard and Richez, 1985; Parrilla *et al.*, 1986; Millot 2009).
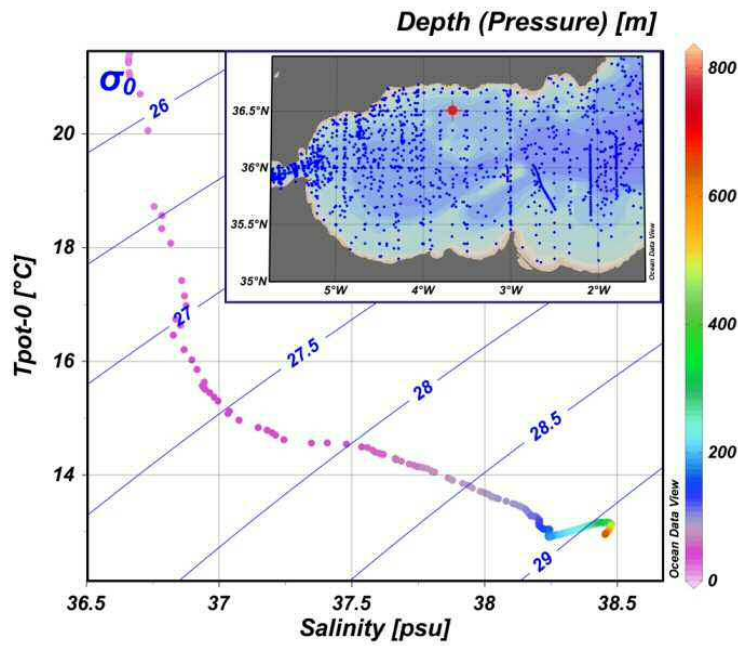
Fig. 2. 14 - Example of a single CTD profile in a T/S diagram, with the colour scale dependent on depth and showing the isopycnals (in blue). Psu - Practical salinity units (equivalent to ‰); Tpot-0 - Potential temperature. σ₀ - Potential density.
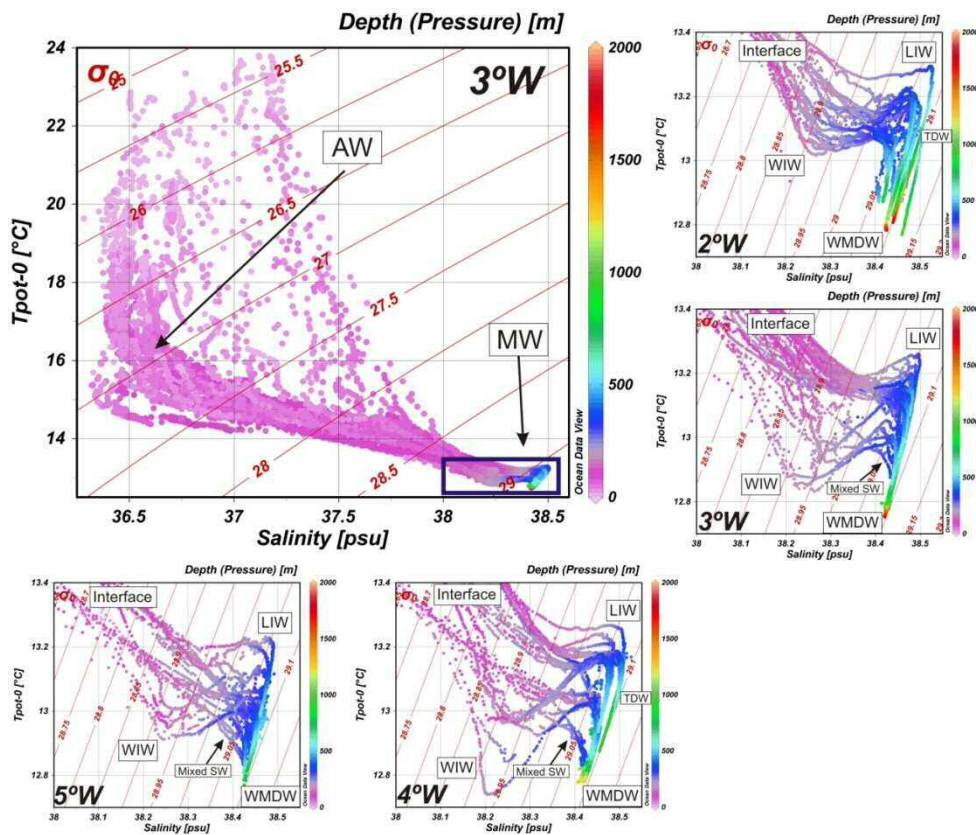
Fig. 2. 15 - North-south T/S diagrams showing all water masses (AW, WIW, LIW, TDW, WMDW) and mixed waters (interface, shelf waters) that can be identified in the Alboran Sea, based on bibliographic data (Millot, 2009). Psu - Practical salinity units (equivalent to ‰); Tpot-0 - Potential temperature. σ₀ - Potential density.
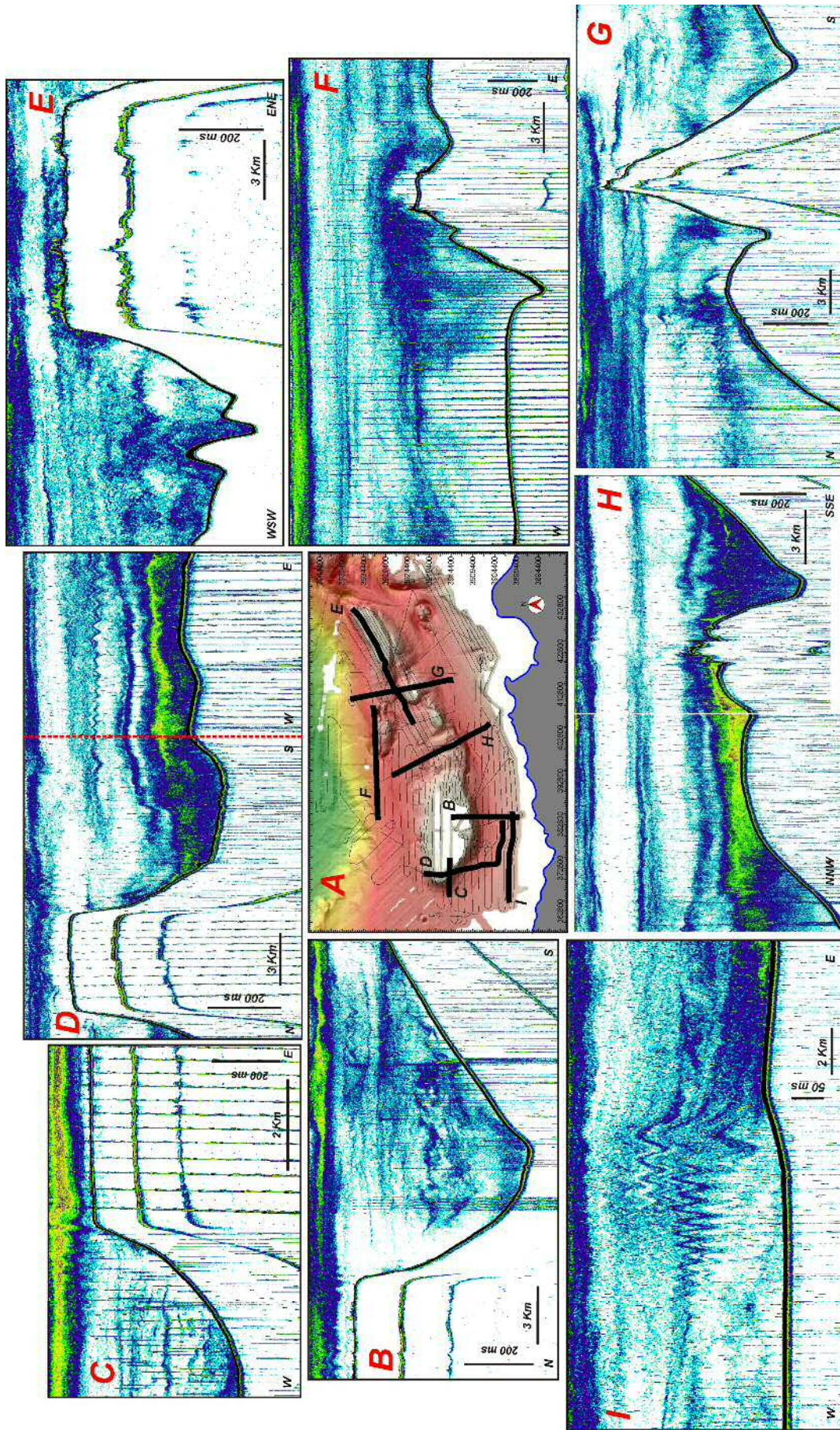
Fig. 2. 16 - EK60 echogram dataset and examples from the Al Hoceima Valley and Xauen and Tofiño banks area.

84

Chapter III - Significance of bottom currents in the deep-sea morphodynamics of the Alboran Sea

Chapter III - Significance of bottom currents in the deep-sea morphodynamics of the Alboran Sea

1. Introduction, objectives and dataset

This Chapter is focused on analysing the potential role of bottom currents in shaping the morphology of the deep sea areas of the Alboran Sea, combining for the first time studies from seismic stratigraphy, sedimentology, geomorphology and physical oceanography.

The general aims of this Chapter are:

> To obtain a new detailed map of the morphosedimentary features of the continental slope and adjacent basins, including the distribution of contourites.
>
> To determine the distribution and circulation patterns of the water-masses in the Alboran Sea.
>
> To evaluate the significance of the bottom currents in deep-sea morphodynamics in order to provide a new model of sedimentation for the Alboran Sea.

The studied dataset includes the compilation of seismic reflection profiles (single-channel and multi-channel seismic profiles) acquired during various campaigns in the last decades (Fig. 3.1A). The base of Quaternary deposits is defined throughout the seismic profiles to have a stratigraphic time reference for the acoustic characterization of the morphosedimentary features. The analysis of the water masses and their hydrographic structures is mostly based on the CTD database as well as ADCP profiles (Fig. 3.1B) recorded in the Spanish and Morocco margins.
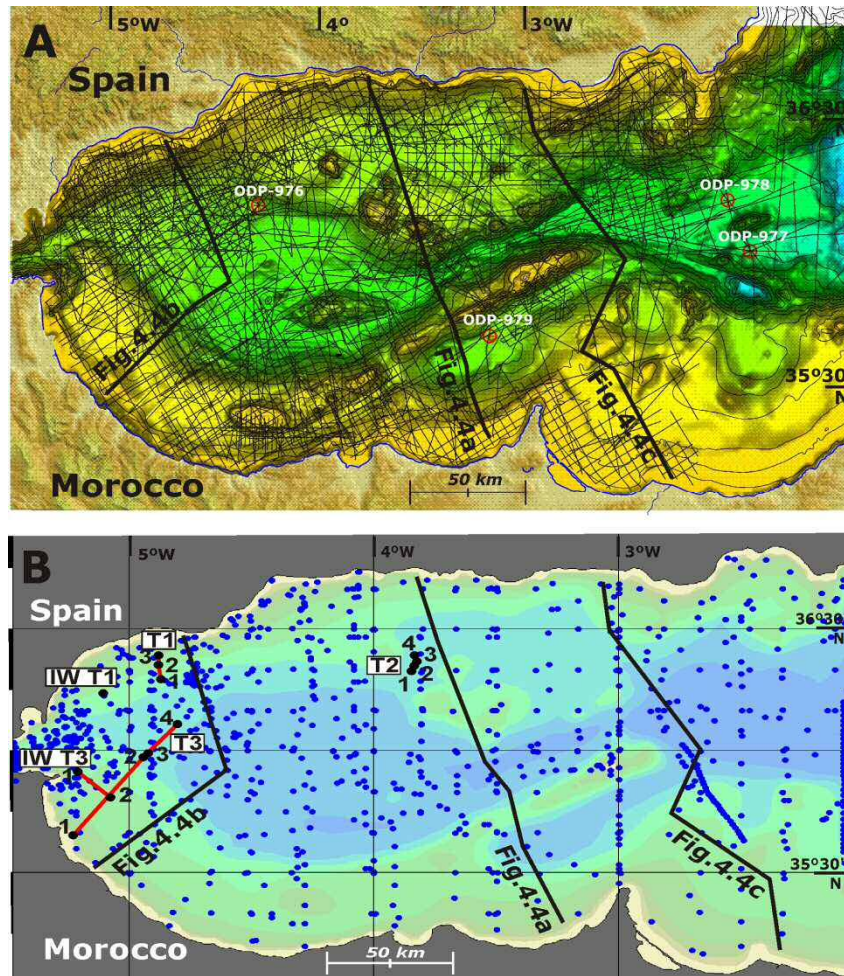
Fig. 3. 1- A) Analysed seismic lines and ODP 976, 977, 978 and 979 sites (red circles). Thick black lines indicate locations of seismic records displayed in Fig. 3.4. B) Analysed CTD (Conductivity, Temperature and Depth) profiles. Thick black lines indicate locations of CTDs used for the hydrographic sections displayed in Fig. 3.4.

2. Geomorphology

2.1. Acoustic facies analysis

Three main acoustic facies were differentiated based on their acoustic amplitude, lateral continuity, geometry and internal configuration: stratified facies (with five subtypes), chaotic facies (with two subtypes), and semitransparent facies (Table 3.1).

The **stratified** or **layered** facies is defined by reflections with low to very high lateral continuity with (sub)parallel to divergent/convergent internal configuration, occasionally undulated. The acoustic amplitude varies from low to very high values, but usually shows intermediate values. Several subtypes have been defined based on the internal configuration:

88

The *stratified (sub)parallel* facies shows low to high acoustic amplitude, very high lateral continuity and (sub)tabular geometry. This facies is usually very homogeneous, although in the late Quaternary shows cyclic vertical variations of its acoustic amplitude.

The *stratified wavy* facies is characterized by low to medium acoustic amplitude with rhythmic lateral variations, low lateral continuity and variable geometry.

The *stratified irregular* facies shows medium to high acoustic amplitude with frequent lateral variations, low lateral continuity and variable geometry. Its internal configuration is characterized by slightly deformed discontinuous reflections.

The *stratified downward concave* (or *layered mounded*) facies is characterized by a medium to high acoustic amplitude, medium lateral continuity and low to high concave geometry. The lateral continuity is variable.

The *stratified oblique* and *sigmoidal* facies shows low to medium acoustic amplitude, medium to high lateral continuity and wedged geometry.

The **chaotic** facies is characterized by reflections of low to high acoustic amplitude, with low to medium lateral continuity and variable geometry. Two types are distinguished according to their internal configuration:

The *chaotic indistinct* facies shows low to medium lateral continuity and mostly lenticular geometry, although it has also been identified in the WAB showing columnar geometry. It is characterized by highly discontinuous reflections with no internal organization.

The *chaotic disrupted* facies is characterized by a low lateral continuity and variable geometry, with a highly disrupted organization. Sometimes few internal reflections with low to medium lateral continuity can be distinguished within.

Last, the **semitransparent** facies is composed by reflections of very low to medium acoustic amplitude, low to medium lateral continuity and (sub)tabular geometry. The internal configuration is parallel to subparallel, with faint reflections of low lateral continuity.
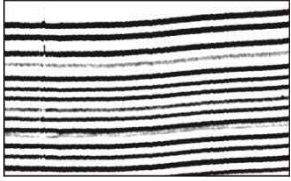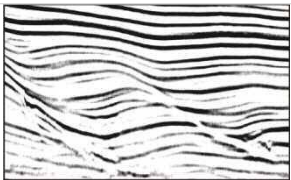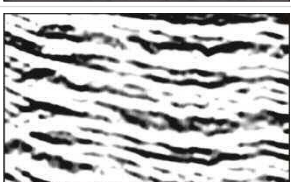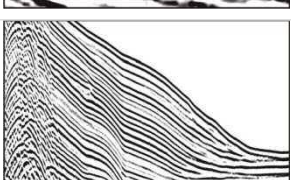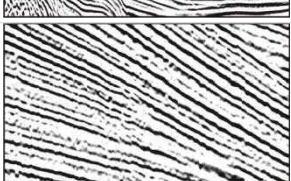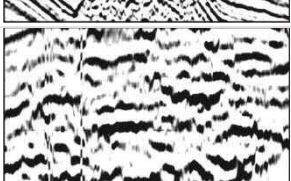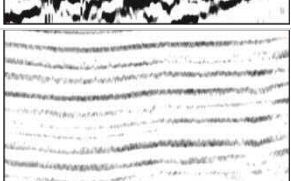
Type	Subtype	Seismic expression	Acoustic amplitude	Lateral continuity	Geometry	Internal configuration
Stratified or layered	(sub) Parallel		Low to high	Very high	(Sub) Tabular	Parallel to subparallel
	Wavy		Low to medium	Low	Variable	Parallel to subparallel undulated layers
	Irregular		Medium to high	Low	Variable	Parallel to subparallel deformed reflections
	Downward concave or mounded		Medium to high	Medium	Low concave to high concave	Divergent/ convergent
	Oblique or sigmoidal		Low to medium	Medium to high	Wedged or sigmoidal	Divergent/ convergent
Chaotic	Indistinct		Low to high	Low-Medium	Mostly lenticular, also columnar	No internal organization
	Disrupted		Low to high	Low	Variable	Highly disrupted
Semitransparent			Very low to medium	Low to medium	Irregular, (Sub) Tabular	Undefined and parallel to subparallel, with reflections of low lateral continuity

Table 3. 1- Characteristics of the acoustic facies identified in the Alboran Basin.

2.2. Major morphosedimentary features

For the first time, a wide spectrum of contourites, including depositional (drifts) and erosive (moats, channels, furrows, terraces and scarps) features, was determined from the shelf break to the basin floor of the Alboran Sea (Figs. 3.2, 3.3 and 3.4).

The dominant contourite features are different types of drifts (Table 3.2), and the largest features are plastered and sheeted drifts. *Large plastered drifts* characterize the Spanish slope and base of slope and the Moroccan slope showing an alongslope trend. *Sheeted drifts* contribute to shaping the Spanish base of slope, and infill the irregular basins, displaying a subtabular geometry that constitutes an almost-flat smooth seafloor. Small-scale drifts are dispersed throughout the Alboran Sea, particularly around the Alboran Ridge and seamounts. In addition to small scale plastered and sheeted drifts, other minor drifts (Figs. 3.2, 3.3 and 3.4) include channel-related, mounded confined, elongated and separated drifts. The *channel-related drifts* are characterized by discontinuous and irregular mounded bodies along the axis and walls of the Alboran Trough. The *mounded confined drifts* form in the narrow passages in between the steep walls of highs. Last, *elongated separated drifts* with a pronounced mounded shape are mapped around seamounts, and recent elongated separated drifts with a subdued mounded morphology are locally identified in the western Moroccan slope.

The erosive contourite features are also distributed locally along margins and basins (Figs. 3.2, 3.3 and 3.4). *Moats* are associated with elongated separated drifts, and have U-shape cross sections. *Contourite channels* develop within the structural corridor between the Moroccan margin and the Xauen Bank (Al Hoceima Valley). The Alboran Trough is a deep passage connecting the east and west basins continuously swept by deep currents (evidenced by the channel-related drifts that form on its axis and walls), and can also be considered as a contourite channel. A few linear and small parallel *furrows* occur near the Strait of Gibraltar. *Terraces* are unmistakable morphological features showing both erosive and depositional characteristics that extend above large plastered and sheeted drifts (Table 3.2), producing long flat areas on the Spanish (T1 and T2) and Moroccan (T3) margins (Figs. 3.2, 3.3 and 3.4). The erosive character occurs in its proximal domains, whereas the depositional character is mostly seen in the distal domains. *Scarps* are identified landward and seaward of these terraces, as narrow steep surfaces that mark the transition from the large-scale plastered drifts on the slope to the large-scale sheeted or plastered drifts in the base of slope and basins.
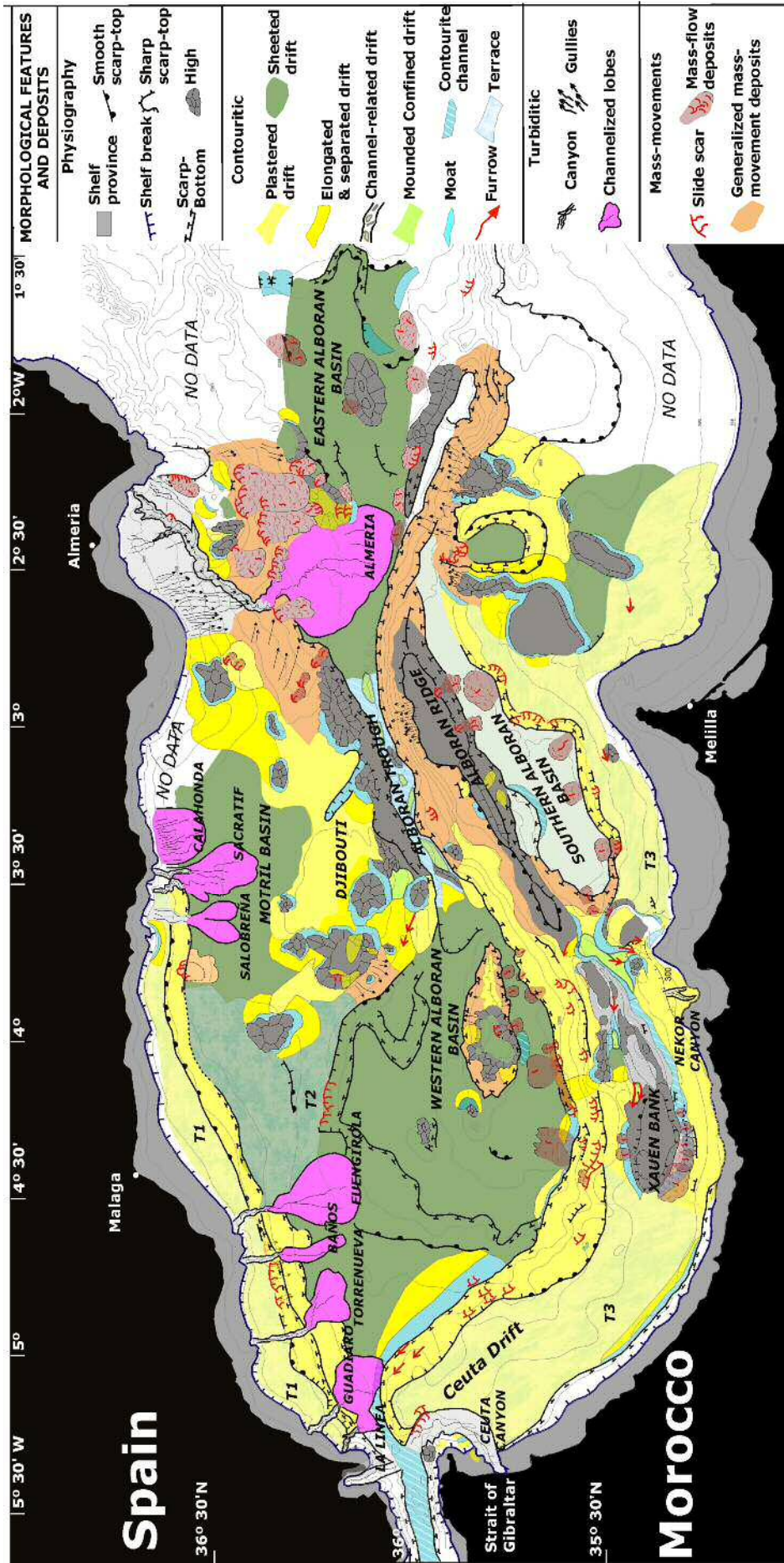
Fig. 3.2 - Map of the uppermost morphosedimentary features, showing the ubiquity of contourites.
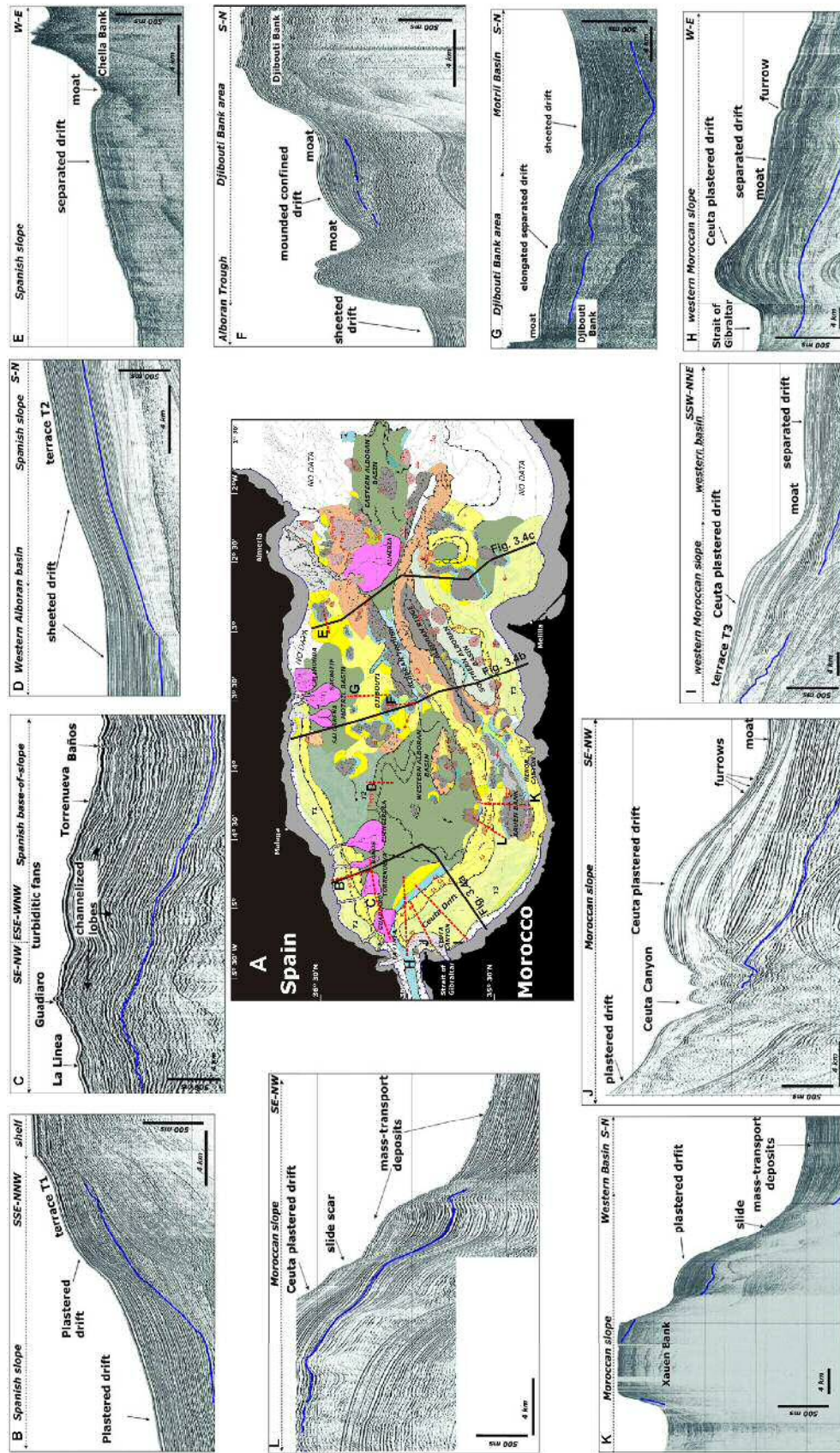
Fig. 3.3 - Segments of seismic profiles illustrating the main morphoseismic characteristics of the sedimentary features mapped in the margins and basins of the Alboran Sea: contourites, turbidites and mass movement deposits. Blue line indicates the base of Quaternary deposits. Short dotted lines indicate locations of seismic profiles. Long thick black lines indicate locations of seismic–hydrographic intersections of the margins and basins illustrated in Fig. 3.4. (For interpretation of the references to colour in A, the reader is referred to the Fig. 3.2)

The lateral continuity of the aforementioned contourites is interrupted by the development of turbiditic features and local mass movement deposits (Figs. 3.2 and 3.4; Table 3.2). Turbidite features are mostly mapped in the Spanish margin, where nine turbiditic systems are defined. They are mostly characterized by a feeder non-leveed canyon that cuts across the slopes and drifts and leads directly, through a short leveed channel, into a lobe with aggrading distributary leveed channels that develop at the base of slope down to the basin. In contrast, no turbidite systems developed in the Moroccan margin, where only the Ceuta Canyon and another relatively shorter canyon (here named Nekor canyon) are mapped. Mass movement deposits with variable dimensions are found locally within slope sheeted drifts, on scarps and on the flanks of structural highs, many of the extending down to the adjacent basins.
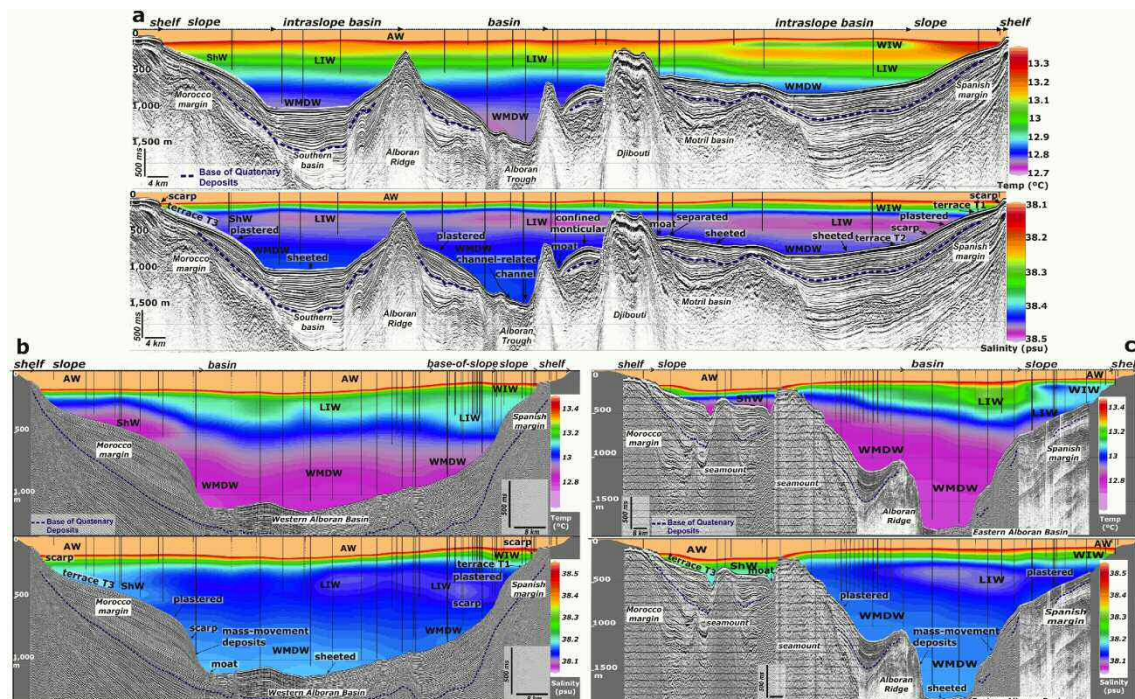
Fig. 3.4 - Seismic–hydrographic intersections of the margins and basins of the Alboran Sea. Note the correlation between the highest density-contrast between water-masses (AW, WIW+LIW, and WMDW) and the main physiographic domains. Types of contourites and water-masses are indicated on the seismic profiles. Colour-coding: temperature (°C) and salinity (psu). The black vertical lines within the water column show the water depth to which the CTD was lowered. Location of seismic–hydrographic intersections is shown in Fig. 3.3.

Contourite drifts represent important accumulations of sediments during the Quaternary, with similar seismic facies along the margins and adjacent basins and affected by tectonic structures (faults and folds). Drift facies (Stow and Faugères, 2008) are defined by layered deposits with internal regional erosive unconformities (Figs. 3.3 and 3.4). Terraces and scarps include truncated reflections, discontinuous and continuous

94

subparallel stratified and oblique to sigmoidal facies. Terraced slope shapes were also enhanced during the Quaternary (Fig. 3.4). Moats, channels and furrows are mainly characterized by truncated reflections, discontinuous stratified and chaotic facies, which generally show relatively high acoustic amplitude compared to those displayed by the associated drifts. These observations set out the contrast between contourite seismic facies and those of turbiditic features and mass movement deposits (Figs. 3.3 and 3.4).

Morphological features & deposits	Acoustic Facies (airgun profiles)	Shape/dimensions	Location
Depositional contourite features			
Plastered drifts	Downward low-concave stratified facies prograding upslope and downslope with internal discontinuities (downlap, onlap, truncations)	Low to high mound shape up to few hundreds of km length (< 300 km), 5.5 to 40 km width and <100 to 600 m of relief	Large drifts: Spanish and Moroccan slopes. Small drifts: seamounts flanks, Spanish base of slope
Sheeted drifts	Parallel and subparallel stratified, occasionally semitransparent facies	Subtabular geometry. < 100 km long, 15 to 50 km wide	Large drifts: Spanish base of slope; Western, Eastern, Southern and Motril basins. Small drifts: Alboran Ridge, seamount tops
Channel-related drifts	Aggrading and prograding downward low-concave stratified facies	Low mound shape. ~ 10 km long, <5 km wide	Alboran Trough
Mounded confined drifts	Downward high-concave stratified facies	High mound shape. Few to tens of km long and wide and 100 to 300 m high	Between highs in the Motril Marginal Plateau
Mounded, elongated and separated drifts	Prograding and aggrading, downward high to low concave stratified facies	Low to high mound shape. <40 km long and 20 km wide	Locally at the foot of seamounts, western Moroccan slope and shelf break scarp
Erosional contourite features			
Scarps	Steep to gentle surface with oblique stratified facies or truncated oblique to sigmoidal prograding facies	Narrow (60 m to 16 km), steep (2º to 11º) scarps hundreds km long	Bounding physiographic domains: -Shelf break & slope: 90 to 161/223 m w.d. (Spanish) and 100/150 to 180/339 m w.d. (Moroccan). -Spanish slope & Motril Basin: 400 to 630 m w.d. -Motril Basin & Western basin: 1000 to 1300 m w.d. -Moroccan slope & Western and Southern basins: 600 to 1000 m w.d.
Moats	Erosive surface truncating underlying stratified or chaotic facies	U-shape cross-section,5 to 43 km in length, < 6.5 km width, and <10 to 85m of relief	Associated to the separated drifts
Channels	Erosive surface truncating underlying stratified or chaotic facies	U-cross-section. 1.4 to 6.5 km wide and 11 to 70 km long	Alboran Trough & Moroccan slope
Furrows	Truncating negative reliefs	Linear features < 25 km long	Western Alboran Basin, Moroccan slope
Terraces	Truncating erosive to conformity surfaces	Flat surface < 30 km wide, <150 km long; mostly abraded in the proximal sectors	Moulding the slope plastered and sheeted drifts of the Spanish (160 to 400 m w.d.) and Moroccan (120 to 600 m w.d.) slopes
Other sedimentary features			
Turbidite systems	Layered irregular and chaotic disrupted facies	Elongated lobular and fan shape, 19 to 53 km long, few km wide	Spanish margin
Mass movement deposits	Chaotic disrupted and indistinct facies	Irregular elongated and lobular shape, hundreds down to few km in scale	Spanish and Moroccan margins, Alboran Trough, Alboran Ridge and seamounts

Table 3.2 - Classification, acoustic facies, shape dimensions and locations of the main morphosedimentary features in the Spanish, Moroccan margins and basins of the Alboran Sea.

3. Identification of water-masses and associated interface processes

The analysed temperature and salinity profiles reveal four major water-masses within the Alboran Sea (Fig. 3.5 and Table 3.3): one of Atlantic origin (AW), and three of Mediterranean origin (Western Intermediate Water [WIW]; Levantine Intermediate Water [LIW]; and Western Mediterranean Deep Water [WMDW]). Additionally, a fifth water-mass lies below the LIW, the Tyrrhenian Deep Water (TDW), but it is poorly defined in the CTD profiles because it shows similar characteristics to the overlying LIW and the underlying WMDW. Here therefore, it is included in the LIW and the WMDW. The WIW and LIW constitute the light (or intermediate) Mediterranean waters (LMW), and the WMDW constitutes the dense (or deep) Mediterranean waters (DMW) (Millot, 2009). The interfaces between the AW and the light and dense MWs are characterized by vertical density gradients (Figs. 3.4 and 3.5).
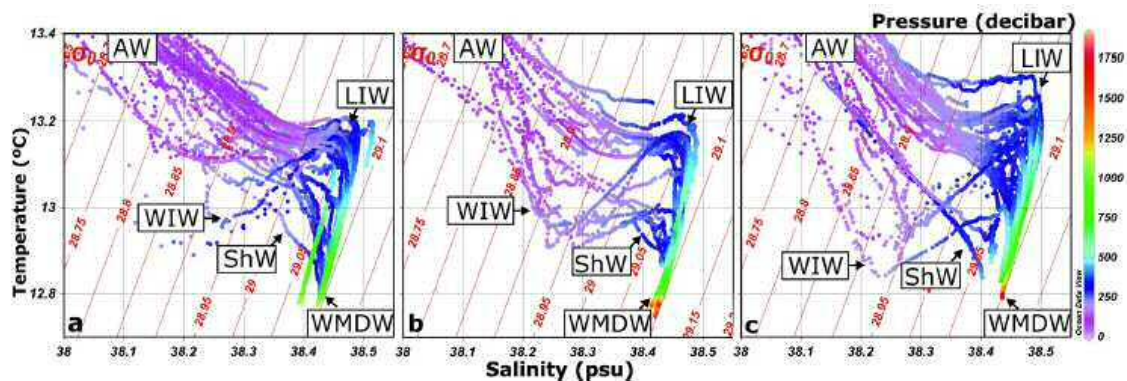
Fig. 3.5 - The main water-masses in the Alboran Sea. Potential temperature and salinity plots from CTD measurements showing the different water-masses that comprise the water column. Their definition matches previous hydrographic analyses of the Alboran Sea and the Strait of Gibraltar (Gascard and Richez, 1985; Parrilla *et al.*, 1986; Millot, 2009, 2013). Location of the hydrographic profiles is shown in Fig. 3.1b. The plots a, b and c correspond to CTDs used for water masses interpretation of the hydrographic vertical sections illustrated, respectively in Fig. 3.4a, b and c.

The superficial AW covers most of the Alboran Sea and has an almost constant salinity (S) of <36–36.5 psu, and an average temperature (T) of 16 °C. It extends from this surface layer down to a w.d. of 150 m and 250 m in the Spanish and Moroccan margins, respectively (Fig. 1.23). In the ADCP profiles, it shows a dominant eastward-moving component (Fig. 3.6).

The LMW are chiefly located in the Spanish margin (Fig. 1.23; Fig. 3.4). Underlying the eastward-moving AW is the westward-moving WIW. This interface can be identified in T–S

diagrams by a drop in T (Fig. 3.5) because the WIW has a temperature of 12.9–13°C and a salinity of 38.1–38.4 psu. This water-mass enters the Alboran Sea along the Spanish slope, and ADCP data shows that it circulates westward along the upper slope at a w.d. between approximately 75 and 300m (Fig. 3.6). The flow intensity varies annually, as previously reported by Millot (2013). Below the WIW, the LIW is identified by an increase in salinity (Figs. 3.4 and 3.5; Table 3.3) and the interface is at 200–300 m w.d. (Table 3.3). The LIW lies at a w.d. of 200–600 m, and typically has a salinity of 38.5 psu, a temperature of 13.1–13.2 °C and circulates westward (Fig. 3.6), mainly interacting along the Spanish margin and adjacent basins, the Alboran Ridge and morphological highs (Fig. 3.4; Table 3.3).

Water-masses	Salinity & temperature	Water depths	Location
Atlantic Water (AW)	< 36-36.5 psu & 16ºC in average	< 150 m on the Spanish margin; <250 m on the Moroccan margin	It covers most of the Alboran Sea
Western Intermediate Water (WIW)	38.1-38.5 psu & 12.9 to 13ºC	Approximately 75 and 300 m	On the Spanish upper slope
Levantine Intermediate Water (LIW)	38.5 psu & >13.1-13.2ºC	Approximately 200 to 600m	On the Spanish margin and adjacent basins
Western Mediterranean Deep Water (WMDW)	38.4 to 38.5 psu & < 12.85ºC	>400 m on the Spanish margin; >180/400 m on the Moroccan margin	On the Spanish and Moroccan (core on the slope) margins, adjacent basins and Alboran Trough
Mixed AW & WMDW: Shelf Waters (ShW)	38.5 psu in average & 13.1-13.2 ºC	< 300 m	On the Moroccan upper slope

Table 3.3 - The main water-masses in the Alboran Sea and their characteristics. Temperature (°C) and salinity (psu) ranges, depth distribution within the water column and primary locations for the four main water-masses making up the Alboran Sea. The mixing layer named Shelf Waters (ShW) (Gascard and Richez, 1985) is not considered a water-mass as it results from local mixing between AW and WMDW. Previous hydrographic analyses of the Alboran Sea and Strait of Gibraltar (Gascard and Richez, 1985; Parrilla *et al.*, 1986; Millot, 2009, 2013) have also been considered.

The WMDW is concentrated along the Moroccan margin (Fig. 1.23; Fig. 3.4). Its greater density is caused by significantly lower temperatures (<12.7–12 °C), and it also has lower salinity (38.4–38.5 psu) (Figs. 3.4 and 3.5; Table 3.3). The WMDW occupies variable water depths depending on the physiographic and geographic domain. As this water-mass enters the Alboran Sea, the complex seafloor relief splits it into three main branches or veins. The northern branch (w.d. >400 m) circulates along the Spanish slope and base of slope; the central branch (w.d. >500 m) is confined along the Alboran Trough and spreads to infill the WAB; and the southern branch enters the SAB and is forced up the parallel western Moroccan slope, reaching water depths of up to 180 m over the terrace (T3) (Fig. 1.23). Here, the WMDW mixes with the AW to form ShW (<300 m) with a salinity of 38.5 °C and a temperature of 13.1–13.2 psu. In the ADCP profiles, the WMDW shows a clear westward-moving near the slope (Fig. 3.6).
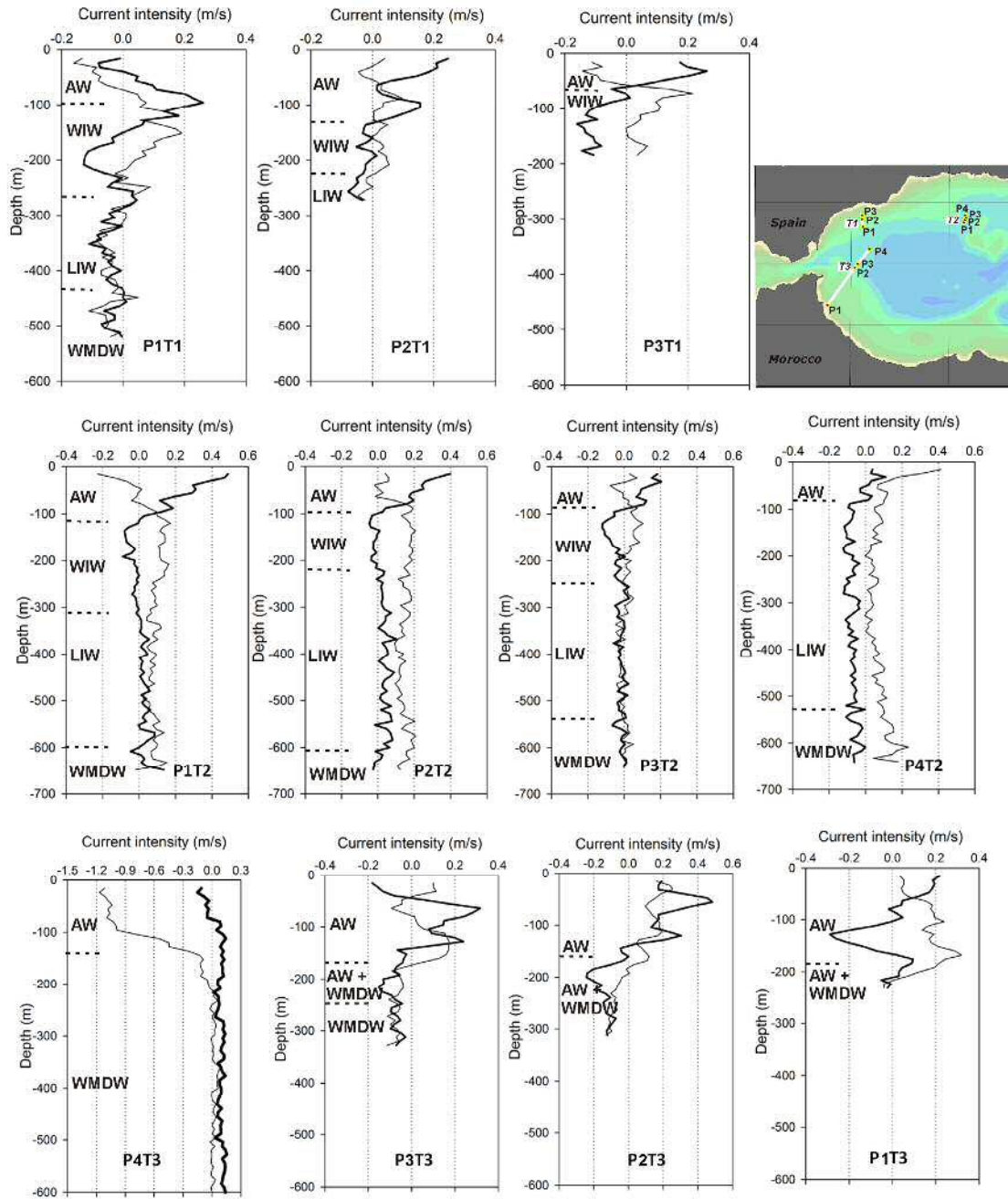
Fig. 3.6 - ADCP measured velocity profiles on contourite terraces. ADCP profiles at stations P1T1, P2T1 and P3T1 on terrace T1, stations P1T2, P2T2, P3T2 and P4T2 on terrace T2 and P1T3, P2T3, P3T3 and P4T3 on terrace T3: east (thick line) and north (thin line) components. Note that the ADCP profiles show the direction component of the water-masses.

Based on the distribution of near-bottom layers of the mentioned water masses (Fig. 3.7), the AW is mainly located on the continental shelves and upper slopes of both margins, the WIW and LIW are on the Spanish slope and the WMDW is on the Moroccan slope, Spanish base of slope and deep basins (Figs. 1.23, 3.4 and 3.7). Thus, the interfaces between the AW and the WIW + LIW, and the WIW + LIW and the WMDW, interact with

the Spanish slope, whereas the interface between AW and WMDW touches the Moroccan slope (Fig. 3.4). These interfaces dip southward and northward for the AW/WIW + LIW/WMDW and the WIW+LIW/WMDW interfaces, respectively. The occurrence of internal waves is associated with these interfaces, inducing large perturbations in the current velocity, and vertically displacing water parcels above and/or below the AW and the WIW+LIW or the WMDW pycnoclines. Internal waves are also observed propagating from the Strait of Gibraltar (Fig. 3.8a) into the Alboran Sea, predominantly above terraces (T1 and T3) (Fig. 3.8b and c). These internal waves are mostly generated within the Strait (Armi and Farmer, 1988; Bruno *et al.*, 2002; Vázquez *et al.*, 2008), and are highly regular (twice a day) following the local rhythm of the oscillatory tidal flow that creates them. Internal waves induce current perturbations that reach bottom depths >400 m, producing current oscillations of up to 0.4 m/s. Fig. 3.6 also illustrates the internal wave occurrences above striking topographic variations, such as the shelf break (Fig. 3.8d).
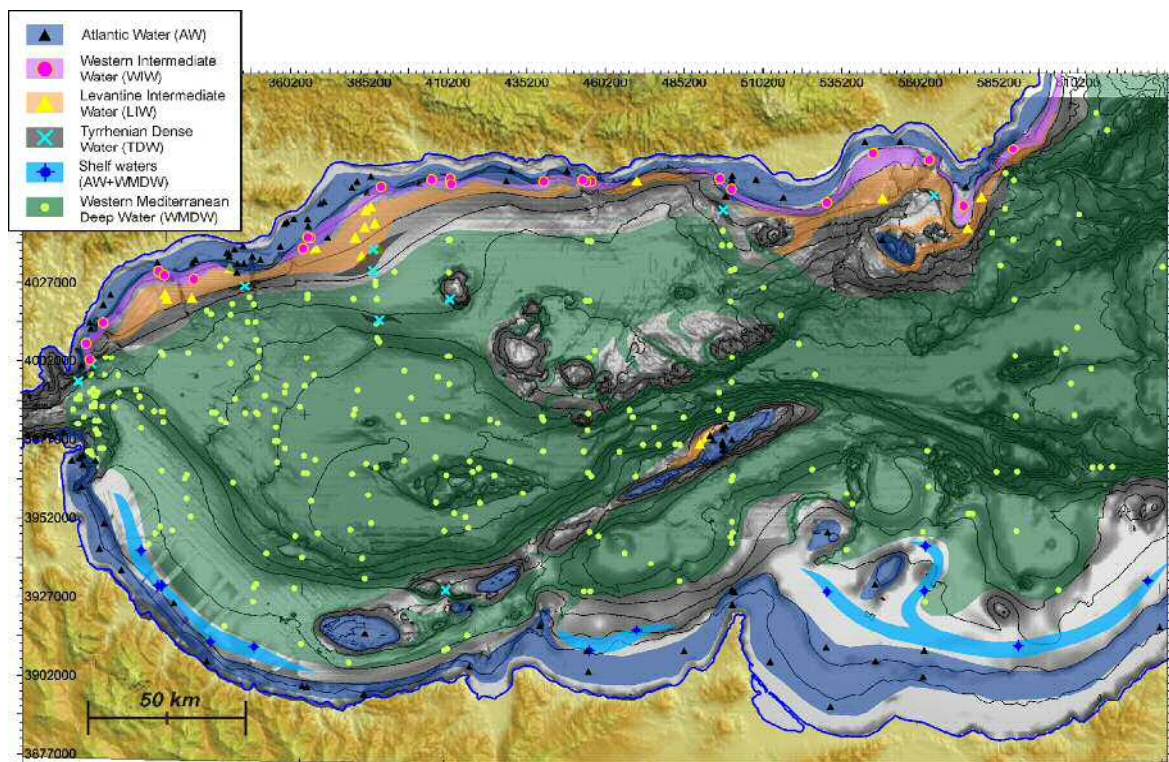
Fig. 3. 7 - Map of the Alboran Sea identifying the near-bottom water masses based on the analysis of their physical characteristics in CTD datasets. Only the CTD datasets that had their last measurement close enough to the seafloor (considering the unequal distribution of the Mediterranean water masses in the water column).
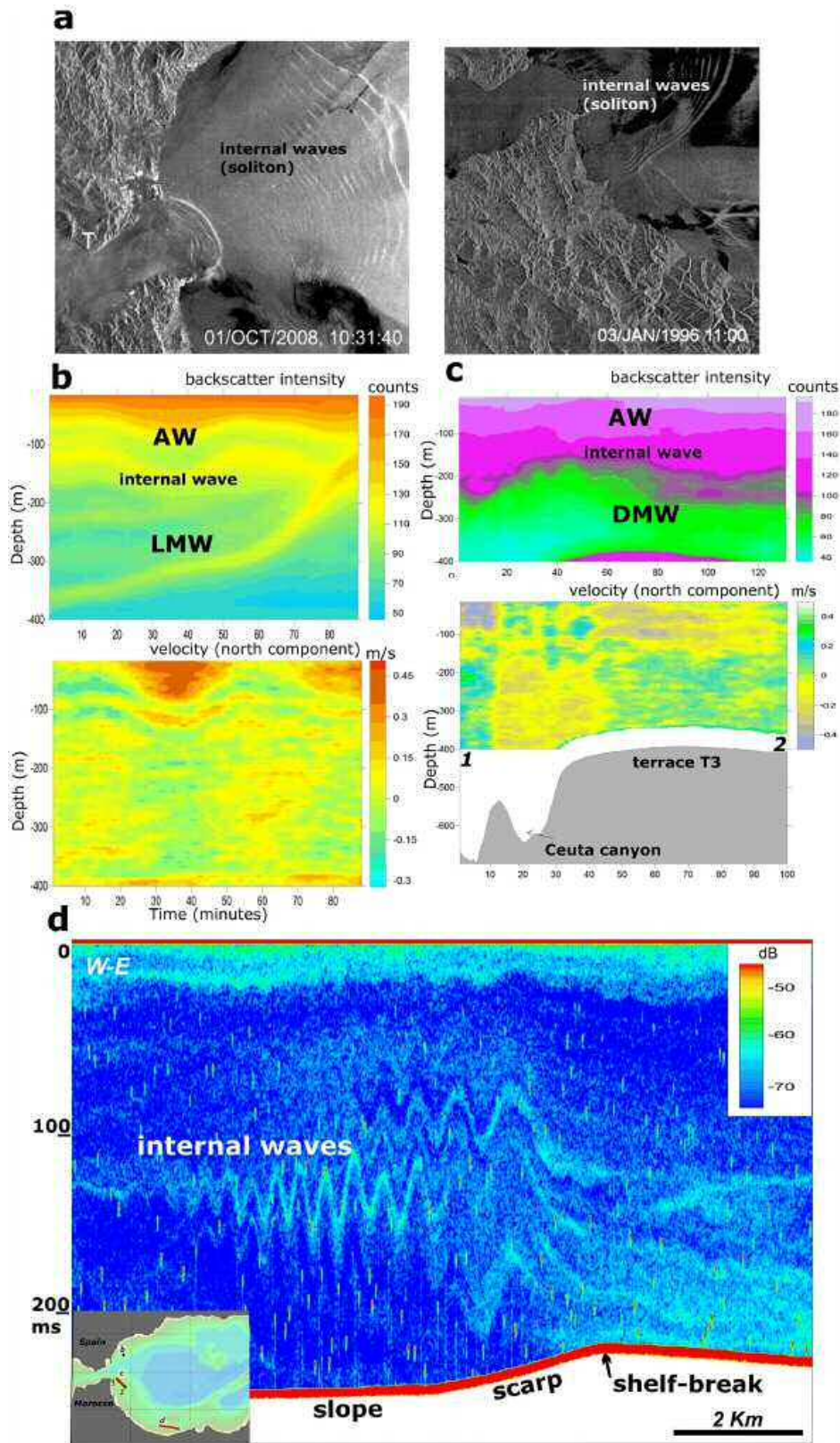
Fig. 3.8 - Internal waves in the Alboran Sea. a) SAR image (ENVISAT) showing the sea surface roughness produced by internal wave packets (solitons) originating in the Strait of Gibraltar; b & c) ADCP profiles at stations on terrace T1 (b) and T3 (c); and d) EK 60 echogram screen capture displaying the occurrence of internal waves at the Moroccan shelf break, taken at a vessel speed of ca. 8 knots, August 2012.

4. Discussion: the role of bottom currents in shaping the seafloor and their scales of action

The new morphosedimentary map combined with descriptive oceanography, are essential for the new interpretation of the dominant processes within the Alboran Sea. This interpretation suggests that bottom currents are key to understand the formation and variability of large and small contourite features, depositional and erosive. Matching the distribution of contourite types with the relevant near bottom water-masses, three scales of action for impinging water-masses are proposed: 1) alongslope bottom-current circulation governs the general physiography; 2) water-mass interfaces sculpt regional contourite terraces; and 3) morphological obstacles are essential in the local control of water masses distribution and associated bottom currents.

4.1. Alongslope bottom current circulation governs the general physiography

The distribution of large-scale plastered and sheeted drifts determines morphological seafloor changes that roughly coincide with the major physiographic provinces (Figs. 3.2, 3.4 and 3.9). Hydrographic sections indicate that these morphological changes match the near-bottom layer distribution of the MWs bounded by the most pronounced density contrasts (pycnoclines) (Figs. 3.4 and 3.9). It is inferred that the formation of the large plastered drifts on the Spanish and Moroccan slopes is influenced by the WIW+LIW and the WDMW, respectively, and the formation of sheeted drifts infilling basins is influenced by the WMDW. These morphosedimentary and hydrographic coincidences lead to propose that the regional physiographic configuration of the Alboran Sea is most likely related to alongslope bottom currents.

Seismic profiles indicate that the present-day physiographic configuration and the subbottom architecture of the large-scale drifts are similar throughout the Quaternary (Figs. 3.2 and 3.4). This fact allows to suggest a long-term, stable behaviour of the water masses or that there appears to be no significant changes in oceanographic model circulation. Also, all observed variability by oceanographers (e.g., seasonal, interannual) would not have significant effect in the long-term shaping of the continental margins. Nevertheless, their apparent not significant effect may simply reflect a poor interpretation because their importance cannot be resolved on the seismic profiles. The literature shows notable examples of the semi-quantitative inferences derived by geologists from the impact of ocean currents on the seafloor sediments, although the time span of most geological processes is quite different from the physical processes analysed by

oceanographers (Rebesco *et al.*, 2008). In this new scenario for the Alboran Sea, it is suggested that the seaward and the landward shifts of the coastline caused by the Quaternary glacioeustatic sea level changes (Ercilla *et al.*, 1994; Hernández-Molina *et al.*, 1995; Chiocci *et al.*, 1997; Lobo *et al.*, 2008) controlled sediment supply variations, but bottom currents transported and deposited sediments along the continental slopes and basins, developing basin-scale contourite drifts and shaping the seafloor morphology.
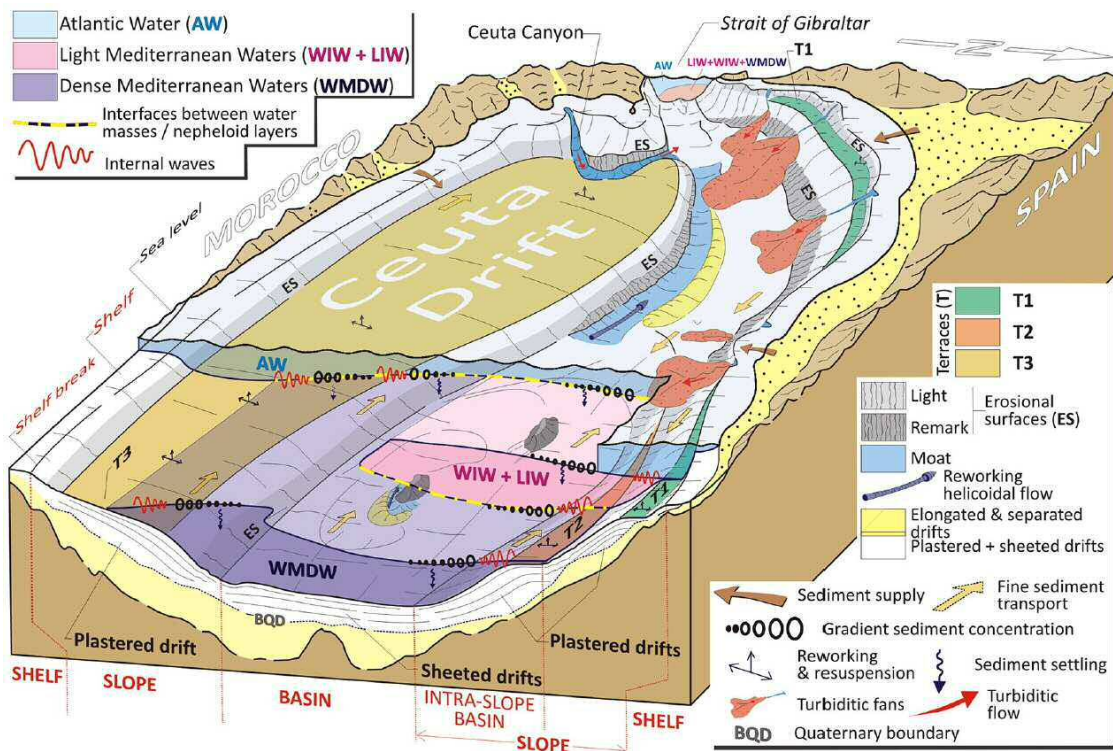
Fig. 3.9 - 3D sketch summarizing the new conceptual model of the effect of bottom-current processes on deep-sea sedimentation. The main characteristics of the depositional and erosive contourites, and the relevant water-masses (with simple and multiple current pathways) are shown, as are the hydrodynamic features governing margin sedimentation.

Some local studies of continental margins show that plastered drifts play an important role in shaping large sections of the continental slope and rise (e.g., Hebrides slope, Stoker *et al.*, 1998; NE Chatam rise, Wood and Davy, 1994; Brazilian upper slope, Viana *et al.*, 2002; Norwegian continental slope, Laberg *et al.*, 1999; Western Spitsbergen continental slope, Rebesco *et al.*, 2013; further examples in Hernández-Molina *et al.*, 2008a,b). Additionally, large deep-sea basins and abyssal plains from the southern and northern hemispheres and equatorials have shown to be shaped by huge plastered and sheeted drifts formed under active bottom water-masses (e.g., Weddell, Scotia, Jane, Powell Basins,

Maldonado *et al.,* 2003, 2006; Rockall Trough, Faugères and Stow, 1993; Silver and Nares Abyssal Plains, Tucholke, 2002).

Physiographic components in continental margins have typically been defined by their structural style, sedimentary and geologic histories (Bouma, 1979). Attempts to categorize the morphological variability of passive siliciclastic margins (O'Grady *et al.,* 2000) have established that differences are governed by the modern sedimentary environment. Based on the results of this study, together with examples from other continental margins, it is suggested that bottom currents are, globally, also a fundamental factor governing the physiographic configuration of continental margins.

4.2. Water-mass interfaces sculpt regional contourite terraces

Contourite terraces are distributed on a regional scale (Table 3.2) and coincide with the present water depth range of various water-mass interfaces: terrace T1 with the AW/WIW+LIW interface, terrace T2 with the WIW+LIW/WMDW interface and terrace T3 with the AW/WMDW interface (Figs. 3.4 and 3.8). As these interfaces are not horizontal surfaces, the terrace water depth locations are different for the Spanish and Moroccan margins. The interfaces represent pycnoclines affected by several baroclinic activities that involve intense bottom currents (e.g., internal waves and tides) (e.g., McCave, 2001; Cacchione *et al.,* 2002). The internal-wave-induced dynamics may mobilize and re-suspend bottom sediments that are then laterally distributed by water-masses over the terraces (Pomar *et al.,* 2012; Shanmugam, 2013b). Fig. 3.8 reports clear evidence for internal wave occurrences over T1 and T3, coinciding with erosional seafloor characteristics of a proximal and/or nearly flat sector of terraces, which denotes a dynamic environment. For T1, Ercilla *et al.* (1994) and Hernández-Molina *et al.* (1995) defined a near-surface alongslope belt of coarse to fine sands extending from the shelf breakdown to approximately 400 m w.d., and Puig *et al.* (2004) demonstrated the effects of internal waves on the formation of nepheloid layers along the terrace. For T2, Masqué *et al.* (2003) defined silts and sandy silts down to approximately 50 cm below the seafloor. All these terraces can be identified throughout the Quaternary sedimentary record in the seismic profiles (Fig. 3.4), suggesting that the action of water-mass interfaces sculpting terraces has been important in different geological time spans, from the present-day to the period scale.

The Atlantic and Mediterranean water mass circulation and spatial fluctuations in water-mass interfaces have been controlled by the high frequency and amplitude glacioeustatic sea level variations (orbital-eccentricity/obliquity/precession variability)

during the Quaternary (e.g., Voelker *et al.,* 2006; Rogerson *et al.,* 2011; Hernández-Molina *et al.,* 2014). These sea level variations would have provoked vertical and lateral variations of the interfaces and the associated oceanographic processes (e.g., internal waves) (Figs. 3.8 and 3.9), determining the dominant erosional processes in the inner terrace sectors and the deposition processes in the distal sectors (Fig. 3.4). This matches the model of Preu *et al.* (2013) for the Argentina continental margin, in which the authors proposed that the large contourite terraces along the upper, middle and lower continental slope and continental rise (500–3500 m w.d.) are conditioned by short- and long-term variations in the interfaces of regional water-masses. They also proposed that interfaces, associated processes (internal waves) and interface variations have favoured the development of contourite terraces because of enhanced turbulence.

4.3. Obstacles are essential to local water-mass distribution and associated bottom currents

The distribution of small-scale drifts and related erosive features as moats and channels is associated, throughout the Quaternary, with obstacles such as seamounts, the Alboran Ridge and related adjacent features (the Alboran Trough and the SAB). There are many examples of contourites associated with seafloor topographic highs in the Atlantic and Mediterranean (e.g., Hernández-Molina *et al.,* 2006a; Stow *et al.,* 2008; Van Rooij *et al.,* 2010; Ercilla *et al.,* 2011). Highs (rounded and linear) act as obstacles, which produce streamline distortions, creating water-mass branches with multiple current dynamics that can winnow, distribute, erode, and rework the near-surface (e.g., Kennett, 1982; Faugères *et al.* 1999; García *et al.,* 2009). The WIW + LIW and the WMDW encounter obstacles such as seamounts and the Alboran Ridge, producing isopycnal domings that create turbulence and faster flows (branches and eddies) along the sides of the obstacles. These processes are in turn responsible for the moats associated with separated and confined drifts at the foot of high walls, as well as the plastered and sheeted drifts along their walls (e.g., Kennett, 1982; Hernández-Molina *et al.,* 2006b; Ercilla *et al.,* 2011) (Figs. 3.2 and 3.4a). Hence, the WMDW is topographically steered by seamounts and the Alboran Ridge. This steering (aided by the occupation of the Spanish slope by the WIW + LIW) constrains the core and holds it against the Moroccan margin, and splits the WMDW into three faster branches which form a) small-scale plastered drifts on the Spanish base of slope; b) channel-related drifts in the Alboran Trough; c) contourite channels in the Alboran Through and the structural corridor between the Moroccan margin and the Xauen Bank (Al Hoceima Valley); and d) a separated drift and furrows in the basin at the foot of Moroccan slope (Fig. 3.2).

4.4. A model for deep-sea sedimentation in the Alboran Sea

In this study a new model to explain deep-sea sedimentation in the Alboran Sea is proposed (Fig. 3.9). When sediments from the continent reach the sea, the AW (i.e., Atlantic Water) quickly disperses the sediment in suspension over a large area, and the WIW+LIW and the WDMW subsequently transport and deposit it along the slopes, base of slope, basins and seamount flanks. The AW/WIW + LIW and the LIW/DMW interfaces in the Spanish margin and the AW/WDMW interface in the Moroccan margin form superimposed nepheloid layers by settling processes (McCave, 1986; Preu *et al.*, 2013). These layers represent the major regional transport path of fine-grained sediment at different water depths, with sediments deposited laterally and basinward, with a dominant alongslope component. Therefore, particles in the Alboran Sea may be transported over long distances before they are deposited. For example, particles arriving from the continent at the Spanish margin are pirated by the western Atlantic anticyclonic gyre, increasing their concentrations towards the gyre's centre (Fabrés *et al.,* 2002).

Interface-generated turbulence processes (e.g., internal waves) and local bottom-current enhancements caused by seafloor irregularities cause bottom currents to re-suspend seafloor sediment (e.g., Pomar *et al.,* 2012; Shanmugam, 2013b). This sweep and winnow of the seafloor may also feed sediment to the nepheloid layers. Fabrés *et al.* (2002) suggested a significantly deep advective input of particles by nepheloid layers stirred by near-bottom layers. Deposition occurs when current velocities decrease, causing rapid settling of suspended particles and contourite drift formation. Large-scale velocity variations along current pathways are related to semi-enclosed margin and basin morphology, Coriolis forces push currents towards the Spanish margin and major seafloor irregularities (e.g., the Alboran Ridge). Additionally, small scale drifts can result from local primary deposition, when topography varies the velocity of an impinging water-mass, or from the reworking of the seafloor by bottom currents. In this case, sediments are primarily deposited near the eroded source area (see Hernández-Molina *et al.,* 2008a).

According to the new integrated model, most of present-day sedimentary processes and their morphosedimentary products in the Alboran Sea resulted from bottom-current processes. The conclusions are corroborated by reports of this phenomenon in other European and South American margins (Hernández-Molina *et al.,* 2011a,b; Rebesco *et al.,* 2013; Preu *et al.,* 2013). The absence of turbidite systems in most of the Moroccan margin (Fig. 3.2) remains unexplained, although Atlantic and Mediterranean alongslope processes could provide a useful proxy, especially during cold periods with an enhanced WMDW. A

possible explanation is that sediment piracy by the AW and the WMDW in the Moroccan margin would avoid the convergence of sediments from Moroccan rivers, inhibiting the local occurrence of erosive gravity flows. Further research and data are required to confirm this hypothesis.

The proposed mechanism offers a more integrated model of deep sea sedimentation, because it highlights the value of further studies on the influence of bottom currents and associated processes in advancing the knowledge of the ocean's physiography, morphology and sedimentary evolution. Understanding the influence of bottom currents is essential, not only for reconstructing present and past water-mass circulation, but also in modelling seafloor shaping and controls for sedimentary stacking patterns in continental margins and deep basins. Additionally, this study highlights the importance of a multidisciplinary approach to future studies of deep-sea sedimentation.

Chapter IV - Seismic evidence of current-controlled sedimentation in the Alboran Sea during the Pliocene and Quaternary: Palaeoceanographic scenarios

Chapter IV - Seismic evidence of current-controlled sedimentation in the Alboran Sea during the Pliocene and Quaternary: Palaeoceanographic scenarios

1. Introduction

This Chapter is focused on the seismic stratigraphic analysis of the Pliocene and Quaternary sequences, to demonstrate the widespread dominance of bottom-current processes in the Alboran Sea, since the opening of the Strait of Gibraltar.

The general aims of this chapter are:

> To improve the Pliocene and Quaternary seismic stratigraphy, as well as updating and renaming the stratigraphic boundaries, to obtain a straightforward nomenclature after the relocation of the base of the Quaternary from 1.8 to 2.6 Ma.
>
> To analyse the seismic and architectural evidence indicating the presence of contourite features.
>
> To determine the sedimentary and palaeoceanographic significance of contourite features.
>
> To establish the factors controlling contourite sedimentation.
>
> To infer the main flow pathways in order to propose the main scenarios for ocean circulation since the opening of the Strait of Gibraltar.

The seismic stratigraphy analysis of the sedimentary deposits is based on the study of the seismic database acquired during various campaigns in the last decades (Fig. 5.1). Five N-S seismic composite profiles based on single-channel (airgun and sparker) and multi-channel seismic lines have been assembled to facilitate the identification of contourite deposits through various environments along the Alboran Sea (Fig. 4.1). These composite profiles range from the deepest area in the east, towards the comparatively shallower WAB, near the Strait of Gibraltar.
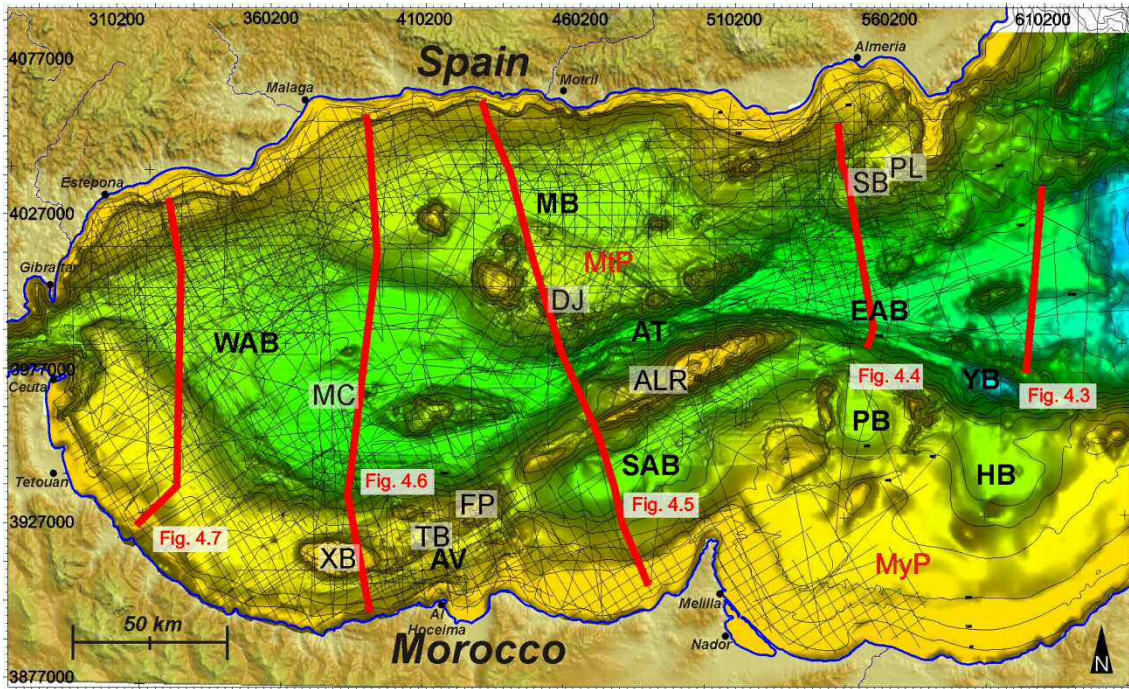
Fig. 4. 1 - Bathymetric map of the Alboran Sea, including the seismic line database and the location of Figs. 4.3-4.7. The basins (AT-Alboran Through; EAB-Eastern Alboran Basin; WAB-Western Alboran Basin; YB-Yusuf Basin), the intra-slope basins (AV-Al Hoceima Valley; HB-Habibas Basin; MB-Motril Basin; PB-Pytheas Basin; SAB-Southern Alboran Basin) and selected seamounts (ALR-Alboran Ridge; DJ-Djibouti Bank; FP-Francesc Pagès Bank; MC-Maria del Carmen Seamount; PB-Pollux Bank; SB-Sabinar Bank; TB-Tofiño Bank; XB-Xauen Bank) and plateaus (MtP-Motril Plateau; MyP-Moulouya Plateau) are indicated in the figure.

2. Pliocene and Quaternary seismic stratigraphy

2.1. Regional stratigraphic boundaries

Following previous local, regional and global criteria (see Fig. 4.2), the following stratigraphic boundaries to constrain the ages of the Pliocene and Quaternary deposits have been used (Figs. 4.3-4.7): a) Messinian (M boundary, 5.96 to 5.33 Ma), b) intra-lower Pliocene ($P0$ boundary, *ca.* 4.5 Ma), c) top of the Zanclean ($P1$ boundary, *ca.* 3.3 Ma), d) base of the Quaternary (BQD boundary, *ca.* 2.6 Ma), e) top of the Gelasian ($Q0$ boundary, *ca.* 1.8 Ma), f) intra-lower Quaternary ($Q1$ boundary, *ca.* 1.12 Ma), and g) top of the Calabrian ($Q2$ boundary, *ca.* 0.7 Ma). Table 4.1 shows these new names and their correlations with their previous counterparts as presented in the literature.
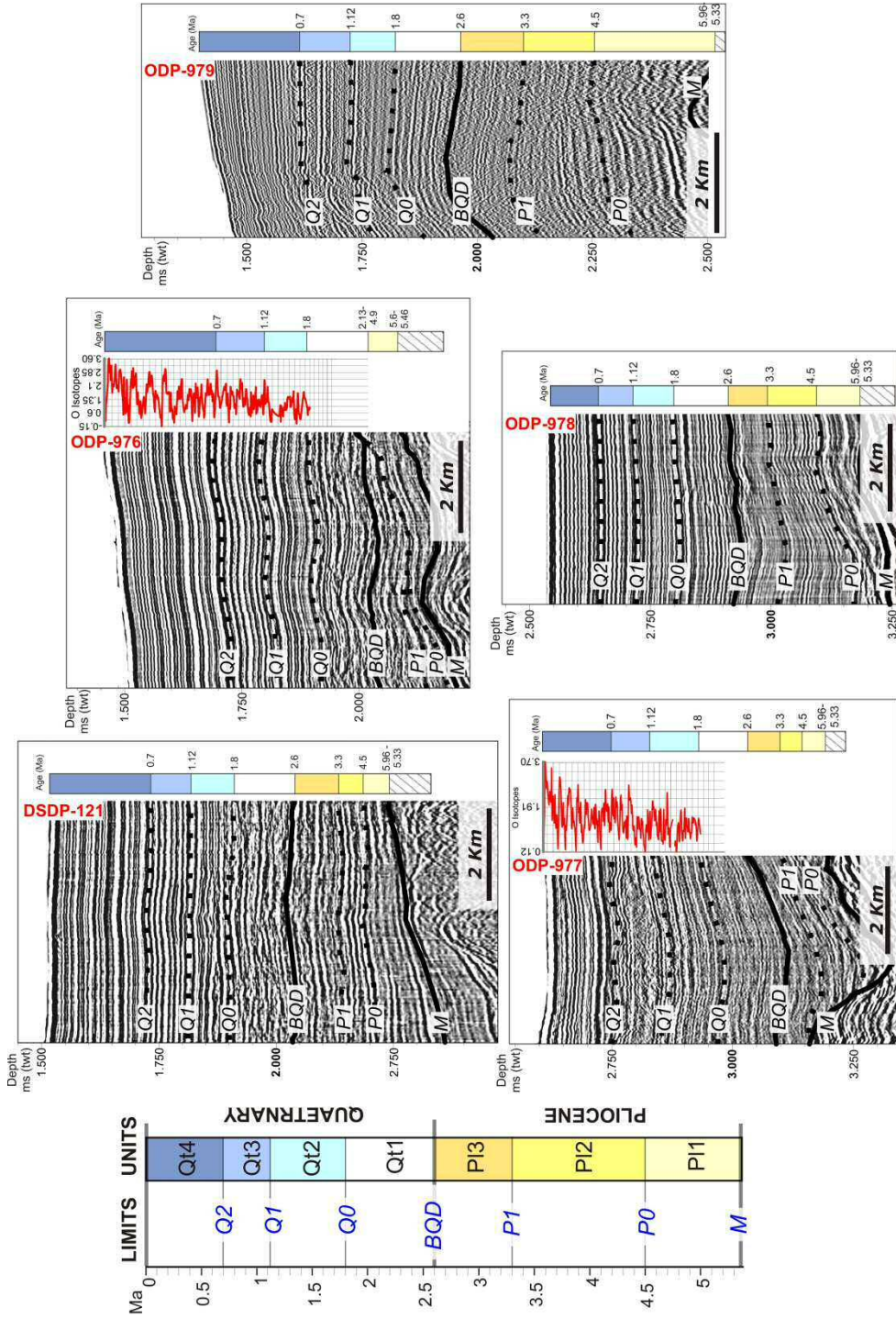
Fig. 4. 2 - Selected portions of seismic lines crossing the locations of the DSDP 121 and ODP 976, 977, 978 and 979 sites, showing the vertical stacking of the Pliocene and Quaternary units and the available δO¹⁸ curves (ODP 976 and 977). The M and BQD reflectors limiting the Pliocene (in yellow) and Quaternary (in blue) sequences are represented in black, whereas the internal boundaries are represented with dashed lines.

The results have been compared with tectonic/sedimentary reflectors in the central and eastern Alboran Sea, as identified by Martínez-García *et al.* (2013), and with the diverse results from other local, regional and global-scale studies (Comas *et al.,* 1996; de Kaenel *et al.,* 1999; Fauquette *et al.,* 1999; González-Donoso *et al.,* 2000; Becker *et al.,* 2005; Lisiecki and Raymo, 2005, 2007; Hayward *et al.,* 2009; Miller *et al.,* 2011; Martínez-García *et al.,* 2013; Hernández-Molina *et al.,* 2014; Rohling *et al.,* 2014) (Fig. 4.8).

The ***M boundary*** is the most prominent and easily recognizable erosional surface on the seismic record due to the frequent truncated reflections and striking erosional character. This surface is a polygenetic product of processes active during different stages of the Messinian salinity crisis. A recent work by Estrada *et al.* (2011) mapped several types of erosional features, including terraces, subaerial canyons and a prominent channel that crosses the entire central Alboran Basin (Figs. 4.3A; 4.6B, C; 4.7B, C).

The remaining seismic boundaries share similar characteristics: discontinuities along the margins and basins that transition laterally to correlative stratigraphic surfaces. The discontinuities include surfaces with reflections truncated to various extents, as well as onlap and downlap terminations primarily located on the western and eastern Spanish and eastern Moroccan upper continental slopes (Figs. 4.3B; 4.5A, C, D; 4.6A; 4.7C). The onlap and downlap surfaces are also particularly evident in a) palaeotopographic depressions that are close to and on the walls of certain seamounts (e.g., the Provençaux), b) on the Alboran Ridge, c) along tectonic structures (e.g., the La Serrata fault), d) on diapiric ridges, and e) on the northern WAB (Fig. 4.6C; Fig. 4.7C). Laterally, these discontinuities change seaward into continuous surfaces.

The ***P0 boundary*** corresponds to a hiatus at sites ODP 976 and 977 (Siesser and de Kaenel, 1999) and coincides with an event of colder temperatures or greater ventilation in the deep waters (Suc and Zagwijin, 1983; Suc *et al.,* 1995; Fauquette *et al.,* 1999; Hayward *et al.,* 2007, 2009). Regional tectonic studies (Martínez-García *et al.,* 2013) have established about 4.57 Ma as being the end of the first shortening phase in the Alboran Basin during the Plio-Quaternary.

The ***P1 boundary*** also appears as a sedimentary hiatus at ODP 976 (Siesser and Kaenel, 1999), coinciding with a cooling event at about 3.3 Ma (Scott *et al.,* 2007) that is the coldest and sharpest one in the δO^{18} register for the entire Pliocene sequence. Regional geologic studies have also recognized an important unconformity of comparable age, probably caused by the uplift of the margins, due to the onset of the second phase of shortening in the Alboran Basin (Martínez-García *et al.,* 2013 and references herein).

Series Epoch	Stage Age	Sequences	Units	Seismic boundaries	Campillo et al., 1992	Jurado and Comas, 1992	Ercilla, 1992	Pérez-Belzuz et al., 1997	Pérez-Belzuz, 1999	Hernández-Molina et al., 2002	Campillo et al., 1992	Pérez-Belzuz, 1999	Other
Quaternary / Pleistocene — Holocene		Qt	4		Seq. 1	Subunit Ia	S.3	Ia	Ct3	Q-II			
	Tarantian (Upper)						S.2						
	Ionian (Middle)			Q2									(Ercilla, 1992) Q2-MPR
	Calabrian (Lower)		3	Q1			S.1		Ct2	Q-1	Q1	B	
			2	Q0	Seq. 2			Ib	Ct1		P2		
	Gelasian (Lower)		1	BQD	Seq. 3	Subunit Ib		Ic	Pl3	P3		A	(Hernández-Molina et al., 2002) UPR
Pliocene	Piacenzian (Upper)	Pl	3	P1					Pl2	P2-II	P1		
										P2-I			
	Zanclean (Lower)		2	P0	Seq. 4			Id	Pl1	M/P1			(Ryan et al., 1973) M
			1	M									

Table 4. 1 - Correlation of the stratigraphy resulting from this study (left) and the most relevant Pliocene-Quaternary stratigraphies of the Alboran Sea area (centre and right).

The *BQD* (Base of Quaternary Deposits) **boundary** is determined by the first major continental glaciation in the Northern Hemisphere (2.6 Ma), which caused an important sea level fall (Lowrie, 1986; Haq *et al.*, 1987; Morrison and Kukla, 1998). In the Alboran Sea, this event roughly coincides with the end of the uplift in the SW sector of the Alboran Ridge (Martínez-García *et al.*, 2013) and matches the sedimentary hiatus at ODP 979 (Siesser and de Kaenel, 1999). Climatic studies also indicate an enhanced dust deposition in the Mediterranean, evidencing the onset of the Sahara aridification at the marine isotope stage (MIS) 100 (2.5 Ma) (Becker *et al.*, 2005).

The *Q0* **boundary** coincides with a shift to colder sea surface temperatures (SST) in the western Mediterranean (Linares, 1999; González-Donoso *et al.*, 2000) and is also coincident with the onset of the last shortening event in the Alboran Basin at about 1.81 Ma (Martínez-García *et al.*, 2013).

The *Q1* **boundary** corresponds to the MIS 34 (1.12 Ma). According to global climate studies, the onset of the Middle Pleistocene Transition occurs at that time, which is

characterized by a progressive shift from 41 ky to 100 ky orbital cycles (Head *et al.*, 2008) and is close to the end of the last shortening event in the Alboran Basin that occurred at about 1.19 Ma (Martínez-García *et al.*, 2013). Although in the different DSDP and ODP sites this boundary exhibits no evidence of erosion or non-deposition, seismic stratigraphic studies show a regional erosional event in the westernmost Alboran Sea (Tesson *et al.*, 1987; Ercilla *et al.*, 2002).

Finally, the **Q2 boundary** corresponds to the MIS 17, at about 700 ky (Comas *et al.*, 1996; de Kaenel *et al.*, 1999). The climatic studies by von Grafenstein *et al.* (1999) indicate that the strong influence of the 100 ky glacial-interglacial cycles occur at approximately this same time in the Alboran Sea. However, this boundary can also roughly correlate with the tectosedimentary unconformity at ca. 0.79 Ma, as defined by Martínez-García *et al.* (2013), in the central and eastern Alboran Sea.

2.2. Pliocene sequence

The Pliocene sequence overlies the prominent erosional *M* boundary and is bounded on top by the *BQD* boundary. Its deposits comprise parallel and subparallel seismic reflections with scattered reflections of high continuity and low-to-medium acoustic amplitude (Figs. 4.4A, B; 4.5D). The highest acoustic responses are recorded in the uppermost Pliocene (Figs. 4.4A; 4.5D; 4.6B, C; 4.7C). Semi-transparent facies are also present. The lateral continuity of the most frequent Pliocene facies (parallel and subparallel stratified facies) is locally interrupted by various facies such as discontinuous, stratified, sigmoidal and oblique stratified, chaotic and transparent facies. Their geometries vary between wedge, lenticular, mounded and irregular configurations (Figs. 4.3A, B; 4.4B; 4.5A; 4.6D; 4.7B). Locally, undulating stratified facies with kilometre-scale wavelengths are also present in the WAB infill and in the SAB (Fig. 4.5A). The deposits are interrupted by numerous structural features such as the Alboran Ridge, other topographic highs and faults (Figs. 4.4-4.6).

The Pliocene deposits range from 0 to 1280 ms thick (twtt) (Fig. 4.9A), generally thinning towards the east. The distribution is irregular and corresponds to several depocentres that dot the margins and basins. The maximum accumulations are located in the basins (700 to 1000 ms), primarily in the WAB and the westernmost Moroccan margin (800 to 1280 ms) near the Strait of Gibraltar. The minimum accumulations are located on structural highs (0 to 100 ms), in the westernmost Spanish margin (0-150 ms) and at the entrance to the Strait of Gibraltar (~100 ms).

114

The Pliocene sequence is internally divided by the *P0* and *P1* regional boundaries that define three seismic units (Fig. 4.2; Figs. 4.3-4.7; Table 4.1).

a) The *Pl1 unit* (Early Lower Pliocene) is bounded by the *M* and *P0* boundaries.

b) The *Pl2 unit* (Late Lower Pliocene) is bounded by the *P0* and *P1* boundaries.

c) The *Pl3 unit* (Upper Pliocene) is bounded by the *P1* and *BQD* boundaries.

The overall geometric configurations of the Pliocene sequence and their units are those of irregular subtabular alongslope sedimentary bodies (Figs. 4.6-4.7) and roughly wedge-shaped bodies in the orthogonal direction such that they pinch out upslope and locally downslope along the Spanish and Moroccan margins. Within the basin, these strata display an overall irregular subtabular geometry (Table 4.2).

Unit	Typical facies	Other remarkable facies	Architecture	Geometry	Remarks
Pl1	Parallel and subparallel stratified with low acoustic amplitude, semitransparent facies.	Subparallel with high reflectivity in central Spanish margin. Local acoustic anomalies in eastern Morocco margin.	Affected by the Messinian palaeotopography, strongly deformed by diapiric activity in the WAB.	Extensive subtabular unit in the WAB and the western margins. Irregular distribution and locally as isolated patches in other areas.	Very thin or absent in the eastern Alboran Sea. Evidences of tectonic activity in eastern Spanish margin.
Pl2	Parallel low to medium amplitude reflectors and highly stratified facies, locally convergent to the south.	Wavy facies is also present in the Morocco margin.	The unit concordantly drapes the previous unit and part of the pre-Messinian units in most cases, and show onlap on the sides of seamounts, scarps and upper slope.	Subtabular deposits fill the overall basin, with irregular patches and local mounded features infilling palaeoreliefs.	Changes in thickness associated to the presence of diapirs and faults.
Pl3	Laminar subparallel facies	Low to medium reflectivity on the base and increasing upwards	Mostly concordant with the Lower Pliocene sedimentary register, showing onlap on the sides of seamounts, scarps and upper slope and erosional surfaces.	Subtabular deposits covering the slopes and draping most of the basins, with mounded sedimentary patches infilling the remaining depressions and gaps between structural highs	Changes in thickness associated to tectonic structures are present (La Serrata fault system, diapirs).

Table 4. 2 - Description (facies, architecture, geometry) of the Pliocene seismic units.
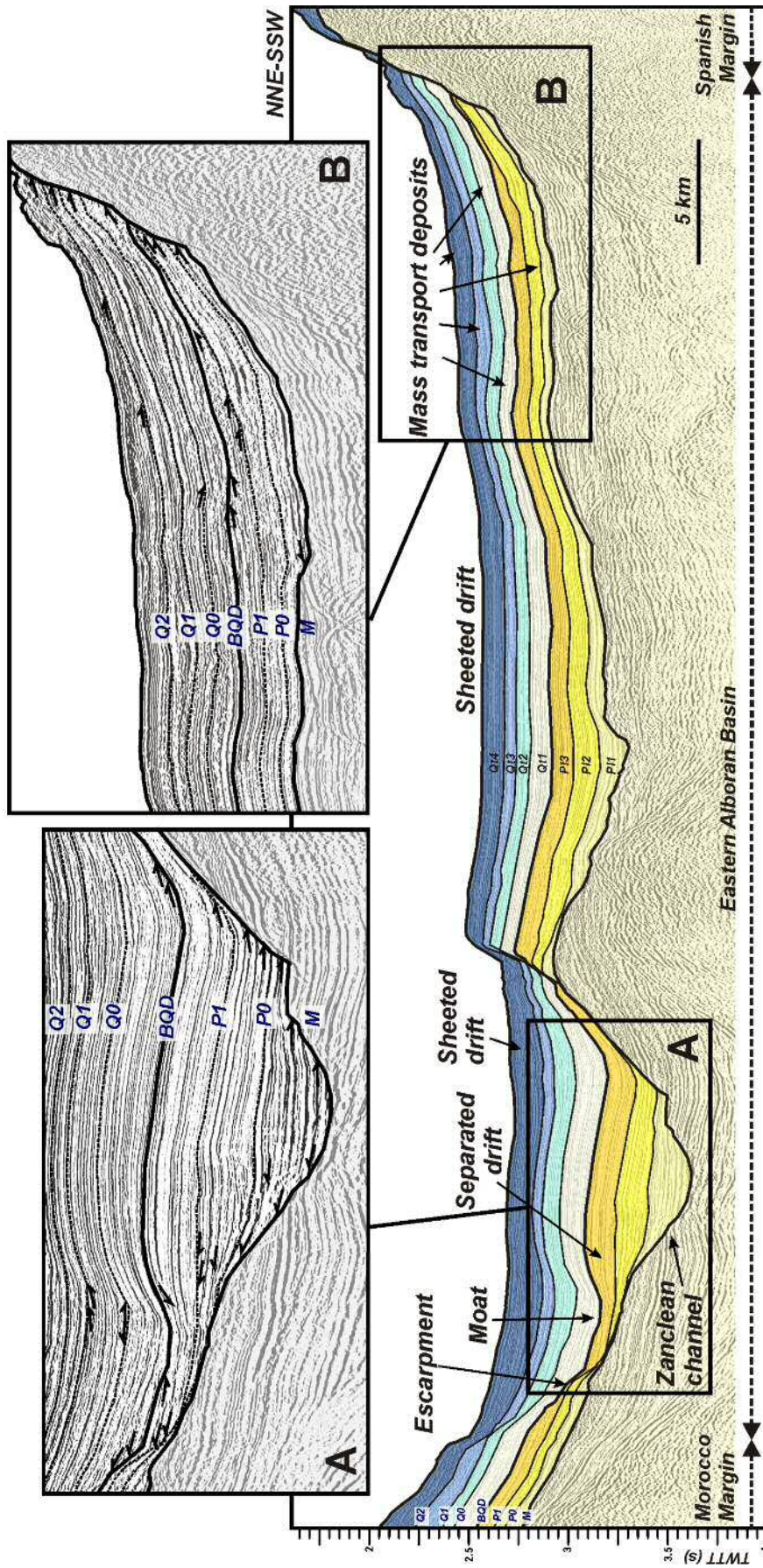
Fig. 4. 3 - Seismic profile in the eastern EAB. See Fig. 1 for location. The Pliocene sequence is represented in yellow and the Quaternary sequence is represented in blue. Unit names are shown in black, and boundary names are shown in blue. Inset A - Buried mounded elongated separated drift. Inset B - Mass movement deposits.

116
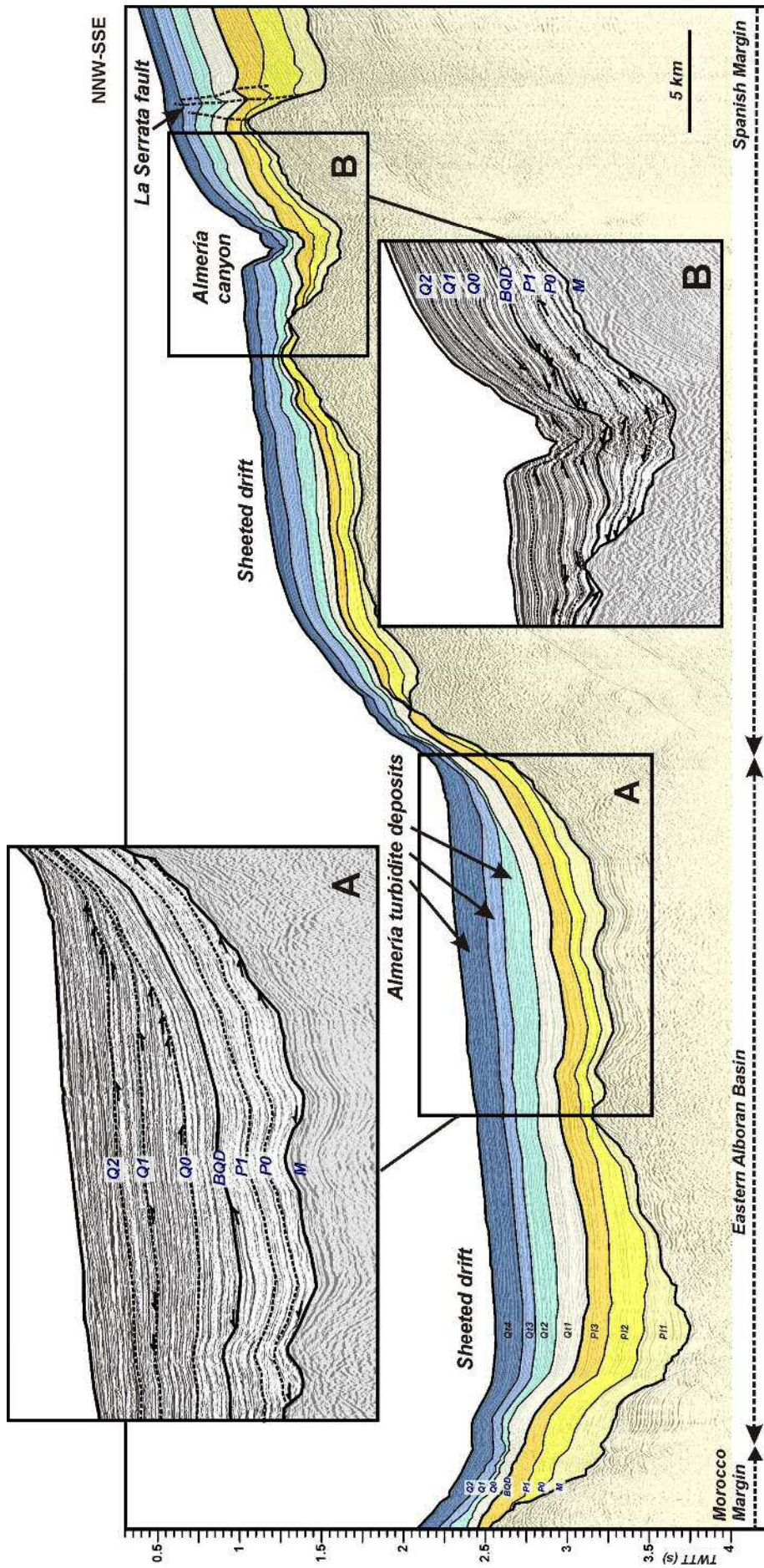
Fig. 4. 4 - Seismic profile in the western EAB. See Fig. 1 for location. Details are as described in Fig. 3. Inset A - Turbidite deposits. Inset B - Turbidite canyon.

117

2.3. Quaternary sequence

The Quaternary sequence overlies the BQD boundary and is bounded above by the seafloor. Its deposits are acoustically similar to the Pliocene sequence, although they generally display higher acoustic amplitudes (Figs. 4.3A; 4.4A, B; 4.5A, B, D; 4.7A, C). They are acoustically defined by parallel and subparallel stratified facies of medium-to-high acoustic amplitude and fill the overall basin (Figs. 4.3A; 4.5A, D; 4.6C; 4.7A). These facies are locally interrupted by reflections of higher amplitude, including discontinuous stratified, sigmoidal, oblique stratified, and chaotic facies with wedged, lenticular, mounded and irregular geometries (Figs. 4.3B; 4.4A, B; 4.7C). Similarly, although to a lesser degree than the Pliocene deposits, the lateral continuity of the Quaternary facies is interrupted by structural features. However, a few of the facies have been progressively draped, thereby totally or partially obliterating their morphology (Figs. 4.6; 4.7B).

The Quaternary sequence is thinner than the Pliocene deposits in the north-western part of the basin, and is not as strongly differentiated between the EAB and WAB (Fig. 4.9B). The Quaternary sequence ranges from 0 to 912 ms thick and shows several depocentres. The main depocentres are located along the Moroccan slope and in certain basins; the thickest (912 ms) is located in the SAB. Other substantial accumulations are observed along the western Moroccan (750 ms) and Spanish margins (up to 600 ms). The minimum accumulations are located on highs (0-150 ms) along the proximal Spanish and Moroccan margins (0-200 ms) and at the entrance to the Strait of Gibraltar (0-150 ms) (Fig. 4.9B). The depocentres along the margin display a more prominent longitudinal trend than those of the Pliocene (Fig. 4.9).

The sequence of Quaternary deposits is internally divided by the *Q0*, *Q1* and *Q2* boundaries, which define the following four seismic units (Figs. 4.2; 4.3-4.7; Table 4.1).

a) The *Qt1 unit* (Early Lower Quaternary) is bounded by the *BQD* and *Q0* boundaries.

b) The *Qt2 unit* (Early Lower Quaternary) is bounded by the *Q0* and *Q1* boundaries.

c) The *Qt3 unit* (Late Lower Quaternary) is bounded by the *Q1* and *Q2* boundaries.

d) The *Qt4 unit* (Middle and Late Quaternary) is bounded by the *Q2* boundary and the modern seafloor.

The overall geometry of the sequence and the internal units primarily display wedge shapes along the Spanish and Moroccan margins (Figs. 4.5A; 4.6D; 4.7A, B, C), subtabular shapes in the basin domains (Figs. 4.3; 4.5D; 4.6B, C), and mounded shapes at the bases

118

and walls of the seamounts and escarpments, on the Alboran Ridge, and in the Alboran Trough (Figs. 4.5C; 4.6A; Table 4.3).

Unit	Typical facies	Other remarkable facies	Architecture	Geometry	Remarks
Qt1	Slightly divergent and convergent oblique reflections in the margins that change into continuous stratified facies showing low-medium reflectivity at the base which increases upwards in the basins	Onlap terminations are observed in the upper margins, onto seamounts, scarps, and tilted Pliocene sediments. Downlapping reflections are observed seawards near the border of erosional scarps and seamounts	Sediments predominantly lay in concordance on the Pliocene sequence	Subtabular deposits draping the distal margins as well as most of the basins slightly wedged and locally sigmoidal in the upper margins, and mounded deposits at the base of structural highs	Still affected by diapiric activity
Qt2	Layered medium-amplitude reflections fill the overall basin, with onlap terminations on the upper margins, seamount walls, scarps, and tilted sediments	Downlap reflections appear locally associated to the distal margins, lensoidal and mounded geometries as well as scarps	Mostly concordant with the previous units	Wedge geometry in the margins, subtabular geometry dominates the basin and subbasin domains, mounded geometry remains confined to the vicinities of seamounts	Onset of progradation of the western margins
Qt3	Layered extensive reflections with medium to high acoustic amplitude increasing upwards	Onlap in the upper margins, scarps and seamounts. Downlap terminations are associated to scarps, distal margins and turbiditic systems in the basins	Mostly concordant with the previous units	Mounded and wedged geometries become more relevant and show higher reliefs. The distal margins, intra-slope basins and deep basins are characterized by subtabular geometry	Progradation of the western margins
Qt4	Highly aggradational pattern in the basins and progradational in the margins, with alternation of high and low amplitude reflectors in the western margins, WAB and MB	Reflections onlap in the upper margins, seamount walls and their vicinities, as well as in scarps.	Mostly concordant	The basins and subbasins are draped by subtabular deposits. Most continental slopes are characterized by wedged deposits with a low-angle erosive surface landwards and a high-angle erosional escarpment seawards. Locally, mounded deposits surround the bases of seamounts.	Wedged deposits in the western Morocco margin are wider than those of the Spanish margin

Table 4. 3 - Description (facies, architecture, geometry) of the Quaternary seismic units.

3. Seismic evidence of contourite features in the Alboran Sea

The detailed analysis of the Plio-Quaternary sediments in the Alboran Sea allowed us to identify seismic and architectural evidence indicating the presence of bottom-current-related features: i.e., contourite drifts and erosional features. These features are ubiquitous, interrupted only by TSs (primarily in the Spanish margin) and mass-wasting deposits (Figs. 4.3B, 4.4A, 4.6B, 4.7C), which have been widely reported in the literature (e.g., Ercilla *et al.*, 1994; Estrada *et al.*, 1997; Alonso *et al.*, 1999, 2014a; Alonso and Ercilla, 2003; García *et al.*, 2006; Casas *et al.*, 2011; Martínez-García *et al.*, 2013).
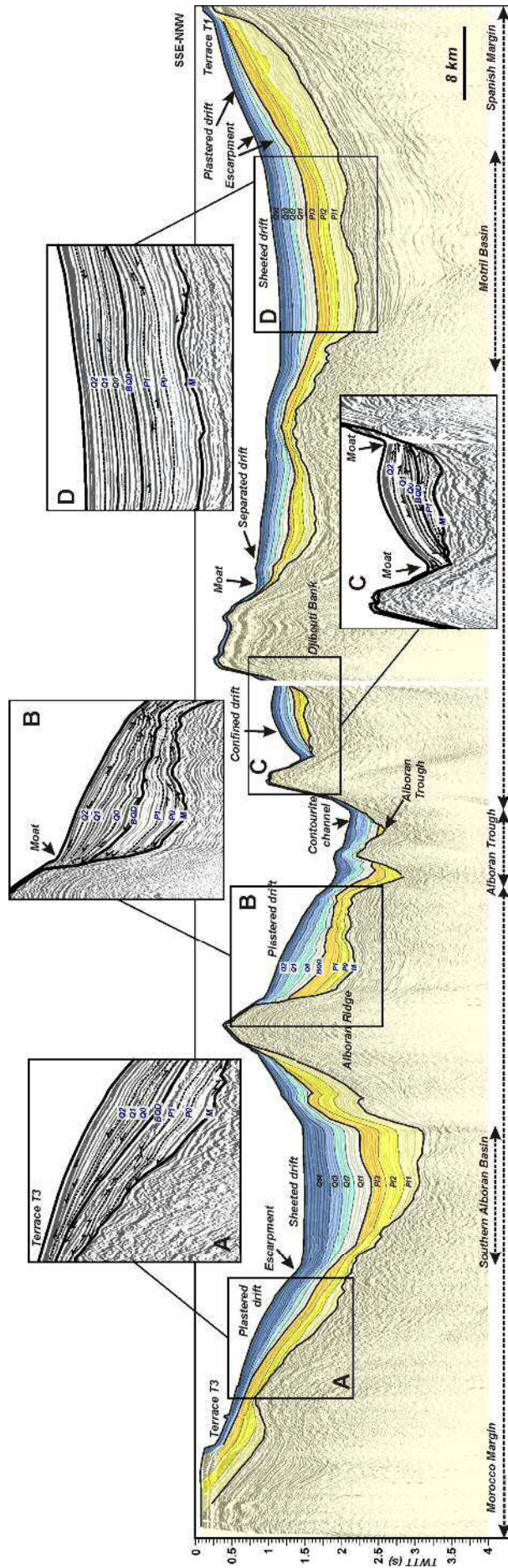
Fig. 4. 5 - Seismic profile in the central Alboran. See Fig. 1 for location. Details are as described in Fig. 3. Inset A - Terraced plastered drift. Inset B - Plastered drift with moat. Inset C - Mounded confined drift. Inset D - Sheeted drift.

120
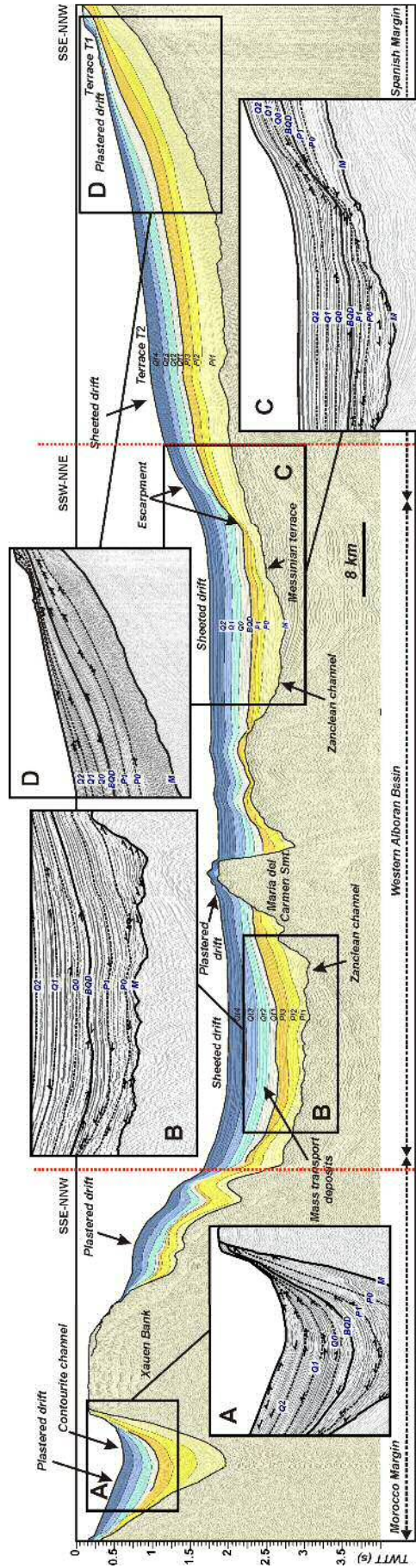
Fig. 4. 6 - Seismic profile in the eastern WAB. See Fig. 1 for location. Details are as described in Fig. 3. Inset A - Contourite channel and plastered drift. Inset B - Messinian erosional channel and mass movement deposits. Inset C - Messinian terrace and erosional channel, erosional escarpment, sheeted drift. Inset D - Terraced plastered drift.

3.1. Contourite drifts

The seismic and architectural evidence of contourite drifts includes the following:

a) Acoustic facies and discontinuities: Well-stratified deposits with upslope and downslope convergent configurations are present on the Spanish and Moroccan continental slopes and on steep areas of the highs (Figs. 4.5A, B, C; 4.6A, D; 4.7A, B, C). In these areas, the deposits display onlap (landward) and downlap (seaward) on stratigraphic discontinuities or continue basinward, displaying a sharp change in strata orientation. In the basins, the stratified facies primarily display a subhorizontal configuration (Figs. 4.5D; 4.6C).

b) Distribution: The facies display a predominantly longitudinal distribution, paralleling the continental margin and the primary alignments of the basins (Figs. 4.5A, B; 4.6D; 4.7A, B, C). This distribution is more evident in the Quaternary deposits (Fig. 4.9B).

c) Geometry: The geometry consists primarily of low to high mounded (Figs. 4.3A; 4.5C) and wedged shapes (Figs. 4.5A, B; 4.6D; 4.7A, B, C) both on the continental slope and on the walls and bases of the highs. In the basins, the geometry is subtabular, although deformed by tectonic features.

d) Facies architecture: The Pliocene and Quaternary deposits display a recurrent sedimentary stacking pattern. The results include an outbuilding pattern with slight progradation of the margins and an aggradational pattern in the subbasins (Figs. 4.5D; 4.6C). The stacking shows variations between the two margins, with major progradation along the Morocco margin, and between the two main basins, with greater aggradation in the WAB.

These characteristics suggest that the most extensive drifts can be classified (Faugères *et al.,* 1999; Rebesco, 2005; Rebesco *et al.,* 2014) as either *plastered drifts*, which accumulated extensively on the relatively steep seafloor of the Spanish and Moroccan continental slopes and morphologic highs, and *sheeted drifts*, which infill the broad areas of the basins. Locally, to a minor extent there are also *elongated separated* and *confined mounded drifts* at the bases of the morphologic highs or escarpments, and plastered and sheeted drifts on the walls/tops of highs and the Alboran Ridge (Fig. 4.5B).
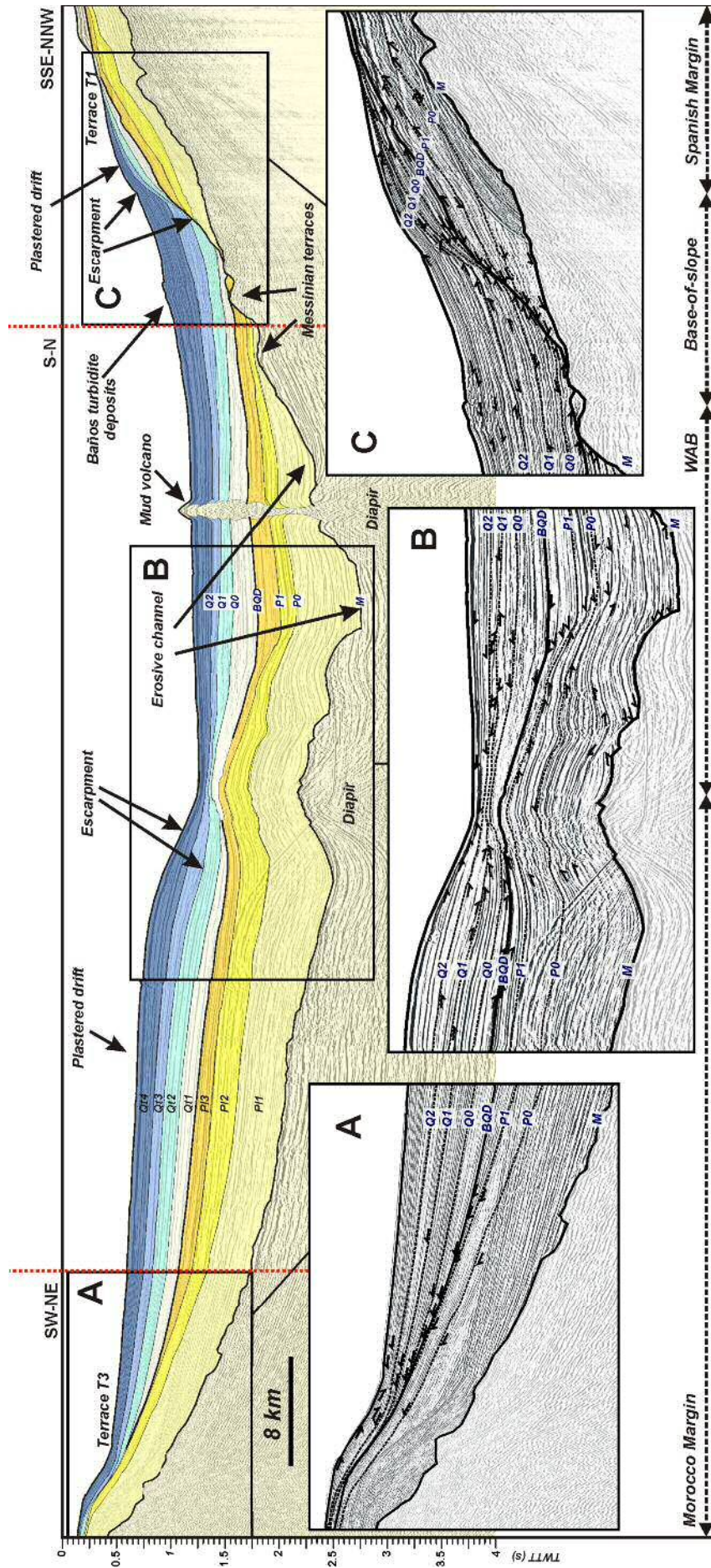
Fig. 4. 7 - Seismic profile in the western WAB. See Fig. 1 for location. Details are as described in Fig. 3. Inset A - Upper terrace in the Ceuta plastered drift. Inset B - Lower terrace and erosional escarpment in the Ceuta plastered drift, and Messinian erosional channel. Inset C - Terraced plastered drift, erosional escarpment, Messinian terrace and turbidite deposits.

3.2. Contourite erosional features

Erosional contourite features display an alongslope (from a few to tens of kilometres in length) distribution and are primarily characterized by laterally confined aggrading and slightly upslope-migrating discontinuous stratified and chaotic facies, that parallel the continental margin or the primary alignments of the basins (Fig. 4.6D). Moreover, their facies architecture indicates that most of them are closely associated in space and time with the drifts, displaying a recurrent sedimentary pattern through the Pliocene and Quaternary sequences (Figs. 4.6C, D; 4.7C).

Based on the classifications of Hernández-Molina *et al.* (2006a, 2014) and García *et al.* (2009), the erosional features consist of terraces (Figs. 4.4; 4.5A; 4.6C, D, 4.7A, B, C), escarpments (Figs. 4.6C; 4.7B, C), moats (Fig. 4.5C) and channels (Figs. 4.3A; 4.6A). Two types of *contourite terraces* can be distinguished based on their horizontal and vertical distribution: (i) terraces affecting the *M* boundary on the Spanish western continental slope and adjacent WAB (Estrada *et al.,* 2011), progressively obliterated by Pliocene strata (Figs. 4.6C; 4.7A, C); and (ii) terraces that shape the continental slope plastered drifts comprising the Pliocene and Quaternary units of the Spanish and Moroccan margins (Figs. 4.5A; 4.6A, D; 4.7A, B, C). These terraces are more pronounced and larger in the Quaternary units and on the Moroccan continental slope (see also Chapter III).

Contourite escarpments are located primarily in the western portion of the Alboran Sea, seaward of the Spanish and Moroccan continental slope terraces. The Pliocene units are affected by a prominent escarpment (Figs. 4.6C; 4.7C) on the lower continental slope of the western Spanish side. Such escarpment is lacking on the Moroccan margin. Based on the geometry of the Quaternary units, this escarpment continues to the Spanish side, and a new escarpment appears on the Moroccan slope that is located seaward of the present-day plastered terraced drift (Fig. 4.7B).

Contourite moats are mostly located at the bases of structural highs, paralleling their trend, and are associated with elongated separated drifts (Fig. 4.5C). Their laterally confined chaotic facies aggraded and migrated slightly upslope. Two contourite *channels* developed within the structural corridor of the Alboran Trough and between the Moroccan margin and the Xauen Bank (Fig. 4.3A; 4.6A).
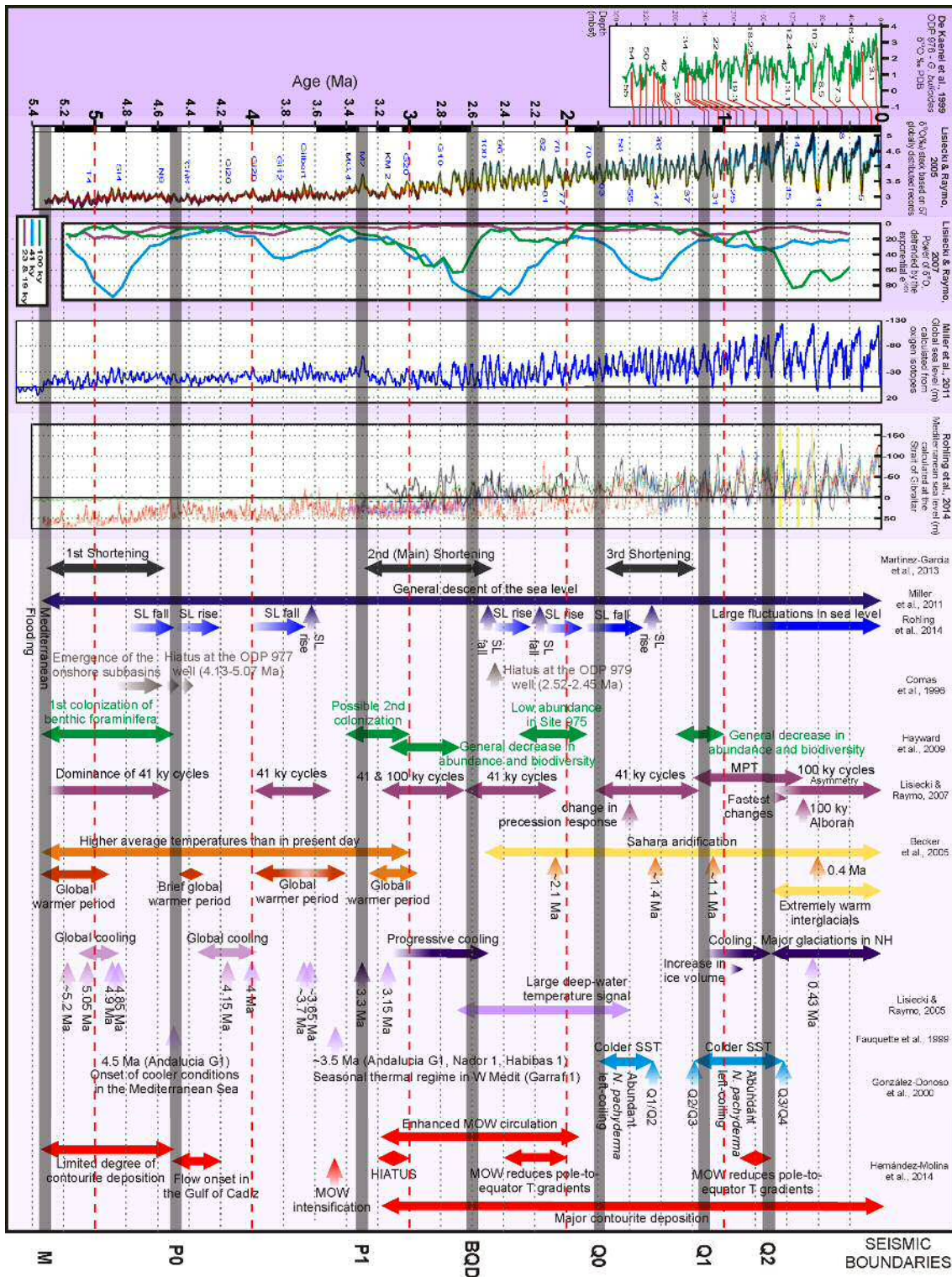
Fig. 4. 8 - Regional and global curves providing information about climatic and sea level fluctuations and events and trends (tectonic, sea level shifts, hiatus, biostratigraphic, orbital, palaeoclimatic and palaeoceanographic) that are useful for reconstructing the sedimentary history of the Alboran Sea.

4. Discussion

4.1. Sedimentary and palaeoceanographic significance of bottom-current features

The nature of Plio-Quaternary bottom-current features in the Alboran Sea leads us to propose new deposition models for the Alboran Basin.

The *longitudinal distribution* of the drifts (Fig. 4.9) differs substantially from that of other marine deposits in which their spatial distribution is related to point sediment sources, such as TSs or mass movement deposits previously mapped in the Alboran Sea (Ercilla *et al.*, 1992; Estrada *et al.*, 1997; Pérez-Belzuz, 1999; Alonso and Ercilla, 2003; García *et al.*, 2006; Lobo *et al.*, 2006; Casas *et al.*, 2011). Thickness variations in plastered and sheeted drifts appear to be independent from the location of the hinterland sediment sources (rivers) and submarine canyons and gullies (Figs. 4.4B; 4.7C). Thus, the distribution of the sediments that comprise these drifts is consistent with a sediment transport direction that is parallel to the margin, i.e., one with an alongslope trend. This dominant alongslope transport and related sedimentation is attributed to the stratified water masses of the Alboran Sea during the Pliocene and Quaternary. In addition, where alongslope flow was enhanced by topographic highs, it created local drifts paralleling the main trends of the highs as follows: elongated, separated and confined drifts at the bases of the highs (Fig. 4.5C) and small-scale, plastered and sheeted drifts on their walls and summits (Figs. 4.4, 4.5B).

The *mounded geometry* of the drifts is related to the action of the Coriolis force on the MWs, which forces them against the slope seafloor or against seamount walls, thereby favouring a lateral velocity gradient that decreases away from the slope. Generally, the geometry of the drifts varies vertically from low mounds and wedges during the Pliocene to high mounds since the Early Quaternary (Fig. 4.5C). This variation could be explained by the deep burial of the Pliocene drifts and their compaction and/or to their development under slower or weaker current regimes, with deposition tending to carpet the slopes. Considering that the lower development of the Gulf of Cadiz CDS at the other side of the Strait of Gibraltar in Pliocene times has been related with a weaker Mediterranean Outflow Water (Hernández-Molina *et al.*, 2016), the second interpretation might more likely be the cause.

Facies architecture in plastered drifts and sheeted drifts indicates that the action of the water masses on deposition was continuous during the Pliocene and Quaternary. Indeed, the deposits directly overlying the M boundary are mostly plastered and sheeted drifts

that remain active (Figs. 4.6D; 4.7B, C). This continuous action generated a stratigraphic architecture defined mostly by the stacking of contourites separated by stratigraphic discontinuities and correlative continuities. This stratigraphic architecture has two palaeoceanographic implications both for the water masses that contributed to its development and for the Pliocene and Quaternary stratigraphic boundaries.

First, because the facies architecture reflects the long-term, stable behaviour of the water masses, the flow direction can be inferred, relative current strength and distribution of past water masses were roughly similar to those of the present. Therefore, the large-scale Pliocene and Quaternary contourite drifts developed due to the action of palaeo MWs via the alongslope currents of the light (LMW) and dense (DMW) waters, both flowing towards the Strait of Gibraltar, after the opening of the strait and the consequent Atlantic flooding (Figs. 4.3, 4.7). The higher-salinity light waters (today consisting of WIW+LIW and flowing between 100 to 600 m) contributed to the deposition of the plastered drifts on the open areas of the Spanish continental slope (these plastered drifts are located on the present seafloor at 90-115 m to depths of 600 m). The relatively colder dense waters (today consisting of WMDW and flowing at depths > 275 m) deposited the plastered drifts on the Moroccan slope (these plastered drifts are located on the present seafloor at 100-150 m to depths of 900 m) and the sheeted drifts of the basins (900 to 1,980 m) (Figs. 4.4, 4.5D) (see Chapter III).

Second, this uninterrupted action of the water masses on the seafloor also has palaeoceanographic implications for the seismic boundaries that divide the Pliocene and Quaternary deposits. Now, with the new results of this study showing the ubiquitous contourites in the Alboran Basin, it is suggested that the regional boundaries defined here are the expression of variations in the bottom-current circulation and characteristics (e.g., bottom-current intensity, depth of water masses interfaces) driven by the interplay of tectonic shortening events as well as climatic and eustatic changes (Table 4.1, Fig. 4.8).

Alongslope erosional features also allow understanding the activity and location of the bottom currents along the margin and basins of the Alboran Sea. The two types of *terraces* described earlier were of two different origins: (i) the terraces incising the *M* boundary (i.e., the upper Miocene deposits) on the Spanish western continental slope and adjacent WAB that resulted from the Zanclean flooding (Estrada *et al.*, 2011) and were progressively obliterated during the Pliocene (Figs. 4.6-4.7); and (ii) the terraces on the continental slope that developed as a result of turbulence processes associated with the interfaces between water masses (Chapter III) during the Pliocene and Quaternary that

eroded the seafloor and shaped the slope-plastered drifts (Figs. 4.5-4.7). The presence of the *escarpments* in the transition between the slope and base of slope (Spanish margin) or basin (Morocco margin) (Figs. 4.5; 4.6C; 4.7B, C) is related to the local acceleration of current flows. *Moats* normally form where water masses meet the highs and produce turbulent and faster flows (helicoidal flows) on both sides of the high (Hernández-Molina *et al.,* 2006b). Their acoustic facies (laterally confined chaotic facies aggrading and migrating slightly upslope, Fig. 4.3A) confirm the action of these turbulent flows. Finally, the *channels* are interpreted as having developed in the structural corridors where bottom flows are funnelled and accelerated by topographic constrictions, thereby eroding the seafloor sediments (Figs. 4.5; 4.6A).

4.2. Factors controlling contourite deposition

Although in this work there is no lithological information about the contourite features, it is proposed that there are at least two main factors controlling the bottom-current-controlled deposition in the Alboran Sea: (i) regional/local tectonic activity, primarily controlling the distribution and geometry of contourite features; and (ii) overprinted climate and related sea level changes, primarily controlling the seismic expression and growth patterns of the drifts, as well as terrace formation.

4.2.1. Regional and local tectonic activity

The morphotectonically active setting that characterized the Alboran Sea during the Pliocene and Quaternary involved a changing seafloor landscape and basin configurations, which controlled the distribution and lateral continuity of the Pliocene and Quaternary seismic stratigraphic divisions and their contourite deposits. Based on the literature (Comas *et al.,* 1992, 1999; Estrada *et al.,* 1997; Pérez-Belzuz *et al.,* 1997; Martínez-García *et al.,* 2013) (Fig. 4.8), several evolving tectonic features are present (basement highs, diapirs, mud volcanoes, scarps), but this study is focused primarily on those of a larger scale that are capable of affecting the flows of water masses and, therefore, the regional morphosedimentary framework.

128
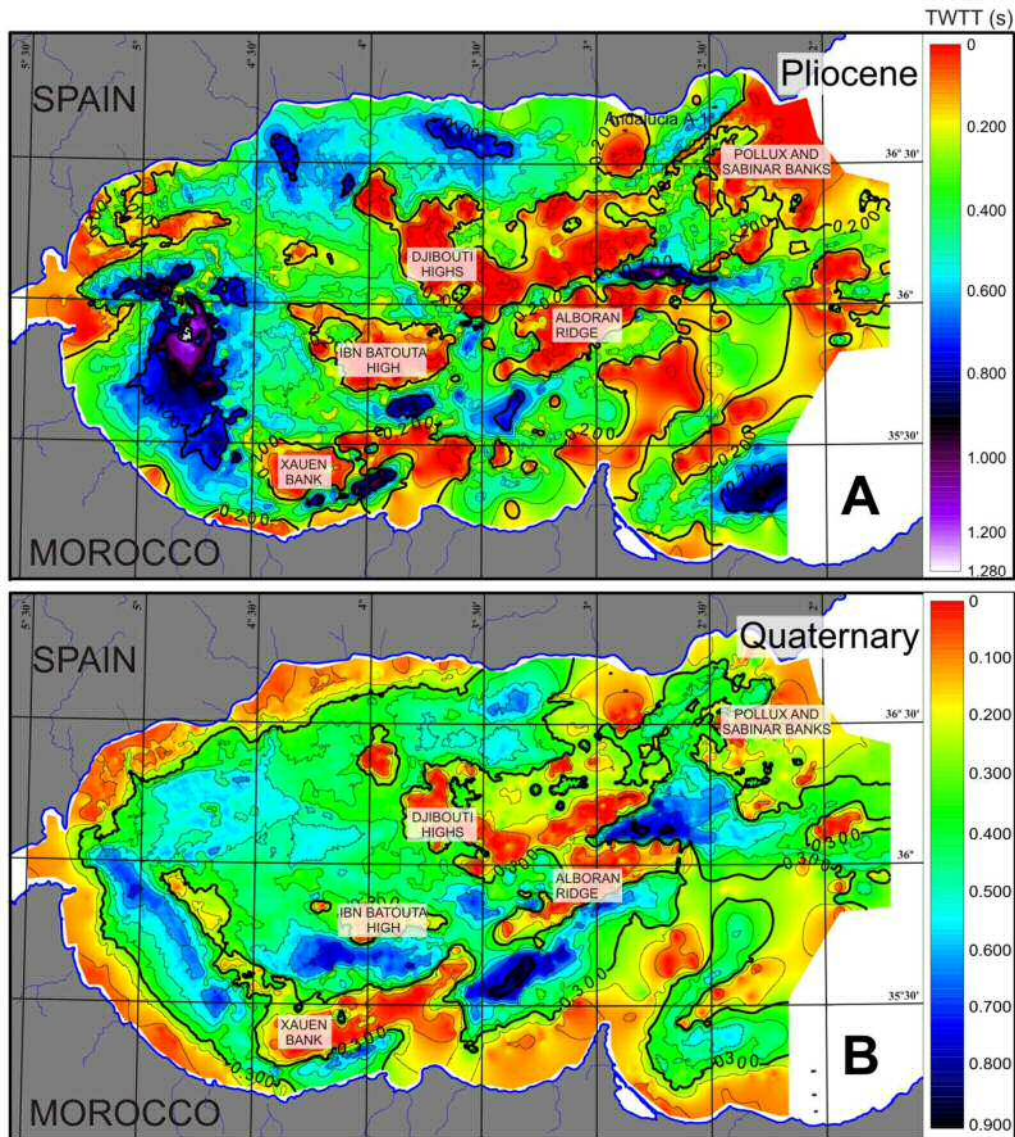
Fig. 4. 9 - Isochore maps of the Pliocene and Quaternary sequences, showing the location of the main depocentres. The colour scales are equivalent until 0.9 s (twtt), with an extended colour scale for the Pliocene due to its greater thickness. Depocentres during the Pliocene are thicker, infilling the Messinian palaeo-relief and with influence of the location of the sediment sources in the Motril Basin and Moulouya Plateau; however, an alongslope trend is already visible in the WAB. During the Quaternary, the alongslope trend of the depocentres is more evident, particularly in the WAB.

One of the most relevant tectonic features is the Alboran Ridge, in which its uplift propagated from NE to SW and split the eastern and WAB (Martínez-García *et al.,* 2013) (Figs. 4.1, 4.9). The Xauen and Tofiño banks area (Figs. 4.1, 4.6) was extensively folded and uplifted (Teurquety, 2012) and, with the Alboran Ridge, progressively led to the formation of a long morphologic barrier in the Late Pliocene (Alboran Ridge, Francesc Pagès, Tofiño, Eurofleet, Ramón Margalef, Petit Xauen, Xauen) (Martínez-García *et al.,* 2013; Ammar *et al.,* 2007) that is presently ~130 km long and 1.75 km tall. This morphologic barrier

controlled the dense circulation, which evolved from a wide, nearly homogenous tabular water mass during the Early Lower Pliocene to a water mass with strong morphological forcing and various flow dynamics from the Later Pliocene to the present (Fig. 4.10B, C), favouring the development of local mounded drifts.

Another large-scale morphotectonic change was related to the basin configurations. During the Pliocene, two major phases of shortening, the related emergence of the onshore subbasins, and the formation of the Alboran Ridge considerably narrowed the Alboran Basin and led to the final development of the WAB, EAB and SAB (Martínez-García *et al.,* 2013). These phases also promoted a general deepening and altered the sizes of the marine basins (Estrada *et al.,* 1997; Comas *et al.,* 1999; Martínez-García *et al.,* 2013). The seismic records (Figs. 4.1, 4.3-4.7), isochore maps (Fig. 4.9) and tectonic subsidence findings in the literature (Docherty and Banda, 1992; Estrada *et al.,* 1997; Rodríguez-Fernández *et al.,* 1999) all indicate that the Pliocene basins were significantly deeper than their Quaternary counterparts, particularly in the WAB. Therefore, it is assumed that during the Pliocene, the dense water flowed at greater depths and the WAB topographic constraint enhanced its action. The combination of this scenario and the prominent alongslope escarpment at the foot of the Spanish continental slope (Figs. 4.6C, 4.7C, 4.9A) suggests the action of a strong, dense countercurrent in the WAB (as modelled by Alhammoud *et al.,* 2010, in a shallow sill situation), which also helps explain its thick Pliocene deposits (up to 1,280 ms) (Fig. 4.9). During the Quaternary this escarpment is active, although less developed (Figs. 4.6C, 4.7C), suggesting a weakening of the countercurrent. The eastward flow of this countercurrent is also supported by the absence of a moat associated with a mounded drift at the foot of the Spanish scarp, which would develop if the flow at the base of this escarpment was directed to the west. Instead, a uniform sheeted drift has developed (Figs. 4.6C, 4.7C). This occurs because the recirculating branch is not constrained by the Coriolis Effect (Faugères *et al.* 1999).

With respect to smaller morphotectonic changes, a) the re-orientation of previous tectonic structures in relation to the Pliocene-Quaternary convergence between the Eurasian and African Plates, b) the changes in the stress field during the Pliocene and Quaternary (e.g., Campos *et al.,* 1992; Maldonado *et al.,* 1992; Woodside and Maldonado, 1992; Rodríguez-Fernández and Martin-Penela, 1993; Estrada *et al.,* 1997; Martínez-García *et al.,* 2013), and c) the uplifting of diapirs in the southwestern subbasin (Pérez-Belzuz *et al.,* 1997; Talukder *et al.,* 2003) all controlled the presence of structural scarps, highs and diapirs. Their roles as obstacles to the light and dense bottom currents were greater during the Pliocene, when they were more exposed (Figs. 4.5, 4.6, 4.9A). In

addition to these smaller tectonic reliefs, during the Early Lower Pliocene, the seafloor was also shaped by the erosional palaeo-relief created by Atlantic flooding (Estrada *et al.,* 2011) (Figs. 4.3, 4.6-4.7). All of these minor features, both tectonic and sedimentary in origin, also produced small-scale isopycnal doming in the light and dense waters and separation of their flows into small-scale branches, forming minor-scale contourite features, such as moats related to elongated separated, confined and sheeted drifts, current-induced bedforms (sediment waves) (Fig. 4.5A), and lateral variations in the acoustic amplitudes of the deposits (Figs. 4.5B, 4.6C).

4.2.2. Climate changes and related sea level changes

The Pliocene was characterized by a sea level highstand due to gradual and general warming and the predominance of small-amplitude, sea level changes (Aguirre, 2000, approx. 30 m; Naish and Wilson, 2009; Do Couto *et al.,* 2014) (Fig. 4.8). In addition, the Pliocene was characterized by a relative landward shift of the coastline on both sides of the Alboran Sea (Aguirre, 2000; Do Couto *et al.,* 2014), which may have resulted in a relatively more distal marine deposition scenario along the distal margin and in the subbasins than during the Quaternary.

However, the Quaternary (*c.a.* 2.6 Ma) was marked by the onset of the Northern Hemisphere glaciations; relatively higher-frequency (41 to 100-ky), higher-amplitude (approx. 120 m) and asymmetric (~1.5 5 m/ka fall vs. 15 m/ka rise; Chiocci *et al.,* 1997) sea level changes (Miller *et al.,* 2011) that occurred primarily since the Middle Pleistocene Revolution (c.c. 900-950 ky); and sharp climatic changes that favoured periods of enhanced thermohaline circulation and MW ventilation (Rogerson *et al.,* 2012) (Fig. 4.8).

Based on the abovementioned glacioeustasy characteristics, it is interpreted that Pliocene contourite deposition occurred in a relatively more distal marine scenario along the distal margin and in the basins than during the Quaternary. This resulted in sediment deposition that was finer during the Pliocene and relatively coarser during the Quaternary. The general vertical change in acoustic amplitudes, i.e., lower in the Pliocene drifts and higher in the Quaternary drifts, would be related to the interplay of those glacioeustatic changes with the palaeoenvironmental conditions and its effects on the sediment sources feeding the contourites.

Variations in the acoustic amplitudes of the drifts can also be related to variations in current strengths (Nielsen *et al.,* 2008). Highly energetic bottom currents sweep away finer sediment and favour the preservation of coarser sediments that are generally

characterized by higher acoustic impedance values. A similar vertical trend was identified in drifts in the nearby areas of the Spanish Atlantic margin (Van Rooij *et al.*, 2010; Hernández-Molina *et al.*, 2014). There, the climatic influence in the MOW evolution, shifting from a weak bottom current during the Pliocene to a high-velocity bottom current during the Quaternary, was the factor suggested to explain the high reflectivity of the Quaternary deposits (Hernández-Molina *et al.*, 2006a). As on those neighbouring continental areas, it is proposed that the climatically and eustatically variable Mediterranean bottom currents, with a prevalence of stronger currents during the Quaternary, may have contributed to the aforementioned vertical increase in acoustic reflectivity in the Plio-Quaternary deposits of the Alboran Sea (Figs. 4.3A; 4.4A, B; 4.5A, B, D; 4.6C; 4.7C).

In addition to this control on seismic expression, it is also suggested that since the Early Lower Quaternary, climate changes may have indirectly controlled the increase in terrace development and progradational patterns of the slope plastered drifts (Figs. 4.5-4.7). Quaternary climate changes may have contributed to better stratification of the water column and sharper interfaces between the water masses, the presence of distinct nepheloid layers associated with those interfaces (Chapter III), a large-scale seaward migration of hinterland sediment sources during the frequent lowstand stages, and better marine ventilation. The major outbuilding of the Moroccan slope (Figs. 4.7, 4.9B) could tentatively suggest the relatively major effect of the Atlantic and WMDW interface on the sediment distribution and deposition.

4.3. Palaeoceanographic scenarios

Based on studies of Atlantic flooding immediately after the opening of the Strait of Gibraltar (García-Castellanos *et al.*, 2009; Estrada *et al.* 2011) and the results of the work presented here, this study proposes a palaeoceanographic model of three phases of palaeocirculation and current conditions (Fig. 4.10) since the opening of the Strait.

The *Atlantic Zanclean flooding* consisted of two inflow phases, one shortly before and another during the flooding. The second phase was characterized by pulses of Atlantic water filling the basin. The erosional channel excavated by this flooding (Figs. 4.3, 4.6, 4.7) and the terraces (Figs. 4.6C, 4.7) resulting from the pulsed infilling (Estrada *et al.*, 2011) allow us to track the path of the AW during this event. A branch of the flow might have flowed through the Southern basin, but more analyses should be performed to confirm this conjecture. No coeval circulation of the MWs was identified in the Alboran Sea (Fig. 4.10A).
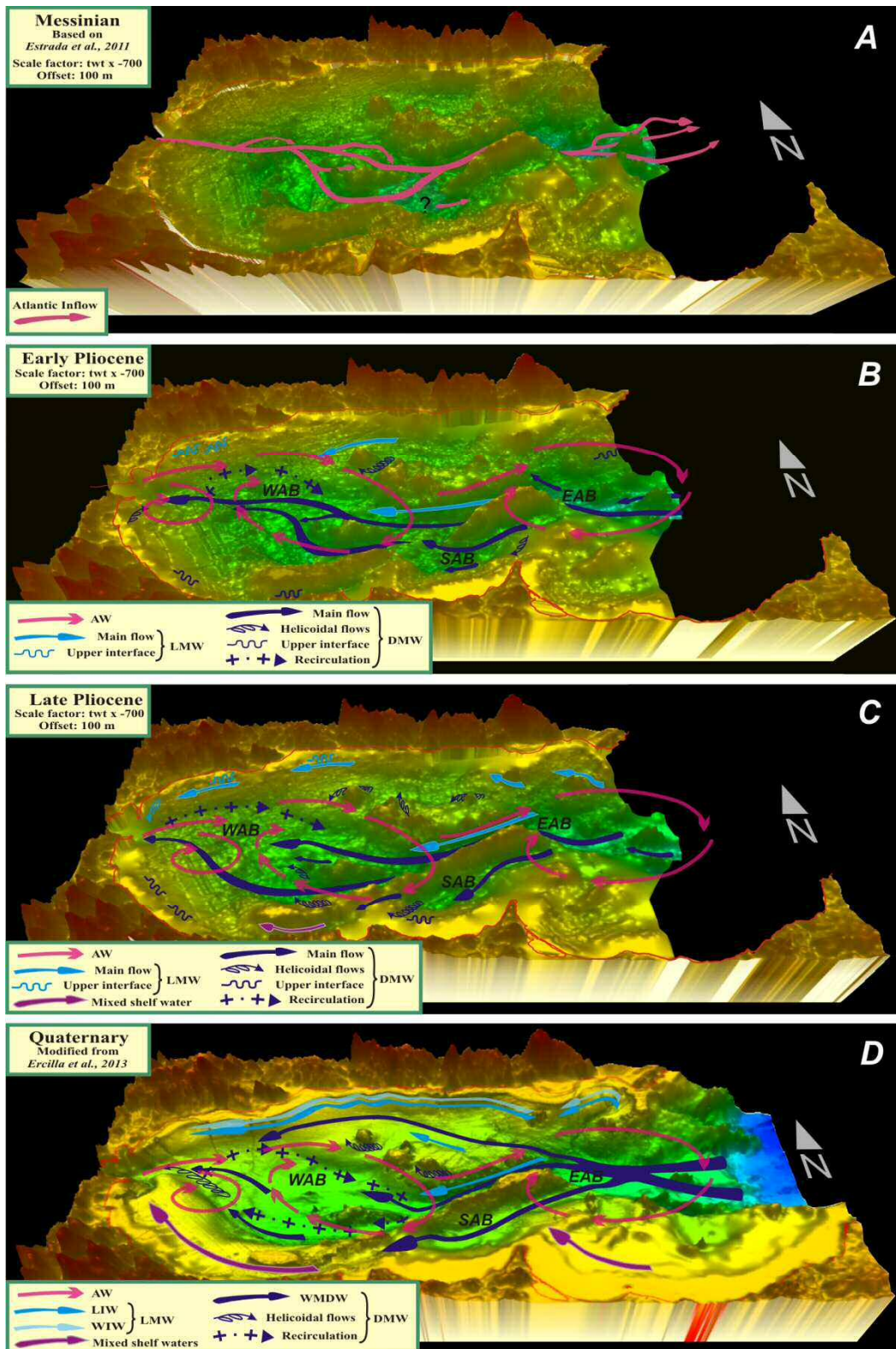
Fig. 4. 10 - **Palaeocirculation models of the Alboran Sea since the opening of the Strait of Gibraltar. A -** **Atlantic flooding. B - First stage of the Pliocene Sea (important recirculation in the WAB, local** **influence of interfaces in very narrow terraces, connection between the SAB and WAB). C - Second** **stage of the Pliocene Sea (important recirculation in the WAB, local influence of interfaces in narrow** **terraces, interrupted connection between the SAB and WAB). D - Quaternary Sea (similar to present,** **with weak recirculation in the WAB and enhanced action of interfaces over wide terraces).**

The *Pliocene Sea* was characterized by a poorly defined water mass structure between the AW and MWs and between the LMW and DMW. The density contrast between these two groups of water masses progressively increased towards the Upper Pliocene, thereby favouring greater terrace development along the Spanish and Moroccan continental slopes (Figs. 4.5-4.7).

The Pliocene Sea was also characterized with a general light and dense bottom current regime of lower strength, as suggested by the widespread sheeted drifts in the subbasins (Figs. 4.3, 4.5, 4.7, 4.9). In addition, it is also proposed that the dense waters displayed two palaeocirculation models in the deepest basin floor: a more homogenous set of tabular water masses during the Early Pliocene (Fig. 4.10B), which evolved into the multiple current dynamics during the Late Pliocene. This was caused by the uplifting of the central part of the Alboran Ridge and the progressive disconnection of the Southern and Western basins (Fig. 4.10B, C). It is proposed that this barrier divided the dense flow into two major branches: one that funnelled into the Alboran Trough and fed the deeper circulation in the WAB; and a second that flowed along the SAB ultimately feeding the western Moroccan alongslope bottom current (Fig. 4.10B, C). In both cases, when the dense waters approached the Strait of Gibraltar, the WAB and sill configuration influenced the formation of a recirculating branch with a strong bottom-current flow eroding an extensive erosional escarpment at the Spanish base of the slope (Figs. 4.6C; 4.7C; 4.9A; 4.10B, C).

The formation of a light and dense local turbulent flow regime associated with helicoidal flows was also significant, primarily during the Early Pliocene, when the Messinian erosional irregularities and the morphologic obstacles (structural, volcanic and diapiric highs) were more numerous (Figs. 4.3, 4.5, 4.6, 4.9A, 4.10B, C).

The *Quaternary Sea* was characterized by multiple current dynamics of the dense waters and its continued recirculating flow, although the latter was weaker (Fig. 4.10D). The "maturity" (better defined and/or stable characteristics) of the AW, and the light and dense MWs favoured the presence of interfaces with greater density contrasts (i.e., well-defined pycnoclines), as suggested by the large scale of terraces in the Spanish and Moroccan margins. Mixed waters between the AW and dense waters occurred and swept the Moroccan slope terrace, due to the upslope topographic forcing of the MW (Fig. 4.10D) (see also Chapter III). The presence of light and dense secondary flows related to helicoidal flows would have decreased due to the sedimentary draping and obliteration of some highs (Fig. 4.9B).

Chapter V - Pliocene and Quaternary sedimentary systems and an architecture model for the Alboran Sea. A geological perspective to palaeoceanographic processes
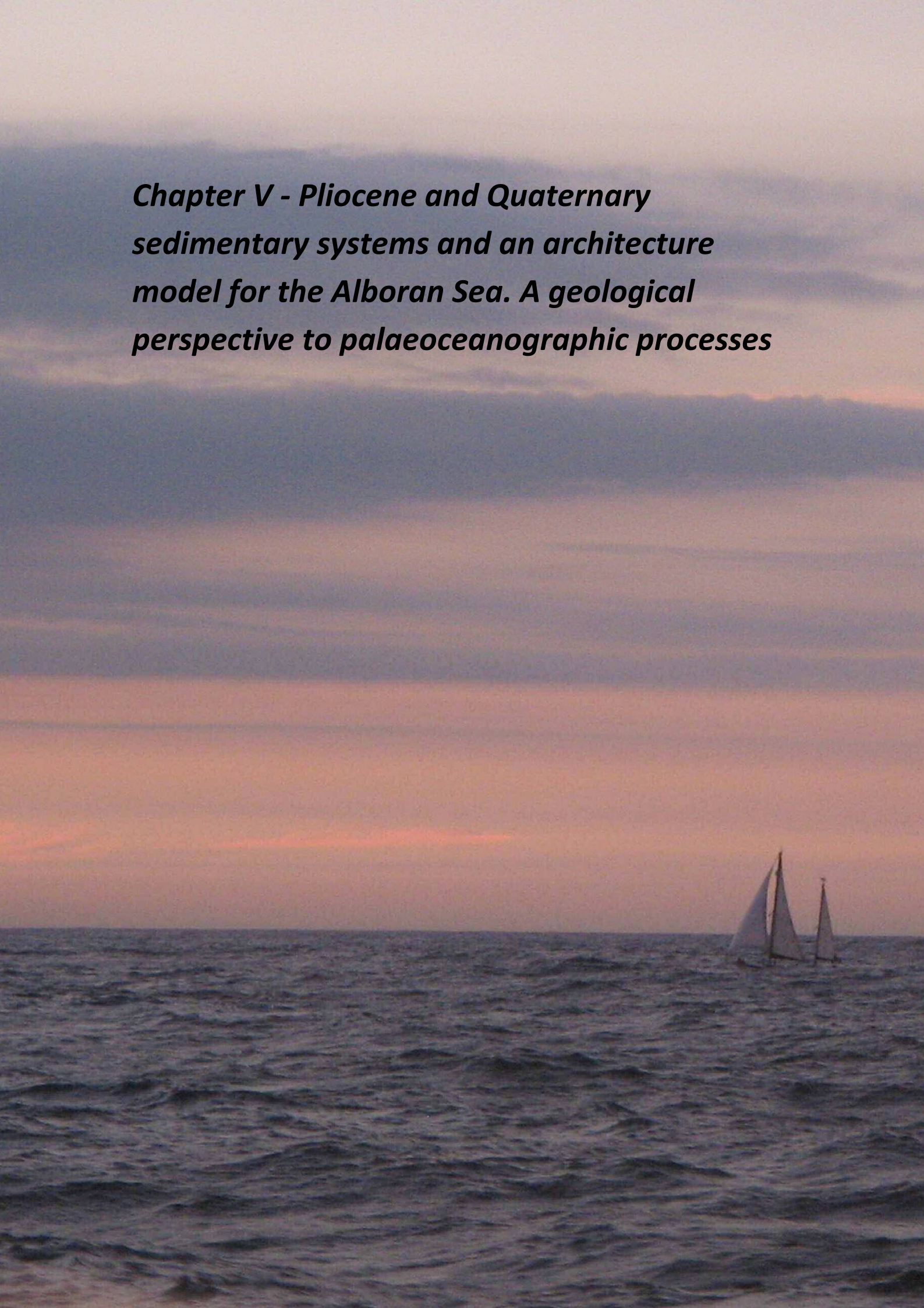
Chapter V - Pliocene and Quaternary sedimentary systems and an architecture model for the Alboran Sea. A geological perspective to palaeoceanographic processes

1. Introduction

This Chapter focuses on the study in detail and at regional scale, of the deep marine sedimentary register of the Alboran Sea, based on a detail stratigraphic analysis to unit scale of the Pliocene and Quaternary sequences, and the classification and characterization of their sedimentary features.

The general aims of this Chapter are:

To analyse in detail the Pliocene and Quaternary seismic units

To define the architectural model in terms of sedimentary systems and discuss their significance in the Plio-Quaternary sedimentary evolution.

To define the palaeoceanographic processes and to determine their occurrence, relative magnitude and energy, and time of action from a geological approach.

The seismic stratigraphy analysis of the sedimentary deposits is based on the study of the compilation of seismic reflection profiles (single-channel and multi-channel seismic profiles) acquired during various campaigns in the last decades (Fig. 5.1). Five different N-S seismic composite profiles based on single-channel (airgun and sparker) and multi-channel seismic lines have been assembled to facilitate the identification of various sedimentary features making up the sedimentary systems through various environments along the Alboran Sea (Fig. 5.1). These composite profiles range again from the deepest area in the east, towards the comparatively shallower WAB, near the Strait of Gibraltar. In addition to these profiles, the composite N-S profiles of the previous Chapter IV, also offer details of the sedimentary features and then, they will be also referenced in this chapter.
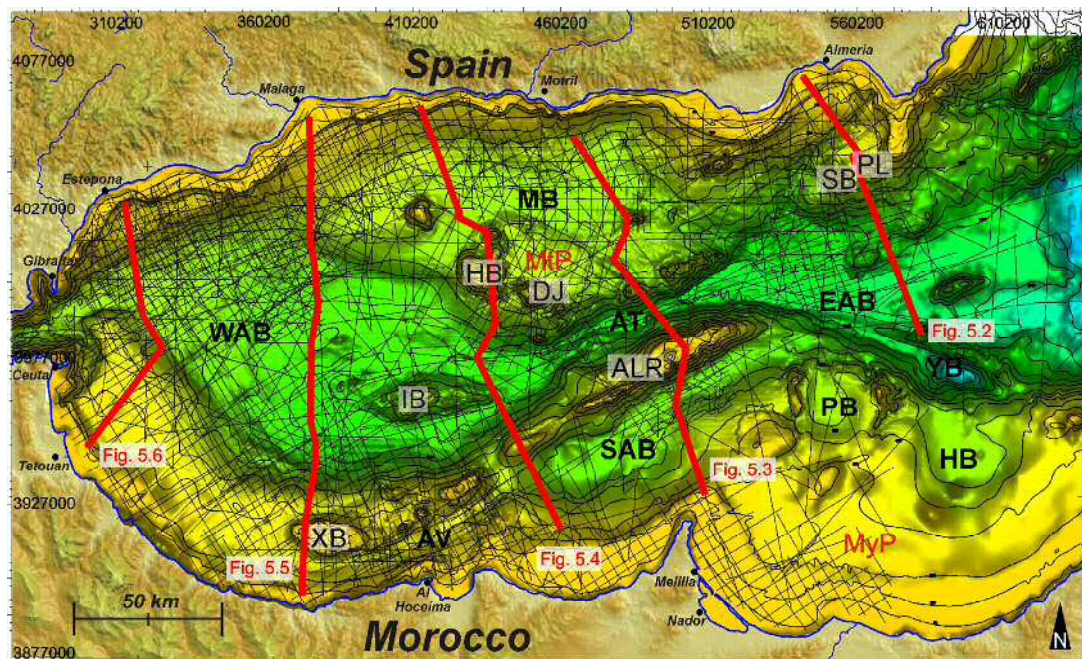
Fig. 5. 1 - Bathymetric map of the Alboran Sea, including the seismic line database and the location of Figs. 5.2-5.6. The basins (AT-Alboran Through; EAB-Eastern Alboran Basin; WAB-Western Alboran Basin; YB-Yusuf Basin), the intra-slope basins (AV-Al Hoceima Valley; HB-Habibas Basin; MB-Motril Basin; PB-Pytheas Basin; SAB-Southern Alboran Basin) and selected seamounts (ALR-Alboran Ridge; DJ-Djibouti Bank; HB-Herradura Bank; IB - Ibn Batouta Seamount; PB-Pollux Bank; SB-Sabinar Bank; XB-Xauen Bank) and plateaus (MtP-Motril Plateau; MyP-Moulouya Plateau) are indicated in the figure.

2. New insights into seismic stratigraphy

The new insights into the seismic stratigraphy of the Pliocene and Quaternary sequences of the Alboran Sea offer a detailed, basin-wide analysis of the seismic units based on acoustic facies (Figs. 5.2-5.6), types of boundaries, isochore maps, geometry, and characterisation of their deposits.

2.1. Pliocene seismic units:

Three seismic units have been identified in the Pliocene sequence (Juan *et al.*, 2016, Chapter IV), which from base to top are: *Pl1*, *Pl2* and *Pl3* (Figs. 5.2-5.6). The limits that bound these seismic units are similar in character, being defined by onlap (Figs. 5.2; 5.3A,B,C; 5.4; 5.5; 5.6B) and local downlap (Figs. 5.2A; 5.3B, D; 5.4A, 5.5A,D; 5.6C) surfaces. The seismic units extend from the uppermost continental slope to the basins, and their distribution is irregular, as they were mostly developed in the basins and are relatively reduced and locally absent in the margins (Figs. 5.2; 5.5; 5.6). Units *Pl1* and *Pl2* have similar acoustic facies and geometry, contrasting with *Pl3*, for which reason these two groups of units will be described separately.

138
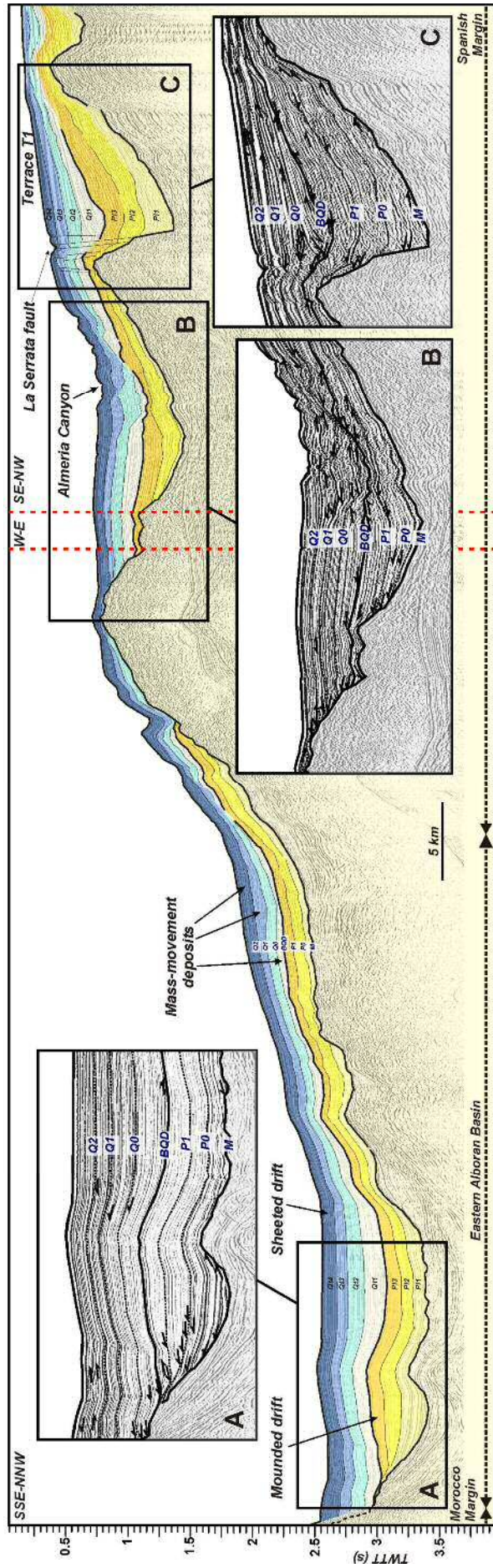
Fig. 5. 2 - Seismic profile located in the eastern EAB. See Fig. 5.1 for location. The Pliocene units are represented in yellow and the Quaternary units are represented in blue. Unit names are shown in black, and boundary names are shown in blue. Inset A - Buried mounded elongated separated drift. Inset B - Almeria canyon. Inset C - Terrace cut by a major fault.

139
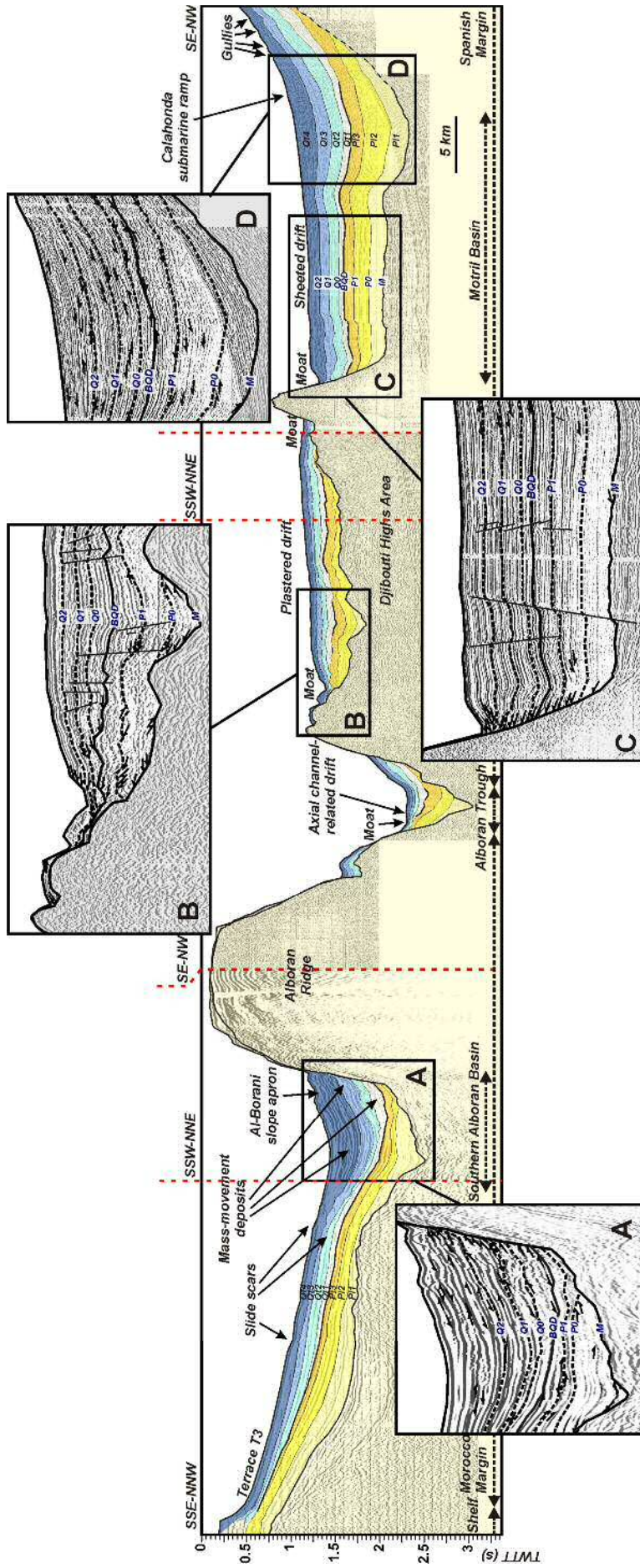
Fig. 5. 3 - Seismic profile in the central Alboran Sea. See Fig. 5.1 for location, details are as described in Fig. 5.2. Inset A - Terraced plastered drift. Inset B - Plastered drift with moat. Inset C - Mounded confined drift. Inset D - Sheeted drift

140

2.1.1. Seismic units Pl1 and Pl2: Lower Pliocene (Zanclean)

Seismic units *Pl1* and *Pl2* are characterized by their relatively lower acoustic amplitude (Figs. 5.2A; 5.3; 5.4B,C; 5.5C,D; 5.6B,C), which is better evidenced in the single-channel seismic profiles. These units mainly consist of tilted subtabular deposits (Figs. 5.3; 5.4; 5.5; 5.6). The tilted subtabular geometry shows a slightly terraced shape locally in the uppermost continental slope of the western margins (Figs. 5.4C, 5.5). These units are internally defined mostly by stratified facies. Also, *Pl1* and *Pl2* deposits form irregular and mounded sedimentary patches draping and infilling the irregular ancient MSC palaeoreliefs (e.g., the Zanclean Channel) with stratified oblique facies in the basins (Figs. 5.2A; 5.4). Locally, undulated facies is also present in the northwestern sector of the WAB. The dominant stratified facies is interrupted, mostly on the distal Spanish margins and in adjacent basins and less so in the Moroccan margins, by laterally confined depositional bodies of discontinuous and continuous stratified and chaotic facies of higher acoustic amplitude with fan and lobate shapes (Figs. 5.3D; 5.5; 5.6).

The *Pl1* and *Pl2* isochore maps (Fig. 5.7) show that sediment distribution is interrupted by highs and Messinian relict reliefs (Estrada *et al.*, 2011). These latter include a notable arcuate, elongated escarpment on the Spanish side of the WAB (Fig. 5.7). This escarpment interrupts the seaward continuation of the subtabular stratified facies between the continental slope and the basin, and the major part of the fan and lobate shape deposits occur at its foot (Figs. 5.5, 5.6). The thickness of *Pl1* varies between 0 and 718 ms twtt, and it is the thickest Pliocene unit (Fig. 5.7A). The sediment distribution shows a striking difference between the EAB and WAB with the highest accumulation being in the WAB (Figs. 5.2; 5.6; 5.7A). There are four large and thick depocentres: two in the WAB (718 ms; 650 ms), one in the MB (575 ms), and one in the EAB (635 ms) (Fig. 5.7A). Smaller depocentres (325 to 550 ms twtt) dot the continental slopes as well as the basins. The depocentres show a parallel, oblique and even perpendicular trend with respect to the margin, mainly due to the irregular palaeotopography of the MSC surface and the local presence of highs (Fig. 5.7A). The thickness of *Pl2* ranges between 0 and 430 ms and no relevant variations in sediment accumulation are observed between the WAB and EAB (Fig. 5.7B). The depocentres maintain their location but their size and thickness generally decrease (200 to 430 ms). The sediment distribution still shows the influence of the MSC palaeotopography in the EAB, where the maximum depocentre is located (434 ms) (Fig. 5.7B). Other important depocentres are located on the Moroccan continental slope (~400 ms twtt) and on both sides of the Alboran Ridge (~300 ms twtt) (Fig. 5.7B).

142
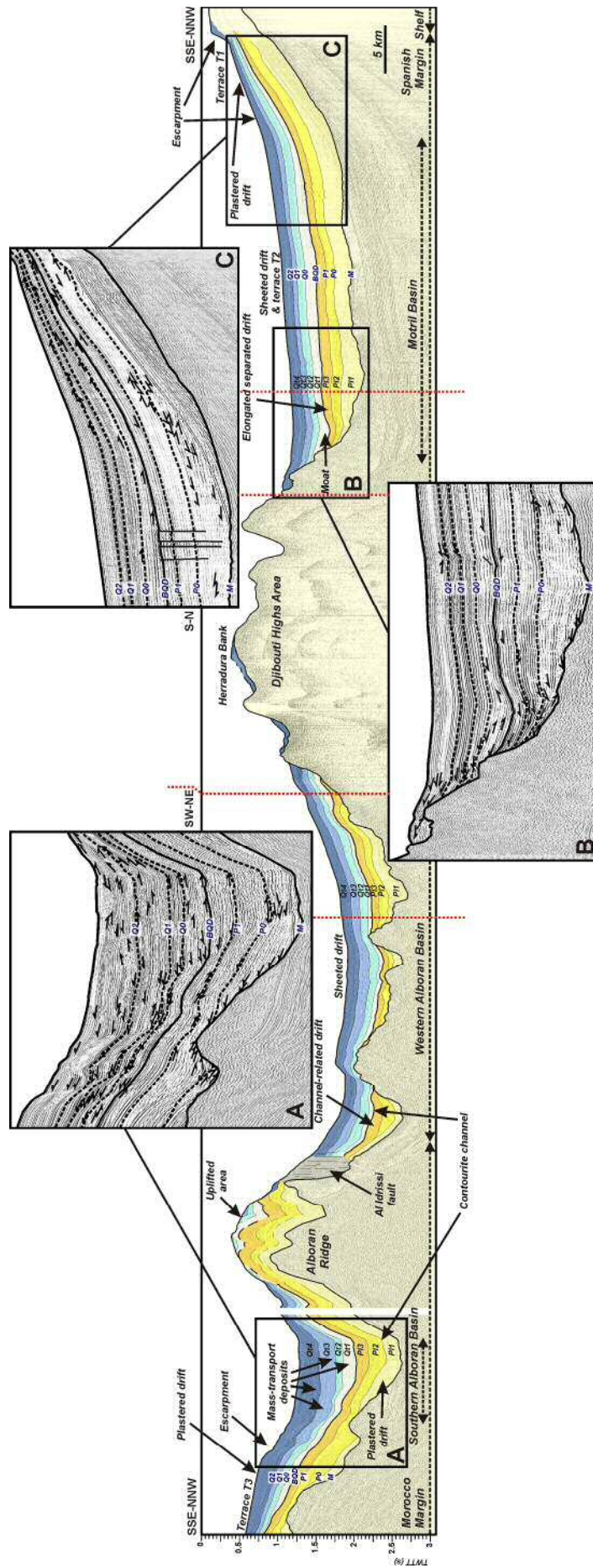
Fig. 5. 4 - Seismic profile in the central Alboran Sea. See Fig. 5.1 for location, details are as described in Fig. 5.2. Inset A - Plastered drift in Lower Pliocene, escarpment and mass movement deposits in the Pliocene. Inset B - Elongated separated drift in the Pliocene. Inset C - Plastered drift and terrace.
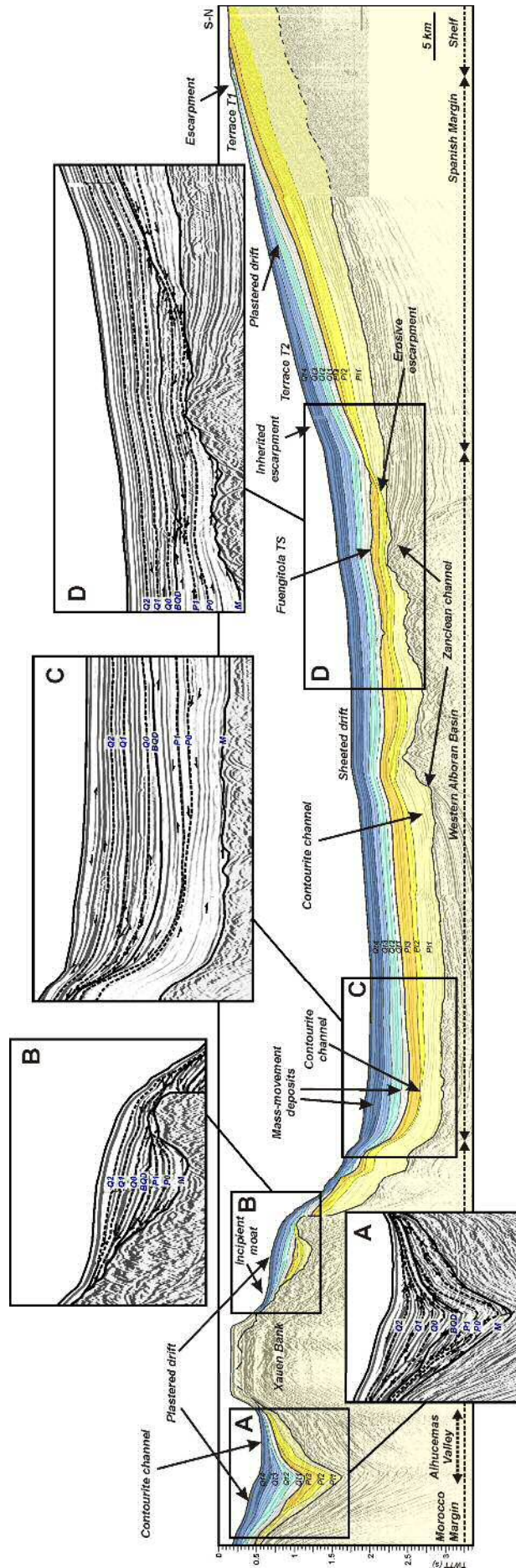
Fig. 5. 5 - Seismic profile in the western Alboran Sea. See Fig. 5.1 for location, details are as described in Fig. 5.2. Inset A - Tilted sediments, plastered drift and the Al Hoceima contourite channel. Inset B - Terraced plastered drift. Inset C - Contourite channel in the Upper Pliocene, mass movement deposits in the Quaternary. Inset D - Erosive escarpment and turbidite deposits in the Pliocene and Lower Quaternary, sheeted drift in the Upper Quaternary.

143
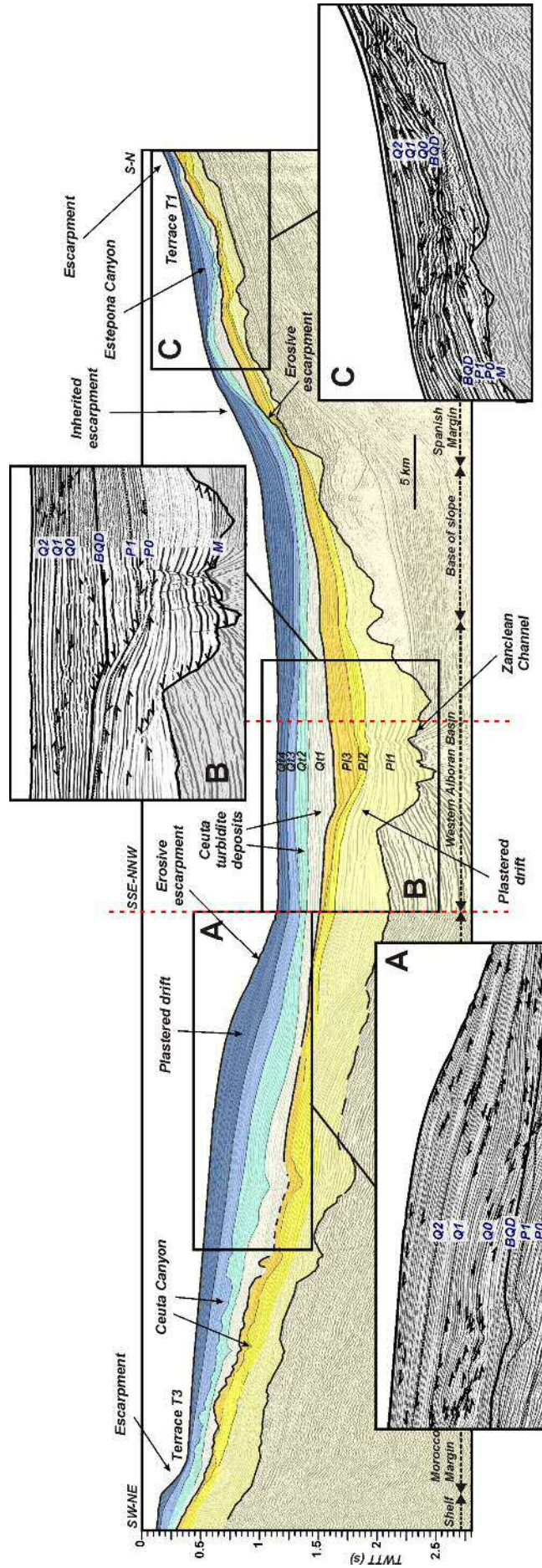
Fig. 5. 6 - Seismic profile in the western Alboran Sea. See Fig. 5.1 for location, details are as described in Fig. 5.2. Inset A - Plastered drifts and erosive escarpment. Inset B - Zanclean channel, Early Pliocene plastered drifts and erosive escarpment, Late Pliocene and Quaternary turbidite deposits. Inset C - Estepona buried canyon deposits and terrace.

144

2.1.2. Seismic unit Pl3: Upper Pliocene (Piacenzian)

Seismic unit *Pl3* is defined by a higher spatial variability of acoustic facies and geometry when compared to *Pl1* and *Pl2*. *Pl3* deposits generally display a subtabular to wedged geometry, mostly characterized by subparallel stratified facies with low to middle reflectivity at the bottom increasing upwards (Figs. 5.3, 5.4A, 5.5C), and by high reflectivity oblique facies on the western Moroccan margin (Fig. 5.6A). Locally, these geometries show terraced shapes (~5 Km long) (Fig. 5.3; 5.4C; 5.6) bounded upslope and downslope by escarpments on the western Spanish and Moroccan continental slopes. Discontinuous stratified and chaotic facies with fan and lobate shapes are less frequent.

The *Pl3* isochore map shows that is the thinnest Pliocene unit (Fig. 5.7) and marks the end of the influence of the MSC palaeotopography on sediment distribution, although the outcropping of the arcuate, elongated escarpment continues (Fig. 5.7C). Sediments are more homogeneously distributed, showing relatively uniform accumulations (0 311 ms) and fewer and smaller depocentres (200 to 311 ms), the thickest (311 ms) being on the Moroccan margin, and the largest (~250 ms) still being located in the WAB (Fig. 5.7C).

2.2. Quaternary seismic units

Four seismic units have been identified within the Quaternary sequence that from base to top are: *Qt1*, *Qt2*, *Qt3*, and *Qt4* (Juan *et al.,* 2016; Chapter IV) (Figs. 5.2-5.6). The limits that bound these seismic units have a similar character, being defined by onlap and local downlap surfaces (Figs. 5.2C; 5.3A,B; 5.4; 5.5A,B,C; 5.36B,C), erosive truncations (Fig. 5.6A,C) and their correlative conformity surfaces (Figs. 5.2A; 5.3C; 5.5D). The seismic units display a higher reflectivity (Figs. 5.2-5.6) and are on average thinner than the Pliocene sequence (Figs. 5.7 and 5.8); they are well developed on the margins and basins and there are no strong differences in deposition between the EAB and WAB (Fig. 5.8). *Qt2* and *Qt3* show similar acoustic facies, geometry and thicknesses which contrast with those of *Qt1* and of *Qt4*, for which reason these three groups of units will be described separately.

2.2.1. Unit Qt1: Gelasian

Seismic unit *Qt1* is mostly defined by oblique stratified facies (Figs. 5.2C, 5.4-5.6) with onlap terminations (Fig. 5.2-5.4, 5.5A,D; 5.6B) and erosive truncations (Fig. 5.3D; 5.5B,C; 5.6A,C) displaying: i) a sloping terraced wedge geometry pinching out landwards at the Spanish and Moroccan continental slopes (Figs. 5.2C; 5.3-5.6); ii) subparallel aggrading stratified facies with subtabular geometry on the distal continental slopes and in the

basins (Figs. 5.2A,B; 5.3C; 5.4B); and iii) mounded stratified facies with a prograding configuration and mounded geometry, at the foot of structural highs (Fig. 5.3). Stratified facies are laterally interrupted by deposits with discontinuous stratified and chaotic facies with fan and lobate geometries (Figs. 5.3D; 5.5D; 5.6B), mostly in the WAB, MB and EAB.

The thickness of *Qt1* ranges between 0 and 430ms twtt, with the main depocentre (340 ms twtt) being in the EAB. Smaller depocentres (185 and 230 ms) also occur in the continental margins and basins, in similar locations to those in the Pliocene (Fig. 5.8A). On the other hand, sediment distribution also reveals that *Qt1* deposits begin to drape the Messinian arcuate escarpment of the Spanish side in the WAB, although its palaeorelief is maintained (Fig. 5.8A).

2.2.2. Seismic units Qt2 and Qt3: Calabrian

Seismic units *Qt2* and *Qt3* are characterized by a relatively major seaward outbuilding of the sloping wedge deposits with oblique stratified facies on the continental slope (Fig. 5.4-5.6). As a result, the aggradational tabular deposits characterized by subparallel stratified facies are progressively confined to basins (Fig. 5.2A; 5.3C; 5.4B; 5.5C). Mounded stratified deposits at the foot of the structural highs and escarpments become more frequent and are better developed (Fig. 5.3; 5.5B). The areas with discontinuous stratified and chaotic facies with fan and lobate geometries decrease in size, mainly during *Qt3* (Fig. 5.5D). From *Qt2* onwards, a rhythmic pattern characterized the reflectivity of facies, with alternating high and low acoustic amplitudes (Fig. 5.2A; 5.4A; 5.6A).

The thickness of the *Qt2* unit varies from 0 to 293 ms twtt (Fig. 5.8B). The depocentres maintain their locations but the thickness and size of many of those located on the margin increase (Fig. 5.8). The thickest (293 ms) and largest (255 ms twtt thick, 80 km long, 10-15 km wide) depocentres occurs on the Moroccan continental slope (Fig. 5.8B). Four other depocentres (220 to 255 ms twtt) are found in the basins. Unit *Qt3* is the thinnest, only reaching 246 ms (Fig. 5.8C). Unlike previous depocentres, the main ones are located in the basins (246 ms in the SAB; >200ms in MB) (Fig. 5.8C). Five other depocentres (160-220 ms twtt) appear evenly distributed across the continental margins and basins. The sediment distribution of the *Qt2* and *Qt3* deposits also reveals that the Messinian arcuate palaeoescarpment relief on the Spanish side of the WAB is maintained (Fig. 5.8B,C).

146
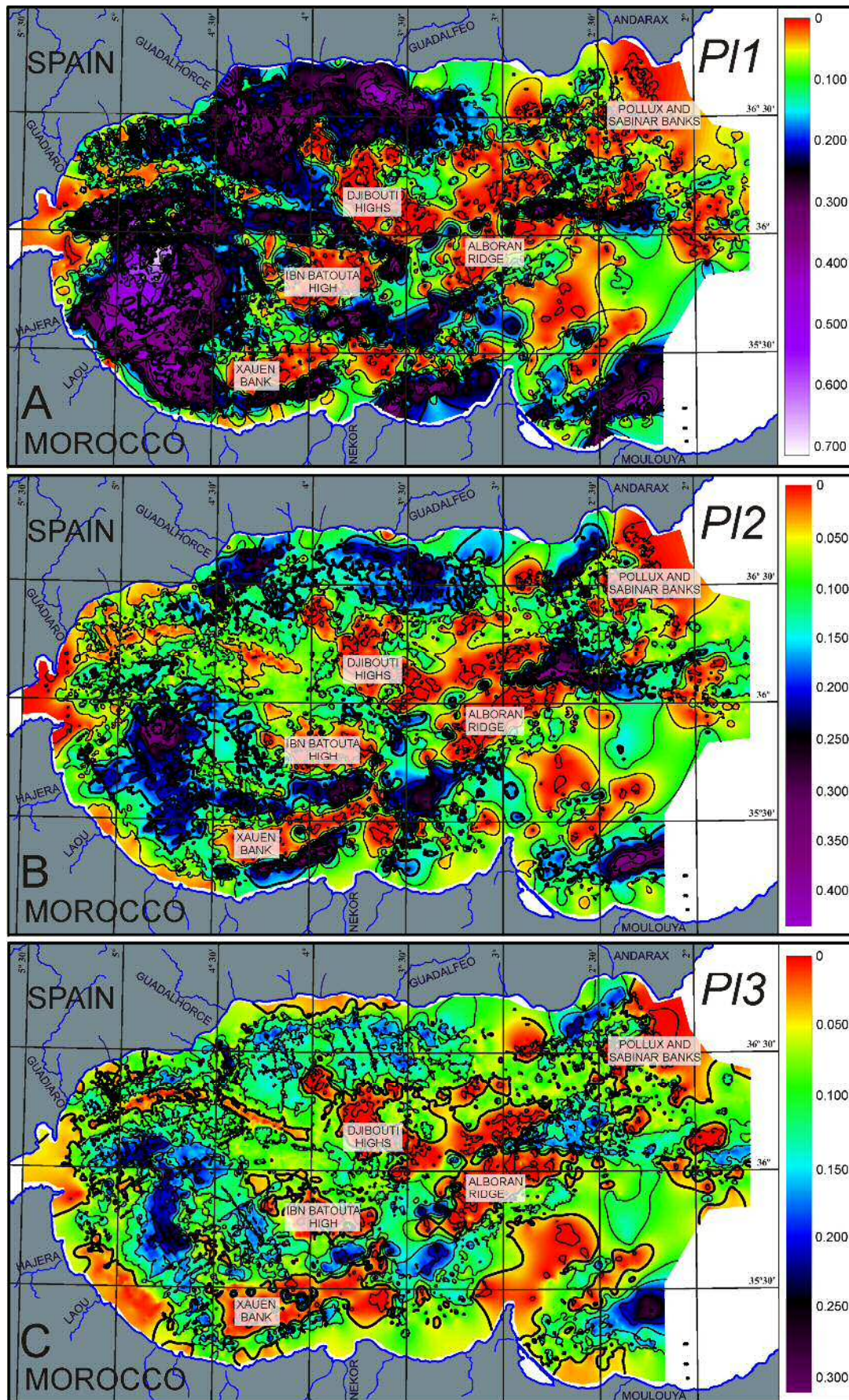
Fig. 5. 7 - Isochore maps of the Pliocene units, showing the location of the main depocentres. The colour scales are equivalent to those of Fig. 5.8.
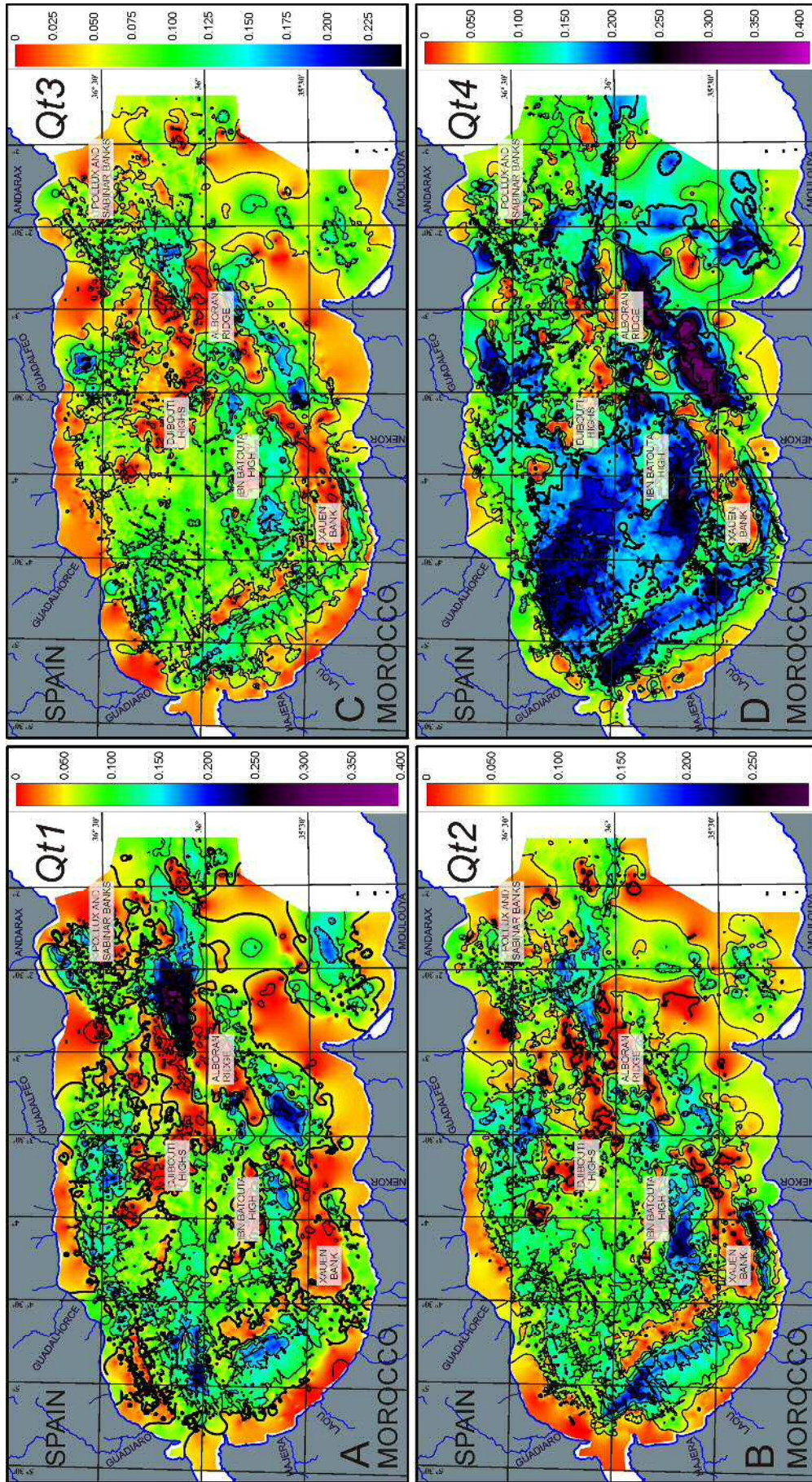
Fig. 5. 8 - Isochore maps of the Quaternary units, showing the location of the main depocentres. The colour scales are equivalent to those of Fig. 5.7

148

2.2.3. Seismic unit Qt4: Middle and Upper Pleistocene and Holocene

The most striking difference with respect to the previous Quaternary units is a decrease in the size of the fan and lobate geometries that are internally characterized by discontinuous stratified and chaotic deposits with high reflectivity. Another difference is that *Qt4* is the thickest Quaternary unit (0 to 407 ms), but it shows a noticeable difference in thickness between the EAB (up to 285 ms) and WAB (up to 340 ms) (Fig. 5.8D). The major depocentre is located in the SAB (407 ms) (Fig. 5.8D). The thinnest depocentres range from 240 to 340 ms twtt and dot the margins and basins in similar locations to the previous units. The sediment distribution reveals that the relief of the Messinian arcuate palaeo-escarpment continues being a striking morphological feature in the present day seafloor (Figs. 5.5; 5.6; 5.8D, Chapter III).

2.3. Growth patterns

The growth pattern changes in style from the Pliocene to Quaternary units. The Pliocene units are mainly aggradational with a stacking that mainly results in the onlapping of units onto the margin and the infilling of the basins (Fig. 5.3-5.5). The growth pattern of the Quaternary units are also aggradational but results in the upward and seaward growth of the margins (Figs. 5.3-5.6) and continued basin infilling (Figs. 5.2-5.6). The degree of outbuilding of the continental slope changes laterally, being more remarkable in the Spanish and Moroccan margins of the WAB.

3. Sedimentary features

The detailed analysis of the acoustic facies, the vertical and lateral distribution and the relationships between them have allowed a great variety of sedimentary features to be identified, that can be categorised into three groups based on their genesis: a) contourites, including depositional (drifts) and erosional features; b) turbidite systems; and c) mass movement deposits.

3.1. Contourite drifts

Contourite drifts are the most prominent features in the Alboran Sea (Chapter III and IV) (Figs. 5.2-5.6). Five different types of drifts have been defined: sheeted, plastered, elongated separated, mounded confined, and channel-related patched drifts. The dominant drifts are the large-scale sheeted and plastered drifts (Figs. 5.9 and 5.10).

Smaller confined, elongated-separated and channel-related drifts have been locally defined scattered throughout the Alboran Basin.

Sheeted drifts are characterized by subtabular geometry with relatively flat surfaces, that mimic the longitudinal trend of the margins and the basin morphologies. They make up a practically flat and smooth (palaeo)seafloor, mainly covering broad, basin-sized areas up to 50-100 km long and wide, being thicker in the Pliocene (100-200 m and up to 280 m thick) than in the Quaternary (60-100 m and up to 265 m thick) units (Tables 5.1 to 5.7). Drifts are defined by (sub)parallel stratified deposits with no remarkable internal discordances, and locally layered wavy facies. Sediments usually end up in onlap terminations at high walls and escarpments. Sheeted drifts are found in all Pliocene and Quaternary seismic units, carpeting the Spanish and Moroccan continental margins, infilling the basins and draping morphological irregularities (Figs. 5.2-5.6; Tables 5.1 to 5.7). Although these deposits have a generally broader extension in the Pliocene units (*Pl1* to *Pl3*) and are mapped on the continental margins and basins, they were more frequently interrupted by TSs and mass movement deposits fragmenting their continuity, whereas in the Quaternary units (*Qt1* to *Qt4*) they are mostly restricted to the basins but show a higher lateral continuity (Figs. 5.9 and 5.10).

Plastered drifts are always located attached to, or plastered against, a slope (continental slope and high walls) (Figs. 5.4-5.6; 5.9; 5.10) and show elongated mound wedge to mound terraced wedge geometries (Figs. 5.4-5.6). These drifts are highly variable in size (tens to hundreds of kilometres long/wide and tens to few hundred metres in relief), and form a low to high mound feature with more prominent relief than sheeted drifts. They are internally defined by oblique stratified deposits with onlap terminations upslope, downlap terminations downslope, and occasional internal erosions (Figs. 5.4C; 5.5; 5.6). Plastered drifts appear scattered within the Early Pliocene units (*Pl1* and *Pl2*) and get wider and longer (up to 300 km long and 5.5 to 40 km wide) in the Quaternary seismic units (*Qt1* to *Qt4*) (Tables 5.4-5.7), eventually covering most of the Spanish and Moroccan continental margins. Plastered drifts are always better developed in the vicinity of the Strait of Gibraltar, both in the Pliocene and the Quaternary seismic units. (Figs 5.5 and 5.6)

Elongated separated drifts show asymmetric mounded geometry in cross-section (Fig. 5.4B) and variable dimensions (< 42 km long and 8 km wide, 75 240 m thick) and appear at the foot of a steep seafloor slope associated with a moat (Tables 5.1 to 5.7). They are defined by mound stratified deposits with convergent configuration toward the mound end that downlap internal erosive reflections onto the adjacent moat (Fig. 5.4B). These

drifts are identified in all Pliocene and Quaternary seismic units, although they are more numerous in the Quaternary units. Their distribution also changes with time: in the Pliocene units (*Pl1* to *Pl3*), the largest elongated separated deposits are located in the deep basins, whereas in the Quaternary units (*Qt1* to *Qt4*), the largest drifts are found on the continental slopes and highs, with smaller ones in the basins.

Confined drifts show low- to high-mounded geometries, with variable dimensions (typically 8 km and up to 20 km long; 5-6 km wide; 100 to 300 m high) and appear between topographic confinements (Tables 5.1 to 5.7). The deposits are well stratified, converging toward the topographic confinements where moats develop. The acoustic amplitude of these deposits is usually higher near the border of the topographic confinement, where they also show downlap and onlap terminations. Confined drifts have been identified in most Pliocene (*Pl2* and *Pl3*) and Quaternary seismic units (*Qt1* to *Qt4*), but are more frequent in Quaternary units. Most Pliocene confined drifts are found in the basins, while the Quaternary drifts occur on the continental slope associated with some structural highs.

Lateral and axial *channel-related patched drifts* usually show mounded (Fig. 5.4), occasionally wedged geometries (3 to 11 km long, < 5 km wide, and up to 220 m thick). They mostly consist of layered mounded and layered (sub)parallel deposits, locally having a layered oblique facies (Fig. 5.4). The strata pattern includes downlap terminations into the channel itself and frequent onlap terminations on the channel sidewalls or structural highs. These drifts are mapped in the Lower Pliocene seismic units (*Pl1* and *Pl2*) in the EAB and WAB, and in the Upper Quaternary seismic units (*Qt4*) on the continental margins and in the basins (Tables 5.1 to 5.7).

3.2. Contourite erosive features

The erosive contourite features identified in the Pliocene and Quaternary units can be grouped into two types based on their linear or planar morphology: valleys, comprising contourite channels and moats, and abraded surfaces, comprising contourite terraces and escarpments.

The *contourite channels* are relatively wide (typically ~1.5 km, and up to 6.5 km) and long (up to 50-70 km) U-shaped features with low (tens of ms) to high relief (hundreds of ms) (Figs. 5.3; 5.4; 5.5A). Their deposits are mostly characterized by discontinuous and continuous stratified facies with high reflectivity chaotic facies (Tables 5.1 to 5.7). Channel deposits are affected by slightly erosive surfaces as well as low-angle onlaps and downlaps

onto internal discontinuities. Locally, they can also contain allochthonous deposits (e.g., mass movement deposits). The presence of contourite channels in the Alboran Sea is conditioned by pre-existing morphosedimentary and structural features (Figs. 5.3; 5.4; 5.5A). The Pliocene contourite channels are mostly constrained to basins and occur in relation to the Zanclean flooding palaeochannel and narrow structural palaeocorridors (i.e., the proto Alboran Trough and SAB) (Fig. 5.4). The Quaternary contourite channels are represented by the narrow structural passages of the Alboran Trough (Fig. 5.3), SAB, and Al Hoceima Valley (Fig. 5.5A).

The *contourite moats* are smaller in size and appear associated to drifts (Figs. 5.3; 5.4). They are relatively narrow U-shaped concave features incised (tens of metres deep and <6 km wide) at the foot of structural highs. Moat deposits comprise the stacking of oblique stratified, discontinuous stratified and chaotic facies, separated by stacked internal erosive surfaces (Figs. 5.3; 5.4). Locally, they can also contain allochthonous deposits (e.g., mass flow deposits and slides). Moat deposits have been identified in the Pliocene and Quaternary units, although they are more frequent in the Quaternary units, associated with the increasing number of elongated separated and confined drifts on the continental margins (Tables 5.1 to 5.7).

The *contourite terraces* represent subhorizontal, narrow erosive surfaces truncating drift deposits, or subhorizontal, wide erosive surfaces that evolve seaward to a conformity surface shaping the contourite drifts (Figs. 5.4-5.6; Tables 5.1 to 5.7). The terraces are bounded upslope and/or downslope by contourite escarpments. Terraces can reach up to 100 km in length and 30 km in width, dipping seaward with gradients typically in the range of 0.5-1º. One of the erosive terraces excavated during the Zanclean (Estrada *et al.,* 2011) outcrops in the northern WAB within the Pliocene seismic units (*Pl1* to *Pl3*) as relict feature, and is obliterated mostly by the Quaternary deposits (*Qt1* to *Qt3*) (Figs. 5.5 and 5.6). On the other hand, three terraces (T1 to T3, Chapter III) have been identified through the Pliocene and Quaternary seismic units at different water depths. The T1 and T3 terraces are shallower and occur on the Spanish (T1, Fig. 5.4C; 5.5; 5.6C) and Moroccan (T3, Fig. 5.6) upper continental slopes (nowadays at 160-400 m w.d. for T1 and 180-600 m w.d. for T3 terraces; Juan *et al.,* 2012, Chapter III), displaying an abrupt enlargement after *Pl3*. T2 occurs in the MB and affect to the sheeted drift infilling that basin (Figs. 5.4 and 5.5); its onset occurs since the late Upper Pliocene (top of *Pl3*), outbuilding mostly in the Quaternary. It is easily identified on the present-day seafloor, between 1000-1300 m w.d. (Fig. 5.5, Chapter III).
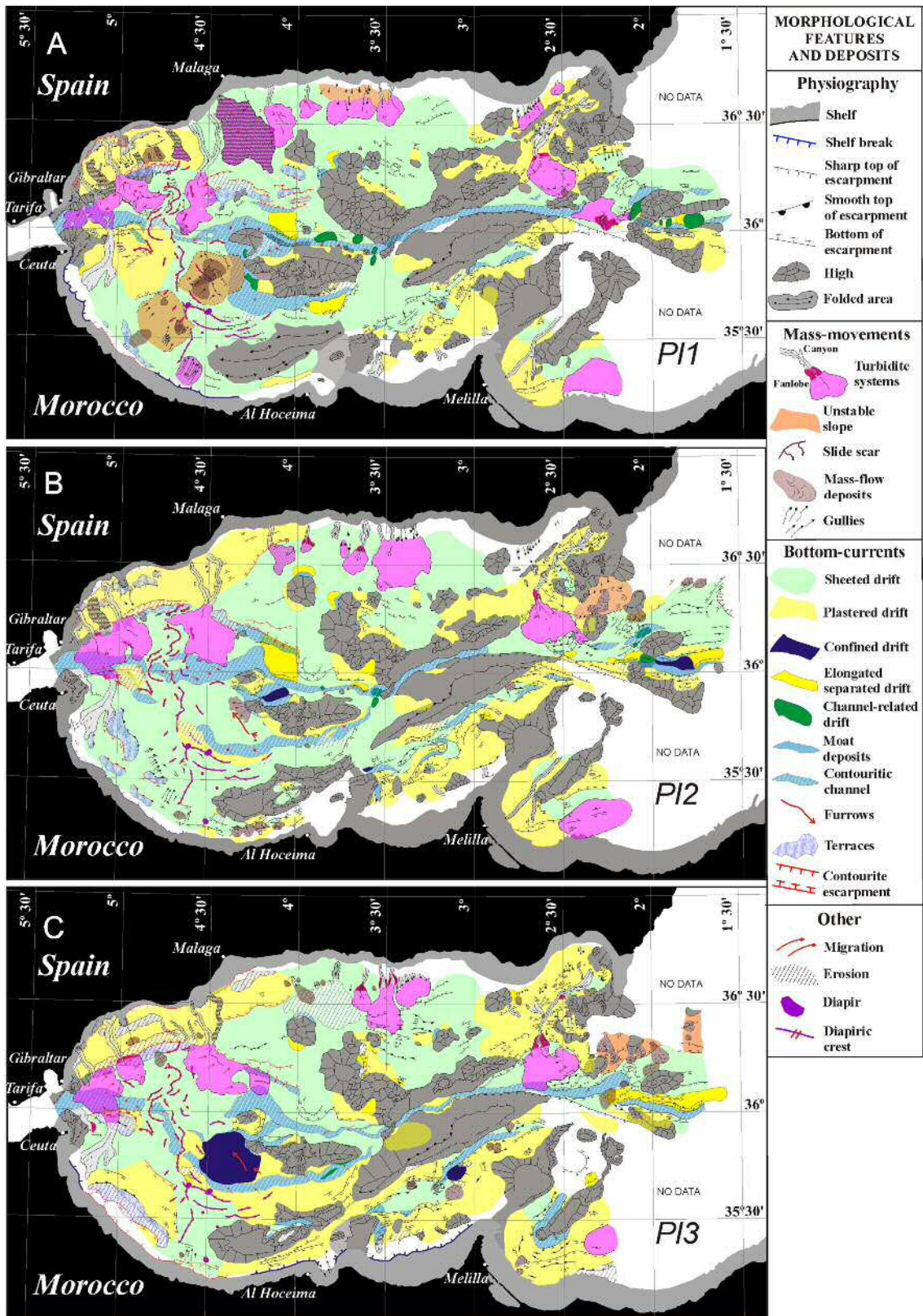
Fig. 5. 9 - Maps showing the distribution of the main morphosedimentary features of each Pliocene unit, based on the seismic database.

Unit *Pl1*

Features & Deposits	Acoustic Facies (airgun profiles)	Shape/ Dimensions	Location
DEPOSITIONAL CONTOURITE FEATURES			
Plastered drifts	Stratified facies onlapping upslope and prograding downslope, with internal discontinuities (downlap, onlap, truncations)	Low mound shape, tilted,<75 km length (typically 30-50 km), 3 to 30 km width and tens to a few hundreds of m (up to 500 m) in thickness	Large drifts: Spanish and Moroccan continental slopes, west of Tres Forcas Cape Ridge. Small drifts: seamounts flanks, base of slope
Sheeted drifts	Parallel and subaparallel stratified facies, with internal low-angle downlaps close to contourite channels at the basin environment	Subtabular geometry. < 100 km long, 10 to 60 km wide, ~250 m thick	Large drifts: Western, Eastern, Southern and Motril basins. Small drifts: North of the Maimónides high, upper Moulouya Plateau.
Channel-related drifts	Mostly layered mounded and layered (sub)parallel facies, with an isolated example of layered oblique facies	Usually mounded shape, occasionally wedged geometry. ~ 12km long, 14 km wide, up to 220 m thick (north WAB)	North and west of Ibn Batouta High (WAB), south of Al-Mansour High (EAB)
Confined drifts	Not observed in this unit		
Elongated separated drifts	Layered mounded and layered subparallel facies	Elongated shape and asymmetric mounded geometry, with variable size (the larger ones are associated to contourite channels acting as a moat). < 8 km long, <5 km wide, and up to 240 m thick	Scattered in the slope and basins, with very local extent: S of Al Mansour High, N and S of Ibn Batouta High, S of Ceuta and W of Herradura Highs.
EROSIONAL CONTOURITE FEATURES			
Escarpments	Truncating steep abraded surface	Up to 25 km long, < 6 km wide (typically ~2.5 km) and steep gradient	Transition between the Spanish slope and base of slope basin at the western Alboran; Northern Yusuf Ridge.
Moats	Erosive surface truncating the underlying layered oblique, layered irregular or chaotic disrupted facies	U-shape cross-section, <10 km long, <2.5 km width, tens of m deep	Base of structural highs, always associated to mounded drifts
Channels	Erosive surface truncating the underlying layered irregular, chaotic disrupted and high-reflectivity layered parallel facies. Also layered wavy facies in the northwestern WAB	Low-relief U-cross-section. 1.5 to 12 km wide and few hundreds km long	All deep basins and western base of slope
Terraces	Seafloor unconformity	Mostly abraded planar surface <4 km wide, <30 km long	Cropping the upper plastered and sheeted drifts at the western Spanish and Moroccan slopes
OTHER SEDIMENTARY FEATURES			
Turbidite systems	Canyons layered irregular to chaotic disrupted; Channel-fill deposits high amplitude, chaotic disrupted with interbedded layered irregular facies; Overbank deposits layered parallel to semitransparent; Levees layered oblique; Lobe deposits- chaotic disrupted and layered irregular	Elongated feeder, the deposits show a lobular morphology in cross-section and wedged in longitudinal cut, showing 16 to 70 km long, up to 26 km wide and 330 m thick	Mostly located at the Spanish margin, cutting across the slope and reaching the base of slope, barely touching the basin environment
Mass movement deposits	Chaotic disrupted and chaotic indistinct, locally layered irregular and semitransparent	Irregular elongated, mounded shape. From tens (< 30 km) down to only a few km long	Spanish and Morocco margins, WAB (mostly at the SW Alboran Basin)

Table 5. 1 - Classification, acoustic facies, shape dimensions and locations of the main sedimentary features in the Spanish, Moroccan margins and basins of the Alboran Sea during the deposition of *Pl1* unit.

Unit *Pl2*

Features & Deposits	Acoustic Facies (airgun profiles)	Shape/ Dimensions	Location
DEPOSITIONAL CONTOURITE FEATURES			
Plastered drifts	Stratified facies onlapping upslope and prograding downslope, with internal low-angle onlap, downlap and erosive truncations. Also layered wavy facies east of Ras Tarf Ridge	Low mound shape, occasionally tilted,<130 km length, 3 to 25km width and tens to a few hundreds of m (up to 210 m)thick	Large drifts: W and E Spanish slope, west of Tres Forcas Cape Ridge. Small drifts: seamount flanks, base of slope, slope to basin transition
Sheeted drifts	Parallel and subaparallel stratified facies, with internal low-angle convergent reflections.	Subtabular geometry, wedging towards the upper slope. <90 km long, 5 to 40 km wide, ~ 200 m thick (up to 280 m)	Large drifts: Western, Eastern, and Motril basins, W Moroccan slope. Small drifts: Southern basin, upper Moulouya Plateau.
Channel-related drifts	Layered mounded and layered (sub)parallel facies	Mostly low-mounded shape, sometimes with higher relief. <8km long, < 5 km wide, up to 165 m thick (W Al-Mansour High)	North of Ibn Batouta High (WAB), north and south of Al-Mansour High (EAB)
Confined drifts	Layered mounded facies	Medium to high mound shape. <20 km long and < 7 km wide, reaching 120 m thick	Larger drifts at central WAB and EAB, smaller one SW of Southern Basin
Elongated separated drifts	Prograding layered mounded and aggrading layered subparallel facies	Elongated shape and asymmetric mounded geometry, with variable size. Up to 25 km long,<18 km wide, and up to 130 m thick	Larger drifts: WAB and EAB, associated to contourite channels acting as a moat Small drifts: Scattered in the slope and basins, with very local extent
EROSIONAL CONTOURITE FEATURES			
Escarpments	Truncating steep abraded surface	Up to 80 km long, <7 km wide (typically ~3 km) and steep gradients	Transition between the Spanish slope and base of slope basin at the western Alboran; Northern Yusuf Ridge.
Moats	Erosive surface truncating the underlying layered oblique, layered irregular or chaotic disrupted facies	U-shape cross-section, <17 km long, <3 km width, tens of m deep	Base of structural highs, associated to mounded drifts
Channels	Erosive surface truncating the underlying sediment and/or thinned layered parallel facies with high reflectivity. Also layered wavy facies in the northwestern WAB	Low-relief U-cross-section. 1.5 to 15 km wide and few hundreds km long	WAB, EAB, Southern intra-slope basin, western base of slope
Terraces	Seafloor unconformity	Mostly abraded planar surface,< 30 km long and <9 km wide	Cropping the upper plastered and sheeted drifts at the western Spanish and Moroccan slopes
OTHER SEDIMENTARY FEATURES			
Turbidite systems	Mostly high amplitude, with layered irregular to chaotic disrupted, save the overbank deposits (layered parallel to semitransparent) and the levees (layered oblique)	Elongated feeder, the deposits show a lobular morphology in cross-section and wedged in longitudinal cut, showing 14 to 68 km long, <30 km wide, up to 300 m thick	Mostly at the Spanish margin, cutting across the slope and reaching the base of slope and even the basin
Mass movement deposits	Chaotic disrupted and chaotic indistinct, locally layered irregular and semitransparent	Irregular elongated, mounded shape. < 15 km long and 13 km wide	Spanish and Morocco margins, mostly at the E Almeria margin and the Al Hoceima Valley

Table 5. 2 - Classification, acoustic facies, shape dimensions and locations of the main sedimentary features in the Spanish, Moroccan margins and basins of the Alboran Sea during the deposition of *Pl2* unit.

Unit *Pl3*

Features & Deposits	Acoustic Facies (airgun profiles)	Shape/ Dimensions	Location
DEPOSITIONAL CONTOURITE FEATURES			
Plastered drifts	Stratified facies onlapping upslope and prograding downslope, with internal low-angle onlap, downlap and erosive truncations. Also layered wavy facies east of Ras Tarf Ridge	Low mound shape, occasionally tilted.<120 km length, 3 to 25km width and tens to a few hundreds of m (up to 175 m) thick	Large drifts: W and E Spanish slope, west of Tres Forcas Cape Ridge, Moulouya Plateau, N Xauen Bank Small drifts: seamount flanks
Sheeted drifts	Parallel and subaparallel stratified facies, with internal low-angle convergent reflections.	Subtabular geometry, wedging towards the upper slope. <60 km long, 1 to 40 km wide, ~ 110 m thick (up to 185 m)	Large drifts: Western, Eastern, and Motril basins Small drifts: Southern basin, upper Moulouya Plateau, and Almeria margin.
Channel-related drifts	Not observed in this unit		
Confined drifts	Layered mounded and layered subparallel facies ending up as layered mounded facies at the ends	Mounded shape, in this stage there's an example of extremely low-mounded drift. <30 km long and <25 km wide, reaching 120 m thick	Central WAB and Southern Basin
Elongated separated drifts	Prograding layered mounded and aggrading layered subparallel, with internal downlap reflections	Asymmetric, elongated mounded geometry shape, with variable size. Up to 60 km long,<9 km wide, and up to 140 m thick	Largest drift: EAB Small drifts: concentrated in the highs of the Motril Marginal Plateau
EROSIONAL CONTOURITE FEATURES			
Escarpments	Truncating steep abraded surface	Up to 55 km long, <8 km wide (typically ~5 km) and steep gradients	Western Alboran: Transition between the Spanish slope and base of slope basin; first evidence of another erosive escarpment at the Morocco lower slope
Moats	Erosive surface truncating the underlying prograding layered oblique facies, with layered irregular or chaotic disrupted facies into it	U-shape cross-section, <20 km long, <5 km width, tens of m deep	Base of structural highs, associated to mounded drifts
Channels	Erosive surface truncating the underlying sediment and/or thinned layered parallel facies with high reflectivity.	Low-relief U-cross-section. <150 km long, 1.5 to 12 km wide	WAB, EAB, Southern intra-slope basin, western base of slope.
Terraces	Seafloor unconformity	Mostly abraded planar surface,<50 km long and <10 km wide	Cropping the upper plastered drifts at the western Spanish and Moroccan slopes
OTHER SEDIMENTARY FEATURES			
Turbidite systems	Mostly high amplitude, with layered irregular to chaotic disrupted, save the overbank deposits (layered parallel to semitransparent) and the levees (layered oblique)	Elongated feeder, the deposits show a lobular morphology in cross-section and wedged in longitudinal cut, showing 14 to 72 km long, < 26 km wide, up to 225 m thick	Mostly at the Spanish margin, cutting across the slope, base of slope and reaching the basin
Mass movement deposits	Chaotic disrupted and chaotic indistinct, locally layered irregular and semitransparent	Irregular elongated, mounded shape. < 12 km long and 10 km wide	Spanish and Morocco margins, mostly at the E Almeria margin and the Southern Intra-slope Basin

Table 5. 3 - Classification, acoustic facies, shape dimensions and locations of the main sedimentary features in the Spanish, Moroccan margins and basins of the Alboran Sea during the deposition of *Pl3* unit.

The *contourite escarpments* are relatively narrow (60 m to 10 km) and elongated (tens to hundreds of km long) continuous, deeply-incised regional features (75-200 m high in the upper slope, 200-400m high in the lower continental slope) characterized by juxtaposed medium to high-reflectivity erosive boundaries sculpting an erosional truncation (Figs. 5.5D; 5.6; Tables 5.1-5.7). These are grouped into proximal and distal escarpments based on their location. The proximal escarpment limiting today's terrace T1 affects the prograding shelf deposits (Lobo *et al.,* 2006, 2008, 2015, Fernández-Salas *et al.,* 2007, 2015) making up the slope side of the shelf break (Figs. 5.2-5.6). There are two distal escarpments on the Spanish continental margin adjacent to the WAB, one bounding the T1 terrace (Figs. 5.4 and 5.6) and the other bounding the T2 terrace (Fig. 5.5D). These distal escarpments coincide partially with the palaeorelief of the Messinian escarpment outcropping within the Pliocene seismic units (*Pl1* to *Pl3*) and the relief fades with time (Figs. 5.5 and 5.6). There is another distal escarpment that limits the T3 terrace on the Moroccan continental margin adjacent to the WAB (Fig. 5.6) since the *Pl2*.

The relief of these escarpments is important from a morphological point of view, as they represent the boundary between the different palaeophysiographic provinces. The proximal one separates the uppermost continental slope from the continental shelf, and the distal ones separate the continental margin and basins (Chapter III). These escarpments also represent the boundary of the Pliocene sheeted drifts and Quaternary plastered drifts developed on the continental margins, with the sheeted drifts developed in the basins (Chapters III and IV).

3.3. Turbidite systems

The new seismic stratigraphic analysis to unit scale of the Pliocene and Quaternary sequences shows the TSs interrupt the ubiquitous contourites that make up the continental margins and basins (Figs. 5.2B; 5.3A,D; 5.5D; 5.6B,C; 5.9; 5.10). The turbiditic development is mostly related to point sources represented by submarine canyons (Figs. 5.2B; 5.6C), or multiple gullies (Fig. 5.3). The TSs have a well-defined 3-D geometry, quasi-perpendicular to the continental margin and with fanlobe elements (Fig. 5.3A) that protrude with respect to the adjacent contourites.

The TSs mostly occur on the Spanish side, where a total of fourteen TSs have been mapped (Fig. 5.9). These systems are, from west to east: La Linea, Guadiaro, Estepona, Baños, Torre Nueva, Fuengirola, Malaga, Velez, Torrox, Salobreña, Guadalfeo, Calahonda, Dalias, and Almeria. A few disappear during the Pliocene (the Malaga fan in *Pl1*; Velez and Torrox fans after *Pl1*; Dalias merges with the Almeria TS after *Pl1*) and Quaternary

(Estepona disappears in or immediately after *Qt3*), and new ones appear in the Pliocene (Calahonda, in *Pl2*) and Quaternary units (Torre Nueva in *Qt2*, Baños in *Qt3*) (Figs. 5.9 and 5.10). The size of the TSs generally decreases in the Quaternary units (Fig. 5.10). In contrast, on the Morocco side only three complete TSs (Moulouya, Ceuta and Ouringa) have been mapped, and none of them remain active today: the Moulouya system became inactive after *Pl3* and the Ceuta fanlobe disappeared during *Qt3* after a change on the course of its feeder canyon (Fig. 5.10B,C,D). Last, in the early lower Pliocene (*Pl1*) one system (Yusuf) occur at the foot of the Habibas escarpment, and in the Late Quaternary (*Qt1*) two systems have developed at the southern Alboran Ridge (Piedra Escuela and Al Borani) (Fig. 5.3A).

The internal seismic character of turbidites can be clearly seen due to their sharp lateral contact with the surrounding dominant contourite deposits (Tables 5.1-5.7). They are recognisable by the chaotic facies that onlap and infill U-shape cut and fill features, defining canyon-fill and turbidite channel-fill deposits (Figs. 5.2B and 5.6C), and discontinuous stratified facies with a lenticular shape that resemble channelised lobes (Figs. 5.3A,D; 5.6B).

The characterisation of the architectural elements reveals that most of the feeder canyons that have been mapped on the top of the Messinian surface have a subaerial origin (Estrada *et al.,* 1997). After the Atlantic flooding they evolved into submarine canyons shaping the Pliocene and Quaternary seafloors. In contrast, the Messinian subaerial canyons mapped on the Moroccan continental margin were draped and infilled by Lower Pliocene contourites. Several Pliocene submarine valleys and TSs located near the Strait of Gibraltar (La Linea, Guadiaro, Ceuta) contributed to the progressive infilling of the Zanclean Channel (Fig. 5.6 and 5.9). Some Pliocene and Quaternary local depocentres (Figs. 5.7 and 5.8) defined on the Spanish continental margin, WAB, MB and EAB, correspond to the larger channelised lobe deposits (i.e., Moulouya TS).

3.4. Mass movement deposits

Mass movement deposits differ from contourites and TSs in sediment source, geometry and facies (Figs. 5.2; 5.3A; 5.4A; 5.5C, Tables 5.1-5.7). They are characterized as wedge and lenticular bodies internally defined by semi-transparent, and chaotic facies, from a few to tens of milliseconds in thickness and surfaces of hundreds to a few km^2 (Tables 5.1-5.7). Their occurrence is related to point or linear slope failures and they generally occur as slides and mass transport deposits mostly associated to the major tectonic features, such as the Alboran Ridge and other seamounts. These deposits have been identified in all the

seismic units and environments (Figs. 5.9 and 5.10). They are more frequent: a) in the western Moroccan continental margin and adjacent WAB in the Lower Pliocene unit; b) in the MB and SAB from the Upper Pliocene unit; c) north (from *Qt2*) and south (from *Qt4*) of the Xauen Bank; and d) along all the northern Alboran Ridge and Habibas High in all Pliocene and Quaternary units (Figs. 5.9 and 5.10).

4. Discussion

4.1 The Alboran Sea: a basin with a complex depositional architecture beyond the shelf break

The results about the significance of role of bottom currents in the deep-sea morphodynamics of the Alboran Sea (Chapter III) and the seismic stratigraphy of the Pliocene and Quaternary sequences (Chapter IV) have revealed the ubiquitous distribution of contourites and their long-term, stable behaviour on the Spanish and Moroccan continental margins and adjacent basins. Here, the detailed analysis of seismic units making up those sequences reveals that the depositional architecture is more complex (Figs. 5.9 and 5.10). In fact, the stratigraphic architecture of the Alboran Sea beyond the shelf break has resulted from the interplay between three types of sedimentary systems: contourite, turbidite and mass movement. Contourite and turbidite sedimentary systems occur on the Spanish margin; contourite sedimentary systems dominate the Moroccan continental margin; and contourite and mass movement systems are mainly found in the basins.

4.1.1 Contourite depositional systems. A multiple case in the Alboran Sea

In the Alboran Sea, most of the bottom-current features and deposits are formed and shaped by the main regional MWs: light and dense MWs (LMW and DMW), but also by the interfaces between the AW and the MWs and also between the MWs (Chapters III and IV). Considering this interpretation, two main contourite depositional systems can be defined in the Alboran Sea: the contourite sedimentary system associated with the LMW (hereafter intermediate contourite depositional system, ICDS) on the Spanish margin, and the contourite sedimentary system associated with the DMW (hereafter deep contourite depositional system, DCDS) on the Moroccan side.
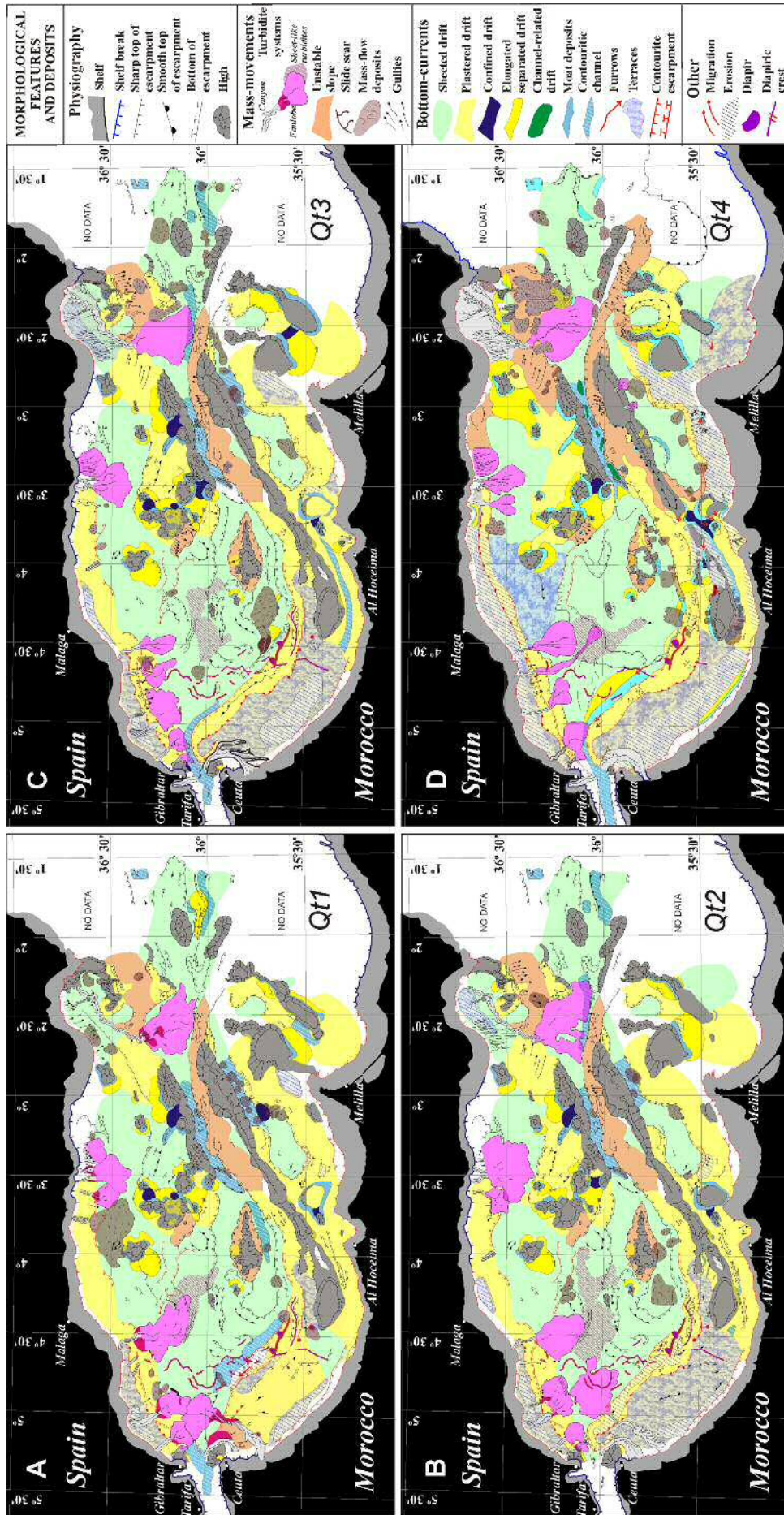
Fig. 5. 10 - Maps showing the distribution of the main sedimentary features of each Quaternary unit, based on the seismic database.

160

Features & Deposits	Acoustic Facies (airgun profiles)	Shape/ Dimensions	Location
DEPOSITIONAL CONTOURITE FEATURES			
Plastered drifts	Stratified facies onlapping upslope and prograding downslope, with internal low-angle onlap, downlap and erosive truncations.	Low mound shape, occasionally tilted, <170 km length, 3 to 40 km width and tens to a few hundreds of m (up to 150 m) thick	Large drifts: W and central Spanish and Moroccan Slopes, Moulouya Plateau. Small drifts: seamount flanks
Sheeted drifts	Parallel and subaparallel stratified facies.	Subtabular geometry, wedging towards the upper slope. < 120 km long, 1 to 70 km wide, ~ 60-80 m thick (up to 175 m at the Southern Basin)	Large drifts: Western, Eastern, and Motril basin, Almeria margin. Small drifts: Southern basin, W of Xauen Bank, Pytheas basin.
Channel-related drifts	Not observed in this unit		
Confined drifts	Layered mounded facies, convergent at the ends.	Mounded shape. <13 km long and < 6,5 km wide, reaching 110 m thick	Djibouti highs and Southern Basin
Elongated separated drifts	Prograding layered mounded and aggrading layered subparallel facies, with internal downlap reflections	Asymmetric, elongated mounded geometry shape, with variable size. Up to 25 km long, <14 km wide, and up to 95 m thick	Largest drift: EAB Small drifts: concentrated in the highs of the Motril Plateau
EROSIONAL CONTOURITE FEATURES			
Escarpments	Truncating steep abraded surface	Up to 32 km long, < 9 km wide (typically ~3 km) and steep gradients	Western Alboran: Transition between the Morocco lower slope and basin
Moats	Erosive surface, truncating the underlying prograding layered oblique facies, with layered irregular or chaotic disrupted facies into it	U-shape cross-section, <25 km long, < 3 km width, tens of m deep	Base of structural highs, associated to mounded drifts
Channels	Erosive surface truncating the underlying sediment and/or thinned layered parallel facies with high reflectivity.	Low-relief U-cross-section. <72 km long, 2.5 to 8 km wide	WAB, EAB, Southern intra-slope basin, Alboran Through
Terraces	Seafloor unconformity	Mostly abraded planar surface, <45 km long and <7 km wide	Cropping the upper plastered drifts at the western Spanish and Moroccan slopes; abrading the Morocco lowermost slope
OTHER SEDIMENTARY FEATURES			
Turbidite systems	Mostly high-amplitude layered irregular to chaotic disrupted facies, save the overbank deposits (layered parallel to semitransparent) and the levees (layered oblique)	Elongated feeder, the deposits show a lobular morphology in cross-section and wedged in longitudinal cut, showing 12 to 90 km long, < 40 km wide, up to 250 m thick	Only in the westernmost Morocco margin; most of them located at the Spanish margin, cutting across the slope, base of slope and reaching the basin.
Mass movement deposits	Chaotic disrupted and chaotic indistinct, locally layered irregular and semitransparent	Irregular elongated, mounded shape. < 24 km long and 38 km wide, up to 140 m thick (Nerja Slide)	Frequent at the E Almeria margin and the Southern Intra-slope Basin, but with a major slide at the central Spanish margin

Unit *Qt1*

Table 5. 4 - Classification, acoustic facies, shape dimensions and locations of the main sedimentary features in the Spanish, Moroccan margins and basins of the Alboran Sea during the deposition of *Qt1* unit.

Unit Qt2

Features & Deposits	Acoustic Facies (airgun profiles)	Shape / Dimensions	Location
DEPOSITIONAL CONTOURITE FEATURES			
Plastered drifts	Stratified facies onlapping upslope and prograding downslope, with internal low-angle onlap, downlap and erosive truncations.	Low mound shape, occasionally tilted, <300 km length, up to 47 km width and tens to a few hundreds of m thick(up to 200 m at Ceuta Drift, 225 m at the folded Xauen intra-slope basin)	Covering most slopes. Large drifts: W to central Spanish and all Moroccan Slopes. Small drifts: seamount flanks
Sheeted drifts	Parallel and subaparallel stratified facies	Subtabular geometry. < 130 km long, up to 70 km wide, ~60-90 m thick (up to 140 m)	Covering most basins. Large drifts: Western, Eastern, Motril basin, Almeria margin. Small drifts: Southern basin, E Provençaux Bank, Pytheas basin.
Channel-related drifts	Not observed in this unit		
Confined drifts	Layered mounded facies, convergent at the ends.	Mounded shape. <10 km long and < 5,5 km wide, reaching 95 m thick	Djibouti highs and Xauen intra-slope basin
Elongated separated drifts	Prograding layered mounded and aggrading layered subparallel facies, with internal downlap reflections	Asymmetric, elongated mounded geometry shape, with variable size. Up to 28 km long, <14 km wide, and up to 110 m thick	Largest drift: Moulouya Plateau. Small drifts: concentrated in the highs of the Motril Marginal Plateau
EROSIONAL CONTOURITE FEATURES			
Escarpments	Truncating steep abraded surface	Up to 75 km long, < 10 km wide (typically ~6km) and steep gradients	Western Alboran: Transition between the Morocco lower slope and basin
Moats	Erosive surface, truncating the underlying prograding layered oblique facies, with layered irregular or chaotic disrupted facies into it	U-shape cross-section, <36 km long, < 3km width, tens of m deep	Base of structural highs, associated to mounded drifts
Channels	Erosive surface truncating the underlying sediment and/or thinned layered parallel facies with high reflectivity.	Low-relief U-cross-section. <55 km long, 2.5 to 8 km wide	EAB, Southern intra-slope basin, Alboran Through
Terraces	Seafloor unconformity	Mostly abraded planar surface, < 145 km long and < 35 km wide	Cropping the upper plastered drifts at the western Spanish and Moroccan slopes
OTHER SEDIMENTARY FEATURES			
Turbidite systems	Mostly high-amplitude layered irregular to chaotic disrupted facies, save the overbank deposits (layered parallel to semitransparent) and the levees (layered oblique)	Elongated feeder, the deposits show a lobular morphology in cross-section and wedged in longitudinal cut, showing 16to 95 km long, < 40 km wide, up to 140 m thick	Most of them located at the Spanish margin, cutting across the slope, base of slope and reaching the basin; few at the W Morocco margin.
Mass movement deposits	Chaotic disrupted and chaotic indistinct, locally layered irregular and semitransparent	Irregular, mostly elongated, mounded shape. < 17 km long and 16 km wide	Frequent at the E Almeria margin, N Xauen Bank, and Southern basin

Table 5. 5 - Classification, acoustic facies, shape dimensions and locations of the main sedimentary features in the Spanish, Moroccan margins and basins of the Alboran Sea during the deposition of *Qt2* unit.

Unit *Qt3*

Features & Deposits	Acoustic Facies (airgun profiles)	Shape / Dimensions	Location
DEPOSITIONAL CONTOURITE FEATURES			
Plastered drifts	Stratified facies onlapping upslope and prograding downslope, with internal low-angle onlap, downlap and erosive truncations.	Low mound shape, occasionally tilted, <300 km length, up to 40 km width and tens to a few hundreds of m thick (maximum 155 m, up to 145 m at the Ceuta Drift)	Covering the slopes. Large drifts: W to central Spanish and all Moroccan Slopes. Small drifts: seamount flanks
Sheeted drifts	Parallel and subparallel stratified facies	Subtabular geometry. <135 km long, 1 to 85 km wide, usually showing a thickness of 60 to 100 m thick but reaching up to 150 m at the Southern Basin	Covering most basins, with the larger drifts located at the deep basins and Motril Plateau, and the smaller ones at intra-slope basins and Almeria upper slope
Channel-related drifts	Layered mounded facies	Asymmetric mounded geometry, 2.5 km long, 50 m thick.	Single example into the Alboran Through
Confined drifts	Layered mounded facies, convergent at the ends.	Mounded geometry. <11 km long and < 6 km wide, reaching 115 m thick	Djibouti highs, Xauen intra-slope basin, Moulouya Plateau
Elongated separated drifts	Prograding layered mounded and aggrading layered subparallel facies, with internal downlap reflections	Asymmetric, elongated mounded geometry shape, with variable size. Up to 28 km long, <15 km wide, and up to 75 m thick	Largest drift: Moulouya Plateau Small drifts: highly concentrated around all the highs of the Motril Plateau
EROSIONAL CONTOURITE FEATURES			
Escarpments	Truncating steep abraded surface	Up to 75 km long in the lower slope and hundreds km long in the upper slope,< 14 km wide (typically ~8 km) and steep gradients	Western Alboran and Southern basin: Transition between the Morocco lower slope and basin.
Moats	Erosive surface, truncating the underlying prograding layered oblique facies, with layered irregular or chaotic disrupted facies into it	U-shape cross-section, <44 km long, < 3km width, tens of m deep	Base of structural highs, associated to mounded drifts
Channels	Erosive surface truncating the underlying sediment and/or thinned layered parallel facies with high reflectivity.	Low-relief U-cross-section. <70 km long, 2.5 to 8 km wide	EAB, Southern intra-slope basin, Alboran Through, Alboran's drain area
Terraces	Seafloor unconformity	Mostly abraded planar surface, < 145 km long and < 32km wide	Cropping the upper plastered drifts at most Spanish and Moroccan slopes
OTHER SEDIMENTARY FEATURES			
Turbidite systems	Mostly high-amplitude layered irregular to chaotic disrupted facies, save the overbank deposits (layered parallel to semitransparent) and the levees (layered oblique)	Elongated feeder, the deposits show a lobular morphology in cross-section and wedged in longitudinal cut, showing 15 to 90 km long, < 34 km wide, up to 165 m thick	Most of them located at the Spanish margin, cutting across the slope, base of slope and reaching the basin; only one in the W Morocco margin. Large slope apron at the southern WAB
Mass movement deposits	Chaotic disrupted and chaotic indistinct, locally layered irregular and semitransparent	Irregular, mostly elongated, mounded shape. < 38 km long and 15 km wide	Frequent at the E Almeria margin and Southern basin

Table 5. 6 - Classification, acoustic facies, shape dimensions and locations of the main sedimentary features in the Spanish, Moroccan margins and basins of the Alboran Sea during the deposition of *Qt3* unit.

Unit Qt4

Features & Deposits	Acoustic Facies (airgun profiles)	Shape/ Dimensions	Location
DEPOSITIONAL CONTOURITE FEATURES			
Plastered drifts	Low-mounded stratified facies prograding upslope and downslope with internal discontinuities (downlap, onlap, truncations)	Low to high mound shape up to few hundreds of km length (< 300 km), 5.5 to 40 km width and <100 to 600 m of relief	Large drifts: Spanish and Moroccan slopes. Small drifts: seamounts flanks, Spanish base of slope
Sheeted drifts	Parallel and subparallel stratified, occasionally semitransparent facies	Subtabular geometry. < 100 km long, 15 to 50 km wide	Large drifts: Spanish base of slope; Western, Eastern, Southern and Motril basins. Small drifts: Alboran Ridge, seamount tops
Channel-related drifts	Aggrading and prograding low-mounded stratified facies	Low mound shape. ~ 10 km long, <5 km wide	Alboran Trough
Confined drifts	High-mounded stratified facies	High mound shape. Few to tens of km long and wide and 100 to 300 m high	Between highs in the Motril Marginal Plateau
Elongated separated drifts	Prograding and aggrading, low to high-mounded stratified facies	Low to high mound shape. <40 km long and 20 km wide	Locally at the foot of seamounts, western Moroccan slope and shelf break scarp
EROSIONAL CONTOURITE FEATURES			
Escarpments	Steep to gentle surface with oblique stratified facies or truncated prograding facies	Narrow (60 m to 16 km), steep (2° to 11°) scarps hundreds km long	Bounding physiographic domains: -Shelf break & slope: 90 to 161/223 m w.d. (Spanish) and 100/150 to 180/339 m w.d. (Moroccan). -Spanish slope & Motril Basin: 400 to 630 m w.d. -Motril Basin & Western basin: 1000 to 1300 m w.d. -Moroccan slope & Western and Southern basins: 600 to 1000 m w.d.
Moats	Erosive surface truncating underlying stratified or chaotic facies	U-shape cross-section,5 to 43 km in length, < 6.5 km width, and <10 to 85m of relief	Associated to the separated drifts
Channels	Erosive surface truncating underlying stratified or chaotic facies	U-cross-section. 1.4 to 6.5 km wide and 11 to 70 km long	Alboran Trough & Moroccan slope
Terraces	Truncating erosive to conformity surfaces	Flat surface < 30 km wide, <150 km long; mostly abraded in the proximal sectors	Molding the slope plastered and sheeted drifts of the Spanish and Moroccan slopes
OTHER SEDIMENTARY FEATURES			
Turbidite systems	Layered irregular and chaotic disrupted facies	Elongated lobular and fan shape, 19 to 53 km long, few km wide	Spanish margin and Southern Basin
Mass movement deposits	Chaotic disrupted and indistinct facies	Irregular elongated and lobular shape, hundreds down to few km in scale	Spanish and Moroccan margins, Alboran Trough, Alboran Ridge and seamounts

Table 5. 7 - Classification, acoustic facies, shape dimensions and locations of the main sedimentary features in the Spanish, Moroccan margins and basins of the Alboran Sea during the deposition of *Qt4* unit. Chapter III.

164

The ICDS mostly comprises the large-scale Pliocene sheeted and Quaternary plastered drifts on the Spanish continental slope. Also, small scale elongated separated drifts and their associated moats, as well as small-scale plastered and sheeted drifts, all of them associated to a few highs swept by the LMW are included. The DCDS is dominant in the Alboran Sea and comprises the large-scale Pliocene sheeted and Quaternary plastered drifts on the Moroccan continental slope, the sheeted drifts infilling the basins, most of the small scale elongated separated, confined and channel-related drifts, and a great variety of erosive features such as contourite channels, moats, and distal escarpments. Most of the contourite features were formed under the action of both MWs, but the T1, T2 and T3 terraces and the proximal escarpments were formed by water masses in combination with one another because the turbulent processes associated with their interfaces were responsible for their formation: i) T1 and the Spanish proximal escarpment by the AW with LMW interface (Fig. 5.11D); ii) T2 and the Moroccan proximal escarpment by the AW and DMW interface; and iii) T3 by the LMW and DMW interface. These contourite elements could, then, be linked to both water masses making up the interfaces. In consequence, T1 and T3 and their adjacent proximal escarpments could be part of an Atlantic Contourite Depositional System (ACDS) or ICDS and DCDS, respectively; and T2 could be part of the ICDS or DCDS.

The literature indicates that there are two different terms used to define the association of contourite features. One is the *Contourite Depositional System (CDS)* that comprises erosive and depositional features sculpted by the same water mass in the same area (Hernández-Molina *et al.*, 2006a; Rebesco and Camerlenghi, 2008); the other term is the *Contourite Depositional Complex (CDC)*, defined by different CDSs formed by the same water mass in the same or adjacent basins (Hernández-Molina *et al.*, 2008b; Rebesco *et al.*, 2014). Neither of these terms defines a set of two or more CDSs located in the same area, each sculpted by multiple water masses during its development. Thus, we propose the term *Multiple Contourite Depositional System (MCDS)* to refer to the entire set of different CDSs in the Alboran Sea that have been generated since the opening of the Strait of Gibraltar and where the contourite features have been growing uninterruptedly until the present day due to the interplay of several water masses throughout this period.

4.1.2 Turbidite systems and the uneven depositional architecture of the Spanish and Moroccan margins

The TSs defined in the Alboran Sea can be grouped into two main types of sedimentary models based on Reading and Richards (1994) and Richards *et al.* (1998): submarine fan

(La Linea, Guadiaro, Estepona, Baños, Torre Nueva, Fuengirola, Malaga, Velez, Torrox, Salobreña, Guadalfeo, Calahonda, Dalias, Almeria, Ceuta-E, Moulouya, Al Borani, Piedra Escuela and Yusuf) and submarine ramp (Ouringa, Dalias, Calahonda) types. The TSs interrupt the lateral continuity of the contourite features of the ICDS and DCDS of the Spanish continental margin and adjacent basin during the Pliocene and Quaternary, and of the DCDS of the Moroccan margin and adjacent basins during the Pliocene. Both margins have been tectonically active during the Plio-Quaternary (Bourgois *et al.,* 1992; Maldonado *et al.,* 1992; Woodside and Maldonado, 1992; Docherty and Banda, 1995; Estrada *et al.,* 1997; Alvarez-Marrón, 1999; Fernández-Ibáñez *et al.,* 2007; Mauffret *et al.,* 2007; Fernández-Ibáñez and Soto, 2008; Martínez-García *et al.,* 2013) and have similar geographic, climatic and fluvial systems supplying sediment load (Stanley *et al.,* 1975; Liquete *et al.,* 2005; Fernández-Salas, 2008; Vázquez *et al.,* 2015; Chapter III), but it is the presence of TSs that provokes the different sedimentary architecture displayed by the two continental margins bordering the Alboran Sea: on the Spanish margin the contourites coexist with TSs, whereas on the Moroccan margins contourite features predominate.

4.1.3 Mass movement system and the reworking of contourites

The mass movement sedimentary systems are mainly associated to the structural highs dotting the basins, and mostly coexist with the relatively small-scale elongated moat-drifts that form at their feet and the plastered and sheeted drifts that drape their walls. The lateral relationships between the two systems and the intercalations of mass movement deposits within the contourites, suggest their occurrence is related to the reworking of the contourites draping the highs due to tectonic activity and/or oversteepening of the seafloor (Martínez-García, *et al.,* 2009; Casas *et al.,* 2011; Ercilla and Casas, 2012; Alonso *et al.,* 2014a; Casas *et al.,* 2015).

4.2 The palaeoceanography of the Alboran Sea: a geological approach

Bottom-current processes in the deep sea area are stable and encompass long periods of time. Consequently, their resulting sedimentary products have a high potential for preservation in the sedimentary record. In this way, contourites constitute the best clues for decoding the palaeoceanography. The geological approach to this involves the need to elucidate the basic oceanographic processes responsible for the contourites. Recent results based on the general contourite characterisation in the Alboran Sea identify three phases of palaeocirculation and current conditions since the opening of the Strait of Gibraltar: the Atlantic Zanclean flooding, the Pliocene Sea, and the Quaternary Sea (Juan *et al.,* 2016; Chapter IV). This chapter characterises in detail a great variety of contourite

elements, both depositional and erosive, within the Pliocene and Quaternary seismic units; in consequence, there are the elements necessary to define the basic oceanographic processes and determine their occurrence, relative magnitude and energy, and time of action. The following paragraphs are concerned with the link between the contourite elements and these processes. The contribution of TSs to decoding water mass characteristics is also briefly discussed.

4.2.1 Erosive contourite features as key elements

Escarpments

The relict and modern escarpments mapped in the Alboran Sea allow us to consider the occurrence of two palaeoceanographic processes: turbulent processes (internal waves) on the shelf breaks (Fig. 5.11A), and the acceleration (Fig. 5.11A,B) and recirculation of flows (current branches and filaments) (Fig. 5.11C,D).

i) *Turbulent processes (internal waves) on the shelf breaks.* Bottom topography produces variations in the stratification of water masses (Smith, 1988), with the edges of continental shelves being one of the topographies that leads to interesting and important physical processes in the ocean (Huthnance, 1981). One of these processes is the generation of turbulence and internal waves at water masses interfaces, which can cause important erosion when one interface intersects the seafloor (e.g., Sarnthein *et al.,* 1982; Pomar *et al.,* 2012; Shanmugam, 2013a,b) (Fig. 5.11A). Indeed, internal waves interacting with a sloping seafloor can lead to the formation of internal boluses whose activity reworks and/or resuspends seafloor sediments (Pomar *et al.,* 2012; Chen *et al.,* 2014). The sharp relief of the shelf break in the Alboran Sea would produce the perturbation of the moving interface between AW and MWs, generating trains of internal waves in the contour water mass. Packets of internal waves have been recorded on the Moroccan (Vázquez *et al.,* 2008; Fig. 3.8d in Chapter III) and Spanish (Puig *et al.,* 2004) shelf breaks which in conjunction with theoretical models (Brandt *et al.,* 1996; Pomar *et al.,* 2012; Shanmugam 2012b), suggest they may be a ubiquitous feature in the Alboran Sea. The high energy of these waves would favour the reworking of the preserved upper Pleistocene prograding regressive deposits that make up the slope side of the shelf break (Ercilla *et al.,* 1994; Hernández-Molina *et al.,* 1994; Lobo *et al.,* 2008, 2015; Fernández-Salas *et al.,* 2015) leading to the formation of the proximal escarpment that bounds the T1 and T3 terraces (Fig. 5.11A).

ii) *The acceleration and recirculation of flows (current filaments and branches).* The literature suggests that the topographic confinement of basins affects the bottom currents,

modifying their velocity and pathway as well as producing turbulent and faster flows at the basin edges (e.g., McCave and Tucholke, 1986; Faugères and Mulder, 2011; García *et al.,* 2009; Rebesco *et al.,* 2014; Hernández-Molina *et al.,* 2015) (Fig. 5.11A,B). Likewise, confined basins may also favour the recirculation of components of the denser and deep-running water mass (Alhammoud *et al.,* 2010). The distal regional escarpment bounding the Spanish margin adjacent to the WAB (Figs. 5.5 and 5.6), points to an acceleration of currents flows(Chapter IV).That acceleration could be produced by (i) flow steering due to local sea-floor topography (e.g., the mound topography of the immediately upslope plastered drift) (Figs. 5.4-5.6), (ii) the margin configuration (the WAB narrows towards the Strait of Gibraltar) (Fig. 5.1), and/or (iii) current recirculation in the WAB and recirculation of a filament of the DMW in that basin (Chapter IV) (Fig. 5.11C). As the escarpment progressively fades during the Quaternary, the third option is the most likely, because the flow steering due to the enhancement of the slope plastered drifts during the Quaternary, and the N-S shortening and W-E stretching that affect to the Alboran Sea due to its convergent tectonic setting between the Eurasia and Africa plates, rather both would contribute to a flow acceleration. Then the cause of the gradually disappearance of the escarpment relief during the Quaternary may suggest that the recirculation was relatively more intense during the Pliocene when the WAB was deeper and confined, keeping the relict Messinian escarpment (Figs. 5.5 and 5.6) free of sediment. As it has been proposed in Chapter IV and based on the Faugères' models (1999), the force of Coriolis would not constrain the counterclockwise flow against the scarp; instead, it would favour its lateral spreading (Fig. 5.9) and the formation of the mapped sheeted drift instead of a moat and a separated drift at the foot of the escarpment (Figs. 5.5 and 5.6).

The other escarpment is the distal escarpment bounding the western Moroccan slope adjacent to the WAB, which began to develop since the Lower Pliocene and became a striking feature after the end of Gelasian (Fig. 5.11B). The formation and evolution of this escarpment could indicate a DMW flow acceleration due to the progressive morphostructural changes of the seafloor that continue today. These changes include the formation of the narrow corridor of the Alboran Trough since the Late Pliocene due to the uplifting of the Alboran Ridge (Martínez-García *et al.,* 2013) (Fig. 5.11D). The Alboran Trough funnels DMW and directs the formation of an accelerated and turbulent branch that enters the WAB. There, part of this branch is also directed by the uplifting highs against the Moroccan continental slope (Parrilla *et al.,* 1986; Millot, 2009; Chapter III) (Fig. 5.11D). This high velocity flow would favour the reworking of the slope plastered drift deposits forming that escarpment (Fig. 5.11B). In conjunction with this flow, the

development of the escarpment would have been also favoured by the action of the DMW recirculation mentioned above. The two flows would merge, increasing the seafloor reworking capacity.

Terraces

Modern and relict terraces in the Alboran Sea point to the occurrence of turbulent processes (internal waves) that characterise the water masses interfaces, and to the acceleration of current flows, respectively.

i) Turbulent processes (internal waves) at water mass interfaces. The results of the Chapter III about the three regional contourite terraces (T1, T2, and T3) that shape the present-day seabed of the Alboran continental margins and MB, have provided information on turbulent processes (internal waves) at the interfaces (i.e., well-defined pycnoclines) between the AW and LMW (T1, Fig. 5.11E), AW and DMW (T3), and LMW and DMW (T2, Fig. 5.11F), where there are strong density, temperature and salinity gradients. The internal waves are able to mobilise and resuspend seafloor sediments, being then laterally distributed by contour water masses over the terraces. The link of contourite terraces with interfaces between two different water masses (and internal waves) was suggested by Hernández-Molina *et al.* (2009) in the Argentine Margin and later proved by Preu *et al.* (2013). The presence of these terraces since the Late Pliocene suggests a new scenario with stronger and permanent pycnoclines of the AW, as well as the LMW and DMW since that time (Juan *et al.*, 2016; Chapter IV). In those areas where those interfaces touch the Spanish and Moroccan slopes and MB, the near-bottom polishing and flattening processes of the internal waves that produce seafloor sediment resuspension, reworking and transport, and the lateral variations of interfaces due to the high frequency and amplitude sea level changes, all these actions have led to a progressive widening of the erosional terraces during the Quaternary.

ii) Acceleration of current flows (filaments). The relief created by the relict Messinian terrace (Fig. 5.11C) on the western Spanish continental margin may have favoured the occurrence of a focused and accelerated DMW filament that remained active until the end of the Pliocene (end of unit *Pl3*, BQD boundary) (Figs. 5.5 and 5.6). The literature provides examples of local changes in seafloor morphology affecting bottom currents and modifying their velocity (Hernández Molina *et al.*, 2006a; Stow *et al.*, 2009, 2013; Rebesco *et al.*, 2014, among others). This terrace has been buried mostly by TSs and a plastered drift since the onset of the Quaternary (Juan *et al.*, 2016) (Figs. 5.5 and 5.6), suggesting a change towards a slower flow of the DMW branch sweeping that area.
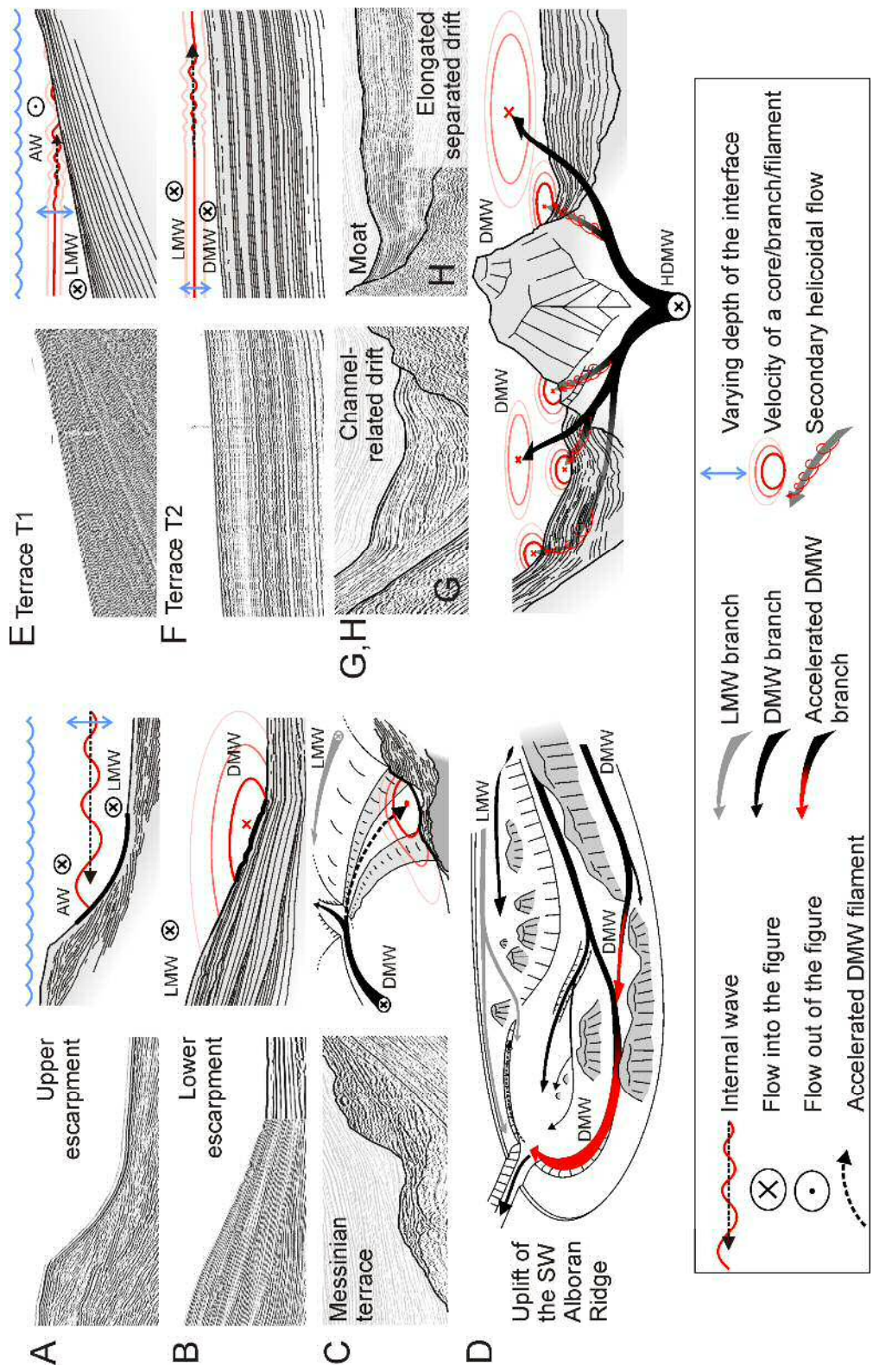
Fig. 5. 11 - Schematic models showing the oceanographic processes sculpting the erosive contourite features.

170

Contourite valleys

Contourite valleys in the Alboran Sea also give us information about the acceleration of branches and formation of secondary flows generated by a complex seafloor morphology.

i)   The acceleration of current flows (branches). The literature suggests that valley-like features are related to the formation of flow instabilities when water masses interact with morphological highs, ridges and steep scarps that act as obstacles (e.g., García *et al.,* 2009). They split branches of the water masses and produce turbulent and faster, secondary flows, i.e., multiple current pathways (Chapter III) (Fig. 5.11D). The channels in the Alboran Sea suggest the splitting of the DMW into accelerated branches by the relict sedimentary Zanclean Channel up to the Late Pliocene, or by structural corridors as the Alboran Trough, SAB and Al Hoceima valley from the Late Pliocene onwards (Fig. 5.11D). Since then, the Quaternary has mainly been characterized by circulation with multiple current pathways, where structural corridors have played an important role in the pathway of the three main DMW branches (Chapter III), as well as their acceleration and deceleration (Fig. 5.11D).

ii)   Secondary flows. The moats, mainly associated to the highs that dot the Alboran seafloor (Fig. 5.11G, H), suggest the formation of secondary flows. The highs represent an obstacle to water masses and on approaching these highs the current breaks up into secondary flows forming helicoidal cores, with velocity values that are sufficient to winnow and redistribute sediment (Fig. 5.11G, H). Recent sedimentological studies of the nearsurface sediment of the modern Djibouti moat, point to a relatively higher velocity of bottom currents as well as their acceleration during cold periods (López-González *et al.,* 2013; Alonso *et al.,* 2013, 2014b). The mapping of the moats through the Pliocene and Quaternary units (Figs. 5.9 and 5.10) point to the fact that secondary flows of the DMW were relatively scarce in the Pliocene, becoming more frequent during the Quaternary.

4.2.2 Contourite drifts as key elements

The drift type points to fundamental differences in the strength of bottom flow.

i)   Bottom flow strength. Sheeted drifts form under a regionally stable tabular water mass that flows with lower velocities operating over relatively large flat seabeds (e.g., Faugères *et al.,* 1999; Stow *et al.,* 2008; Juan *et al.,* 2016) (Fig. 5.11F); the mounded drifts (plastered, elongated separated, confined, Fig. 5.11E,G,H) form under a more intensified bottom motion, mainly of a tabular or multicore water mass operating over steep and/or

irregular seafloors (e.g., Stow *et al.*, 2008; Hernández-Molina *et al.*, 2008a; Ercilla *et al.*, 2011; Chapter III). In the Alboran Sea, the evolution of the large-scale slope drifts over time (Figs. 5.2-5.6; 5.9; 5.10; Tables 5.1-5.7) also provides information on the strength of the bottom flow (Figs. 5.9; 5.10). The drifts show changes from sheeted to plastered type from the Late Pliocene onwards, contributing to the upward and seaward growth of the Spanish and Moroccan margins. This change points to the fact that from the opening of the Strait of Gibraltar to the Late Pliocene, LMW and DMW operated with an overall lower energy bottom motion, and from that point, the general strength of both water masses increased. A similar interpretation has been also suggested from the evolution of the contourite terraces. In addition to the changes in drift morphology, and as it has been mentioned in Chapter IV, the vertical increase in acoustic reflectivity displayed by drift deposits in the Quaternary, points to a shifting from a weak bottom current during the Pliocene to a high-velocity bottom current during the Quaternary

4.2.3 The contribution of the turbidite systems

Interaction between contourites and turbidites occurs when alongslope bottom currents and downslope gravitational processes are present in the same sedimentary basin, either simultaneously or alternating (Mulder *et al.*, 2008; Marchès *et al.*, 2007). The new insights into the Pliocene and Quaternary stratigraphy reveal that both processes have been operating in the Alboran Sea since the opening of the Strait of Gibraltar, leaving a sedimentary record with coexisting contourite and TSs (Figs. 5.9; 5.10). Therefore, it can be tentatively assumed that the evolution of the TSs over time has been influenced by the evolution of the water masses.

The literature on TSs in the Alboran Sea suggests that glacioeustatic changes, morphostructure of the margins, and hinterland sediment sources are the main factors controlling their evolution (Alonso and Maldonado, 1992; Ercilla *et al.*, 1994; Estrada *et al.*, 1997; Alonso and Ercilla, 2003). Nevertheless, none of those works explain the general recession of TSs during the Quaternary. Taking into account the fact that Quaternary glacioeustatic sea level changes and their related sediment supply only could favour turbidity flow activity compared to the Pliocene, it is suggested that bottom circulation has been the main factor controlling the decreased turbidity activity during the Quaternary. Specifically, *enhanced water mass action on sediment transport, the better-defined water mass structure* between the AW and MWs*, and the presence of interfaces with greater density contrasts (i.e., well-defined pycnoclines)* since the

Quaternary are the main oceanographic factors influencing the general recession of the TSs. This oceanographic scenario would affect the turbidity flows in two ways:

i) The formation of gravity flows with less sediment charge. This is because when sediment from the continent arrives in the sea, the AW first quickly disperses the sediment in suspension over a large area, and then MWs and their interfaces distribute the sediment over long distances before they deposit it (Chapter III).

ii) The piracy of the fine sediment transported by gravity flows running along the TSs. This privacy would cause gravity flows with lower concentration, affecting to the canyon and channel axial incision and undercutting, to the downslope transfer of sediment (it decreases), and then to TSs development and their architecture.

Chapter VI - Bottom-current signatures in the uneven turbidite systems of the Alboran Sea

Chapter VI - Bottom-current signatures in the uneven turbidite systems of the Alboran Sea

1. Introduction

Previous results from the Alboran Sea (Chapters III, IV, and V) suggest that this sedimentary basin is an ideal context in which to analyse the interaction between alongslope and downslope sedimentary processes. Its complex morphostructural and oceanographic contexts, and their changes during the Pliocene and Quaternary have favoured a complex interaction between contourite, turbidite and gravitational systems, resulting in a depositional architecture that changes alongslope and basinward over short distances. The distribution of contourites in the Alboran Sea demonstrates that the action of bottom-current alongslope processes are a common phenomenon on both margins. This contrasts sharply with TSs distributions: these suggest that gravity flow downslope processes commonly occur on the Spanish margin where contourites coexisted with canyon- and gully-fed TSs during the Pliocene as well as in the Quaternary. In contrast, only three TSs have been mapped on the Moroccan margin, and none of these are active today.

The purpose of this Chapter is to look at the influence of contourite alongslope processes on the uneven development of TSs in the Alboran Sea. The general aims of this Chapter are:

> To outline the morphological and sedimentary signatures resulting from the interaction of alongslope contourite and downslope sedimentary processes in order to interpret the different levels of interaction through the Pliocene and Quaternary TSs.
> To create conceptual models showing how the uneven development of TSs also conditions the different sedimentary models for the Spanish and Moroccan continental margins.

The dataset used in this chapter is a compilation of single- and multi-channel seismic reflection profiles acquired during various campaigns over recent decades (Fig. 2.3). The

dataset also includes the sedimentological analysis of 17 sediment cores available from the Continental Margins Group at the ICM-CSIC (Lebreiro and Alonso, 1998; Alonso *et al.*, 1999b; Pérez-Belzuz, 1999). These cores were recovered from some of the WAB and MB TSs (Fig. 2.5). The Figure 6.1 shows the different areas that are analysed in this chapter:
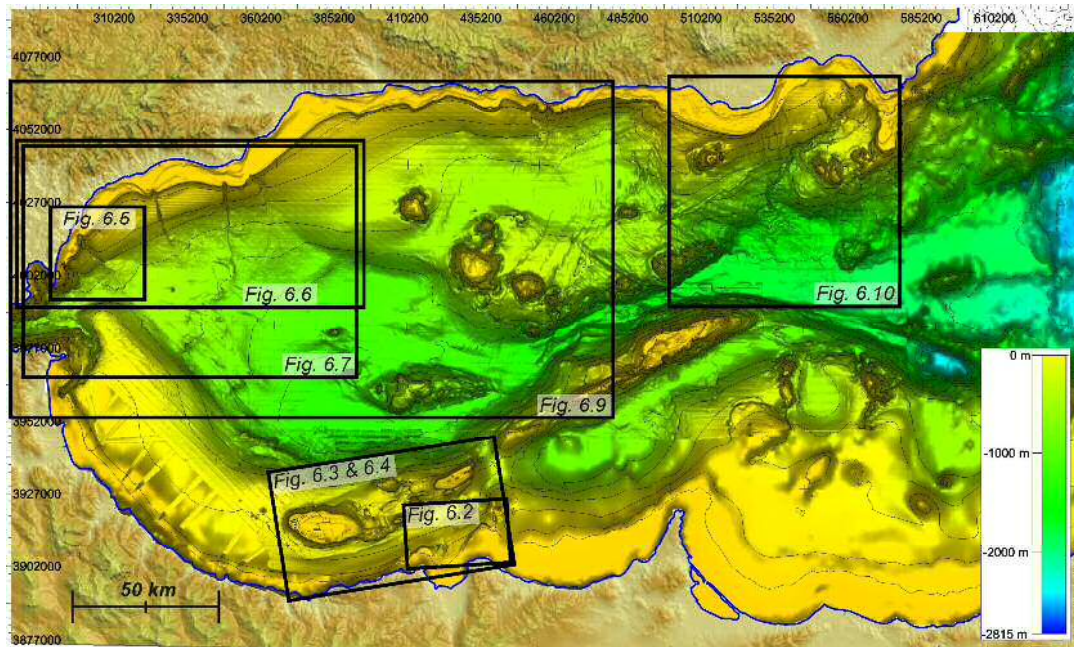
Fig. 6. 1 - Bathymetric map showing the TSs of the Alboran Sea. The black rectangles refer to the location figures 6.2 to 6.7, 6.9 and 6.10.

2. Levels of interaction between alongslope and downslope processes

Different levels of interaction between alongslope and downslope processes have been identified in the Alboran TSs based on the morphological and sedimentary architecture analysis and their spatial and temporal relationships with contourite features. The classification summarised by Marchès *et al.* (2010) has been used to define the levels of interaction.

The following interaction processes are characterised and interpreted:

a) Alongslope processes dominate downslope processes

b) Alternating downslope and alongslope processes

c) Alongslope processes influence downslope processes

d) Downslope processes dominate alongslope processes

2.1. Alongslope processes dominate downslope processes

The morphosedimentary signature: The main morphosedimentary signature of alongslope processes dominating downslope ones is found on the Moroccan margin (Figs. 6.1 and 6.2). First, from the bathymetric map of the Nekor Canyon it can be seen that the canyon disappears abruptly at 300 m water depth, crosscut by the alongslope Al Hoceima contourite channel (Fig. 6.2).
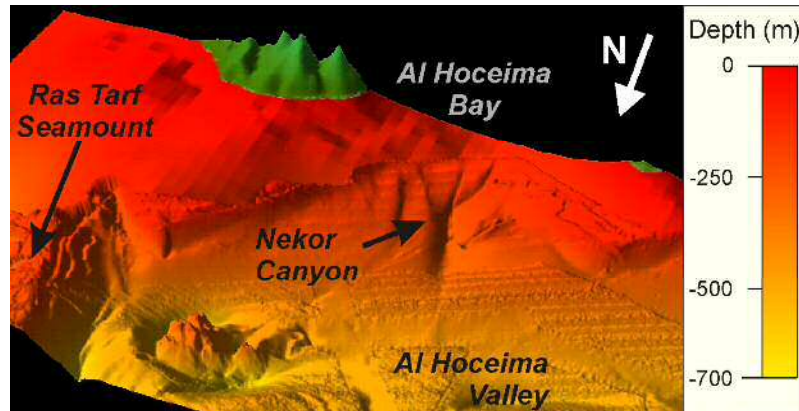
Fig. 6. 2 - Bathymetric map showing the truncation of the Nekor Canyon when reaching the Al Hoceima Valley, whose axis is eroded by a contourite channel.

The analysis of the seismic database evidences this canyon incises slope plastered drift deposits (Figs. 4.6 in Chapter IV and 5.5 in Chapter V), and displays reflectors truncated against the wall, as well as several phases of scour and fill features infilled by onlapping stratified and chaotic facies (Fig. 6.3A,B, Lafosse *et al.*, 2016). This all suggests the action of gravity flow deposits, at least since *Qt2* (Fig. 5.10, Chapter V). However, the seismic profiles show a lack of depositional bodies related to the gravity flows running along the canyon. Instead, the canyon mouth passes laterally to the U-shaped cross-section of the Al Hoceima contourite channel (Fig. 6.3C,D), whose floor is defined by stratified facies truncated in an alongslope direction, parallel to the trend of the margin.

Interpretation: The downslope truncation of the Nekor canyon and lack of lobe deposits at its mouth (Figs. 6.2 and 6.3C,D) point to contour current activity dominating the downslope processes. Specifically, this contour current activity must be related to the strong action of the WDMW running along the Moroccan margin (Fig. 6.4). The southernmost branch of this water mass is funnelled within the Al Hoceima Valley, which represents a corridor created by the Moroccan continental margin, and the morphological highs of the Tofiño area (Fig. 6.4). At this location, the vigorous DWM prevents any deposition of the sedimentary load from the gravity flows running along the canyon. When this sediment reaches the water depths affected by the WMDW, it is

quickly dispersed and transported along the contourite channel towards the Strait of Gibraltar (Fig. 6.4).
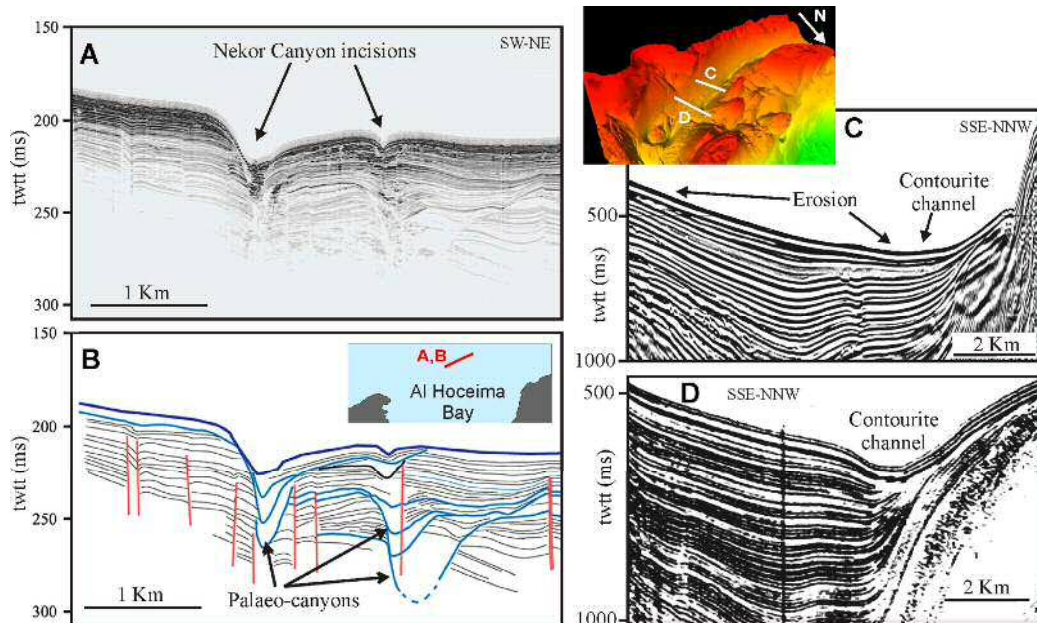
Fig. 6. 3 - Seismic profiles in the vicinities of the Nekor Canyon: A) Transverse TOPAS seismic profile of the Nekor Canyon, registered during the SARAS cruise; B) Interpretation of the same profile, highlighting the Nekor palaeocanyons. A and B are modified from Lafosse et al. (2016). C) Profile at the mouth of the Nekor Canyon, showing a wide section of the Al Hoceima contourite channel; D) Downstream profile next to the Nekor Canyon, showing a deeply incised section of the Al Hoceima contourite channel.
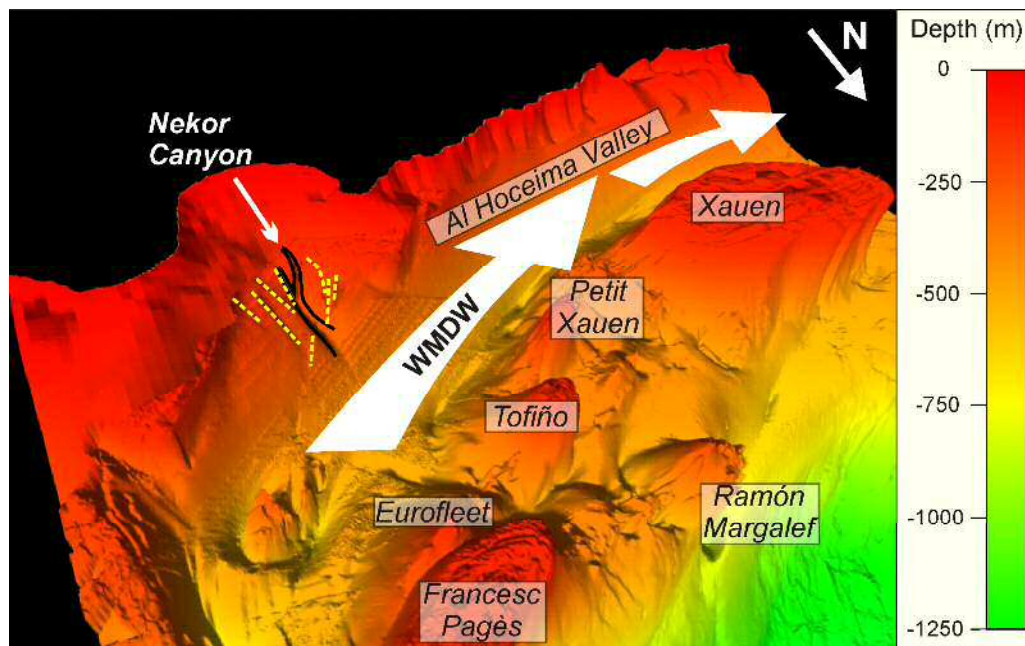
Fig. 6. 4 - WMDW sweeping the seafloor within the Al Hoceima Valley, next to the mouth of the Nekor canyon. Legend: Large white arrows - WMDW flow; Dashed yellow lines - Outcropping faults in the vicinities of the Nekor Canyon; Solid black lines - Nekor canyon walls.

2.2. Alternating downslope and alongslope processes

The morphosedimentary signature: The main morphosedimentary signature of alternating downslope and alongslope processes is found in the WAB, in the most recent lobe deposits of the Guadiaro TS (Fig. 6.5). The recentmost deposits of the eastern side of the Guadiaro lobe is characterised by levels of wedge-shaped chaotic facies that extend and thin from the Guadiaro turbiditic channel toward the lobe fringe. These levels of chaotic facies alternate with levels of stratified facies that have a high lateral continuity and acoustic amplitude with mound morphology that pinches out toward the Guadiaro channel (Fig. 6.5C). Their vertical arrangement suggests an apparent upslope migration that progressively onlaps the bulge created by the lobe deposits. The stratified facies passes laterally into the Guadiaro channel deposits or a moat-like feature defined by high acoustic amplitude reflections.
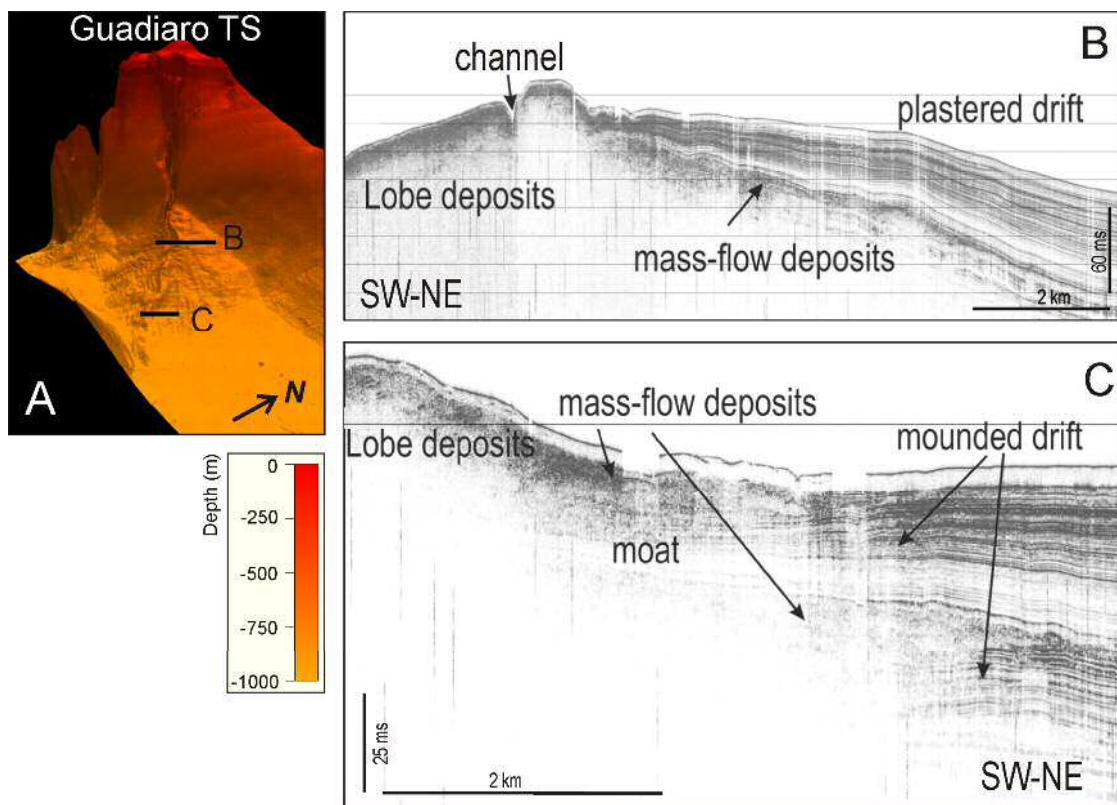
Fig. 6. 5 –Example of the downslope and alongslope processes alternating in the Guadiaro TS (Spanish margin). A) Bathymetric map showing the location of the TOPAS profile; B) and C) TOPAS seismic records showing the alternation of mass-flow deposits and contourites on the right margin of the Guadiaro lobe deposits (WAB).

Interpretation: The most recent pattern of lobe deposits from the Guadiaro TS is interpreted as the vertical stacking of alternating mass-flow deposits and contourites (Fig. 6.5). The chaotic deposits are recognised as mass-flow deposits formed by the gravity flows running along the Guadiaro channel. The levels of stratified facies are interpreted as plastered drifts, one of them having an incipient moat. The drifts have an aggrading pattern and rest unconformably on the mass-flow deposits.

It is proposed that the deposition of the mass-flow deposits was most important during the late Quaternary sea level falls, in agreement with previous works on the Alboran TS evolution (Ercilla *et al.*, 1994; Estrada *et al.*, 1997; Alonso and Ercilla, 2003). At those times, the seaward migration of the shoreline led to an increased sediment supply and basinward transport, generating a heavy sediment load that induced high energy processes with greater erosive power that cut and deepened the Guadiaro canyon and channel. This channelised downslope transport decreased during the relative sea level rises and highstands. When there was reduced or no downslope sediment transport, the permanent steady bottom flows of the DMW would have favoured drift formation until the arrival of new mass flow avenues. The sediment for constructing the drift may have been provided by low density gravity flows running along the canyon or by the reworking of the mass-flow deposits. In fact, at the present time nepheloid layers have been observed when the Guadiaro River, whose mouth is close to the Guadiaro canyon, is in spate (Puig *et al.* 2004).

On the other hand, the formation of a recirculating filament of the WMDW with a strong bottom-current flow in the WAB (Juan *et al.*, 2016, Chapter V), suggests that it could be current flow that conditions the deposition of contourites alternating with mass-flow deposits on the eastern side of the Guadiaro lobe. In this sense, the prominent bulge formed by the Guadiaro lobe deposits would represent an obstacle affecting the pathway and velocity of that filament, favouring the deposition of plastered drifts over the lobe slope.

2.3. Alongslope processes influence on downslope processes

Three main morphological and sedimentary signatures from this type of interaction have been identified in the central and western TSs on the Spanish margin. These signatures are related to: i) the spatial distribution of the lobe deposits; ii) the similarities and differences in the architectural elements; and iii) the sedimentological characteristics of the deposits.

i) The morphosedimentary signature on the spatial distribution of the lobe deposits: One place that shows the morphosedimentary signature of alongslope processes influencing downslope ones are the lobe deposits of the TSs on the western Spanish margin. The depositional architecture of the Pliocene (La Linea, Guadiaro, Estepona, and Fuengirola) and Quaternary (La Linea, Guadiaro, Baños, Torre Nueva, and Fuengirola) TSs developed in that sector indicate the spatial and temporal variations in the distribution of their channelised lobe deposits (Figs. 5.9 and 5.10, Chapter V). A detailed analysis of these lateral changes has revealed a concomitant eastward migration in the Guadiaro lobe deposits, as well as in Estepona and Fuengirola lobe deposits during the Pliocene units, and more enhanced in the unit *Pl3* (Fig. 6.6). In contrast, the direction of lateral migrations do not reveal a similar pattern in the Quaternary seismic units.
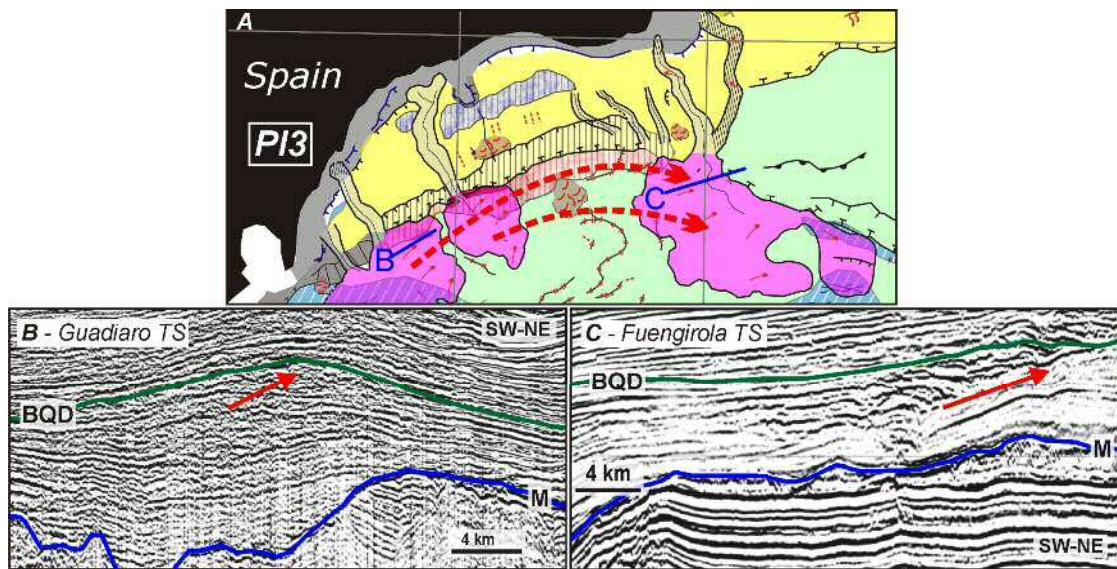
Fig. 6. 6 –Examples of the influence of alongslope processes on downslope processes on the Spanish margin. A) Map showing the eastward migration of channelised lobe deposits in the WAB, mainly during the Upper Pliocene. B) Single channel profile of the Guadiaro TS, with the eastward migration of the stacked lobes. C) Multichannel profile of the Fuengirola TS, showing the eastward and upslope migration of leveed channels and lobes. Legend: M, top of Messinian; BQD, Base of Quaternary Deposits; see also Fig. 5.9.

Interpretation: These relocations in the lobe deposits imply that TS development involved significant lateral changes in the gravity flows. In the absence of regional palaeotopographic control over the route of the gravity flows feeding the mentioned TSs on the western Spanish margin, the simultaneous eastward migration of the lobe deposits suggests the existence of a vigorous bottom current that redistributed the gravity flow sediments. Results from the Chapters IV and V indicate that during the Upper Pliocene (*Pl3*), the WAB was about to attain its semi-confined configuration after the uplifting of the SW Alboran Ridge and the Xauen, Petit Xauen, Tofiño, Eurofleet,

Ramon Margalef and Francesc Pagès highs in the area (Figs. 4.10B,C and 5.11D), that progressively led to the formation of a long morphological barrier (Martínez-García *et al.,* 2013; Ammar *et al.,* 2007). It is tentatively suggested that the quasi-confined geometry of the WAB in the Late Pliocene favoured the acceleration of the DMW filament that recirculated in that deep domain (Fig. 5.11D). This accelerated filament winnowed the fine particles transported down-current by the gravity flows during and/or after deposition in the TSs, and settled them downstream.

ii) The morphosedimentary signature on the architectural elements: Another signature related to the influence of alongslope over downslope processes is found in the recent morphoarchitecture of the abovementioned La Linea, Guadiaro, Baños, Torre Nueva, and Fuengirola TSs in the WAB, that display both similarities and differences in their elements. The similar architectural elements are the canyons, mostly characterised by non-leveed margins. The TS feeder canyons cross the continental slope eroding the contourite terraces and the alongslope plastered drifts. Canyons mouth directly into fanlobes (i.e., main leveed channel, channelised lobe, and lobe fringe, Shanmugam and Moiola, 1988) on the base of slope and adjacent basin, with aggrading and migrating leveed channels. The differences are mostly related to the architectural changes of the fanlobes. They display an E-W variation, from a single linear to lower sinuous leveed channel in those TSs close to the Strait of Gibraltar (La Linea and Guadiaro), to a single main leveed channel linked downslope to distributary channels in the other TSs (Baños, Torre Nueva, and Fuengirola) (Fig. 6.7). The channel pathways are mostly rectilinear, although sinuous channels are more frequent in the fan lobes located in the east (Fig. 6.7).

Interpretation: It is widely known that the dimensions and architecture of deep marine turbidite systems may reflect the type of sediment (grain size) and the way it is transported and deposited (Richards and Bowman, 1998; Richards *et al.,* 1998), although the receiving province configuration and sediment delivery sources are also factors that govern the overall size (Kenyon *et al.,* 2000; García *et al.,* 2015). The architecture, dimensions, and plan-view morphology of the TS elements based on the classifications of Reading and Richards (1994) and Richards and Bowman (1998) suggest that the sedimentary composition of the TSs ranges from mixed sand-mud (Baños, Torre Nueva and Fuengirola TSs), becoming sandier towards the Strait of Gibraltar (La Linea and Guadiaro TSs). There are several indicators that support this interpretation: a) the scale of the elements can be considered moderate (length/width: up to 40km/20km) to small (length/width: <17km/<8 km) towards the Strait of Gibraltar; b) their sediment sources

are mostly steep, seasonal rivers and streams that erode the Betic mountains and coastal deposits, mainly during sea level falls and lowstand stages (Ercilla *et al.,* 1994; Estrada *et al.,* 1997; Alonso and Ercilla, 2003). During these periods, the heavy sediment load supplied by these hinterland sediment sources induces high energy gravity flow processes, whose deposition leads to a complex facies architecture with a great variety of seismo-facies that change over relatively short distances (a few to tens of km) (Estrada *et al.,* 1997; Alonso and Ercilla, 2003).
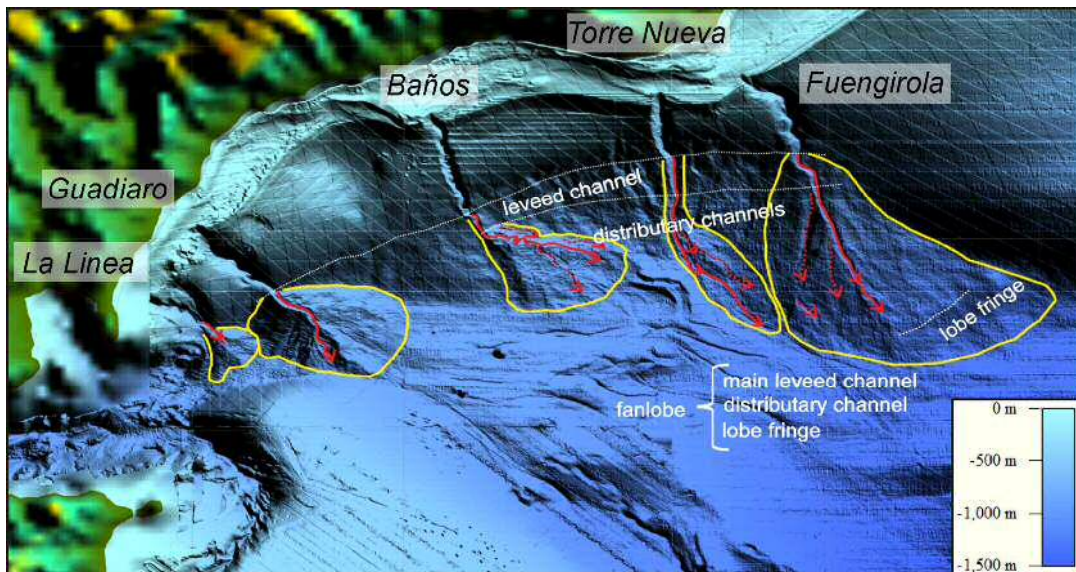
Fig. 6. 7 - Multibeam bathymetry displaying the morphoarchitecture (plan-view) of the TSs in the WAB. Variation from a single linear to lower sinuous leveed channel in the fans close to the Strait of Gibraltar, to a single main leveed channel linked downslope to distributary channels in the eastern fanlobes. The channel pathways are mostly rectilinear, although sinuous channels are more frequent in the eastern fanlobes.

Taking into account the fact that the La Linea, Guadiaro, Baños, Torre Nueva and Fuengirola TSs can be classified as mixed sand-mud and mud-sand, the similarities and differences in their architectural elements are interpreted in terms of the influence of bottom currents on the composition of the gravity flows feeding the TSs, and how this influence changes along and across the slope. In this sense, the architectural characteristics of the TSs could be explained as being a consequence of the alongslope activity of the AW and MWs. Specifically, they could be a consequence of the interplay between the WAG of the AW, whose velocity decreases eastwards (Viúdez *et al.,* 1998; Periáñez, 2006, 2007; Naranjo *et al.,* 2012), and the activity of the LMW and DMW that accelerate toward the Strait of Gibraltar (Gascard and Richez, 1985; Pistek *et al.,* 1985; Millot, 2011, 2014; Ercilla *et al.,* 2003; Chapters III and V). The AW and MWs therefore have higher velocities in the areas closest the Strait of Gibraltar, favouring relatively

greater piracy of the fine fraction of the gravity flows in those areas. Piracy results in fine sediment deprivation in the downslope flows feeding the TSs, explaining the lack of defined levees on the canyon margins and the sandier fanlobes towards the Strait of Gibraltar, where the DMW currents are faster.

iii) Sedimentological signature: The last sedimentary signature of the influence of alongslope over downslope processes can be found in the sedimentological analyses from sediment cores recovered from the central (Calahonda and Sacratif) and western (Guadiaro and Ceuta Canyon) TSs. The canyon floor cores are characterised by abundant turbidite gravels, sand, and silt layers (Ta-d) alternating with turbidite mud layers (Te) (Fig. 6.8).

These turbidites show regional grain-size differences (Fig. 6.9). It is apparent that sediment cores from the western canyons (Ceuta and Guadiaro) are characterised by the highest proportions of coarse-grained turbidites (gravels and sands), which are similar to the main channel fill. Well- and moderately-sorted fine gravels (65%-91%) and well- and moderately-sorted fine and medium sands (71%-95%) forming thick layers (up to 86 cm) predominate in the Ceuta Canyon (core k-23). Moderately-sorted fine and medium sands (46% to 91%) forming thick layers (30-80 cm), dominate in the Guadiaro Canyon (cores k-17, k-18, k-19 and k-20), while the cores from the eastern canyons/channels (Sacratif Canyon/channels and Calahonda gullies) comprise thin, fine-grained turbidites (silts and muds) (Fig. 6.9). A high proportion of moderate-poorly sorted medium silt layers alternating with turbidite mud predominate in the Sacratif Canyon (cores TG8, TG10, TG11 and TG13). Mud dominates with a minor presence of thinly bedded (< 8 cm) poorly-sorted medium and fine silt with occasional, thin, fine sand layers in the Calahonda gullies (cores TG16, TG17 and TG18). The channel cores can be differentiated from those of the erosive environment in the canyon on the basis of fewer and thinner, rhythmically distributed sand beds. On the other hand, the vertical distribution of the turbidite levels in the sediment cores indicates that the Guadiaro TS, close to the Strait of Gibraltar, is dominated by Ta-c Bouma sequences, i.e., lacking the finest, top level (Te), whereas TSs further away from the Strait of Gibraltar (Sacratif and Calahonda) are dominated by Ta-e Bouma sequences (Fig. 6.8).

186
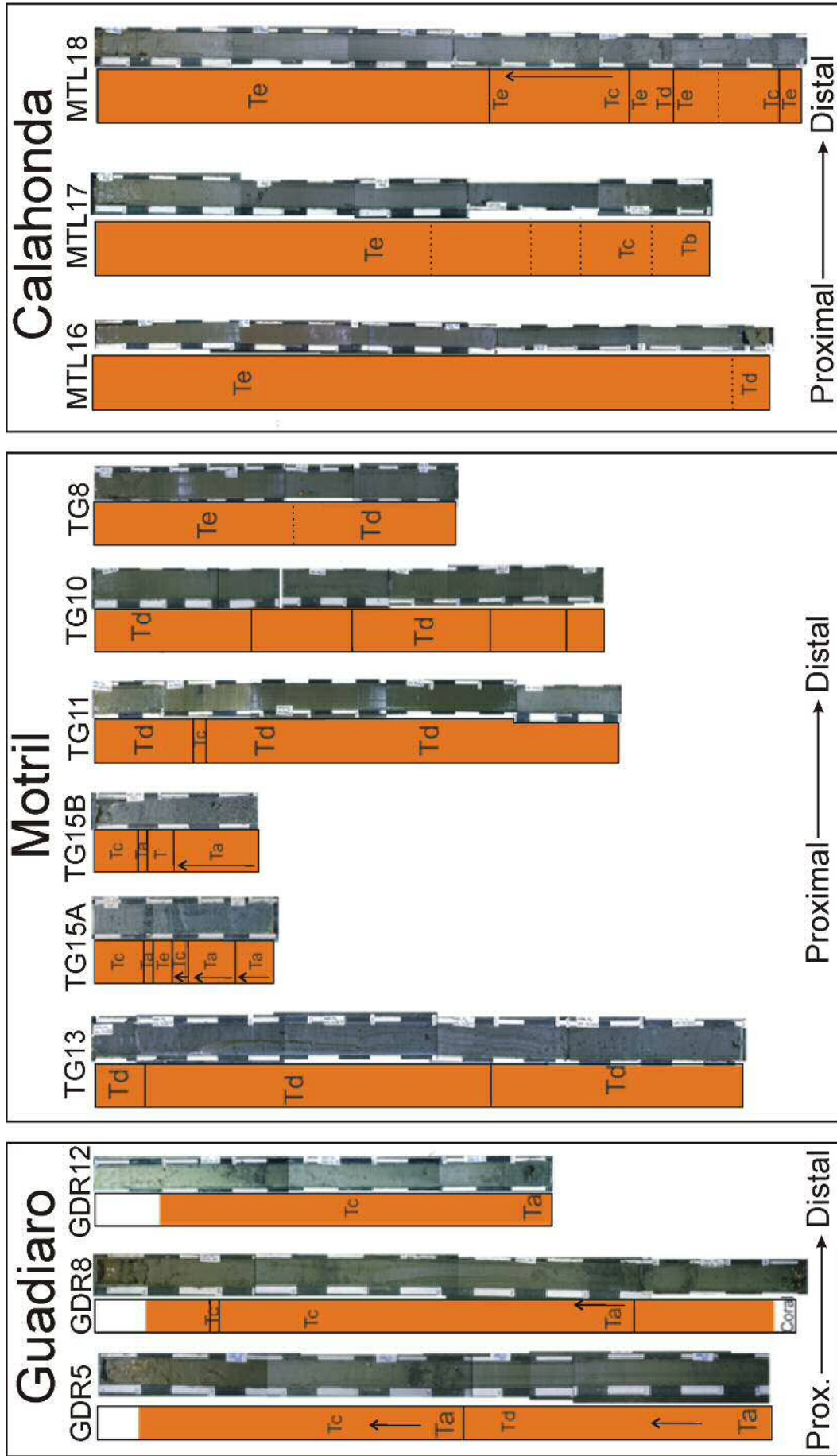
Fig. 6. 8 - Sediment core facies in the gravity cores recovered in the TSs that mouth in the Motril Basin. Legend: Ta-d are turbidite gravels, sand, and silt layers; Te are turbidite mud layers (Lebreiro and Alonso, 1998). See Fig. 2.5 for location.
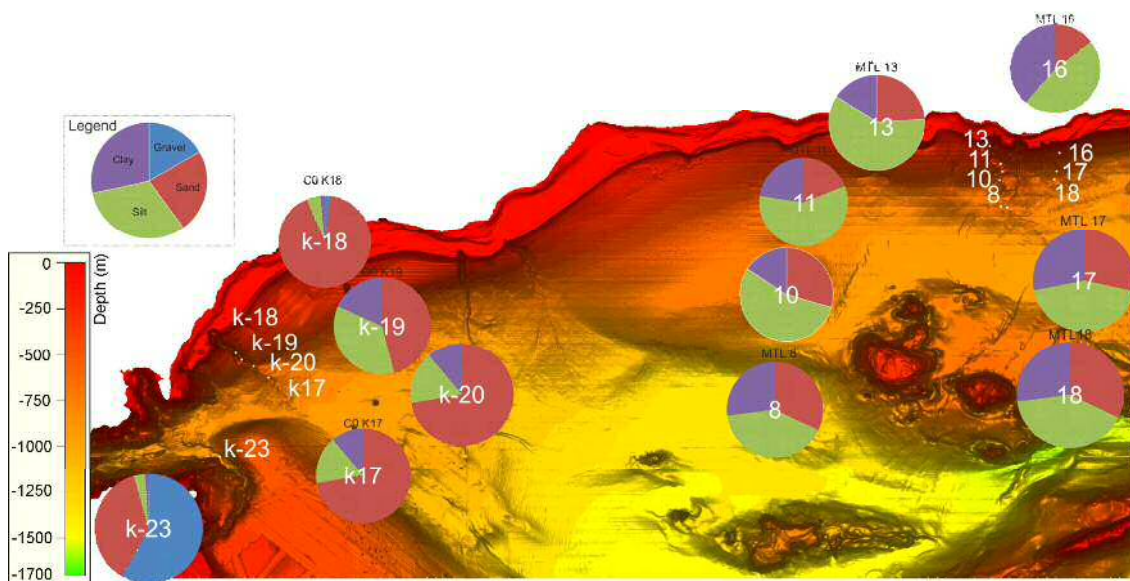
Fig. 6. 9 - Sedimentary composition (grain size) of samples recovered along various TSs (Guadiaro TS, k-17 to k-20; Ceuta Canyon mouth, K-23; Motril Canyon, 8, 10, 11, 13 and Calahonda submarine ramp, 16-18). See Fig. 2.5 for location.

The interpretation: The sedimentological results support the interpretation of the morphological and seismic sedimentary signatures as alongslope bottom currents influencing gravity flow processes in the TSs, with this influence becoming increasingly important towards the Strait of Gibraltar. The higher proportions of coarse-grained turbidites (gravels and sands) and truncated Bouma sequences in the westernmost TSs is due to the fact that the AW and MWs have higher velocities in the areas closest the Strait of Gibraltar (Gascard and Richez, 1985; Pistek *et al.*, 1985; Viúdez *et al.*, 1998; Ercilla *et al.*, 2003; Periáñez, 2006, 2007; Millot, 2011, 2014; Naranjo *et al.*, 2012; Chapters III and V), favouring relatively greater piracy of the sediment supplied by the gravity flows in those areas.

2.4. Downslope dominate alongslope processes

Morphosedimentary signature: The main morphosedimentary evidence of this dominance is found on the eastern Spanish margin, where the Almeria TS develops. This TS represents the largest turbiditic system in the Alboran Sea. It comprises a long submarine canyon (55 km) with a sinuous to meandering thalweg, three important tributary systems (Gata, Andarax and Dalias) and a leveed channel (García *et al.*, 2006). At about 1200 m water depth the canyon evolves into the Almeria leveed channel that enters into the EAB at about 1500 m water depth. There, the overbank area widens and

the main leveed channel branches into sinuous to meandering distributary channels that make up the lobe deposits extending down to 1800 m in the EAB (Alonso and Ercilla 2003), and which display a lobate shape (Fig. 6.10). The lobe deposits are seismically characterised by broad, irregular lens-shaped packages (Fig. 6.10B,D) with thicknesses of up to 65 ms, and lengths of 2–4 km. The top of these deposits are incised by small channels (Fig. 6.10A,B,D), and characterized by downlapping reflections (Fig. 6.10D). The stacked lobes partially overlap each other, prograding eastwards. At sedimentological facies scale, the Late Pleistocene sediments of the Almeria Channel are characterised by sandy to muddy turbidite levels, and at least for the last 10 ky (11.2–1.3 ka) this channel has not been traversed by any major turbidity current able to overspill the channel walls and form turbidite deposits on the overbank area (Bozzano et al., 2009).
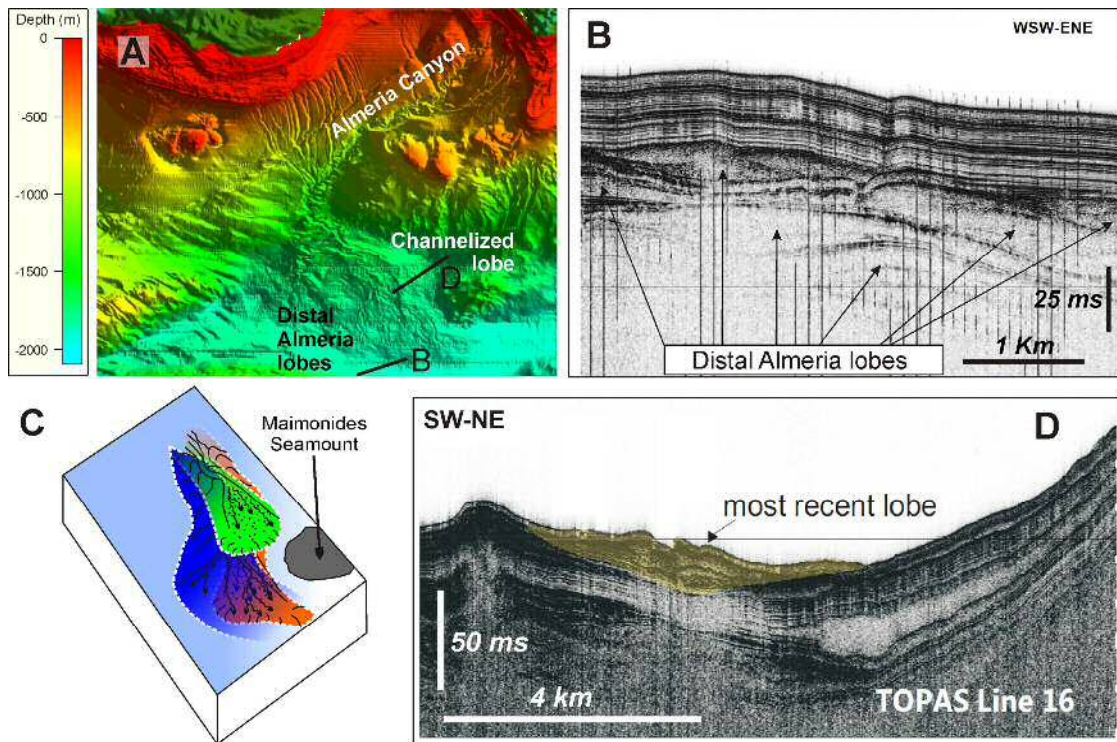
Fig. 6. 10 – Example of downslope processes dominating alongslope processes. A) The sedimentation pattern of the Almeria TS is governed by the gravity flows feeding the systems and the morphostructural configuration of the area. B) TOPAS profile of the distal Almeria lobes, located in the lateral prolongation of the Alboran Trough (in the present day draped by sheeted drift due to the lateral migration of the lobes). Modified from Alonso et al. (2010). C) Diagram showing the lateral migration and vertical stacking of the Almeria lobes. D) TOPAS profile showing a cross-section of the most recent lobe. C and D were modified from Alonso et al. (2011).

Interpretation: The abovementioned characteristics of the Almeria canyon, its complex tributary systems, as well as the main leveed channel and channelised lobe deposits, have all been primarily conditioned by the characteristics (load and energy) of the gravity flows. This interpretation also agrees with previous results reported in the literature on the sedimentary processes controlling the development of the Almeria TS (Alonso *et al.*, 1992; Estrada *et al.*, 1997; Alonso and Ercilla, 2003). Its Pliocene and Quaternary depositional architecture reveals that the trajectories and morphologies of the sinuous channels appear to result from the balance between gravity flow power (product of flow density, discharge and gradient) and the erodibility of the sediment at the channel perimeter, following a pattern analogous to that of rivers (Schumm *et al.*, 1987; Pirmez, 1994). The occurrence of these flows has mainly been governed by glacioeustasy and spatial relocation by tectonics during the Pliocene and the Quaternary (Estrada *et al.*, 1997; Alonso and Ercilla, 2003; Alonso *et al.*, 2012). This dominance of gravity flows over bottom currents that characterises the Almeria TS occurs because the energy of the LMW and DMW contour currents is not strong enough to pirate the finest suspension of the frequent gravity flows that run along the canyon, channel, overbank and channelised lobe areas.

3. The Spanish margin versus the Moroccan margin: sedimentary models of alongslope and downslope interactions in the turbidite systems

The different levels of interaction between alongslope contourite and downslope gravity flow processes have governed the uneven turbidite system development in the Alboran Sea. This uneven development has allowed to create conceptual models that explain the complex spatial interplay between along- and downslope processes and their implications for the Spanish and Moroccan margins architecture.

3.1 The Spanish margin

The Spanish margin is characterised by three levels of interaction that change from east to west and from the proximal to distal sectors: i) the eastern sector of the Spanish margin is where gravity flows dominate over the AW, DMW and LMW contour currents (Fig. 6.11A); ii) this level of interaction changes toward the west where these gravity flows are influenced by bottom currents (Fig. 6.11B); and iii) in the westernmost sector, where the action of bottom currents and gravity flows also alternate.
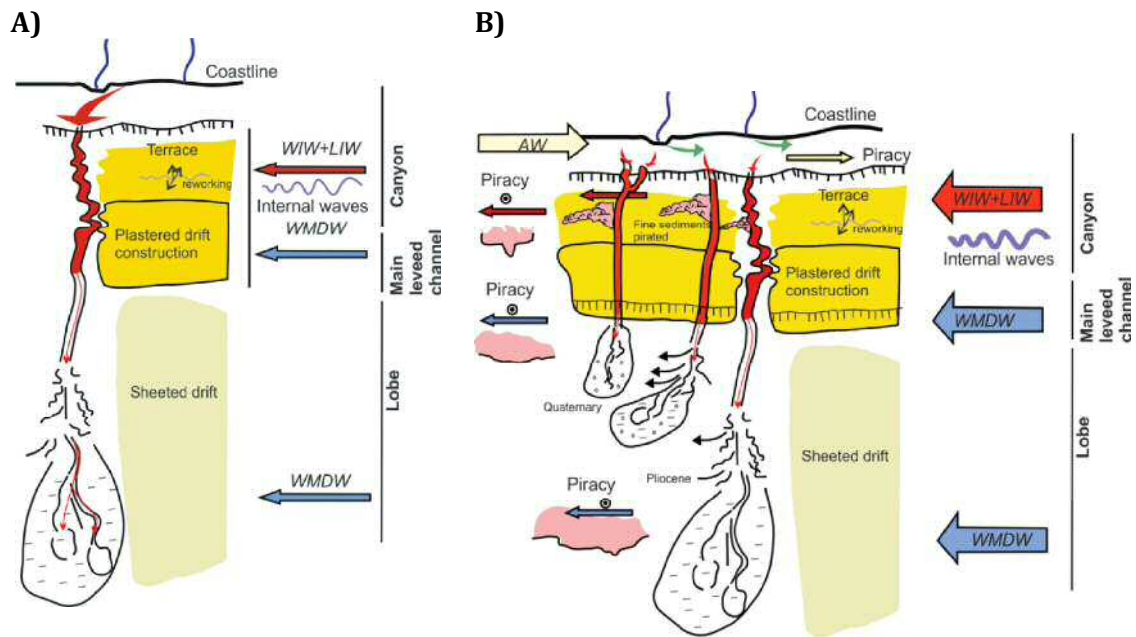
Fig. 6. 11– Sedimentary models of the Spanish margin. A) Eastern Spanish margin: the downslope processes influence alongslope processes. B) Western Spanish margin: the alongslope processes influence downslope processes. Modified from Mulder et al. (2008).

When gravity flows dominate bottom currents (i) the less energetic alongslope processes do not significantly influence the downslope processes of the TSs and, as a result, gravity flow deposits predominate (Fig. 6.11A). When the AW, DMW and LMW contour currents influence the gravity flows (ii) these water masses favour the piracy of the sediment supplied by the gravity flows, conditioning the geometry, sediment distribution (TSs migrate in the direction of the bottom currents, Fig. 6.11B), scarce presence or lack of levee/overbank deposits, grain size of TSs sediments, and truncating turbidite sequences. This level of interaction changes longitudinally and transversally (Fig. 6.11B). This occurs because the morphoarchitecture of the TSs is influenced at different water depths by the vertical superposition of different water masses: the AW and MWs and their interfaces. This influence has conditioned that the TSs can have: a) similar architectural elements, such as feeder canyons. This is because they have similar levels of bottom-current influence; specifically, turbulence and internal waves at water masses interfaces between AW and MWs; and b) fanlobes with different architectural elements. This is because they are affected by a WMDW whose bottom-current energy changes alongslope, increasing its energy towards the Strait of Gibraltar (Fig. 6.11B). In addition, the results of this work suggest that these influences have also changed with time; in fact, stronger and permanent interfaces between the AW and MWs (then turbulent processes are more important) have occurred since the Quaternary, and most

191

of the fanlobes in the WAB were affected by a stronger recirculation of the DMW during the Pliocene. Finally, when both alongslope and downslope sedimentary processes alternate (iii), gravity flow deposits and contourites may also alternate in the sedimentary record of the TSs.

3.2 The Moroccan margin

On the Moroccan margin, bottom-current interaction is stronger and has conditioned the scarce presence of turbidite canyons and the lack of fanlobe deposits. The interplay between piracy by the Atlantic anticyclonic gyres, and the dispersion of suspended sediment due to the enhanced density contrast between the AW and DMW, as well as the fact that the DMW core impinges on and accelerates along the Moroccan margin being forced to flow upslope, all favour intense alongslope sediment transport (Fig. 6.12). This intense transport prevents the convergence of sediment along the Moroccan margin, inhibiting the local occurrence of potential, erosive gravity flows that could lead to the formation of canyons and/or their related fan lobes. Instead, there is non-deposition or erosion (Fig. 6.12).
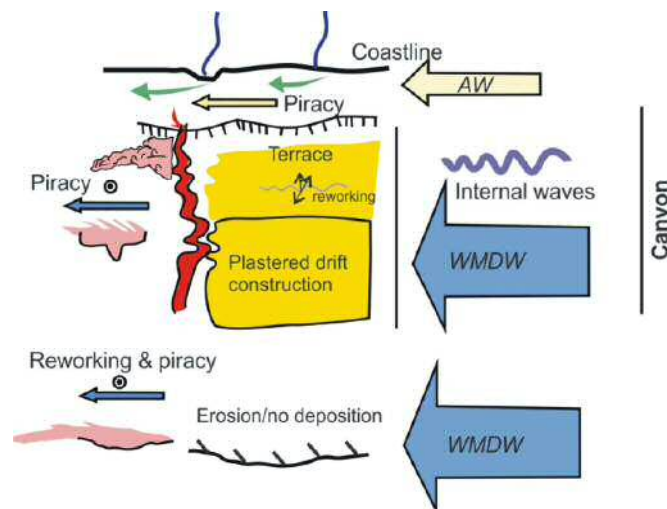
Fig. 6. 12– Sedimentary model of the Moroccan margin: alongslope processes dominate downslope processes. Modified from Mulder et al. (2008).

Chapter VII - Conclusions

Chapter VII - Conclusions

This PhD thesis looks at the influence of bottom currents on the morphology of the Alboran Sea and the sedimentation in these deep-sea environments, as well as how this influence has evolved through the Pliocene and Quaternary. The use of disciplines as varied as geomorphology, sedimentology, seismic stratigraphy and physical oceanography allows to: i) obtain a comprehensive understanding of the role played by the bottom-currents in shaping the deep-water environments; ii) provide evidence, for the first time, of the widespread dominance of contourites in the Alboran Sea and their controlling factors, as well as reconstruct the distinct palaeoceanographic scenarios that have existed since the opening of the Strait of Gibraltar; iii) gain comprehensive knowledge of the sedimentary architecture of both the Spanish and Moroccan margins and basins, giving us clues as to how to geologically define the palaeoceanographic processes; and iv) demonstrate that turbidite systems bear the imprint of the interaction between downslope gravity flows and contourite alongslope processes.

1. Major achievements

The major contributions of this PhD research are summarised in the following four points:

> It offers a **new morphodynamic scenario** for the deep-sea environments of the Alboran Sea, based on the recognition of contourite deposits, including depositional (plastered, sheeted, channel-related, mounded confined, elongated and separated drifts), and erosive (moats, channels, furrows, terraces and escarpments) features. Hydrographic data offers **new insights into the distribution of the Mediterranean water masses**, and reveals that the bottom circulation of the Western Intermediate Water (WIW) and Levantine Intermediate Water (LIW) interacts with the Spanish slope, and the Western Mediterranean Deep Water (WMDW) on the Moroccan slope, Spanish base-of-slope and deep basins. The integration of distinct datasets and approaches allows a **new sedimentary model** to be proposed for the Alboran Sea that highlights the significance of bottom-current processes in shaping deep-sea morphology. Basic tenets of this model are that the bottom circulation of water masses governs physiography, that interface positions of water-masses with contrasting

densities sculpt terraces on a regional scale, and that morphological obstacles play an essential role in the local control of processes and water-mass distribution.

It asserts **chronological constraints on the Pliocene and Quaternary deposits** at a regional scale. The boundaries of these stratigraphic divisions have been updated and renamed as follows: the Messinian (M at 5.96 to 5.33 Ma), the intra-lower Pliocene (P0 at ca. 4.5 Ma), the top of the Zanclean (P1 at ca.3.3 Ma), the base of the Quaternary (BQD at ca. 2.6 Ma), the top of the Gelasian (Q0 at ca. 1.8 Ma), the intra-lower Quaternary (Q1 at ca. 1.12 Ma), and the top of the Calabrian (Q2 at ca. 0.7 Ma). This seismic analysis of the Plio-Quaternary stratigraphy facilitates the presentation and discussion of **evidence for contourite features** comprising the entire stratigraphic architecture of the Spanish and Moroccan margins as well as the basins of the Alboran Sea. Contourite features postdating the opening of the Gibraltar Strait have been identified, with plastered drifts dominating the Spanish and Moroccan continental slopes and sheeted drifts dominating the basins. The widespread distribution of contourites in the Alboran Basin and their spatial and temporal continuity suggest that the action of the Mediterranean waters (LMW and DMW) flowing toward the Strait of Gibraltar has continued uninterrupted during the Pliocene and Quaternary. At least **two main factors** have controlled **contourite deposition**: (i) **tectonics** and (ii) **climate and related sea-level changes**. The morphotectonically active seafloor landscape (i.e., the Alboran Ridge and the Xauen and Tofiño Banks) and basin configurations (WAB, EAB, and SAB) have controlled the main flow pathways and their circulation. Climate and related sea-level changes primarily affect water mass conditions (interfaces) and hinterland sediment sources, thereby controlling the morphoseismic characteristics of the drifts (facies and geometry) and terraces (dimensions). **A model of three main phases of palaeocirculation and current conditions** (the Atlantic Zanclean flooding, the Pliocene Sea, and the Quaternary Sea) since the opening of the Strait of Gibraltar is proposed. This evolution includes: a) the impact of the pulsed Atlantic water inflow into the Alboran Basin at the time of the opening of the strait, b) a great DMW circulation evolving from a wide, nearly homogenous tabular water mass during the Early Lower Pliocene to a water mass with multiple current dynamics from the Late Pliocene until the present day, and c) better-defined and/or stable characteristics of the Atlantic, light and dense Mediterranean waters during the Quaternary.

It offers a **comprehensive view of the Plio-Quaternary** subsurface through a detailed analysis of the **sedimentary architecture** of the Spanish and Moroccan margins and basins. Sedimentary maps spanning the entire Alboran Sea, including precise distribution of contourites, turbidites and mass-movement deposits and their relationship to each other, are presented and analysed. This has led to the definition of: i) **three contourite depositional systems**; the Intermediate Contourite Depositional System (ICDS), formed under the action of the LMW on the Spanish margin; the deep contourite depositional system contourite (DCMW) formed under the action of the DMW mainly on the Moroccan margin and basins; and the Atlantic Contourite Depositional System (ACDS) developed by the Atlantic Water on the upper continental slope of both margins. Also new terms for describing contourites have been formulated; ii) **twenty turbidite systems**, their onsets and spatial and temporal relocations; and iii) the reworking of contourites by **mass-movements**. Basic oceanographic **processes**, their occurrence, relative magnitude and energy, and time of action can be determined, principally using contourites and to a lesser extent turbidites.

It recognises the morphological, sedimentary and sedimentological signatures generated by the **different levels of interaction between the alongslope bottom currents and downslope gravity flows in the turbidite systems** during the Pliocene and Quaternary. On the Spanish margin, the interaction is especially varied and complex, impacting the turbidite systems both regionally and locally. Here, the interaction occurs at various levels that change across- and downslope: the alongslope processes influence the downslope processes, the downslope and alongslope processes alternate; and downslope processes dominate alongslope processes.On the Moroccan margin, the strong action of the DMW is dominant, inhibiting the local occurrence of potential erosive gravity flows and thus, the formation of canyons and their associated deposits. **Conceptual models** are presented to explain this complex spatial interplay between along- and downslope processes occurs, as well as their imprint on the **uneven development of turbidite systems** and therefore, sedimentation on the Spanish and Moroccan margins.

The **findings of this PhD** research demonstrate the pivotal role of bottom water circulation in seafloor shaping, sedimentary stacking patterns and the sedimentary evolution of continental margins and basins, **establishing a new outlook for future studies on deep marine sedimentation**.

2. Implications for the Mediterranean basins

The oceanographic context of the Alboran Sea, where Atlantic and Mediterranean water masses meet close to the Strait of Gibraltar, and the tectonically-controlled morphological context of its margins and adjacent deep sea areas, has conditioned the ubiquity of contourite features (Chapters III to IV). In addition, the results suggest that the interplay between the two contexts and their changes during the Pliocene and Quaternary have favoured complex interaction between contourite, turbidite and mass-movement systems resulting in a depositional architecture that changes laterally and basinward over short distances (Chapters V to VI). Similar complex oceanographic and morphological contexts to those found in the Alboran Sea are also characteristic of other basins in the Mediterranean Sea, although to our knowledge, no other detailed study at basin scale, like this, has yet been carried out on the other basins.

The Mediterranean basin comprises a marginal sea formed by two major basins: eastern and western. Both have a complex morphostructure that favours the enclosing of several regional seas separated by straits and channels, including the Straits of Sardinia, Sicily, Otranto, the Cretan Arc, and the channels of the Balearic and Corsica Channel. These straits and channels favour water mass exchange and control their characteristics (Astraldi *et al.*, 1999, and references therein; Millot, 2009; Millot and García-Lafuente, 2011). There are four main water masses making up the Mediterranean water column: the Modified Atlantic Water (MAW), Levantine Intermediate Water (LIW), Eastern Mediterranean Deep Water (EMDW), and Western Mediterranean Deep Water (WMDW). These run throughout the Mediterranean, their characteristics being modified where they cross the various straits and channels.

The regional seas are characterised by complex regional physiography and seafloor morphology, flow regime, and stratification of the water column (Shanmugam, 2013), where alongslope currents (Millot, 2009; 2013), turbulent processes at the interfaces between the water masses, overflows (e.g., Astraldi *et al.*, 1998b; Kinder and Bryden, 1990), formation of dense shelf water cascades (e.g., Skliris *et al.*, 2004; Dufau-Julliand *et al.*, 2004; Trincardi *et al.*, 2007; Palanques *et al.*, 2009; Puig *et al.*, 2010, 2013; Ribó *et al.*, 2011; Foglini *et al.*, 2016), strong mesoscale eddies (e.g., Millot and Taupier-Letage, 2005), secondary circulation (e.g., Wåhlin and Walin, 2001; Muench *et al.*, 2009a,b; Cossu *et al.*, 2010; Rebesco *et al.*, 2014); solitons (e.g., Velegrakis *et al.* 1999), internal tides (e.g., Horton and Clifford, 2005; Abdennadher and Boukthir, 2013; Shanmugam 2013, 2014), and other oceanographic processes have been described using physics. We

therefore suggest that bottom currents and their related oceanographic processes are more relevant in shaping the margins and adjacent basins of the regional Mediterranean basins than hitherto suspected. The literature shows examples of contourites in the Mediterranean basin (Table 1.2), but these have frequently been considered local features or even rare curiosities in the bigger picture of this basin (e.g., Velasco *et al.*, 1996; Ercilla *et al.*, 2002; Roveri, 2002; Verdicchio and Trincardi, 2008; Palomino *et al.*, 2011; Vandorpe *et al.*, 2011; Martorelli *et al.*, 2011; Micallef *et al.*, 2013; Rebesco *et al.*, 2014). In fact, most studies have focused on recognising downslope gravitational processes (e.g., Casas *et al.*, 2003, 2011, 2015; Minisini *et al.*, 2007; Garziglia *et al.*, 2008; Martínez-García *et al.*, 2009; Dalla Valle *et al.*, 2013; Alonso *et al.*, 2014). Based on the results of this work, the long-term impact of bottom-current circulation and related processes, as well as their interplay with downslope gravitational processes must be seriously considered in order to fully understand the stratigraphy and depositional architecture of the Mediterranean marginal seas.

In addition, the Alboran Sea represents the final arrival area of the Mediterranean water masses and opens to the Atlantic Ocean through the Strait of Gibraltar. Therefore, sedimentological studies of the contourites and sedimentary products resulting from the interplay between the alongslope and downslope processes in this sea, could also be relevant in the understanding of water mass exchange between the Mediterranean regional seas and consequently the role played by the MWs in the formation of the Mediterranean Outflow Water and its impact on the circulation and climate of the North Atlantic region.

3. Applied interest of this study

In addition to the major scientific achievements, the results of this Ph.D. are also important in a variety of application areas.

For geological hazards: The Alboran Sea represents one of the most tectonically active areas surrounding Iberia. This Ph.D. research provides essential information and the results comprise a powerful tool for evaluating potential hazards in this sea. In fact, they provide important regional clues that help establish the evolution of the erosive and depositional features in relation to neotectonic effects. The results will therefore contribute to increasing both our knowledge and understanding of the tectonic and related sedimentary processes, acting at different spatial and temporal scales, that are responsible for potentially catastrophic earthquakes, slope failures and tsunamis.

Geohazard assessment in the densely-populated westernmost Mediterranean region will benefit significantly from this study.

For economy: Knowledge of contourites and turbidite systems is of great interest for potential hydrocarbon reserves. In the Alboran Sea, seismic research and exploratory drilling have been undertaken for more than 30 years. The results of this study, particularly the sedimentary models, will enhance the interpretation of and research in basins with hydrocarbon exploration potential. In this sense, the results of this Ph.D. will have implications for our understanding of reservoir connectivity (facies association), geometry, and the stacking patterns of contourites and turbidites. This work points to the fact that when different water masses affect the architecture of TSs, it can be difficult to define or predict stratigraphic patterns associated with the main architectural elements of the TS, such as canyons, channels, overbank and lobe deposits. This is because the different contourite processes can affect and condition lithofacies distribution. On the other hand, this work also supports the growing interest in contourites as potential hydrocarbon reservoirs. The morphological, seismic and evolutive characteristics of certain contourite features, such as the terraces (that represent features formed by geologically persistent turbulence processes), point to the fact that they can have high concentrations of coarse-grained sediments with a high degree of lateral continuity, and are therefore good potential traps for hydrocarbons. Moreover, they are laterally bounded by plastered drifts that can seal them. For this reason, the results of this work will be of great help in assessing the economic importance of contourites, turbidites, and turbidites under the influence of bottom currents, from their seismic and sedimentological characteristics.

For seabed management and use: The detailed knowledge of the seafloor topography and surface characteristics of the sedimentary cover obtained from this Ph.D. research will be very useful both from the scientific point of view, in terms of anchoring tools, the modelling of oceanic circulation including topographic effects, fishing tests, and so on, as well as from an applied point of view, with regard to activities such as the laying of cables and pipelines, waste disposal, and military applications.

Bionomy of the seafloor: This study highlights the fact that particular geomorphological and oceanographic characteristics converge in the Alboran Sea. The meeting of Atlantic and Mediterranean water masses and the variety of: i) oceanographic structures, such as the large quasi-permanent Western Alboran Gyre (WAG) and the variable Eastern Alboran Gyre (EAG), fronts (geostrophic fronts of Almeria, Oran, and

Algeria); ii) bottom-current processes, like internal waves, branch acceleration, filaments, secondary flows, upwelling and downwelling; iii) morphological features, such as submarine canyons and seamounts of various kinds; and iv) fluid dynamic structures including mud-volcanoes, makes the Alboran Sea an excellent natural laboratory for studying biodiversity and ecosystems as these features mean it has such an abundance of biological resources.

4. Outstanding questions

During this study the research has raised issues that are still outstanding or not yet fully resolved. These are questions whose answers should be properly addressed in future research. They can be grouped based on disciplines:

Physics Oceanography:

The water masses above and below the main interfaces in the Alboran Sea flow in different directions on the Spanish (AW flowing eastward, LMW flowing westward) and Moroccan (AW and DMW flowing westward and northwestward along the margin) margins. How does this affect the propagation of internal waves along the interfaces, and how does it affect sediment piracy and redistribution on both margins?

According to Naranjo *et al.* (2012), the rotational energy of the WAG is capable of aspiring and uplifting the WMDW from depths as great as 700 m in the WAB. These authors also consider the gyre to be the main reason the WMDW banks against the African slope. The question is, then, how does this upper gyre affect the bottom-current processes of the intermediate and deep circulation?

The clockwise rotation of the two Atlantic gyres, WAG and EAG, could transport sediment from the Spanish margin to the Moroccan margin, and redistribute it along the margin. Is it possible that this scenario offers a possible explanation for the large slope plastered drifts (e.g., Ceuta Drift) on the Moroccan margin when compared to the Spanish margin, despite being fed by a similar network of small rivers excavating similar mountain ranges under similar climatic conditions?

It has been described in the literature that the WAG collapses under extremely cold winter conditions (Bormans and Garrett, 1989; Vargas-Yáñez *et al.*, 2002; Periáñez, 2006, 2007; García-Lafuente *et al.*, 2008). On the other hand, the Atlantic inflow is the greatest and forces the WAG to shift eastward when low-pressure systems on the

Western Mediterranean cause arise of the sea surface and westerlies prevail (Grazzini and Pierre, 1991). It has also been described that the westerlies were displaced southwards to the Mediterranean during the last glacial maximum (COHMAP, 1988; Grazzini and Pierre, 1991). Thus, the WAG collapses and the eastward migrations of the gyre must have been more frequent during glaciations, changing the upper layer circulation in the Alboran Sea as well as altering sediment redistribution patterns. How did this affect drift outbuilding? And is it possible to extrapolate the circulation patterns seen during extremely cold winters in the present day to past glacial times?

There are hardly any physics oceanography studies about the bottom-current processes in the deep-sea environments of the Alboran Sea. Additional regional studies on near-bottom layers of the MWs are much needed to properly study the bottom-current influence on sedimentation.

Stratigraphy:

This study provides new insights into Pliocene and Quaternary seismic stratigraphy with regard to the chronology of ages/stages. Establishing a higher resolution seismic stratigraphy based on very high-resolution seismic profiles (e.g., TOPAS and parasound) will improve our understanding of the interplay between the contourite, turbidite and gravitational sedimentary systems, at least during the Upper Quaternary, as well as the relationship between the downslope and alongslope sedimentary processes.

During the analysis of the seismic stratigraphy, the definition of and correlation between units in the contourites that drape or are affected by structural features, such as highs, faults and folds, highlights changes in their stratigraphic architecture. The characterisation of the bottom-current processes could therefore be improved by decoding the dynamics of structural features, as well as their role as triggering factors in mass-movement deposits.

The seismic stratigraphy reveals that climate and related sea-level changes primarily affected water mass conditions. Taking into account the fact that the MWs have different temperature and salinity characteristics, the question that arises is: does climate affect the LMW and DMW to the same extent?

The relationships between the alongslope and downslope processes may be better constrained through a more detail analysis of the STs than here presented. A task for future research should be to study with more detail the depositional architecture of

the TSs and the relocation of their architectural elements for each stratigraphic division.

Sedimentology and gemorphology:

This study gives detail information about the seismic characteristics of the contourite features based on the analysis and reinterpretation of a large extend of geophysics data. In the Alboran Sea, there is also a large database of sediment cores, ODP and commercial sites. The results here presented, "knock at the door" to review the previous results and re-interpret them in the new scenario dominated by the bottom currents. In addition, they will be important for ground true observations and then will provide clues for better understanding of the bottom-current processes responsible of contourite features.

The study of sediment could also offer interesting clues to differentiate between contourites, turbidites and debrites.

The recovering of long sediment cores in those domains affected by the vertical movement of MW interfaces during the glacioeustatic changes, could help to understand how climate changes affect to the LMW and to the DMW.

As it has been mentioned in this manuscript, the time span of most geological processes are quite different from the physical processes analysed by oceanographers. In this sense, one of the questions that should be addressed in future is the long-term preservation of deposits related to different oceanographic processes. This is because only the high-magnitude events that are capable to produce thick deposits are generally preserved in the sedimentary record.

Chapter VIII - References

Chapter VIII - References

ABC

Abdennadher, J., Boukthir, M. 2013. Internal tides distribution in the central Mediterranean Sea. Rapport of the Commission Internationale pour l'Exploration Scientifique de la Mer Méditerranée 40, 120.

Abrantes, F., Alt-Epping, U., Lebreiro, S., Voelker, A., Schneider, R., 2008. Sedimentological record of tsunamis on shallow-shelf areas: the case of the 1969 AD and 1755 AD tsunamis on the Portuguese shelf off Lisbon, Marine Geology 249, 283-293.

Aguirre, J., 2000. Evolución paleoambiental y análisis secuencial de los depósitos Pliocenos de Almayate (Málaga, sur de España). Revista de la Sociedad Geológica de España 13(3-4), 431-443.

Alhammoud, B., Meijer, P.T., Dijkstra, H.A., 2010. Sensitivity of Mediterranean thermohaline circulation to gateway depth: A model investigation. Paleoceanography 25(2), PA2220.

Alonso, B., Ercilla, G., 2000. Valles Submarinos y Sistemas Turbidíticos Modernos. Editorial CSIC-CSIC Press, Barcelona. 296pp.

Alonso, B., Ercilla, G., 2002. Architecture of modern turbidite systems in different geological settings on the Spanish margins (NW and SW Mediterranean Sea). In: Briand, F. (Ed.). Turbidite systems and deep-sea fans of the Mediterranean and the Black seas. CIESM Workshop 17, 19–22.

Alonso, B., Ercilla, G., 2003. Small turbidite systems in a complex tectonic setting (SW Mediterranean Sea): morphology and growth patterns. Marine and Petroleum Geology 19(10), 1225-1240.

Alonso, B., Maldonado, A., 1992. Pliocene-Quaternary margin growth patterns in a complex tectonic setting (Northeastern Alboran Sea). Geo-Marine Letters 12, 137–143.

Alonso, B., Canals, M., Got, H., Maldonado, A., 1991. Sea valleys and related depositional systems in the Gulf of Lion and Ebro continental margins. American Association of Petroleum Geologist Bulletin 75(7), 1195–1214.

Alonso, B., Comas, M.C., Ercilla, G., Palanques, A., 1996. Data Report: Textural and mineral composition of Cenozoic sedimentary facies off the western Iberian Peninsula, Sites 897, 898, 899, and 900. In: Whitmarsh, R.B., Sawyer, D.S., Klaus, A., Masson D.G. (Eds.). Proceedings of the Ocean Drilling Program, Scientific Results 149, 741-754.

Alonso, B., Ercilla, G., Martínez-Ruiz, F., Baraza, J., A. Galimont, 1999a. Pliocene-Pleistocene sedimentary facies at site 976: Depositional history in the northwestern Alboran Sea. In: Zahn, R., Comas, M.C., Klaus, A., (Eds.), Proc. ODP Scientific Results 161, 57-68.

Alonso, B., Baraza, J., Ercilla, G., Estrada, F., Galimont, A., Gueneoux, L., Pérez-Belzuz, F., 1999b. Modern Turbidite Systems Developed in the Western Mediterranean Sea and Eastern Atlantic Ocean. Internal Report -NORSK HYDRO– Norway. Barcelona, Spain. 230pp.

Alonso, B., SAGAS and UTM teams, 2010. Informe científico-técnico de la campaña SAGAS bis (SDG-017). Institut de Ciències del Mar de Barcelona, 105pp.

Alonso, B., Ercilla, G., Casas, D., Juan, C., Estrada, F., Garcia, M., Vázquez, J. T., Giralt, S., Farran, M., MONTERA, CONTOURIBER and SAGAS teams, 2011. Late Pleistocene and Holocene geochemical record of the most recent turbidite lobe of the Almeria Fan (Alboran Sea). 28th IAS Meeting. Zaragoza, Spain. Abstract Book, 277.

Alonso, B., Ercilla, G., Juan, C., Casas, D., Estrada, F., Vázquez, J.T., García, M., Farran, M., D'Acremont, E., Gorini, C., 2012. El abanico distal de Almería: Arquitectura estratigráfica y evolución durante el Pleistoceno Superior (SO Mediterráneo). Geo-Temas 13, 557-560.

Alonso, B., Ercilla, G., Juan, C., Estrada, F., García, M., 2013. The Djibouti Drift, Alboran Sea (SW Mediterranean Sea): Sediment dynamics over the last 300 ka. 30th IAS Meeting of Sedimentology. Conference abstracts volume, T3S4_P15.

Alonso, B., Ercilla, G., Garcia, M., Vázquez, J.-T., Juan, C., Casas, D., Estrada, F., D´Acremont, E., Gorini, C., El Moumni, B., Farran, M., 2014a. Quaternary Mass-Transport Deposits on the North-Eastern Alboran Seamounts (SW Mediterranean Sea). In: Krastel, S., Behrmann, J.-H., Völker, D., et al. (Eds.), Submarine Mass Movements and Their Consequences. Advances in Natural and Technological Hazards Research 37, 561-570.

Alonso, B., López-González, N., Bozzano, G., Casas, D., 2014b. Djibouti Ville Drift (SW Mediterranean): Sedimentation and record of bottom-current fluctuations during the Pleistocene and Holocene. 2nd Deep-Water Circulation Congress. Ghent, Belgium. Vliz Special Publication, 93-94.

Alvarez-Marrón, J., 1999. Pliocene to Holocene structure of the eastern Alboran Sea (Western Mediterranean). In: Zahn, R., Comas, M.C., Klaus, A. (Eds.), Proceedings of Ocean Drilling Program, Scientific Results 161, 345–355.

Ammar, A., Mauffret, A., Gorini C., Jabour, H., 2007. The tectonic structure of the Alboran margin of Morocco. Revista de la Sociedad Geológica de España 20(3-4), 247-271.

Apel, J.R. 2000. Solitons near Gibraltar: views from the European remote sensing satellites. Report GOA 2000, 1. Global Ocean Association, Silver Spring, MD.

Apel, J.R. 2004. Oceanic internal waves and solitons, In: Jackson C.R., Apel J.R. (Eds.), Synthetic aperture radar marine user's manual.US Department of Commerce, National Oceanic and Atmospheric Administration, Silver Spring, 189-206.

Arhan, M., Carton, X., Piola, A. and Zenk, W. 2002. Deep lenses of circumpolar water in the Argentine Basin. Journal of Geophysical Research 107, C1-3007.

Arhan, M., Mercier, H. and Park, Y.-H. 2003. On the deep water circulation of the Eastern South Atlantic Ocean. Deep Sea Research Part I: Oceanographic Research Papers 50, 880-916.

Armentrout, J. M., 1991. Paleontologic Constraints on Depositional Modeling: Examples of Integration of Biostratigraphy and Seismic Stratigraphy, Pliocene-Pleistocene, Gulf of Mexico. In: Weimer, P., Link, M. H., Seismic Facies and Sedimentary Processes of Submarine Fans and Turbidite Systems, 137-170.

Armi, L., Farmer, D.M., 1988. The flow of Mediterranean water through the Strait of Gibraltar. Progress in Oceanography 21, 1–105.

Astraldi, M., Gasparini, G., Sparnocchia, S., 1998. Water masses and seasonal hydrographic conditions in the Sardinia-Sicily-Tunisia region. Rapport du Commission International de la Mer Mediterranee 35, 122-123.

Astraldi, M., Balopoulos, S., Candela, J., Font, J., Gacic, M., Gasparini, G.P., Manca, B., Theocharis, A., Tintoré, J., 1999. The role of straits and channels in understanding the characteristics of Mediterranean circulation. Progress in Oceanography 44, 65-108.

Auzende, J.-M., Rehault, J.-P., Pastouret, L., Szep, B., Olivet, J.-L., 1975. Les bassins sédimentaires de la mer d'Alboran. Bulletin de la Société Géologique de France 17(1), 98-107.

Ballesteros, M., Rivera, J., Muñoz, A., Muñoz-Martín, A., Acosta, J., Carbó, A., Uchupi, E., 2008. Alboran Basin, southern Spain — Part II: Neogene tectonic implications for the orogenic float model. Mar. Pet. Geol. 25, 75–101.

Baro, J., Rueda J.L., Díaz-del-Río, V., 2012. South iberian submarine canyons in the Alboran sea: geohabitats, associated communities and fisheries resources. Mediterranean Submarine Canyons, 145.

Becker, J., Lourens, L.J., Hilgen, F.J., van der Laan, E., Kouwenhoven, T.J., Reichart, G.-J., 2005. Late Pliocene climate variability on Milankovitch to millennial time scales: A high-resolution study of MIS100 from the Mediterranean. Palaeogeography, Palaeoclimatology, Palaeoecology 228(3-4), 338-360.

Belderson, R.H., Kenyon, N.H., 1976. Long-range sonar views of submarine canyons. Marine Geology 22(3), M69-M74.

Bellaiche, G., Mart, Y., 1995. Morphostructure, growth patterns, and tectonic control of the Rhône and Nile deep-sea fan: a comparison. American Association of Petroleum Geologist Bulletin 2, 259–284.

Bellaiche, G., Loncke, L., Gaullier, V., Droz, L., Mascle, J., Courp, T., Moreau, A., Radan, S., Sardou, O., 2002. The Nile cone and its channel-levee system: results the prismed II and Fanil cruises. In: Briand, F. (Ed.). Turbidite systems and deep-sea fans of the Mediterranean and the Black seas, CIESM Workshop 17, 49–52.

Biju-Duval, B., Letouzey, J., Montadert, L., 1978. Structure and evolution of the Mediterranean basins. Initial Reports of the Deep Sea Drilling Project 42, 951-984.

Blikra, L.H., Nemec, W., 1998. Postglacial colluvium in western Norway: depositional processes, facies and palaeoclimatic record. Sedimentology 45(5), 909-959.

Blum, P., Okamura, Y., 1992. Pre-Holocene sediment dispersal systems and effects of structural controls and Holocene sea level rise from acoustic facies analysis: SW Japan forearc. Marine Geology 108, 295–322.

Boillot, G., Dupeuble, P.A., Hennequin-Marchand, I., Lamboy, M., Lepretre, J.P., Musellec, P., 1974. Le rôle des décrochements "tardi-hercyniens" dans l'évolution structurale de la marge continentale et dans la localisation des grands canyons sous-marins à l'ouest et au nord de la péninsule ibérique. Révue de géographie physique et de géologie dynamique 16(2), 75-86.

Booth, J.S., Sangrey, D.A., Fugate, J.K. 1985. A nomogram for interpreting slope stability of fine-grained deposits in modern and ancient marine environments. Journal of Sedimentary Research, 55, 29-36.

Booth-Rea, G., Ranero, C.R., Martinez-Martinez, J.M., Grevemeyer, I., 2007. Crustal types and Tertiary tectonic evolution of the Alboran sea, western Mediterranean. Geochemistry, Geophysics, Geosystems 8, Q10005.

Borisov, D.G., Murdmaa, I.O., Ivanova, E.V., Levchenko, O.V., Yutsis, V.V., Frantseva, T.N., 2013. Contourite systems in the region of the Southern São Paulo Plateau escarpment, South Atlantic. Oceanology 53, 460–471.

Bormans, M., Garrett, C., 1989. A Simple Criterion for Gyre formation by the Surface Outflow From a Strait, With Application to the Alboran Sea. Journal of Geophysical Research 94, 12637-12644.

Bouma, A.H., 1979. Continental slopes. Soc. Econ. Paleontol. Mineral. Spec. Publ. 27, 1–15.

Bourgois, J., Mauffret, A., Ammar, A., Demnati, A., 1992. Multichannel Seismic Data Imaging of Inversion Tectonics of the Alboran Ridge (Western Mediterranean Sea). Geo-Marine Letters 12, 117-122.

Bozzano, G., Alonso, B., Ercilla, G., Estrada, F., García, M., 2009. Late Pleistocene and Holocene depositional facies of the Almeria Channel (Alboran Sea, Western Mediterranean). External Control on Deep-Water Depositional Systems, SPEM Special Publication 82, 199-206.

Brackenridge, R.E., Hernández-Molina, F.J., Stow, D.A.V., Llave, E., 2013. A Pliocene mixed contourite–turbidite system offshore the Algarve Margin, Gulf of Cadiz: Seismic response, margin evolution and reservoir implications. Marine and Petroleum Geology 46, 36-50.

Brandt, P., Alpers, W., Backhaus, J.O., 1996. Study of the generation and propagation of internal waves in the Strait of Gibraltar using a numerical model and synthetic aperture radar images of the European ERS 1 satellite. Journal of Geophysical Research: Oceans 101(C6), 14237-14252.

Brankart, J.M., Pinardi, N., 2001. Abrupt cooling of the Mediterranean Levantine intermediate water at the beginning of the 1980s: observational evidence and model simulation. Journal of Physical Oceanography 31 (8), 2307–2320.

Brodie, I., Kemp, A.E.S., 1994. Variation in biogenic and detrital fluxes and formation of laminae in late Quaternary sediments from the Peruvian coastal upwelling zone. Marine Geology, 116, 385-398.

Bruno, M., Alonso, J.A., Cózar, A., Vidal, A., Ruiz-Canavete, A., Echevarria, F., Ruiz, J., 2002. The boiling-water phenomena at Camarinal Sill, the Strait of Gibraltar. Deep-Sea Research II Topical Studies in Oceanography 49 (19), 4097–4113.

Bryden, H.L., Stommel, H., 1982. Origin of the Mediterranean outflow. Journal of Marine Research 40, 55–71.

Butzer, K.W., 1961. Paleoclimatic implications of Pleistocene stratigraphy in the Mediterranean Area. Annals New York Academy of Sciences 95, 449-456.

Cacchione, D.A., Pratson, L.F., Ogston, A.S., 2002. The shaping of continental slopes by internal tides. Science 296, 724–727.

Cacho, I., Grimalt, J. O., Canals, M., Sbaffi, L., Shackleton, N. J., Schönfeld, J., Zahn, R., 2001. Variability of the western Mediterranean Sea surface temperature during the last 25,000 years and its connection with the Northern Hemisphere climatic changes. Paleoceanography 16, 40-52.

Camerlenghi, A., Crise, A., Accerboni, E., Laterza, R., Pudsey, C.J., Rebesco, M., 1997b. Ten month observation of the bottom current regime across a sediment drift of the Pacific margin of the Antarctic Peninsula. Antarctic Science 9, 424–431.

Campillo, A. C., Maldonado, A., Mauffret, A., 1992. Stratigraphic and tectonic evolution of the western Alboran Sea: late Miocene to Recent. Geo-Marine Letters 12(2/3), 165–172.

Campos, J., Maldonado, A., Campillo, A. C., 1992. Post-Messinian evolutional patterns of the Central Alboran Sea. Geo-Marine Letters 12, 173-178.

Canals, M., Lastras, G., Urgeles, R., Casamor, J.L., Mienert, J., Cattaneo, A., De Batist M., Haflidason, H., Imbo, Y., Laberg, J.S., Locat, J., Long, D., Longva, O., Masson, D.G., Sultan, N., Trincardi, F., Bryn, P. 2004. Slope failure dynamics and impacts from seafloor and shallow sub-seafloor geophysical data: case studies from the COSTA project. Marine Geology 213, 9-72.

Casas, D., Ercilla, G., Baraza, J., Alonso, B., Maldonado, A., 2003. Recent mass-movement processes on the Ebro continental slope (NW Mediterranean). Marine and Petroleum Geology 20, 445-457.

Casas, D., Ercilla, G., Yenes, M., Estrada, F., Alonso, B., García, M., Somoza, L., 2011. The Baraza Slide: model and dynamics. Marine Geophysical Research 32(1-2), 245-256.

Casas, D., Casalbore, D., Yenes, M., Urgeles, R., 2015. Submarine mass movements around the Iberian Peninsula. The building of continental margins through hazardous processes. Boletín Geológico y Minero 126, 257-278.

Cattaneo, A., Jouet, G., Charrier, S., Théreau, E., Riboulot, V., 2014. Submarine landslides and contourite drifts along the Pianosa Ridge (Corsica Trough, Mediterranean Sea). In: Krastel, S., Behrmann, J.H., Völker, D., Stipp, M., Berndt, C., Urgeles, R., Chaytor, J., Huhn, K., Strasser, M., Harbitz, C.B. (Eds.). Submarine mass movements and their consequences. Advances in Natural and Technological Hazards Research 37, 435-445.

Ceramicola, S., Rebesco, M., De Batist, M., Khlystov, O., 2001. Seismic evidence of smallscale lacustrine drifts in Lake Baikal (Russia). Marine Geophysical Research 22, 445–464.

Chalouan, A., Michard, A., El Kadiri, K., Negro, F., Frizon de Lamotte, D., Soto, J.I., Saddiqi, O., 2008. The Rif Belt. In: Michard, A., Saddiqi, O., Chalouan, A., Frizon de Lamotte, D. (Eds.). Continental Evolution: The Geology of Morocco. Springer 116, 203-302.

Chen, H., Xie, X., Van Rooij, D., Vandorpe, T., Su, M., Wang, D., 2014. Depositional characteristics and processes of alongslope currents related to a seamount on the northwestern margin of the Northwest Sub-Basin, South China Sea. Marine Geology 355, 36-53.

Chiocci, F.L., Ercilla, G., Torres, J., 1997. Stratal architecture of Western Mediterranean Margins as the result of the stacking of Quaternary lowstand deposits below 'glacio-eustatic fluctuation base-level'. Sedimentary Geology 112, 195-217.

Cloetingh, S.A.P.L., Van der Beek, P.A., Van Rees, D., Roep, T.B., Biermann, C., Stephenson, R.A., 1992. Flexural interaction and the dynamics of Neogene extensional basin formation in the Alboran-Betic region. Geo-Marine Letters 12(2-3), 66-75.

Comas, M.C., Soto, J.I., 1999. Brittle deformation in the metamorphic basement at site 976: implications for middle Miocene extensional tectonics in the western Alboran basin. In: Zahn, R., Comas, M.C., Klaus, A. (Eds.), Proceedings of the Ocean Drilling Program, Scientific Results 161, 331-334.

Comas, M.C., García-Dueñas, V., Jurado, M.J., 1992. Neogene tectonic evolution of the Alboran Sea from MCS data. Geo-Marine Letters 12, 157-164.

Comas, M.C., Dañobeitia, J.L., Álvarez-Marrón, J., Soto, J.I., 1995. Crustal reflections and structure in the Alboran basin: preliminary results of the ESCI-Alboran survey. Revista de la Sociedad Geológica de España 8, 529-542.

Comas, M. C., Zahn, R., Klaus, A., et al. 1996. Proceedings of the Ocean Drilling Program, Initial Reports, 161. College Station, TX (Ocean Drilling Program).

Comas, M.C., Platt, J.P., Soto, J.I., Watts, A.B., 1999. The origin and tectonic history of the Alboran basin: insights from Leg 161 results. In: Zahn, R., Comas, M.C., Klaus, A. (Eds.), Proceedings of the Ocean Drilling Program, Scientific Results, pp. 555-580.

Cossu, R., Wells, M., 2013. The evolution of submarine channels under the influence of Coriolis forces: experimental observations of flow structures. Terra Nova 25, 65-71.

Cossu, R., Wells, M., Wåhlin, A., 2010. Influence of the Coriolis force on the flow structure of turbidity currents in submarine channel systems. Journal of Geophysical Research Oceans 115 (11), C11016.

Cremer, M., 1981. Distribution des turbidites sur l'éventail subaquatique du Canyon du Cap-Ferret. Bulletin De L'institut De Géologie Du Bassin d'Aquitaine 30, 51-69.

DEF

D'Acremont, E., Gorini, C., Ceramicola, S., Ercilla, G., Farran, M., López-González, N., Vandorpe, T.P. Vázquez, J.T., Do Couto, D., 2012. EUROFLEETS Cruise Summary Report: South Alboran Research in Active Systems. SARAS Cruise, R/V Ramon Margalef, 37 pp.

D'Acremont, E., Gutscher, M.-A., Rabaute, A., de Lépinay, B.M., Lafosse, M., Poort, J., Ammar, A., Tahayt, A., Le Roy, P., Smit, J., Do Couto, D., Cancouët, R., Prunier, C., Ercilla, G., Gorini, C., 2014. High-resolution imagery of active faulting offshore Al Hoceima, Northern Morocco. Tectonophysics 632, 160-166.

Dalla Valle, G., Gamberi, F., Rocchini, P., Minisini, D., Errera, A., Baglioni, L., Trincardi, F., 2013. 3D seismic geomorphology of mass transport complexes in a foredeep basin: Examples from the Pleistocene of the Central Adriatic Basin (Mediterranean Sea). Sedimentary Geology 294, 127-141.

Damuth, J.E., 1980. Use of high-frequency (3.5–12 kHz) echograms in the study of near-bottom sedimentation processes in the deep-sea: A review. Marine Geology 38, 51-75.

de Kaenel, E., Siesser, W. G., Murat, A., 1999. Pleistocene calcareous nannofossil biostratigraphy and the western Mediterranean sapropels, Sites 974 to 977 and 979. In: Zahn, R., Comas, M. C., Klaus, A. (Eds.), Proceedings of the Ocean Drilling Program, Scientific Results 161, 159-183.

Deptuck, M.E., Steffens, G.S., Barton, M. and Pirmez, C. 2003. Architecture and evolution of upper fan channel belts on the Niger Delta slope and in the Arabian Sea. Marine and Petroleum Geology 20, 649-676.

Dewey, J.F., Helman, M.L., Turco, E., Hutton, D.H.W., Knott, S.D., 1989. Kinematics of the western Mediterranean. In: Coward, M.P., Dietric, D., Park, R.G. (Eds.) Alpine Tectonics, Geological Society, London, Special Publications 45, 265-283.

Dickson, R., McCave, I.N., 1986. Nepheloid layers on the continental slope west of Porcupine Bank. Deep-Sea Research Part A: Oceanographic Research Papers, 33, 791-818.

Dillon, W. P., Robb, J. M., Greene, H. G., Lucena, J. C., 1980. Evolution of the continental margin of southern Spain and the Alboran sea. Marine Geology 36, 205-226.

Divins, D. L., 2003. Total Sediment Thickness of the World's Oceans and Marginal Seas. NOAA National Geophysical Data Center, Boulder, CO.

Do Couto, D., Popescu, S.-M., Suc, J.-P., Melinte-Dobrinescu, M.C., Barhoun, N., Gorini, C., Jolivet, L., Poort, J., Jouannic, G., Auxietre, J.-L., 2014. Lago Mare and the Messinian Salinity Crisis: Evidence from the Alboran Sea (S. Spain). Marine and Petroleum Geology 52, 57-76.

Do Couto, D., Gorini, C., Jolivet, L., Lebret, N., Augier, R., Gumiaux, C., d'Acremont, E., Ammar, A., Jabour, H., Auxietre, J.-L., 2016. Tectonic and stratigraphic evolution of the Western Alboran Sea Basin in the last 25Myrs. Tectonophysics 677-678, 280-311.

Docherty, J.I.C., Banda, E., 1992. A note on the subsidence history on the northern margin of the Alboran Basin. Geo-Marine Letters 12: 82-87.

Docherty, C., Banda, E., 1995. Evidence for the eastward migration of the Alboran Sea based on regional subsidence analysis: a case for basin formation by delamination of the subcrustal lithosphere?. Tectonics 14, 804–818.

Domzig, A., Gaullier, V., Giresse, P., Pauc, H., Déverchère, J., Yelles, K., 2006. Role of tectonics in deposition processes along the western Algerian margin (Oran-Tenes) from echo-character. Geophysical Research Abstracts 8, 04793.

Dónde Va Group, 1984. Donde va? An oceanographic experiment in the Alboran Sea. EOS Trans. Am. Geophys. Union 65, 682–683.

Dufau-Julliand, C., Marsaleix, P., Petrenko, A., Dekeyser, I., 2004. Three-dimensional modeling of the Gulf of Lion's hydrodynamics (northwest Mediterranean) during January 1999 (MOOGLI3 Experiment) and late winter 1999: Western Mediterranean Intermediate Water's (WIW's) formation and its cascading over the shelf break. Journal of Geophysical Research: Oceans (1978–2012) 109(C11), C11002.

Duggen, S., Hoernle, K., Bogaard, Pvd., Harris, C., 2004. Magmatic evolution of the Alboran Region: the role of subduction in forming the western Mediterranean and causing the Messinian Salinity Crisis. Earth and Planetary Science Letters 218, 91-108.

Duggen, S., Hoernle, K., Klügel, A., Geldmacher, J., Thirlwall, M., Hauff, F., Lowry, D., Oates, N., 2008. Geochemical zonation of the Miocene Alborán Basin volcanism (westernmost Mediterranean): geodynamic implications. Contributions to Mineralogy and Petrology 156, 577-593.

Durán, R., Canals, M., Sanz, J.L., Lastras, G., Amblas, D., Micallef, A., 2014. Morphology and sediment dynamics of the northern Catalan continental shelf, northwestern Mediterranean Sea. Geomorphology 204, 1-20.

Dykstra, M. 2012. Deep-Water Tidal Sedimentology. In: Davis Jr., R.A., Dalrymple, R.W. (Eds.). Principles of Tidal Sedimentology, 371-395.

Eden, C., Willebrand, J. 1999. Neutral density revisited. Deep Sea Research Part II: Topical Studies in Oceanography 46, 33-54.

Egloff, J., Johnson, G.L., 1975. Morphology and Structure of the Southern Labrador Sea. Canadian Journal of Earth Sciences 12, 2111-2133.

Einsele, G., 1992. Sedimentary Basins, Evolution, Facies and Sediment budget.. Springer-Verlag, 628pp.

Einsele, G., Chough, S.K., Shiki, T., 1996. Depositional events and their records: an introduction. Sedimentary Geology 104, 1-9.

El Moumni, B., Gensous, B., 1992. Sur la sédimentation actuelle et post-glaciaire dans le plateau continental du Rif oriental (Maroc). Bull. Inst. Sci. 16, 65-73.

Ercilla, 1992. Sedimentación en márgenes continentales y cuencas del Mediterráneo Occidental durante el Cuaternario (Península Ibérica). Universitat Politècnica de Catalunya, Ph.D Thesis.

Ercilla, G., Alonso, B., 1996. Quaternary siliciclastic sequence stratigraphy of western Mediterranean passive and tectonically active margins: the role of global versus local controlling factors. Geological Society, London, Special Publications 117(1), 125-137.

Ercilla, G., Casas, D. 2012. Submarine Mass Movements: Sedimentary Characterization and Controlling Factors. INTECH Open Access Publisher.

Ercilla, G., Alonso, B., Baraza, J., 1992. Sedimentary Evolution of the Northwestern Alboran Sea during the Quaternary. Geo-Marine Letters 12, 144-149.

Ercilla, G., Alonso, B., Baraza, J., 1994. Post-Calabrian sequence stratigraphy of the northwestern Alboran Sea (southwestern Mediterranean). Marine Geology 120, 249-265.

Ercilla, G., Baraza, J., Alonso, B., Estrada, F., Casas, D., Farran, M., 2002. The Ceuta Drift, Alboran Sea, southwestern Mediterranean. In: Stow, D.A.V., Pudsey, C.J., Howe, J.A., Faugères, J.-C., Viana, A.R. (Eds.), Deep-Water Contourite Systems: Modern Drifts and Ancient Series, Seismic and Sedimentary Characteristics. Geological Society, London, Memoirs, pp. 155-170.

Ercilla, G., García-Gil, S., Estrada, F., Gràcia, E., Vizcaino, A., Váquez, J.T., Díaz, S., Vilas, F., Casas, D., Alonso, B., Dañobeitia, J., Farran, M., 2008a. High-resolution seismic stratigraphy of the Galicia Bank Region and neighbouring abyssal plains (NW Iberian continental margin). Marine Geology 249(1-2), 108-127.

Ercilla, G., Casas, D., Estrada, F., Vázquez, J.T., Iglesias, J., García, M., Gómez, M., Acosta, J., Gallart, J., Maestro-González, A., 2008b. Morphosedimentary features and recent depositional architectural model of the Cantabrian continental margin. Marine Geology 247(1-2), 61-83.

Ercilla, G., Casas, D., Vázquez, J.T., Iglesias, J., Somoza, L., Juan, C., Medialdea, T., León, R., Estrada, F., García-Gil, S., Farran, M., Bohoyo, F., García, M., Maestro, A., ERGAP Project and Cruise Teams, 2011. Imaging the recent sediment dynamics of the Galicia Bank region (Atlantic, NW Iberian Peninsula). Marine Geophysical Research 32 (1–2), 99–126.

Ercilla, G., Juan, C., Estrada, F., Casas, D., Alonso, B., García, M., Farran, M., Palomino, D., Vázquez, J.T., Llave, E., Hernández-Molina, F.J., Medialdea, T., Gorini, C., D'Acremont, E., El Moumni, B., Gensous, B., Tesson, M., Maldonado, A., Ammar A., CONTOURIBER and MONTERA TEAMS, 2012. Contourite sedimentation in the Alboran Sea: morphosedimentary characterization. Geo-Temas 13, 542-544.

Ercilla, G., Juan, C., Alonso, B., J., Estrada, F., Casas, D., García, M., Hernández-Molina, F., Vázquez, J.T., Llave, E., Palomino,D., Farran, M., Gorini, C., D'Acremont, E., El Moumni, B., Ammar, A., 2014. Water mass footprints in uneven turbidite system development in the Alboran Sea. In: D. Van Rooij and A. Rüggeberg (eds.). 2nd Deep-Water Circulation Congress, The Contourite Log-Book. Ghent, Vilzz Special Publication 69, 83-84.

Ercilla, G., Juan, C., Hernández-Molina, F.J., Bruno, M., Estrada, F., Alonso, B., Casas, D., Farran, M., Llave, E., García, M., Vázquez, J.T., D'Acremont, E., Gorino, C., Palomino, D., Valencia, J., El Moumni, B., Ammar, A, 2016. Significance of bottom currents in deep-sea morphodynamics: an example from the Alboran Sea. Marine Geology 378, 157-170.

Estrada, F., Ercilla, G., Alonso, B., 1997. Pliocene-Quaternary tectonic-sedimentary evolution of the NE Alboran Sea (SW Mediterranean Sea). Tectonophysics 282, 423-442.

Estrada, F., Ercilla, G., Gorini, C., Alonso, B., Vázquez, J. T., García-Castellanos, D., Juan, C., Maldonado, A., Ammar A., Elabbassi M., 2011. Impact of pulsed Atlantic water inflow into the Alboran Basin at the time of the Zanclean flooding. Geo-Marine Letters 31(5-6), 361-376.

Fabrés, J., Calafat, A., Sánchez-Vidala, A., Canals, M., Heussner, S., 2002. Composition and spatio-temporal variability of particle fluxes in theWestern Alboran Gyre, Mediterranean Sea. J. Mar. Syst. 33–34, 431–456.

Faccenna, C., Piromallo, C., Crespo-Blanc, A., Jolivet, L., Rossetti, F., 2004. Lateral slab deformation and the origin of the western Mediterranean arcs. Tectonics 23, TC1012.

Farmer, D.M. and Armi, L. 1988. The flow of Atlantic water through the Strait of Gibraltar. Progress in Oceanography, 21, 1-105.

Faugères, J.-C., Mulder, T., 2011. Contour currents and contourite drifts. In: Hüneke, H., Mulder, T. (Eds.). Deep-sea sediments 63, 149-214.

Faugères, J.-C., Stow, D.A.V., 1993. Bottom-current-controlled sedimentation: a synthesis of the contourite problem. Sediment. Geol. 82, 287–297.

Faugères, J.-C., Stow, D.A.V., 2008. Contourite drifts: nature, evolution and controls. In: Rebesco, M., Camerlenghi, A. (Eds.), Contourites. Developments in Sedimentology, 60. Elsevier, Amsterdam, pp. 257–288.

Faugères, J.-C.,Mezerais, M.L., Stow, D.A.V., 1993. Contourite drift types and their distribution in the North and South Atlantic Ocean basins. Sedimentary Geology 82, 189–203.

Faugères, J.-C., Stow, D.A.V., Imbert, P., Viana, A.R., 1999. Seismic features diagnostic of contourite drifts. Marine Geology 162, 1-38.

Fauquette, S., Suc, J.-P., Guiot, J., Diniz, F., Feddi, N., Zheng, Z., Bessais E., Drivaliari, A., 1999. Climate and biomes in the West Mediterranean area during the Pliocene. Palaeogeography, Palaeoclimatology, Palaeoecology 152, 15-36.

Fernández-Ibáñez, F., Soto, J.I., 2008. Crustal rheology and seismicity in the Gibraltar Arc (western Mediterranean). Tectonics 27, TC2007.

Fernández-Ibáñez, F., Soto, J.I., Zoback, M.D., Morales, J., 2007. Present-day stress field in the Gibraltar Arc (western Mediterranean). Journal of Geophysical Research: Solid Earth (1978–2012) 112(B8), B08404.

Fernández-Salas, L.M., 2008. Los depósitos del Holoceno Superior en la plataforma continental del sur de la Península Ibérica: caracterización morfológica y estratigráfica. PhD Thesis, Universidad de Cádiz, Puerto Real, Spain.

Fernández-Salas, L.M., Lobo, F.J., Hernández-Molina, F.J., Somoza, L., Rodero, J., Díaz-del-Río, V., Maldonado, A., 2003. High-resolution architecture of late Holocene highstand prodeltaic deposits from southern Spain: the imprint of high-frequency climatic and relative sea-level changes. Continental Shelf Research 23, 1037-1054.

Fernández-Salas, L.M., Lobo, F.J., Sanz, J.L., Díaz-del-Río, V., García, M.C., Moreno, I., 2007. Morphometric analysis and genetic implications of pro-deltaic sea-floor undulations in the northern Alboran Sea margin, western Mediterranean Basin. Marine Geology 243, 31-56.

Fernández-Salas, L.M., Durán, R., Mendes, I., Galparsoro, I., Lobo, F.J., Bárcenas, P., Rosa, F., Ribó, M., García-Gil, S., Ferrín, A., Carrara, G., Roque, C., Canals, M., 2015. Shelves of the Iberian Peninsula and the Balearic Islands (I): Morphology and sediment types. Boletín Geológico y Minero 126, 327-376.

Field, M.E., Gardner, J.V., Prior, D.B., 1999. Geometry and significance of stacked gullies on the northern California slope. Marine Geology 154, 271–286.

Flood, R.D., Shor, A.N. 1988. Mudwaves in the Argentine Basin and their relationship to regional bottom circulation patterns. Deep Sea Research 35, 943-972.

Flood, R.D., Manley, P.L., Kowsmann, R.O., Appi, C.J., Pirmez, C., 1991. Seismic facies and late Quaternary growth of Amazon submarine fan. In: Weimer, P., Link, M.H. (Eds.). Seismic Facies and Sedimentary Processes of Modern and Ancient Submarine Fans and turbidite systems. Frontiers in sedimentary geology. Springer-Verlag, New York, 415–433.

Foglini, F., Campiani, E., Trincardi, F., 2016. The reshaping of the South West Adriatic Margin by cascading of dense shelf waters. Marine Geology 375, 64-81.

Folk, R.L., Ward, W.C., 1957. Brazos River bar: a study in the significance of grain size parameters. Journal of Sedimentary Research, 27(1), 3-26.

Friedman, G.M., Sanders, J.E., 1978. Principles of sedimentology. Wiley, New York. 792 pp.

Frigola, J., Moreno, A., Cacho, I., Canals, M., Sierro, F. J., Flores, J. A., and Curtis, J. H., 2007. Holocene climate variability in the western Mediterranean region from a deepwater sediment record. Paleoceanography 22(2), PA2209.

GHI

Gani, M.R., 2004. From Turbid to Lucid: A Straightforward Approach to Sediment Gravity Flows and Their Deposits. The Sedimentary Record 2(3), 4-8.

García, M, Alonso, B., Ercilla, G., Gràcia, E., 2006. The tributary valley systems of the Almeria Canyon (Alboran Sea, SW Mediterranean): Sedimentary architecture. Marine Geology 226 (3-4), 207-223.

García, M., Hernández-Molina, F. J., Llave, E., Stow, D.A.V., León, R., Fernández-Puga, M.C., Díaz del Río, V., Somoza, L., 2009. Contourite erosive features caused by the Mediterranean Outflow Water in the Gulf of Cadiz: Quaternary tectonic and oceanographic implications. Marine Geology 257, 24-40.

García, M., Ercilla, G., Alonso, B., Estrada, F., Jané, G., Mena, A., Alvés, T., Juan, C., 2015. Deep-water turbidite systems: a review of their elements, sedimentary processes and depositional models. Their characteristics on the Iberian margins. Boletín Geológico y Minero 126, 189-218.

García-Castellanos, D., Estrada, F., Jimenez-Munt, I., Gorini, C., Fernandez, M., Verges J., De Vicente, R., 2009. Catastrophic flood of the Mediterranean after the Messinian salinity crisis. Nature 462(7274), 778-781.

García-Dueñas, V., Balanyá, J.C., Martínez-Martínez, J.M., 1992. Miocene extensional detachments in the outcropping basement of the northern Alboran basin (Betics) and their tectonic implications. Geo-Marine Letters 12(2-3), 88-95.

García-Lafuente, J., Delgado, J., Criado, F., 2002. Inflow interruption by meteorological forcing in the Strait of Gibraltar. Geophysical Research Letters 29(19), 21-24.

Garrett, C., 2003. Internal tides and ocean mixing. Science 301, 1858–1859.

Garrison, R.E., 1981. Pelagic and hemipelagic sedimentation in active margin basins. Depositional Systems of Active Continental Margins: Short Course Notes, 15-38.

Garziglia, S., Migeon, S., Ducassou, E., Loncke, L., Mascle, J., 2008. Mass-transport deposits on the Rosetta province (NW Nile deep-sea turbidite system, Egyptian margin): Characteristics, distribution, and potential causal processes. Marine Geology 250, 180-198.

Gascard, J.C., Richez, C., 1985. Water masses and circulation in the Western Alboran Sea and in the Straits of Gibraltar. Proggress in Oceanography 15, 157–216.

Gaudin, M., Berné, S., Jouanneau, J.-M., Palanques, A., Puig, P., Mulder, T., Cirac, P., Rabineau, M. and Imbert, P. 2006. Massive sand beds attributed to deposition by dense water cascades in the Bourcart canyon head, Gulf of Lions (northwestern Mediterranean Sea). Marine Geology 234, 111-128.

Gaullier, V., Loncke, L., Mascle, J., Vendeville, B. C., Maillard, A., 2002. Salt tectonics in the Nile and Rhône deep-sea fans: comparison on the basis of seismic data and physical modelling. In: Briand, F. (Ed.). Turbidite systems and deep-sea fans of the Mediterranean and the Black seas, CIESM Workshop 17, 39–42.

Gervais, A., Mulder, T., Savoye, B., 2006. Sandy modern turbidite lobes: a new insight from high resolution seismic data. Marine and Petroleum Geology 23, 485–502.

Gladstone, R., Flecker, R., Valdes, P., Lunt, D., Markwick, P., 2007. The Mediterranean hydrological budget from a Late Miocene global climate simulation. Palaeogeography, Palaeoclimatology, Palaeoecology 251, 254–267.

Golik, A., 1993. Indirect evidence for sediment transport on the continental shelf off Israel. Geo-Marine Letters 13, 159–164.

Gómez-Ballesteros, M., Druet, M., Muñoz, A., Arrese, B., Rivera, J., Sánchez, F., Cristobo, J., Parra, S., García-Alegre, A., González-Pola, C., Gallastegui, J., Acosta, J., 2014. Geomorphology of the Avilés Canyon System, Cantabrian Sea (Bay of Biscay).Deep-Sea Research II 106, 99-117.

Gong, C., Wang Y., Zhu, W., Li, W. and Xu, Q. 2013. Upper Miocene to Quaternary unidirectionally migrating deepwater channels in the Pearl River Mouth Basin, northern South China Sea. AAPG Bulletin, 97, 285-308.

Gonthier, E.G., Faugères, J.C., Stow, D.A.V., 1984. Contourite facies of the Faro Drift, Gulf of Cadiz. Geological Society, London, Special Publications 15, 275-292.

González-Donoso, J. M., Serrano, F., Linares, D., 2000. Sea surface temperature during the Quaternary at ODP Sites 976 and 975 (western Mediterranean). Palaeogeography, Palaeoclimatology, Palaeoecology 162, 17-44.

Griffin, D.L., 2002. Aridity and humidity: two aspects of late Miocene climate of North Africa and the Mediterranean. Palaeogeography, Palaeoclimatology, Palaeoecology 182, 65–91.

Gutscher, M-.A., Malod, J., Rehault, J-.P., Contrucci, I., Klingelhoefer, F., Mendes-Victor, L., Spakman, W., 2002. Evidence for active subduction beneath Gibraltar. Geology 30, 1071–1074.

Haflidason H., Sejrup, H.P., Nygard, A., Mienert, J., Bryn, P., Lien, R., Forsberg, C.F., Berg, K., Masson, D., 2004. The Storegga slide: architecture, geometry and slide development. Marine Geology 213, 201-234.

Hampton, M.A., Lee, H.J. and Locat, J. 1996. Submarine landslides. Reviews of Geophysics 34 (1), 33-59.

Haq, B.U., Hardenbol, J., Vail, P.R., 1987. Chronology of Fluctuating Sea Levels Since the Triassic. Science 235, 1156-1166.

Hayward, B. W., Kawagata, S., Grenfell, H. R., Sabaa, A. T., O'Neill, T., 2007. Last global extinction in the deep sea during the mid-Pleistocene climate transition. Paleoceanography 22(3), PA3103.

Hayward, B. W., Sabaa, A.T., Kawagata, S., Grenfell, H.R., 2009. The Early Pliocene re-colonisation of the deep Mediterranean Sea by benthic foraminifera and their pulsed Late Pliocene–Middle Pleistocene decline. Marine Micropaleontology 71(3-4), 97-112.

Haywood, A.M., Sellwood, B.W., Valdes, P.J., 2000. Regional warming: Pliocene (3 Ma) paleoclimate of Europe and the Mediterranean. Geology 28, 1063-1066.

Head, M.J., Pillans, B., Farquhar, S.A., 2008. The Early-Middle Pleistocene transition: characterization and proposed guide for the defining boundary. Episodes 31(2), 255.

Heezen, B.C., Hollister, C.D., Ruddiman, W.F., 1966. Shaping of the continental rise by deep geostrophic contour currents. Science 152, 502–508.

Heezen, B.C., Johnson, G.L., 1969. Mediterranean undercurrent and microphysiography west of Gibraltar. Bulletin de l'Institut Océanographique 67, 1–95.

Hernández-Molina, F. J., Somoza, L., Rey, J., Pomar, L., 1994. Late Pleistocene-Holocene sediments on the Spanish continental shelves: Model for very high resolution sequence stratigraphy. Marine Geology 120, 129-174.

Hernández-Molina, F.J., Somoza, L., Rey, J., 1995. Late Pleistocene–Holocene High-Resolution Sequence Analysis on the Alboran Sea Continental Shelf. In: De Batist, M., Jacobs, P. (Eds.), Geology of Siliciclastic Shelf Seas. Geological Society, London, Special Publication 117, pp. 139–154.

Hernández-Molina, F. J., Somoza, L., Vázquez, J. T., Lobo, F., Fernández-Puga, M. C., Llave, E., Díaz-del-Río, V., 2002. Quaternary stratigraphic stacking patterns on the continental shelves of the southern Iberian Peninsula: their relationship with global climate and palaeoceanographic changes. Quaternary International 92, 5-23.

Hernández-Molina, F. J., Llave, E., Somoza, L., Fernández-Puga, M.C., Maestro, A., León, R., Medialdea, T., Barnolas, A., García, M., Díaz-del-Río, V., Fernández-Salas, L.M., Vázquez, J.T., Lobo, F.J., Alveirinho Dias, J.M., Rodero, J., Gardner, J., 2003. Looking for clues to paleoceanographic imprints: A diagnosis of the Gulf of Cadiz contourite depositional systems. Geology 31, 19-22.

Hernández-Molina, F.J., Llave, E., Stow, D.A.V., García, M., Somoza, L., Vázquez, J.T., Lobo, F.J., Maestro, A., Díaz del Río, V., León, R., Medialdea, T., Gardner, J., 2006a. The contourite depositional system of the Gulf of Cádiz: A sedimentary model related to the bottom current activity of the Mediterranean outflow water and its interaction

with the continental margin. Deep Sea Research Part II: Topical Studies in Oceanography 53, 1420-1463.

Hernández-Molina, F. J., Larter, R. D., Rebesco, M., Maldonado, A., 2006b. Miocene reversal of bottom water flow along the Pacific Margin of the Antarctic Peninsula: Stratigraphic evidence from a contourite sedimentary tail. Marine Geology 228(1–4), 93-116.

Hernández-Molina, F.J., Llave, E., Stow, D.A.V., 2008a. Continental Slope Contourites. In: Rebesco, M., Camerlenghi, A. (Eds.), Contourites, Developments in Sedimentology 60, 379-408.

Hernández-Molina, F.J., Maldonado, A., Stow, D.A.V., 2008b. Abyssal plain contourites. In: Rebesco, M., Camerlenghi, A. (Eds.), Contourites, Developments in Sedimentology 60, 347-378.

Hernández-Molina, F.J., Paterlini, M., Violante, R., Marshall, P., de Isasi, M., Somoza, L., Rebesco, M., 2009. Contourite depositional system on the Argentine slope: An exceptional record of the influence of Antarctic water masses. Geology 37, 507-510.

Hernández-Molina, F.J., Stow, D.A.V., Llave, E., Rebesco, M., Ercilla, G., Van Rooij, D., Mena, A., Vázquez, J.T., Voelker, A.H.L., 2011a. Deep-water circulation: processes & products (16–18 June 2010, Baiona): introduction and future challenges. Geo-Mar. Lett. 31, 285–300.

Hernández-Molina, F.J., Serra, N., Stow, D.A.V., Llave, E., Ercilla, G., Van Rooij, D., 2011b. Along-slope oceanographic processes and sedimentary products around Iberia. Geo-Mar. Lett. 31, 315–341.

Hernández-Molina, F., Llave, E., Preu, B., Ercilla, G., Fontan, A., Bruno, M., Serra, N., Gomiz, J., Brackenridge, R., Sierro, F., 2014. Contourite processes associated with the Mediterranean Outflow Water after its exit from the Strait of Gibraltar: Global and conceptual implications. Geology 42, 227-230.

Hernández-Molina, F. J., Wahlin, A., Bruno, M., Ercilla, G., Llave, E., Serra, N., Roson, G., Puig, P., Rebesco, M., Van Rooij, D., Roque, C., González-Pola, C., Sánchez, F., Gómez, M., Preu, B., Schwenk, T., Hanebuth, T.J.J., Sánchez-Leal, R.F., García Lafuente, J., Brackenridge, R.E., Juan, C., Stow, D.A.V., Sánchez-González, J.M., 2015. Oceanographic processes and products around the Iberian margin: a new multidisciplinary approach. Boletín Geológico y Minero 126, 279-326.

Hernández-Molina, F. J., Sierro, F. J., Llave, E., Roque, C., Stow, D. A. V., Williams, T., Lofig, J., Van der Scheeb, M., Arnáizh, A., Ledesmai, S., Rosalesh, C., Rodríguez-Tovarj, F.J., Pardo-Igúzquiza, E., Brackenridge, R. E., 2016. Evolution of the gulf of Cadiz margin and southwest Portugal contourite depositional system: Tectonic, sedimentary and paleoceanographic implications from IODP expedition 339. Marine Geology 377, 7-39.

Hiscott, R.N., Hall, F.R., Pirmez, C., 1997. Turbidity current overspill from the Amazon Channel: texture of the silt/sand load, paleoflow from anysotropy of magnetic susceptibility, and implications for flow processes. In: Flood, R.D., Piper, D.J.W., Klaus, A. and Peterson, L.C. (eds.), Proceedings of the Ocean Drilling Program, Scientific Results, 155, College Station, TX, 53–78.

Hodell, D. A., Kennett, J.P., 1986. Late Miocene-Early Pliocene stratigraphy and paleoceanography of the South Atlantic and southwest Pacific Oceans: A synthesis. Paleoceanography 1, 285-311.

Hodell, D.A., Curtis, J.H., Sierro, F. J., Raymo, M. E., 2001. Correlation of late Miocene to early Pliocene sequences between the Mediterranean and North Atlantic. Paleoceanography 16, 164-178.

Hoernle, K., van den Bogaard, P., Duggen, S., Mocek, B., Garbe-Schönberg, D., 1999. Evidence for Miocene subduction beneath the Alboran Sea: $^{40}Ar/^{39}Ar$ dating and geochemistry of volcanic rocks from holes 977A and 978A. In: Zahn, R., Comas, M.C., Klaus, A., Proceedings of the Ocean Drilling Program, Scientific Results 161, 357-373.

Holbrook, W.S., Lizarralde, D., Pecher, I.A., Gorman, A.R., Hackwith, K.L., Hornbach, M., Saffer, D., 2002. Escape of methane gas through sediment waves in a large methane hydrate province. Geology 30, 467-470.

Holger, K. 1987. Benthic storms, vortices, and particle dispersion in the deep western Europe. Deutsche Hydrographische Zeitschrift, 40, 88-12.

Hollister, C.D. and McCave, I.N. 1984. Sedimentation under deep-sea storms. Nature, 309, 220-225.

Horton, C., Clifford, M, 2005. Comparison of forecast and observed internal tides in the Eastern Mediterranean Sea. Geophysical Research Abstracts 7, 01834.

Hübscher, C., Dullo, C., Flögel, S., Titschack, J., Schönfeld, J., 2010. Contourite drift evolution and related coral growth in the eastern Gulf of Mexico and its gateways. International Journal of Earth Sciences 99, 191-206.

Hüneke, H., Henrich, R. 2011. Pelagic sedimentation in modern and ancient oceans. In: Hüneke, H., Mulder, T. (Eds.). Deep-Sea Sediments 63, 215-351.

Hüneke, H., Mulder, T., 2011. Deep-Sea Sediments. Developments in Sedimentology 63. Elsevier. 849 pp.

Hungr, O., Lerouell, S., Picarelli, L., 2014. The Varnes classification of landslides types, an update. Landslides, 11, 167-194.

Hunter, S.E., Wilkinson, D., Stanford, J., Stow, D.A.V., Bacon, S., Akhmetzhanov, A.M., Kenyon, N.H., 2007. The Eirik Drift: a longterm barometer of north Atlantic deepwater flux south of Cape Farewell, Greenland. In: Viana, A., Rebesco, M. (Eds.), Economic and Paleoceanographic Importance of Contourites. Geological Society, London, Special Publication, 276, pp. 245–264.

Huthnance, J., 1981. Waves and currents near the continental shelf edge. Progress in Oceanography 10, 193-226.

Iglesias, J., 2009. Sedimentation on the Cantabrian Continental Margin from Late Oligocene to Quaternary, Universidade de Vigo & Institut de Ciències del Mar CSIC. PhD Thesis, 214 pp.

Iribarren, L., Vergés, J., Fernàndez,M., 2009. Sediment supply from the Betic–Rif orogen to basins through Neogene. Tectonophysics 475, 68–84.

Ivanov, V.V., Shapiro, G.I., Huthnance, J.M., Aleynik, D.L., Golovin, P.N. 2004. Cascades of dense water around the world ocean. Progress in Oceanography, 60, 47-98.

JKL

Jabaloy, A., Galindo-Zaldívar, J., González-Lodeiro, F., 1993. The Alpujárride–Nevado–Filábride extensional shear zone, Betic Cordillera, SE Spain. J. Struct. Geol. 15, 555–569.

Jiménez-Espejo, F.J., Martínez-Ruiz, F., Rogerson, M., González-Donoso, J.M., Romero, O.E., Linares, D., Sakamoto, T., Gallego-Torres, D., Rueda-Ruiz, J.L., Ortega-Huertas, M., Perez Claros, J.A., 2008. Detrital input, productivity fluctuations, and water mass circulation in the westernmost Mediterranean Sea since the Last Glacial Maximum. Geochem. Geophys. Geosyst. 9 (11).

Johnson, H.D., Baldwin, C.T., 1996. Shallow clastic seas. Sedimentary environments: processes, facies and stratigraphy 3, 232-280.

Jolivet, L., Augier, R., Faccenna, C., Negro, F., Rimmele, G., Agard, P., Robin, C., Rossetti, F., Crespo-Blanc, A., 2008. Subduction, convergence and the mode of backarc extension in the Mediterranean region. Bull. Soc. géol. Fr. 179, 525–550.

Juan, C., Ercilla, G., Hernández-Molina, F. J., Estrada, F., Alonso, B., Casas, D., García, M., Farran, M., Llave, E., Palomino, D., Vázquez, J.T., Medialdea, T., Gorini, C., D'Acremont, E., El Moumni, B., Gensous, B., Tesson, M., Maldonado, A., Ammar, A., CONTOURIBER and MONTERA TEAMS, 2012a. Contourite sedimentation in the Alboran Sea: morphosedimentary characterization. Geo-Temas 13, 1809-1812.

Juan, C., Ercilla, G., Estrada, F., Casas, D., Alonso, B., García, M., Farran, M., Palomino, D., Vázquez, J.T., Llave, E., Hernández-Molina, F. J., Medialdea, T., Gorini, C., D'Acremont, E., El Moumni, B., Ammar, A., 2012b. The Pliocene-Quaternary stratigraphy in the Eastern Alboran Sea. Rendiconti Online della Società Geologica Italiana 21 (2), 970-972.

Juan, C., Ercilla, G., Hernández-Molina, F.J., Estrada, F., Alonso, B., Casas, D., García, M., Farran, M., Llave, E., Palomino, D., Vázquez, J.-T., Medialdea, T., Gorini, C., D'Acremont, E., El Moumni, B., Ammar, A., 2016. Seismic evidence of current-controlled sedimentation in the Alboran Sea during the Pliocene and Quaternary: Palaeoceanographic implications. Marine Geology 378, 292-311.

Jurado, M. J., Comas, M. C., 1992. Well Log Interpretation and Seismic Character of the Cenozoic Sequence in the Northern Alboran Sea. Geo-Marine Letters 12, 129-136.

Kemp, A.E.S., 1990. Sedimentary fabrics and variation in lamination style in Peru continental margin upwelling sediments. In: Proceedings of the Ocean Drilling Program, Scientific Results 112, 43-58.

Kennett, J.P., 1981. Marine Geology. Prentice Hall, Englewood Cliffs, New Jersey.

Kenyon, N.H., 1987. Mass-wasting features on the continental slope of northwest Europe. Marine Geology 74(1), 57-77.

Kenyon, N., 2001. Channelised deep-sea depositional systems in the Mediterranean: The value of sonar back-scatter mapping. IOC Workshop Report 175, 6–10.

Kenyon, N.H., Belderson, R.H., Stride, A.H., 1978. Channels, canyons and slump folds on the continental slope between South-West Ireland and Spain. Oceanol. Acta 1, 369–380.

Killworth, P.D. 1983. Deep convection in the world ocean. Reviews of Geophysics and Space Physics, 21, 1-26.

Kinder, T. H., Bryden, H.L., 1990. Aspiration of deep waters through straits. In: Pratt, L.J. (Ed.), The physical oceanography of sea straits. Springer, Netherlands. NATO ASI Series 318, 295-319.

Knutz, P.C., 2008. Paleoceanographic Significance of Contourite Drifts. In: Rebesco, M., Camerlenghi, A. (Eds.), Contourites. Developments in Sedimentology 60, 457–516.

Köhler, C.M., Heslop, D., Dekkers, M.J., Krijgsman, W., van Hinsbergen, D.J.J., von Dobeneck, T., 2008. Tracking provenance changes during the late Miocene in the Eastern Mediterranean Metochia section using geochemical and environmental magnetic proxies. Geochemistry, Geophysics, Geosystems 9, Q12018.

Köhler, C.M., Heslop, D., Krijgsman, W., Dekkers, M.J. 2010. Late Miocene paleoenvironmental changes in North Africa and the Mediterranean recorded by geochemical proxies (Monte Gibliscemi section, Sicily). Palaeogeography, Palaeoclimatology, Palaeoecology 285, 66-73.

Krantz, D.E. 1991. A chronology of Pliocene sea-level fluctuations: the U.S. Middle Atlantic coastal plain record. Quaternary Science Reviews 10, 163-174.

Krijgsman, W., Hilgen, F.J., Raffi, I., Sierro, F.J., Wilson, D.S., 1999a. Chronology, causes and progression of the Messinian salinity crisis. Nature, 400, 652-655.

Krijgsman, W., Langerels, C.G., Zachariasse, W.J., Boccaletti, M., Moratti, G., Gelati, R., Iaccarion, S., Papani, G., Villa, G., 1999b. Late Neogene evolution of the Taza-Guercif basin (Rifian Corridor, Morocco) and implications for the Mediterranean salinity crisis. Marine Geology 153, 147-160.

Krijgsman, W., Fortuin, A.R., Hilgen, F.J., Sierro, F.J., 2001. Astrochronology for the Messinian Sorbas basin (SE Spain) and orbital (precessional) forcing for evaporite cyclicity. Sedimentary Geology 140, 43-60.

Kuenen, P.H., 1938. Density currents in connection with the problem of submarine canyons. Geol. Mag. 75, 241–249.

Kuenen, P.H., 1951. Properties of turbidity currents of high density. Society of Economic Paleontologists and Mineralogists, Special Publication 2, 14–33.

Kuenen, P.H., Migliorini, C.I., 1950. Turbidity currents as a cause of graded bedding. The Journal of Geology 58, 91–127.

Kunze, K., Rosenfeld, L.K., Carter, G.S., Gregg, M.C., 2002. Internal waves in Monterey submarine canyon. Journal of Physical Oceanography 32, 1890–1913.

Laberg, J.S., Vorren, T.O., Knutsen, S.M., 1999. The Lofoten contourite drift off Norway. Marine Geology 159, 1–6.

Laberg, J. S., Dahlgren, T., Vorren, T.O., Haflidason, H., Bryn, P., 2001. Seismic analyses of Cenozoic contourite drift development in the Northern Norwegian Sea. Marine Geophysical Researches 22: 401-416.

Lafosse, M., d'Acremont, E., Rabaute, A., Mercier de Lépinay, B., Tahayt, A., Ammar, A., Gorini, C., 2016. Evidence of Quaternary transtensional tectonics in the Nekor basin (NE Morocco). Basin Research, In Press.

Larrasoaña, J.C., Roberts, A.P., Rohling, E.J., Winklhofer, M., Wehausen, R., 2003. Three million years of monsoon variability over the northern Sahara. Climate Dynamics 21, 689–698.

Lebreiro, S., Alonso, B., 1998. The Guadiaro Turbidite System: Morphology, sedimentary facies and Holocene depositional history. Norsk-Hydro Internal Report of the Marine Geology Group-Institute of Marine Science (pp. 1–5). Barcelona: Consejo Superior de Investigaciones Científicas.

Lee, H.J., Locat, J., Desgagnés, P., Parsons, J.D., McAdoo, B.G., Orange, D.L., Puig, P., Wong, F.L., Dartnell, P., Boulanger, E., 2009. Submarine Mass Movements on Continental Margins. In: Nittrouer, C.A., Austin, J.A., Field, M.E., Kravitz, J.H., Syvitski. J.P.M., Wiberg. P.L. (Eds.). Continental Margin Sedimentation: From Sediment Transport to Sequence Stratigraphy. International Association of Sedimentologists Special publication 37, 213-275.

Legg, S., Briegleb, B., Chang, Y., Chassignet, E.P., Danabasoglu, G., Ezer, T., Gordon, A.L., Griffies, S., Hallberg, R., Jackson, L., Large, W., Özgökmen, T.M., Peters, H., Price, J., Riemenschneider, U., Wu, W., Xu, X., Yang, J., 2009. Improving Oceanic overflow representation in climate models. The Gravity Current Entrainment Climate Process Team. Bulletin of the American Meteorological Society 90, 657-670.

Lihoreau, F., Boisserie, J.-R., Viriot, L., Coppens, Y., Likius, A., MacKaye, H.T., Tafforeau, P., Vignaud, P., Brunet, M., 2006. Anthracothere dental anatomy reveals a late Miocene Chado–Libyan bioprovince. PNAS 103 (23), 8763–8767.

Linares, D., González-Donoso, J. M., Serrano, F., 1999. Paleoceanographic conditions during the Quaternary at Sites 976 (Alboran Sea) and 975 (Menorca Rise) inferred from the planktonic foraminiferal assemblages: basis for a biostratigraphy, in: Zahn, R., Comas, M.C., Klaus, A. (Eds.). Proceedings of the Ocean Drilling Program, Scientific Results 161, 441-455.

Liquete, C., Arnau, P., Canals, M., Colas, S., 2005. Mediterranean river systems of Andalusia, southern Spain, and associated deltas: A source to sink approach. Marine Geology 222-223: 471-495.

Lisiecki, L.E., Raymo, M.E., 2005. A Pliocene-Pleistocene stack of 57 globally distributed benthic d18O records. Paleoceanography 20, PA1003.

Lisiecki, L.E., Raymo, M.E., 2007. Plio–Pleistocene climate evolution: trends and transitions in glacial cycle dynamics. Quaternary Science Reviews 26, 56-69.

Llave, E., Hernández-Molina, F.J., Somoza, L., Díaz del Río, V., Stow, D.A.V., Maestro, A., Alveirinho Dias, J.M., 2001. Seismic stacking pattern of the Faro-Albufeira contourite system (Gulf of Cadiz): a Quaternary record of paleoceanographic and tectonic influences. Marine Geophysical Researches 22, 487-508.

Llave, E., Schönfeld, J., Hernández-Molina, F.J., Mulder, T., Somoza, L., Díaz del Río, V., Sánchez-Almazo, I., 2006. High-resolution stratigraphy of the Mediterranean outflow contourite system in the Gulf of Cadiz during the late Pleistocene: The impact of Heinrich events. Marine Geology 227, 241-262.

Llave, E., Hernández-Molina, F.J., Somoza, L., Stow, D.A.V., Diaz Del Rio, V., 2007. Quaternary evolution of the contourite depositional system in the Gulf of Cadiz. Geological Society, London, Special Publications 276, 49-79.

Lobo, F. J., Fernández-Salas, L.M., Moreno, I., Sanz J.L., Maldonado, A., 2006. The sea-floor morphology of a Mediterranean shelf fed by small rivers, northern Alboran Sea margin. Continental Shelf Research 26, 2607-2628.

Lobo, F.J., Maldonado, A., Hernández-Molina, F.J., Fernánndez-Salas, L.M., Ercilla, G., Alonso, B., 2008. Growth patterns of a proximal terrigenous margin offshore the Guadalfeo River, northern Alboran Sea (SW Mediterranean Sea): glacio-eustatic control and disturbing tectonic factors. Marine Geophysical Research 29, 195–216.

Lobo, F.J., Durán, R., Roque, C., Ribó, M., Carrara, G., Mendes, I., Ferrín, A., Fernández-Salas, L.M., García-Gil, S., Galparsoro, I., Rosa, F., Bárcenas, P., 2015. Shelves around the Iberian Peninsula (II): Evolutionary sedimentary patterns. Boletín Geológico y Minero 126, 377-408.

Locat, J., Lee, H., 2000. Submarine landslides: advances and challenges. Canadian Geotechnical Journal 39(1), 193-212.

Loncke, L., Gaullier, V., Mascle, J., Vendeville, B., 2002. Shallow structure of the Nile deep-sea fan: interactions between structural heritage and salt tectonic; consequences on sedimentary dispersal. In: Briand, F., (Ed.). Turbidite systems and deep-sea fans of the Mediterranean and the Black seas, CIESM Workshop 17, 43–48.

López-González, N., Alonso, B., Ercilla, G., Juan, C., Estrada, F., García, M., 2013. Sediment availability and bottom current intensity vs climatic conditions: the case of the Djibouti contourite system (Alboran Sea, SW Mediterranean). 30th IAS Meeting of Sedimentology. Conference abstracts volume, T3S4_P21.

Lowrie, A., 1986. Climate, Seismic Stratigraphy, and Sea-Level Changes. Geophysics 51, 1513-1513.

Lüdmann, T., Wiggershaus, S., Betzler, C., Hübscher, C., 2012. Southwest Mallorca Island: A cool-water carbonate margin dominated by drift deposition associated with giant mass wasting. Marine Geology 307-310: 73-87.

MNO

Maldonado, A., Campillo, A., Mauffret, A., Alonso, B., Woodside, J., 1992. Alboran Sea Cenozoic tectonic and stratigraphic evolution. Geo-Marine Letters 12, 179-186.

Maldonado, A., Barnolas, A., Bohoyo, F., Galindo-Zaldívar, J., Hernández-Molina, J., Lobo, F., Rodríguez-Fernández, J., Somoza, L., Vázquez, J.T., 2003. Contourite deposits in the central Scotia Sea: the importance of the Antarctic Circumpolar Current and the Weddell Gyre flows. Palaeogeography, Palaeoclimatology, Palaeoecology 198, 187–221.

Maldonado, A., Barnolas, A., Bohoyo, F., Escutia, C., Galindo-Zaldívar, J., Hernández-Molina, F.J., Jabaloy, A., Lobo, F., Nelson, C.H., Rodríguez-Fernández, J., Somoza, L., Vázquez, J.-T., 2005. Miocene to Recent contourite drifts development in the northern Weddell Sea (Antarctica). Global and Planetary Change 45, 99-129.

Maldonado, A., Bohoyo, F., Galindo-Zaldívar, J., Hernández-Molina, F.J., Jabaloy, A., Lobo, F., Rodríguez-Fernández, J., Suriñach, E., Tomás Vázquez, J.T., 2006. Ocean basins near the Scotia-Antarctic plate boundary: influence of tectonics and paleoceanography on the Cenozoic deposits. Marine Geophysical Research 27, 83–107.

Marani, M., Argnani, A., Roveri, M., Trincardi, F., 1993. Sediment drifts and erosional surfaces in the central Mediterranean: seismic evidence of bottom-current activity. Sedimentary Geology 82, 207-220.

Marchès, E., Mulder, T., Cremer, M., Bonnel, C., Hanquiez, V., Gonthier, E., Lecroart, P., 2007. Contourite drift construction influenced by capture of Mediterranean Outflow Water deep-sea current by the Portimão submarine canyon (Gulf of Cadiz, South Portugal). Marine Geology 242, 247-260.

Marchès, E., Mulder, T., Gonthier, E., Cremer, M., Hanquiez, V., Garlan, V., Lecroat, P. 2010. Perched lobe formation in the Gulf of Cadiz: Interactions between gravity processes and contour currents (Algarve Margin, Southern Portugal). Sedimentary Geology 229, 81-24.

Martin, J.M., Braga, J.C., 1996. Tectonic signals in the Messinian stratigraphy of the Sorbas Basin (Almeria, SE Spain). In: Friend, P.F., Dabri C.J. (Eds.). Tertiary Basins of Spain: The Stratigraphic Record of Crustal Kinematics. World and Regional Geol. Ser. 6, 387-391.

Martínez-García, P., 2012. Recent tectonic evolution of the Alboran Ridge and Yusuf regions. Universidad de Granada, PhD Thesis. 274 pp.

Martínez García, P., Comas, M., Soto, J.I., Lonergan, L., Pérez-Hernández, S., 2009. Deslizamientos submarinos recientes en la Cresta de Alborán (Mar de Alborán). Geogaceta 47, 89-92.

Martínez-García, P., Soto, J.I., Comas, M., 2010. Recent structures in the Alboran Ridge and Yusuf fault zones based on swath bathymetry and sub-bottom profiling: evidence of active tectonics. Geo-Marine Letters 31, 19-36.

Martínez-García, P., Soto, J., Comas, M., 2011. Recent structures in the Alboran Ridge and Yusuf fault zones based on swath bathymetry and sub-bottom profiling: evidence of active tectonics. Geo-Mar. Lett. 31, 19–36.

Martínez-García, P., Comas M., Soto J., Lonergan, L., Watts, T., 2013. Strike-slip tectonics and basin inversion in the Western Mediterranean: the Post-Messinian evolution of the Alboran Sea. Basin Research 25(4), 361-387.

Martorelli, E., Falcini, F., Salusti, E., Chiocci, F.L., 2010. Analysis and modeling of contourite drifts and contour currents off promontories in the Italian Seas (Mediterranean Sea). Marine Geology 278, 19-30.

Martorelli, E., Petroni, G., Chiocci, F.L., 2011. Contourites offshore Pantelleria Island (Sicily Channel, Mediterranean Sea): depositional, erosional and biogenic elements. Geo-Marine Letters 31, 481-493.

Martos, Y., Maldonado, A., Lobo, F.J., Hernández-Molina, F.J., Pérez, L.F., 2013. Tectonics and palaeoceanographic evolution recorded by contourite features in southern Drake Passage (Antarctica). Marine Geology 343, 73–91.

Maslin, M. A., Ridgwell, A.J., 2005. Mid-Pleistocene revolution and the 'eccentricity myth'. Geological Society, London, Special Publications 247, 19-34.

Masqué, P., Fabres, J., Canals, M., Sanchez-Cabeza, J.A., Sánchez-Vidal, A., Cacho, I., Calafat, A.M., Bruach, J.M., 2003. Accumulation rates of major constituents of hemipelagic sediments in the deep Alboran Sea: a centennial perspective of sedimentary dynamics. Marine Geology 193, 207–233.

Masson, D.G., Kenyon, N.H., Waver, P.P.E., 1996. Slides, debris flows, and turbidity currents. In: Summerhayes, C.P., Thorpe, S.A. (Eds.), Oceanography.Manson Publishing, London (UK), pp. 136–151.

Masson, D.G., Harbitz, C.B., Wynn, R.B., Pedersen, G., Lovholt, F., 2006. Submarine Landslides: processes, triggers and hazard prediction. Philosophical Transactions of the Royal Society A, 364, 2009-2039.

Masson, D., Harbitz, C.B., Wynn, R.B., Pedersen, G., Lovholt, F., 2011. Submarine landlsides: processes, triggers and hazard prediction. Philosophical Transactions of the Royal Society 364, 2009-2039.

Mauffret, A., Maldonado, A., Campillo, A.C., 1992. Tectonic framework of the eastern Alboran and western Alboran basins, western Mediterranean. Geo-Marine Letters 12, 104–110.

Mauffret, A., Ammar, A., Gorini, C., Jabour, H., 2007. The Alboran Sea (Western Mediterranean) revisited with a view from the Moroccan Margin. Terra Nova 19, 195–203.

Mazzoli, S., Helman, M., 1994. Neogene patterns of relative plate motion for Africa-Europe: some implications for recent central Mediterranean tectonics. Geologische Rundschau 83(2), 464-468.

McCave, I.N., 1986. Local and global aspects of the bottom nepheloid layers in the world ocean. Netherlands. Journal of Sedimentary Research 20, 167–181

McCave, I.N., 2001. Nepheloid Layers. In: Steele, J.H., Thorpe, S.A., Turekian, K.K. (Eds.), Encyclopedia of Ocean Sciences 4. Academic Press, London, pp. 1861–1870.

McCave, I.N., Tucholke, B.E., 1986. Deep current-controlled sedimentation in the western North Atlantic. In: Vogt, P.R., Tucholke, B.E. (Eds.), The Geology of North America The Western North Atlantic Region, Decade of North American Geology. Geological Society of America, Boulder, pp. 451–468.

Mézerais, M. L., Faugères, J.C., Figueiredo, A.G., Massé, L., 1993. Contour current accumulation off the Vema Channel mouth, southern Brazil Basin: pattern of a contourite fan. Sedimentary Geology 82, 173-187.

Micallef, A., Georgiopoulou, A., Le Bas, T., Mountjoy, J., Huvenne, V., Lo Iacono, C., 2013a. Processes on the precipice: seafloor dynamics across the upper Malta-Sicily escarpment. Rapport of the Commission Internationale pour l'Exploration Scientifique de la Mer Méditerranée 40, 39.

Micallef, A., Foglini, F., Le Bas, T., Angeletti, L., Maselli, V., Pasuto, A., Taviani, M., 2013. The submerged paleolandscape of the Maltese Islands: Morphology, evolution and relation to Quaternary environmental change. Marine Geology 335, 129-147.

Middleton, N.J., 1985. Effects of drought on dust production in the Sahel. Nature 316, 431–434.

Miller, K., Mountain, G., Wright, J., Browning, J., 2011. A 180-Million-Year Record of Sea Level and Ice Volume Variations from Continental Margin and Deep-Sea Isotopic Records. Oceanography 24(2), 40-53.

Millot, C., 1987. Circulation in the western Mediterranean Sea. Oceanol. Acta 10 (2), 143–149.

Millot, C., 1999. Circulation in the Western Mediterranean Sea. Journal of Marine Systems 20 (1-4), 23–442.

Millot, C., 2009. Another description of the Mediterranean Sea outflow. Progress in Oceanography 82, 101-124.

Millot, C., 2013. Levantine Intermediate Water characteristics: an astounding general misunderstanding! Sci. Mar. 77 (2), 217–232.

Millot, C., 2014. Heterogeneities of in- and out-flows in the Mediterranean Sea. Progress in Oceanography 120, 254-278.

Millot, C., García-Lafuente, J., 2011. About the seasonal and fortnightly variabilities of the Mediterranean outflow. Ocean Science 7, 421-428.

Millot, C., Taupier-Letage, I., 2005a. Additional evidence of LIW entrainment across the Algerian subbasin by mesoscale eddies and not by a permanent westward flow. Progress in Oceanography 66, 231-250.

Millot, C., Taupier-Letage, I., 2005b. Circulation in the Mediterranean Sea. In: Saliot, A. (Ed.), The Mediterranean Sea. Springer. Handbook of Environmental Chemistry 5K, 29-66.

Millot, C., Candela, J., Fuda J.-L., Tber, Y., 2006. Large warming and salinification of the Mediterranean outflow due to changes in its composition. Deep Sea Research Part I: Oceanographic Research Papers 53(4), 656-666.

Minisini, D., Trincardi, F., Asioli, A., Canu, M., Foglini, F., 2007. Morphologic variability of exposed mass-transport deposits on the eastern slope of Gela Basin (Sicily channel). Basin Research 19, 217-240.

Miramontes, E., Cattaneo, A., Jouet, G., Garziglia, S., Thereau, E., Gaillot, A., Roubi, A., Rovere, M., 2014. The Pianosa Contourite Depositional System (Corsica Trough, North Tyrrhenian Sea): stratigraphic evolution and possible role in slope instability. Vliz Special Publication, 15-16.

Moraes, M.A.S., Maciel, W.B., Braga, M.S.S., Viana, A.R., 2007. Bottom-current reworked Palaeocene–Eocene deep-water reservoirs of the Campos basin, Brazil. In: Viana, A.R., Rebesco, M. (Eds.), Economic and Palaeoceanographic Significance of Contourite Deposits. Geological Society, London, Special Publication, 276, pp. 81–94.

Moreno, A., Cacho, I., Canals, M., Prins, M.A., Sánchez-Goñi, M.-F., Grimalt, J.O., Weltje, G.J., 2002. Saharan dust transport and high-latitude glacial climatic variability: the Alboran Sea record. Quaternary Research 58 (3), 318–328.

Morrison, R., Kukla, G., 1998. The Pliocene-Pleistocene (Tertiary-Quaternary) boundary should be place at about 2.6 Ma, not at 1.8 Ma! GSA Today August, 9.

Moscardelli, L., Wood, L., 2008. New classification system for mass transport complexes in offshore Trinidad. Basin Research, 20, 73-98.

Mudelsee, M., Stattegger, K., 1997. Exploring the structure of the mid-Pleistocene revolution with advanced methods of time-series analysis. Geologische Rundschau 86(2), 499-511.

Muench, R., Padman, L., Gordon, A., Orsi, A., 2009a. A dense water outflow from the Ross Sea, Antarctica: mixing and the contribution of tides. Journal of Marine Systems 77, 369–387.

Muench, R.D., Wåhlin, A.K., Özgökmen, T.M., Hallberg, R., Padman, L., 2009b. Impacts of bottom corrugations on a dense Antarctic outflow: NW Ross Sea. Geophysical Research Letters 36, L23607.

Mulder, T. 2011. Gravity processes and deposits on continental slope, rise and abyssal plains. In: Hüneke, H., Mulder, T. (Eds.). Deep-Sea Sediments. Developments in Sedimentology, 63, 1-24.

Mulder, T., Alexander, J., 2001. Abrupt change in slope causes variation in the deposit thickness of concentrated particle-driven density currents. Marine Geology 175, 221-235.

Mulder, T., Cochonat, P., 1996. Classification of offshore mass movements. Journal of Sedimentary Research, 66, 43–57.

Mulder, T., Voisset, M., Lecroart, P., Le Drezen, E., Gonthier, E., Hanquiez, V., Faugères, J.C., Habgood, E., Hernandez-Molina, F.J., Estrada, F., Llave-Barranco, E., Poirier, D., Gorini, C., Fuchey, Y., Voelker, A., Freitas, P., Lobo Sanchez, F., Fernandez, L.M., Kenyon, N.H., Morel, J., 2003. The Gulf of Cadiz: an unstable giant contouritic levee. Geo-Marine Letters 23, 7-18.

Mulder, T., Cirac, P., Gaudin, M., Bourillet, J.-F., Tranier, J., Normand, A., Weber, O., Griboulard, R., Jouanneau, J.-M., Anschutz, P., Jorissen, F.J., 2004. Understanding continent-ocean sediment transfer. EOS American Geophysical Union Transaction 257, 261–262.

Mulder, T., Faugères, J.C., Gonthier, E., 2008. Mixed Turbidite–Contourite Systems. In: Rebesco, M., Camerlenghi, A. (Eds.). Contourites, Developments in Sedimentology 60, 435-456.

Mulder, T., Hüneke, H., van Loon, A.J., 2011. Progress in Deep-Sea Sedimentology. In: Hüneke, H., Mulder, T. (Eds.), Deep-Sea Sediments. Developments in Sedimentology 63, 1–22.

Mutti, E., Normark, W.R., 1991. An integrated approach to study of turbidite systems. In: Weimer, P., Link, M.H. (Eds.). Seismic facies and sedimentary processes of submarine fans and turbidite systems, Springer-Verlag, 75–106.

Mutti, E., Ricci Lucchi, F., 1975. Turbidite facies and facies association. In: Mutti, E., Parea, G.C., Ricci Lucchi, F., Sagri, M., Zanzucchi, G., Ghibaudo, G., Iaccarino, S. (Eds.). Example of Turbidite Facies Associations from Selected Formation of Northern Apennines, IAS Congress, Nice. p. 21-36.

Naish, T. R., Wilson, G.S., 2009. Constraints on the amplitude of Mid-Pliocene (3.6-2.4 Ma) eustatic sea-level fluctuations from the New Zealand shallow-marine sediment record. Philosophical Transactions of the Royal Society A; Mathematical, Physical & Engineering Sciences 367(1886), 169-187.

Naranjo, C., García Lafuente, J., Sánchez Garrido, J. C., Sánchez Román, A., Delgado-Cabello, J., 2012. The Western Alboran Gyre helps ventilate the Western Mediterranean Deep Water through Gibraltar. Deep Sea Research Part I 63, 157-163.

Nardin, T. R., Hein, F. J., Gorsline, D. S., Edwards, B. D., 1979. A review of mass movement processes, sediment and acoustic characteristics, and contrasts in slope and base-of-slope systems versus canyon-fan-basin floor systems. In: Pilkey, O.H. and Doyle, L. J. (eds.), Geology of continental slopes. Society of Economic Paleontologists and Mineralogists. Special Publication, 27, 61-73.

Nielsen, T., Knutz, P.C., Kuijpers, A., 2008. Seismic Expression of Contourite Depositional Systems. In: Rebesco, M., Camerlenghi, A., Contourites, Developments in Sedimentology, 60, 301-321.

Normark, W. R., Posamentier, H., Mutti, E., 1993. Turbidite systems: state of the art and future directions. Reviews of Geophysics 32(2), 91–116.

Normark, W.R., Piper, D.J.W., Posamentier, H., Pirmez, C., Migeon, S., 2002. Variability in form and growth of sediment waves on turbidite channel levees. Marine Geology 192(1-3), 23-58.

O'Grady, D.O., Syvitski, J.P.M., Pratson, L.F., Sarg, J.F., 2000. Categorizing the morphologic variability of siliciclastic passive continental margins. Geology 28, 207–210.

Orange, D.L., 1999. Tectonics, sedimentation, and erosion in northern California: submarine geomorphology and sediment preservation potential as a result of three competing processes. Marine Geology 154, 369–382.

PQR

Palanques, A., Puig, P., Latasa, M., Scharek, R., 2009. Deep sediment transport induced by storms and dense shelf-water cascading in the northwestern Mediterranean basin. Deep Sea Research Part I: Oceanographic Research Papers 56, 425-434.

Palomino, D., Vázquez, J.-T., Ercilla, G., Alonso, B., López-González, N., Díaz-del-Río, V., 2011. Interaction between seabed morphology and water masses around the seamounts on the Motril Marginal Plateau (Alboran Sea, Western Mediterranean). Geo-Marine Letters 31, 465-479.

Palomino, D., Alonso, B., Lo Iacono, C., Casas, D., D'Acremont, E., Ercilla, G., Gorini, C., Vázquez, J., 2015. Seamounts and Seamount-like Structures of the Alborán Sea. Atlas of the Mediterranean seamounts and seamount-like structures 1, 19-55. International Union for Conservation of Nature.

Panin, N., Jipa, D., 2002. River Danube-Black Sea geosystem. birth and development. In: Briand, F., (Ed.). Turbidite systems and deep-sea fans of the Mediterranean and the Black seas, CIESM Workshop 17, 63–68.

Parrilla, G., Kinder T.H., 1987. Oceanografía física del mar de Alborán. Bol. Inst. Esp. Oceanogr 4(1), 133-165.

Parrilla, G., Kinder, T. H., Preller, R. H., 1986. Deep and Intermediate Mediterranean Water in the western Alboran Sea.Deep Sea Research 33(1), 55-88.

Pérez-Belzuz, F., 1999. Geología del Margen y Cuenca del mar de Alborán durante el Plio-Quaternario: Sedimentación y Tectónica. Doctoral Thesis, Universitat de Barcelona, 554 pp.

Pérez-Belzuz, F., Alonso, B., Ercilla, G., 1997. History of mud diapirism and trigger mechanisms in the Western Alboran Sea. Tectonophysics 282, 399-422.

Periáñez, R., 2006. Modelling surface radioactive spill dispersion in the Alboran Sea. Journal of Environmental Radioactivity 90(1): 48-67.

Periáñez, R., 2007. Chemical and oil spill rapid response modelling in the Strait of Gibraltar–Alborán Sea. Ecological Modelling 207(2-4), 210-222.

Pickering, K.T., Hiscott, R.N., Hein, F.J., 1989. Deep-marine environments: clastic sedimentation and tectonics. Allen & Unwin Australia.

Piola, A.R. and Matano, R.P. 2001. Brazil and Falklands (Malvinas) currents. In: Steele, J.H., Thorpe, S.A,Turekian, K.K. (Eds.). A Derivative of the Encyclopedia of Ocean Sciences: Ocean Currents. Academic Press, London, p. 35-43.

Piper, D.J.W., Normark, W.R., 1983. Turbidite depositional patterns and flow characteristics. Navy Submarine fan, California Borderland. Sedimentology 30, 681–694.

Pistek, P., de Strobel, F., Montanari, C., 1985. Deep-Sea circulation in the Alboran Sea. Journal of Geophysical Research 90, 4969-4976.

Platt, J.P., Vissers, R.L.M., 1989. Extensional collapse of thickened continental lithosphere: A working hypothesis for the Alboran Sea and Gibraltar Arc. Geology 17 (6), 540-543.

Pomar, L., Morsilli, M., Hallock, P., Bádenas, B., 2012. Internal waves, an under-explored source of turbulence events in the sedimentary record. Earth Sci. Rev. 111 (1–2), 56–81.

Pratson, L.F., Haxby, W.F., 1996. What is the slope of the U.S. continental slope?. Geology 24, 3-6.

Preu, B., Javier Hernández-Molina, F.J., Violantem R., Piola, A.R., Paterlini, M., Schwenk, T., Voigt, I., Krastel, S., Spiess V., 2013. Morphosedimentary and hydrographic features of the northern Argentine margin: the interplay between erosive, depositional and gravitational processes and its conceptual implications. Deep Sea Research Part I Oceanographic Research Papers 75, 157-174.

Prior D.B., 1984. Submarine landslides. In: Proceedings of the 4th international symposium on landslides, Toronto, vol 2, pp 179–196.

Prior, D.B., Coleman, J.M., 1984. Submarine slope instability. In: Brunsden, D., Prior, D.B (Eds.). Slope Instability, 419-455.

Prior, D.B., Doyle, E.H., 1985. Intra-slope canyon morphology and its modification by rockfall processes, US Atlantic continental-margin. Marine Geology 67(1-2), 177-196.

Prior, D.B., Suhayada, J.N., 1979. Submarine mudslide morphology and development mechanism. Mississippi Delta. 11th Offshore Technology Conference, Houston, Texas, 2, 1055-1061.

Puig, P., Palanques, A., Guillen, J., El Khatab, M., 2004. Role of internal waves in the generation of nepheloid layers on the northwestern Alboran slope: implications for continental margin shaping. Journal of Geophysical Research, Oceans C09011.

Puig, P., Durrieu de Madron, X., Schroeder, K., Salat, J., López-Jurado, J.L., Gasparini, G.P., Palanques, A., Emelianov, M., 2010. Formation of a basin wide bottom nepheloid layer in the western Mediterranean after the winter 2005 dense shelf water cascading event. Geo-Temas 11, 141-142.

Puig, P., Durrieu de Madron, X., Salat, J., Schroeder, K., Martín, J., Karageorgis, A.P., Palanques, A., Roullier, F., Lopez-Jurado, J.L., Emelianov, M., Moutin, T., Houpert, L., 2013. Thick bottom nepheloid layers in the western Mediterranean generated by deep dense shelf water cascading. Progress in Oceanography 111, 1-23.

Raymo, M. E., 1994. The initiation of Northern Hemisphere glaciation. Annual Review of Earth and Planetary Sciences 22, 353-383.

Reading, H.G., Richards, M., 1994. Turbidite systems in deep water basin margins classified by grain size and feeder system. AAPG Bulletin 78, 792-822.

Rebesco, M., 2005. Sedimentary environments: Contourites. In: Selley, R.C., Cocks, L.R.M., Plimer, I.R. (Eds.), Encyclopedia of Geology. Elsevier, Oxford, pp. 513–527.

Rebesco, M., Camerlenghi, A., 2008. Contourites, Developments in Sedimentology vol. 60. Elsevier, Amsterdam. 663 pp.

Rebesco, M., Stow, D.A.V., 2001. Seismic expression of contourites and related deposits: a preface. Marine Geophysical Research 22, 303–308.

Rebesco, M., Camerlenghi, A., Van Loon, A., 2008. Contourite research: a field in full development. In: Rebesco, M., Camerlenghi, A. (Eds.), Contourites, Developments in Sedimentology. Elsevier, pp. 3-10.

Rebesco, M., Wåhlin, A., Laberg, J.S., Schauer, A., Brezcynska-Möller, A., Lucchi, R.G., Noormets, R., Accettella, D., Zarayskaya, Y., Diviacco, P., 2013. Quaternary contourite drifts of the Western Spitsbergen margin. Deep-Sea Research I Oceanographic Research Papers 79, 156–168.

Rebesco, M., Hernandez-Molina, F.J., Van Rooij, D., Wåhlin, A., 2014. Contourites and associated sediments controlled by deep-water circulation processes: State-of-the-art and future considerations. Marine Geology 352, 111-154.

Ribó, M., Puig, P., Palanques, A., Lo Iacono, C., 2011. Dense shelf water cascades in the Cap de Creus and Palamós submarine canyons during winters 2007 and 2008. Marine Geology 284, 175-188.

Ribó, M., Puig, P., Salat, J., Palanques, A., 2013. Nepheloid layer distribution in the Gulf of Valencia, northwestern Mediterranean. Journal of Marine Systems 111-112, 130-138.

Richards, M., Bowman, M., 1998. Submarine fans and related depositional systems ii: variability in reservoir architecture and wireline log character. Marine and Petroleum Geology 15, 821-839.

Richards, M., Bowman, M., Reading, H., 1998. Submarine fans systems I: characterization and stratigraphic prediction. Mar. Pet. Geol. 15, 689–717.

Rind, D., Chandler, M.A., 1991. Increased ocean heat transports and warmer climate. Journal of Geophysical Research 96, 7437–7461.

Roden, G.I. 1987. Effects of seamount chains on ocean circulation and thermohaline structure, In: Keating B.H. et al., (Eds.). Seamounts, Islands and Atolls. AGU Geophysics Monograph 96, 335-354.

Rodríguez-Fernández, J. Martin-Penela, A. J., 1993. Neogene evolution of the Campo de Dalias and the surrounding offshore areas-(Northeastern Alboran Sea).Geodinamica Acta 6(4), 255-270.

Rodríguez-Fernández, J., Comas, M.C., Soria, J., Martín-Pérez, J.A., Soto, J.I., 1999. The sedimentary record of the Alboran Basin: an attempt at sedimentary sequence correlation and subsidence analysis. In: Zahn, R., Comas, M.C., Klaus, A. (Eds.), Proceedings of the Ocean Drilling Program, Scientific results 161, 69-76.

Rogers, A.D. 1994. The Biology of Seamounts. Advances in Marine Biology, 30, 305-340.

Rogerson, M., Colmenero-Hidalgo, E., Levine, R.C., Rohling, E.J., Voelker, A.H.L., Bigg, G.R., Schönfeld, J., Cacho, I., Sierro, F.J., Löwemark, L., Reguera, M.I., de Abreu, L., Garrick, K., 2010. Enhanced Mediterranean-Atlantic exchange during Atlantic freshening phases. Geochemistry, Geophysics, Geosystems 11, Q08013.

Rogerson, M., Schönfeld, J., Leng, M.J., 2011. Qualitative and quantitative approaches in palaeohydrography: a case study from core-top parameters in the Gulf of Cadiz. Marine Geology 280 (1–4), 150–167.

Rogerson, M., Rohling, E.J., Bigg, G.R., Ramirez, J., 2012. Paleoceanography of the Atlantic-Mediterranean exchange: Overview and first quantitative assessment of climatic forcing. Reviews of Geophysics 50, RG2003.

Rohling, E. J., Foster, G.L., Grant, K.M., Marino, G., Roberts, A.P., Tamisiea, M.E., Williams, F., 2014. Sea-level and deep-sea-temperature variability over the past 5.3 million years. Nature 508, 477-482.

Roque, C., Duarte, H., Terrinha, P., Valadares, V., Noiva, J., Cachão, M., Ferreira, J., Legoinha, P., Zitellini, N., 2012. Pliocene and Quaternary depositional model of the Algarve margin contourite drifts (Gulf of Cadiz, SW Iberia): seismic architecture, tectonic control and paleoceanographic insights. Marine Geology 303–306, 42–62.

Rosenbaum, G., Lister, G. S., Duboz, C., 2002. Relative motions of Africa, Iberia and Europe during Alpine orogeny. Tectonophysics, 359(1), 117-129.

Roveri, M., 2002. Sediment drifts of the Corsica Channel, northern Tyrrhenian Sea. In: Stow, D.A.V., Pudsey, C.J., Howe, J.A., Faugeres, J.C., Viana, A.R. (Eds.), Deep-Water

Contourite Systems: Modern Drifts and Ancient Series, Seismic and Sedimentary Characteristics. Geological Society of London, Memoirs 22, 191-208.

Ruddiman, W.F., Sarnthein, M., Backman, J., Baldauf, J.G., Curry, W., Dupont, L.M., Janecek, T., Pokras, E.M., Raymo, M.E., Stabell, B., Stein, R., Tiedemann, R., 1989. Late Miocene to Pleistocene evolution of climate in Africa and the low-latitude Atlantic: overview of Leg 108 results. Proceedings of the Ocean Drilling Program, Scientific Results 108, 463–484.

Ryan, W.B.F, Hsu., K.J., Cita, M.B., Dumitricia, P., Lort, J., Maync, W., Nesteroff, W.D., Pautot,G., Stradner, H., Wezel, F.C., 1973. Western Alboran Basin — Site 121. Initial Reports of the Deep Sea Drilling Project, 13(1–2), 43-89. U.S. Govt. Printing Office, Washington, D.C (1973), 1447 pp.

STU

Salusti, E., Bellacicco, M., Anagnostou, C., Rinaldi, E., Tripsanas, E., 2015. On dense water formation in shelves of the Aegean Sea during the year 1987. 2015 EGU General Assembly 17, 2659.

Sarnthein, M., Thiede, J., Pflaumann, U., Erlenkeuser, H., Fütterer, D., Koopmann, B., Lange, H., Seibold, E., 1982. Atmospheric and oceanic circulation patterns off Northwest Africa during the past 25 million years. Geology of the Northwest African continental margin, 545-604.

Scott, G. H., Kennett, J. P., Wilson, K. J., Hayward, B. W., 2007. Globorotalia puncticulata: Population divergence, dispersal and extinction related to Pliocene–Quaternary water masses. Marine Micropaleontology 62(4), 235-253.

Serra, N., Ambar, I., Boutov, D., 2010. Surface expression of Mediterranean Water dipoles and their contribution to the shelf/slope–open ocean exchange. Ocean Science 6, 191–209.

Shackleton, N.J., Backman, J., Zimmerman, H.T., Kent, D.V., Hall, M.A., Roberts, D.G., Schnitker, D., Baldauf, J.G., Desprairies, A., Homrighausen, R., Huddleston, P., Keene, J.B., Kaltenback, A.J., Krumsiek, K.A.O., Morton, A.C., Murray, J.W., Westberg-Smith, J., 1984. Oxygen isotope calibration of the onset of ice-rafting and history of glaciation in the North Atlantic region. Nature 307, 620-623.

Shanmugam, G. 2000. 50 years of the turbidite paradigm, (1950s-1990s): deep-water processes and facies models. A critical perspective. Marine and Petroleum Geology, 17, 285-342.

Shanmugam, G., 2006. The tsunamite problem. Journal of Sedimentary Research 76, 718-730.

Shanmugam, G., 2008. Deep-water Bottom Currents and their Deposits. In: Rebesco, M., Camerlenghi, A. (Eds.). Contourites. Developments in Sedimentology 60,59-81.

Shanmugam, G., 2011. Discussion of He et al. (2011, Geo-Marine Letters) Evidence of internal-wave and internal-tide deposits in the Middle Ordovician Xujiajuan Formation of the Xiangshan Group, Ningxia, China. Geo-Marine Letters 32,359-366.

Shanmugam, G., 2012a. New perspectives on deep-water sandstones: origin, recognition, initiation, and reservoir quality. Handbook of Petroleum Exploration and Production. Elsevier, Amsterdam, v. 9 (524 pp.).

Shanmugam, G. 2012b. Process-sedimentological challenges in distinguishing paleo-tsunami deposits, In: A. Kumar and I. Nister, (eds.), Paleo-tsunamis: Natural Hazards, 63, 5-30.

Shanmugam, G., 2013a. Modern internal waves and internal tides along oceanic pycnoclines: challenges and implications for ancient marine baroclinic sands. Am. Assoc. Pet. Geol. 97, 799–843.

Shanmugam, G., 2013b. Comment on "Internal waves, an under-explored source of turbulence events in the sedimentary record" by L. Pomar, M. Morsilli, P. Hallock, and B. Bádenas [Earth-Science Reviews, 111 (2012), 56-81]. Earth-Science Reviews 116, 195-205.

Shanmugam, G., 2014. Modern internal waves and internal tides along oceanic pycnoclines: Challenges and implications for ancient deep-marine baroclinic sands: Reply. AAPG Bulletin 98, 858–879.

Shanmugam, G., and Moiola, R.J., 1988. Submarine fans: characteristics, models, classification, and reservoir potential. Earth-Science Reviews 24(6), 383-428.

Shepard, F.P., 1976. Tidal components of currents in submarine canyons. Journal of Geology 84, 343–350.

Shepard, F.P., 1981. Submarine canyons: multiple causes and long-time persistence. American Association of Petroleum Geologists Bulletin, 65, 1062-1981.

Shepard, F.P., Dill, R.F., 1966. Submarine Canyons and other sea-valleys. Rand McNally, Chicago, IL. 381pp.

Shepard, F.P., Marshall, N.F., McLoughlin, P.A., Sullivan, G.G., 1979. Currents in submarine canyons and other sea valleys. Studies in Geology, 8. AAPG, Tulsa.

Sierro, F.J., Hodell, D.A., Curtis, J.H., Flores, J.A., Reguera, I., Colmenero-Hidalgo, E., Bárcena, M.A., Grimalt, J.O., Cacho, I., Frigola, J., Canals M., 2005. Impact of iceberg melting on Mediterranean thermohaline circulation during Heinrich events, Paleoceanography, 20, PA2019.

Siesser, W.G., de Kaenel, E.P., 1999. Neogene calcareous nannofossils: western Mediterranean biostratigraphy and paleoclimatology, in: Zahn, R., Comas, M.C., Klaus, A., (Eds.), Proceedings of the Ocean Drilling Program, Scientific Results 161, 223–237.

Simpson, J.E. 1982: Gravity currents in the laboratory, atmosphere and ocean. Annual Review of Fluid Mechanics, 14, 213-234.

Sivkov, V., Gorbatskiy, V., Kuleshov, A., Zhurov, Y., 2002. Muddy contourites in the Baltic Sea: an example of a shallow-water contourite system. In: Stow, D.A.V., Pudsey, C.J., Howe, J.A., Faugères, J.-C., Viana, A.R., Deep-Water Contourite Systems: Modern Drifts and Ancient Series, Seismic and Sedimentary Characteristics. Geological Society, London, Memoirs 22, 121-136.

Skliris, N., Lacroix, G., Djenidi, S., 2004. Effects of extreme meteorological conditions on coastal dynamics near a submarine canyon. Continental Shelf Research 24, 1033-1045.

Smith, S.D., 1988. Coefficients for sea surface wind stress, heat flux, and wind profiles as a function of wind speed and temperature. Journal of Geophysical Research: Oceans 93, 15467-15472

Somoza, L., Medialdea, T., León, R., Ercilla, G., Vázquez, J.T., Farran, M., Hernández-Molina, F.J., González, J., Juan, C., Fernández-Puga, M. C., 2012. Structure of mud volcano systems and pockmarks in the region of the Ceuta Contourite Depositional System (Western Alborán Sea). Marine Geology 332-334, 4-26.

Spakman, W., Wortel, R., 2004. A tomographic view on western Mediterranean geodynamics. In: Cavazza, W., Roure, F., Spakman, W., Stampfli, G.M., Ziegler, P. (Eds.), The TRANSMED Atlas, The Mediterranean Region from Crust to Mantle, pp. 31–52.

Sprovieri, R., 1990. Plio-Pleistocene paleoclimatic evolution at ODP Leg 107 Site 653 (Tyrrhenian sea-western Mediterranean). Mem. Soc. Geol. It. 44, 135-144.

Stanley, D., Kelling, G., Vera, J.A., Sheng, H., 1975. Sands in the Alboran Sea: a model of input in a deep marine basin. Smithsonian Contributions to Earth Science 15, 51 pp.

Stewart, R.H., 2008. Introduction to Physical Oceanography. Texas A&M University. 345 pp.

Stoker, M.S., Akhurst, M.C., Howe, J.A., Stow, D.A.V., 1998. Sediment drifts and contourites on the continental margin off northwest Britain. Sediment. Geol. 115 (1–4), 33–51.

Stow, D.A.V., Faugères, J.C., 2008. Contourite Facies and the Facies Model. In: Rebesco, M., Camerlenghi, A., Contourites, Developments in Sedimentology 60, 223-256.

Stow, D.A.V., Lovell, J.P.B., 1979. Contourites: Their Recognition in Modern and Ancient Sediments. Earth-Science Reviews 14, 251-291.

Stow, D.A.V., Mayall, M., 2000. Deep-water sedimentary systems: new models for the 21st century. Mar. Pet. Geol. 17, 125– 135.

Stow, D.A.V., Tabrez, A.R., 1998. Hemipelagites: processes, facies and model. Geological Society, London, Special Publications 129, 317-337.

Stow, D.A.V., Reading, H.G., Collinson, J.D., 1996. Deep seas. Sedimentary environments: processes, facies and stratigraphy 3, 395-453.

Stow, D.A.V., Faugères, J.-C., Howe, J.A., Pudsey, C.J., Viana, A.R., 2002a. Bottom Currents, Contourites and Deep-Sea Sediment Drifts: Current State-of-the-Art. In: Stow, D.A.V., Pudsey, C.J., Howe, J.A., Faugères, J.-C., Viana, A.R. (Eds.), Deep-Water Contourite Systems: Modern Drifts and Ancient Series, Seismic and Sedimentary Characteristics. Geological Society of London, Memoire 22, pp. 7–20.

Stow, D.A.V., Faugères, J.C., Gonthier, E., Cremer, M., Llave, E., Hernandez-Molina, F.J., Somoza, L., Diaz-Del-Rio, V., 2002b. Faro-Albufeira drift complex, northern Gulf of Cadiz. Geological Society, London, Memoirs 22, 137-154.

Stow, D.A.V., Hunter, S.,Wilkinson, D., Hernández-Molina, J., 2008. The Nature of Contourite Deposition. In: Rebesco,M., Camerlenghi, A. (Eds.), Contourites. Developments in Sedimentology 60. Elsevier, Amsterdam, pp. 143–155.

Stow, D.A.V., Hernández-Molina, F.J., Llave, E., Sayago-Gil, M., Díaz-del Río, V., Branson, A., 2009. Bedform-velocity matrix: the estimation of bottom current velocity from bedform observations. Geology 37, 327–330.

Stow, D.A.V., Hernández-Molina, F.J., Llave, E., Bruno, M., García, M., Díaz del Río, V., Somoza, L., Brackenridge, R.E., 2013. The Cadiz Contourite Channel: sandy contourites, bedforms and dynamic current interaction.Marine Geology 343, 99–114.

Suc, J.P., Bessais, E., 1990. Perennite d'un climat thermo-xeric en Sicile avant, pendant, apres la crise de salinite Messinienne, C. R. Acad. Sci., Ser. II, 310, 1701-1707.

Suc, J.-P., Zagwijn, W. H., 1983. Plio-Pleistocene correlations between the northwestern Mediterranean region and northwestern Europe according to recent biostratigraphic and palaeoclimatic data.Boreas 12(3), 153-166.

Suc, J.-P., Diniz, F., Leroy, S., Poumot, C., Bertini, A., Dupont, L., Clet, M., Bessais, E., Zheng, Z., Fauquette, S., Ferrier, J., 1995. Zanclean (~Brunssumian) to early Piacenzian (~early–middle Reuverian) climate from 4º to 54º north latitude (West Africa, West Europe and West Mediterranean areas). Mededelingen Rijks Geologische Dienst 52, 43–56.

Sweeney, E.M., Gardner, J.V., Johnson, J.E., Mayer, L.A., 2012. Geological interpretations of a low-backscatter anomaly found on the New Jersey continental margin. Marine Geology 326–328, 46–54.

Tahchi, E., Cabello, P., Benkhelil, J., 2010. Contour current and drift deposition at the Latakia Ridge off Syria in the Eastern Mediterranean. Geo-Temas 11, 169–170.

Talukder, A.R., Comas, M.C., Soto, J.I., 2003. Pliocene to Recent mud diapirism and related mud volcanoes in the Alboran Sea (Western Mediterranean). Geological Society, London, Special Publications 216(1), 443-459.

Tarbuck, E.J., Lutgens, F.K., Tasa, D., 2005. Ciencias de la Tierra: Una introducción a la geología física. Madrid, Pearson Educación. 686pp.

Tesson, M., Gensous, B., Labraimi, M., 1987. Seismic analysis of the southern margin of the Alboran Sea.Journal of African Earth Sciences 6(6), 813-821.

Tesson, M., Gensous, B., 1989. Les bases d'une stratigraphie sismique du Neogene post-nappes en mer d'Alboran, au large du Maroc. Implications structurales et paleogeographiques. Journal of African Earth Sciences 9(3-4), 421-433.

Teurquety, G., 2012. Etude tectono-sédimentaire des bancs de Xauen et Tofino au sud de la mer d'Alboran. Master Thesis, Université Pierre et Marie Curie.

Tiedemann, R., Sarnthein, M., Shackleton, N.J., 1994. Astronomic timescale for the Pliocene Atlantic $\delta^{18}O$ and dust flux records of Ocean Drilling Program Site 659. Paleoceanography 9, 619-638.

Thunnell, R.C., Rio, D., Sprovieri, R., Vergnaud-Grazzini, C., 1991. An overview of the post-Messinian paleoenvironmental history of the western Mediterranean. Paleoceanography 6, 143-164.

Toucanne, S., Jouet, G., Ducassou, E., Bassetti, M.-A., Dennielou, B., Angue Minto'o, C.M., Lahmi, M., Touyet, N., Charlier, K., Lericolais, G., Mulder, T., 2012. A 130,000-year record of Levantine Intermediate Water flow variability in the Corsica Trough, western Mediterranean Sea. Quaternary Science Reviews 33, 55-73.

Trincardi, F., Foglini, F., Verdicchio, G., Asioli, A., Correggiari, A., Minisini, D., Piva, A., Remia, A., Ridente, D., Taviani, M., 2007. The impact of cascading currents on the Bari Canyon System, SW-Adriatic Margin (Central Mediterranean). Marine Geology 246, 208-230.

Tucholke, B.E., 2002. The Greater Antilles Outer Ridge: development of a distal sedimentary drift by deposition of fine-grained contourites. In: Stow, D.A.V., Pudsey, C.J., Howe, J.A., Faugères, J.-C., Viana, A.R. (Eds.), Deep-Water Contourite Systems: Modern Drifts and Ancient Series, Seismic and Sedimentary Characteristics. The Geological Society of London, Memoire 22, pp. 39–55.

VWXYZ

Vandorpe, T., Van Rooij, D., Stow, D.A.V., Henriet, J.-P., 2011. Pliocene to recent shallowwater contourite deposits on the shelf and shelf edge off south-western Mallorca, Spain. Geo-Marine Letters 31, 391–403.

Van Rooij, D., Iglesias, J., Hernández-Molina, F. J., Ercilla, G., Gomez-Ballesteros, M., Casas, D., Llave, E., De Hauwere, A., Garcia-Gil, S., Acosta J., Henriet, J. P., 2010. The Le Danois Contourite Depositional System: Interactions between the Mediterranean Outflow Water and the upper Cantabrian slope (North Iberian margin). Marine Geology 274(1-4), 1-20.

Vargas-Yáñez, M., Plaza, F., García-Lafuente, J., Sarhan, T., Vargas, J.M., Vélez-Belchí, P., 2002. About the seasonal variability of the Alboran Sea circulation. Journal of Marine Systems 35, 229-248.

Vázquez, A., Bruno, M., Izquierdo, A., Macías, D., Ruiz-Cañavate, A., 2008. Meteorologically forced subinertial flows and internal wave generation at the main sill of the Strait of Gibraltar. Deep-Sea Research I Oceanographic Research Papers 55 (10), 1277–1283.

Vázquez, J.-T., Bárcenas, P., Palomino, D., Alonso, B., Ercilla, G., Díaz-del-Río, V., López-González, N., Fernández-Salas, L.M., Sayago-Gil, M., 2010. Sedimentary instabilities along the southwestern slope of the Alboran Ridge (SW Mediterranean). 39th CIESM Congress. Venice (Italy), Rapport of the Commission Internationale pour l'Exploration Scientifique de la Mer Méditerranée 39, 76.

Vázquez, J. T., Alonso, B., MONTERA and UTM teams, 2012. Informe científico-técnico: Campaña Montera-0412. B/O Sarmiento de Gamboa. 147 pp.

Vázquez, J.-T., Ercilla, G., Alonso, B., Juan, C., Rueda, J.L., Palomino, D., Fernández-Salas, L.M., Bárcenas, P., Casas, D., Díaz del Río, V., Estrada, F., Farran, M., García, M., González, E., López-González, N., El Moumni, B., CONTOURIBER, MONTERA and MOWER Teams, 2015. Submarine canyons and related features in the Alboran Sea: continental margins and major isolated reliefs. In: Briand, F. (Ed.), Submarine canyon

dynamics in the Mediterranean and tributary seas, an integrated geological, oceanographic and biological perspective. CIESM Workshop Monographs 47, 183-196.

Velasco, J.P.B., Baraza, J., Canals, M., Balón, J., 1996. La depression periférica y el lomo contourítico de Menorca: evidencias de la actividad de corrientes de fondo al N del talud Balear. Geogaceta 20, 359–362.

Velegrakis, A.F., Michel, D., Collins, M.B., Lafite, R., Oikonomou, E.K., Dupont, J.P., Huault, M.F., Lecouturier, M., Salomon, J.C., Bishop, C., 1999. Sources, sinks and resuspension of suspended particulate matter in the eastern English Channel. Continental Shelf Research 19, 1933-1957.

Verdicchio, G., Trincardi F., 2008. Mediterranean shelf-edge muddy contourites: examples from the Gela and South Adriatic basins. Geo-Marine Letters 28, 137-151.

Viana, A.R., Faugères, J.-C., Stow, D.A.V., 1998. Bottom-current controlled sand deposits: a review from modern shallow to deep water environments. Sedimentary Geology 115, 53–80.

Viana, A.R., De Almeida Jr., W., De Almeida, C.W., 2002. Upper Slope Sands: Late Quaternary Shallow-Water Sandy Contourites of Campos Basin, SW Atlantic Margin. In: Stow, D.A.V., Pudsey, C., Howe, J.A., Faugères, J.-C., Viana, A.R. (Eds.), Deep-Water Contourites: Modern Drifts and Ancient Series, Seismic and Sedimentary Characteristics. Geological Society of London, Memoire 22, pp. 261–270.

Viana, A.R., Almeida Jr., W., Nunes, M.C.V., BulhÕes, E.M., 2007. Economic and Paleoceanographic Significance of Contourite Deposit. In: Viana, A.R., Rebesco, M. (Eds.), Economic and Paleoceanographic Significance of Contourite Deposit. The Geological Society of London, Sep. Publ. 276, pp. 1–23.

Voelker, A., Lebreiro, S., Schönfeld, J., Cacho, I., Exlenkenser, H., Abrantes, F., 2006. Mediterranean outflow strengthenings during Northern Hemisphere coolings: a salt sources for the glacial Atlantic? Earth Planet. Sci. Lett. 245, 39–55.

Völker, C., 2007. A short introduction to physical oceanography. Bremerhaven, Germany, Alfred-Wegener-Institut für Polar- und Meeresforschung, 57pp.

von Grafenstein, R., Zahn, R., Tiedemann, R., Murat. A., 1999. Planktonic $\delta 18O$ records at sites 976 and 977, Alboran sea: stratigraphy, forcing, and paleoceanographic implications, in: Zahn, R., Comas, M.C., Klaus, A., (Eds.): Proc. ODP Scientific Results 161, 469-479.

von Lom-Keil, H., Speiss, V. and Hopfauf, V. 2002. Fine grained sediment waves on the western flank of the Zapiola Drift, Argentine Basin -Evidence for variations in Late Quaternary bottom flow activity. Marine Geology 192, 239-258.

Wagner, B., Aufgebauer, A., Vogel, H., Zanchetta, G., Sulpizio, R., Damaschke, M., 2012. Late Pleistocene and Holocene contourite drift in Lake Prespa (Albania/F.Y.R. of Macedonia/Greece). Quaternary International 274, 112-121.

Wåhlin, A. 2004. Topographic advection of dense bottom water. Journal of Fluid Mechanics, 210, 95-104.

Wåhlin, A., Walin, G., 2001. Downward migration of dense bottom currents. Environmental Fluid Mechanics 1, 257–279.

Webb, D.L., 1993. Seabed and sub-seabed mapping using a parametric system. Hydrographic J. 68, 5-13.

Weijermars, R., 1988. Neogene tectonics in the western Mediterranean may have caused the Messinian salinity crisis and an associated glacial event. Tectonophysics 148, 211-219.

Wille, P., 2005. Sound images of the ocean in research and monitoring. Berlin, Springer Science & Business Media. 471pp.

Wood, R., Davy, B., 1994. The Hikurangi Plateau. Mar. Pet. Geol. 118, 153–173.

Woodside, J. M., Maldonado, A., 1992. Styles of Compressional Neotectonics in the Eastern Alboran Sea. Geo-Marine Letters 12, 111-116.

Wright, S.G. and Rathje, E.M. 2003. Triggering Mechanisms of Slope Instability and their Relationship to Earthquakes and Tsunamis. Pure and Applied Geophysics 160, 1865-1877.

Wynn, R.B., Cronin, B.T., Peakall, J., 2007. Sinuous deepwater channels: Genesis, geometry and architecture. Marine and Petroleum Geology, 24, 341-387.

Zazo, C., 1999. Interglacial sea levels. Quaternary International 55, 101-113.

Zazo, C., Goy, J. L., Dabrio, C. J., Lario, J., González-Delgado, J. A., Bardají, T., Hillaire-Marcel, C., Cabero, A., Ghaleb, B., Borja, F., Silva, P. G., Roquero E., Soler, V., 2013. Retracing the Quaternary history of sea-level changes in the Spanish Mediterranean–Atlantic coasts: Geomorphological and sedimentological approach. Geomorphology 196, 36-49.

Chapter IX - Annex: scientific contributions
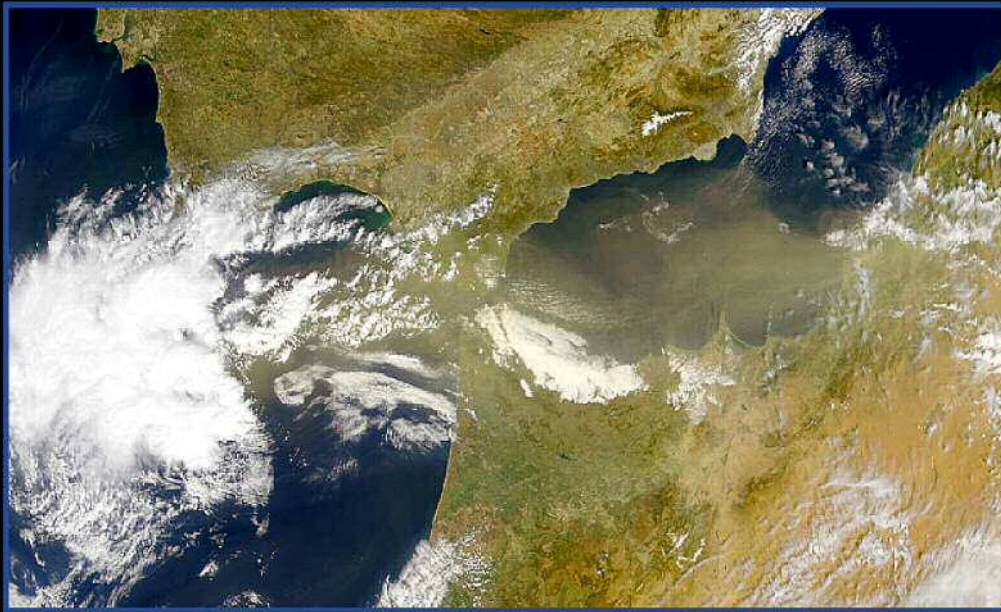
Carmen Juan Valenzuela

Tesis Doctoral 2016

UNIVERSITAT DE BARCELONA

CSIC
CONSEJO SUPERIOR DE INVESTIGACIONES CIENTÍFICAS

ICM
Institut de Ciències del Mar